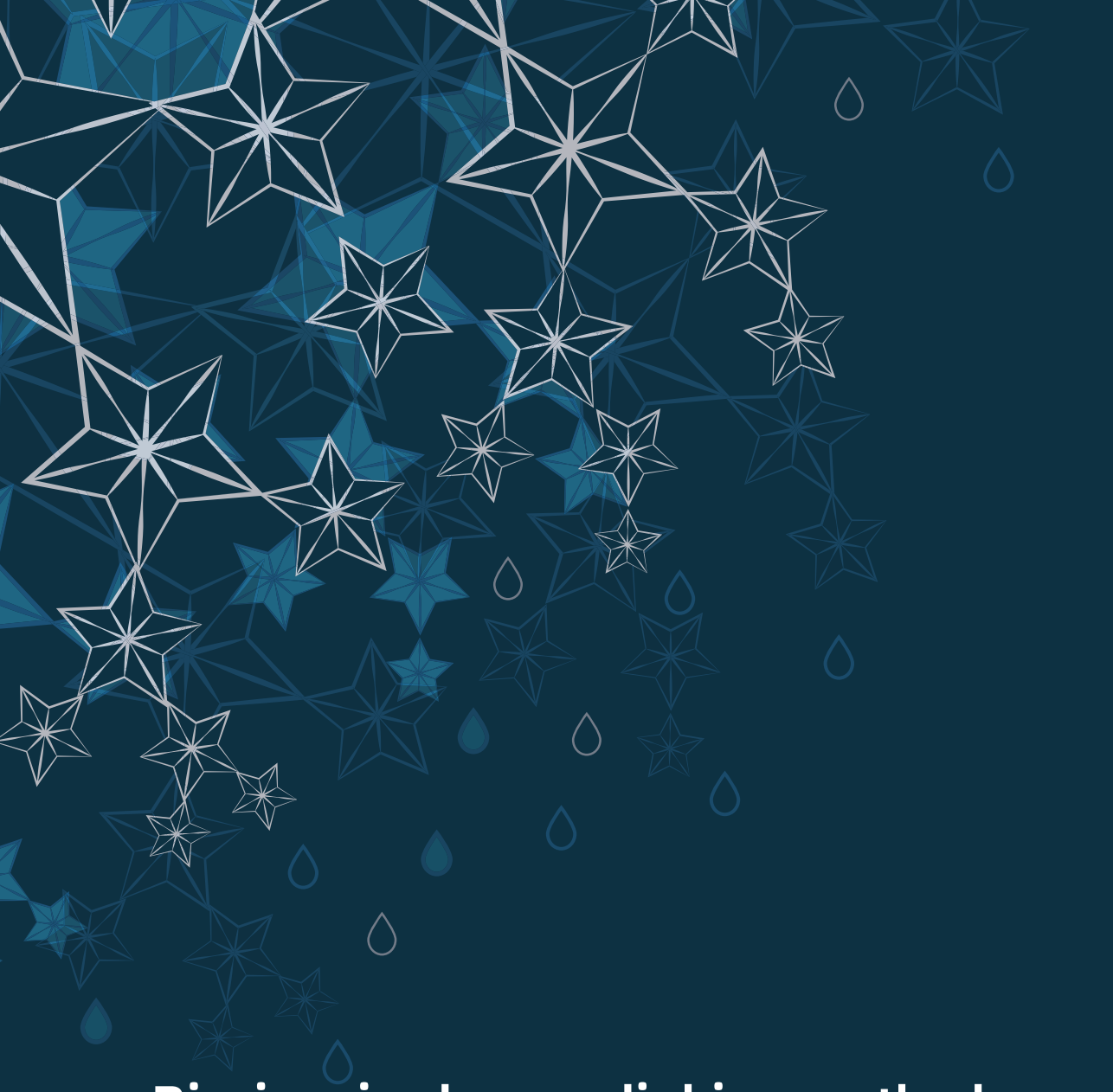

Bio-inspired cross-linking methods for hydrogel formation

Anika M. Jonker

Bio-inspired cross-linking methods for hydrogel formation

Proefschrift

ter verkrijging van de graad van doctor
aan de Radboud Universiteit Nijmegen
op gezag van de rector magnificus,
volgens besluit van het college van decanen
in het openbaar te verdedigen op woensdag 20 januari 2016
om 14.30 uur precies

door

Anika Maartje Jonker

geboren op 30 maart 1987
te Almere

Promotor
Prof. dr. ir. J.C.M. van Hest

Co-promotor
Dr. D.W.P.M. Löwik

Manuscriptcommissie
Prof. dr. A.E. Rowan
Prof. dr. R.P. Sijbesma (TU Eindhoven)
Dr. K.M. Bonger

Paranimfen
Saskia Bode
Annika Borrmann

Cover design
Angela van de Weg
Kristel Schumacher, Studio Lakmoes, Arnhem
Barbara Wagensveld, Studio Lakmoes, Arnhem

Layout and printed by Gildeprint - Enschede

ISBN: 978-94-6233-183-9

Netherlands Enterprise Agency

The research presented in this thesis was financially supported by Agentschap NL, Ministry of Education, Culture and Science

Table of Contents

List of abbreviations

α-cyano	α-cyano-4-hydroxycinnamic acid
BCN	(1*R*,8*S*,9*S*)-bicyclo[6.1.0]non-4-yn-9-yl
Boc	*tert*-Butyloxycarbonyl
BOP	Benzotriazol-1-yl-oxy-tris dimethylaminophosphonium hexafluorophosphate
CD	Circular dichroism
CuAAC	Cu(I)-catalyzed azide-alkyne cycloaddition
DCM	Dichloromethane
DIPCDI	*N,N'*-diisopropylcarbodiimide
D*i*PEA	N,N-diisopropylethylamine
DLS	Dynamic light scattering
DMEM	Dulbecco's Modified Eagle Medium
DMF	Dimethylformamide
DMSO	Dimethylsulfoxide
DOPA	3,4-dihydroxyphenylalanine
DHPA	3,4-dihydroxyphenylacetic acid
DMPC	1,2-dimyristoyl-sn-glycero-3-phosphocholine
DPPC	1,2-dipalmitoyl-sn-glycero-3-phosphocholine
ECM	Extracellular matrix
EDTA	Ethylenediaminetetraacetic acid
EthD-1	Ethidium homodimer-1
Et_3N	Triethylamine
Et_2O	Diethylether
EtOAc	Ethylacetate
Fmoc	Fluorenylmethyloxycarbonyl
G'	Storage modulus
G''	Loss modulus
HBTU	*N,N,N',N'*-Tetramethyl-*O*-(1*H*-benzotriazol-1-yl)uronium hexafluorophosphate
HeLa	Henrietta Lacks
HMPA	Hexamethylphosphoramide
HOAc	Acetic acid
HOBt	*N*-hydroxybenzotriazole
HOS	Human osteosarcoma
HPLC	High Performance Liquid Chromatography
IR	Infrared
ITC	Isothermal calorimetry

LC-MS	Liquid chromatography-Mass Spectrometry
MALDI-TOF	Matrix-assisted laser desorption/ionization – time of flight
MAS	Magic-angle spinning
MeCN	Acetonitrile
MeOH	Methanol
MMP	Matrix metalloproteinase
MS	Mass Spectrometry
MT	Mushroom Tyrosinase
MW	Molecular weight
$NaIO_4$	Sodium periodate
NHS	*N*-hydroxy succinimide
NMR	Nuclear Magnetic Resonance
OSu	*N*-hydroxysuccinimide
PBS	Phosphate buffered saline
PEG	Poly(ethylene)glycol
PyBOP	Benzotriazol-1-yl-oxy-tripyrrolidinophosphonium hexafluorophosphate
PyBrOP	Bromotripyrrolidinophosphonium hexafluorophosphate
r.t.	Room temperature
Rt	Retention time
SEC	Size-exclusion chromatography
SPAAC	Strain-promoted azide-alkyne cycloaddition
SPOCQ	Strain-promoted oxidation-controlled cyclooctyne–1,2-quinone cycloaddition
SPPS	Solid phase peptide synthesis
TEM	Transmission electron microscopy
TFA	Trifluoroacetic acid
TFE	Trifluoroethanol
TIS	Triisopropylsilane
TLC	Thin-layer chromatography
δ	Chemical shift

List of amino acids

Ala	A	Alanine
Arg	R	Arginine
Asp	D	Aspartic acid
Asn	N	Asparagine
Cys	C	Cysteine
Gln	Q	Glutamine
Glu	E	Glutamic acid
Gly	G	Glycine
His	H	Histidine
Ile	I	Isoleucine
Leu	L	Leucine
Lys	K	Lysine
Met	M	Methionine
Phe	F	Phenylalanine
Pro	P	Proline
Ser	S	Serine
Thr	T	Threonine
Trp	W	Tryptophan
Tyr	Y	Tyrosine
Val	V	Valine

Chapter 1

Peptide- and protein based hydrogels

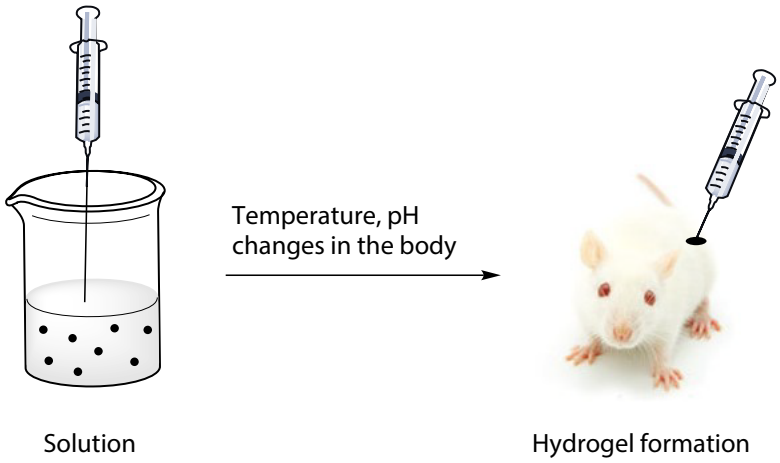

Part of this chapter has been published as:

Jonker, A. M.; Löwik, D. W. P. M.; van Hest, J. C. M. *Chem. Mater.* **2012**, *24*, 759-773

1.1. Introduction

Hydrogels are three-dimensional, hydrophilic polymer networks, capable of absorbing large amounts of water or biological fluids, up to thousand times their dry weight. They are insoluble due to the presence of cross-links between the constituents that form the polymeric network. They are often made of homopolymers or copolymers, but can also consist of small molecules that self-assemble into high molecular weight structures.[1,2] The first hydrogel report dates back to the study by Wichterle and Lim (1960), who polymerized and cross-linked 2-hydroxyethyl methacrylate into a transparent gel, which showed promising results in the manufacturing of contact lenses.[3] Since this pioneering work, the number of publications on hydrogels has increased every year.[4,5] Hydrogels can be classified in a number of ways. They can for example be categorized based on the nature of their building blocks, being either neutral or ionic, or natural or synthetic in origin. Furthermore, hydrogels are often distinguished based on their mechanical and structural characteristics, such as the degree of cross-linking and the integrity of the gels. Finally, an important classification is the way in which cross-linking occurs, which can be either chemical or physical.[2] Hydrogels formed by chemical cross-links undergo significant volume changes during the transition from solution (sol) to gel state. These chemical cross-links can be formed in many different ways, such as disulfide formation, (photo)polymerisation or the reaction between thiols and acrylates or sulfones. The density of cross-linking can easily be varied and with this also the mechanical properties of the final material. Physically cross-linked hydrogels, on the other hand, do not undergo significant volume changes during the sol-gel transition. They can be prepared via the self-assembly of polymers, which occurs in response to external stimuli such as pH and temperature. The polymers generally provide relatively low viscous solutions that can rapidly form a gel when an external trigger is applied. Often physical cross-linking leads to weaker gels than chemical cross-linking; therefore these gels are more susceptible to mechanical forces such as shear. This can also be used to its advantage, as it makes physical hydrogels suitable as injectable materials (**Figure 1.1**). Another advantage of physical cross-linking is that it mostly does not depend on the addition of organic solvents or cross-linking reagents, offering possibilities for these hydrogels in biomedical applications such as the controlled delivery of drugs and cells and in tissue engineering.[6]

Tissue engineering is an important research field, since every year millions of people suffer from the loss or failure of organs or tissues. These patients are treated by organ or tissue transplantations. Since there is a huge shortage of donors, new treatments such as tissue engineering gain increasing attention.[7-10] In this research field, man-made organs or tissues are developed to restore, improve or maintain tissue function.[9] These materials are usually made by incorporation of the patient's own cells into polymer scaffolds, such as poly(glycolic acid) (PGA) and poly(lactic acid) (PLA). These scaffolds are capable of delivering the cells into the body,

thereby providing a site for new tissue formation. Administration of these polymer scaffolds into the body occurs via cuts or incisions. In addition, polymer scaffolds can also be used as a substrate for the attachment and migration of cell populations.[7,8] As an alternative, hydrogels are thought to constitute an excellent starting point as a matrix to grow new tissue in. The gels can be designed to be biodegradable and their mechanical and structural properties to resemble those of many tissues. Importantly, hydrogels can be designed to be able to transplant the cells into the body by simple injection, thereby minimizing the invasive manner (**Figure 1.1**).[11]

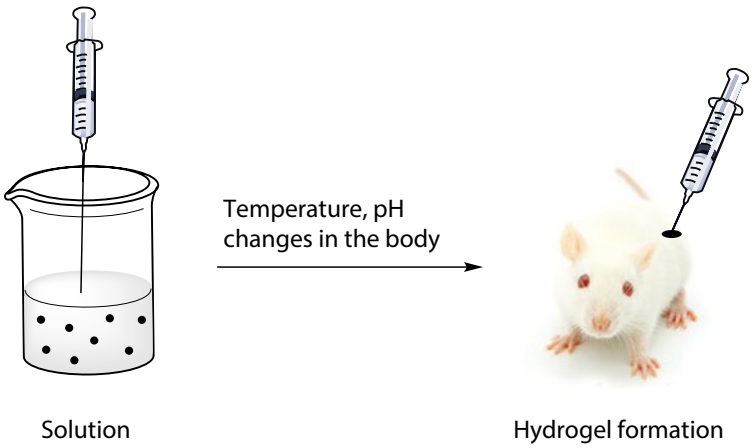

Figure 1.1. A schematic representation of an injectable hydrogel. At low temperatures, these hydrogels are soluble. Cells or drugs (represented by the black dots) are mixed with the solvent. After injection, temperature or pH changes in the body are responsible for hydrogel formation, resulting in the delivery of the cells or drugs to the body.

In the design of these hydrogels, several criteria have to be taken into account. A highly important factor is the biocompatibility. The injectable materials should be biocompatible, in the sense that they do not damage adjacent cells or in some other way induce undesired responses. Another issue that needs to be addressed is cell adhesion; hydrogels should interact favourably with the type of cells they want to deliver. Inappropriate interaction might lead to undesirable tissue formation. Furthermore, the degradation behaviour of the hydrogels is important for tissue engineering applications. The rate of degradation should be in line with the tissue development, since the degradation of the hydrogels may influence the mechanical properties. Importantly, the degradation products should be biocompatible as well.[7]

An important guide in the design of hydrogels for tissue engineering is the extracellular matrix (ECM). The ECM is the biological material that surrounds cells in tissues. It is furthermore responsible for mechanical support and provides an environment for new tissue formation.[12] The ECM itself consists mainly of proteoglycan filaments, collagen fibres and elastin. The collagen

fibres provide tensile strength and durability to the surrounding tissue. Elastin enables the stretch and recoil of the ECM network. The proteoglycan filaments are built up from proteins and hyaluronic acid to form coiled structures. Proteoglycan binds water, sequesters growth factors and supplies compression resistance. At low protein concentrations, the ECM structure can be considered gel-like.[13,14] Hence, mimicking the ECM is an important goal in the design of hydrogels for tissue engineering and is considered as a good way to develop biomaterials with control over cell adhesion, proliferation, migration and differentiation.[15]

Peptides and proteins are often used in the development of hydrogels, since they exhibit some advantageous characteristics, such as biocompatibility and biodegradability. The incorporation of peptides into biomaterials can be performed using several chemical reactions including click chemistry, Michael addition of cysteine residues to vinyl sulfones or maleimides, UV-initiated cross-linking and native chemical ligation. These reactions all take place with a high level of chemical specificity. This is often not possible for proteins, since the exact composition of the interaction region is not precisely known. Incorporation of proteins into biomaterials is therefore often performed via non-specific amine-carboxylic acid couplings. Peptides can be incorporated into biomaterials to infer a number of functions. This includes cell-binding, growth factor binding, surface binding and/or proteolytic susceptibility.[16] The most frequently used peptide sequence in this respect is the arginine-glycine-aspartic acid (RGD) sequence.[17] The incorporation of this cell adhesion motif into biomaterials has already been reviewed extensively in literature.[8,18-21] Efforts are being made to introduce combinations of peptides during the synthesis of biomaterials, in order to integrate multiple functions.[16]

On the other hand, peptides and proteins can also be employed as moieties that provide structural integrity to a gel, e.g. via self-assembly or aggregation. In this chapter an overview is given of hydrogels in which peptides and proteins are structural elements of the polymer network. Starting from hydrogels which are derived from naturally occurring structural proteins, we will gradually move from all-protein and peptide-based synthetic systems to hybrid hydrogels which are composed of synthetic polymeric and peptide structural elements. We will illustrate the potential of these hydrogels with applications which are mainly derived from the field of tissue engineering. Finally, an overview of chemical cross-linking methods is described. For articles which give a broader overview of biomaterials used in hydrogel formation or which discuss in more detail the mechanical properties of peptide-based hydrogels one is referred to excellent reviews by Schacht et al. and Pochan et al.[4,22]

In summary, hydrogels are promising materials for use as biomaterials, since they have high water content, have a tuneable viscoelasticity, are biocompatible and can be made injectable. Both peptides and proteins have advantageous features for use as building blocks in the synthesis of

biomaterials and hydrogels in particular. As mentioned above, an important requirement for the design of hydrogels is the biocompatibility. Hydrogels based on peptides or proteins often fulfil this prerequisite and are easily degraded by the body.

1.2. Natural protein-based hydrogels

As described above, proteins display interesting properties for use in the synthesis of hydrogels. Especially their excellent biocompatibility and biodegradability make them promising candidates in biomedical applications. A concise description of proteins derived from natural sources which are used for the preparation of biomaterials is provided. Since usually biosynthetic procedures are used to mimic the sequences of natural proteins, these are more extensively described in **Paragraph 1.3**. One is referred to excellent reviews for more information about elastin[23,24], collagen and gelatin.[25,26]

1.2.1. Elastin

Elastin is a major structural protein of the extracellular matrix (ECM) that regulates the cell/cell interactions and the cell/ECM interactions. Elastin provides the ECM with tensile strength and elasticity, required for proper functioning.[27] Typically, natural elastin hardly has been used as a biomaterial in tissue engineering. An important requirement when using proteins as biomaterial is the purity. In the synthesis of elastin, elastic fibres are formed on microfibrillar components acting as scaffold. Elastin then has to be purified from the elastic fibres. Contaminations from the preparation, like calcium-binding microfibrillar components, can lead to immunological responses in the human body. Moreover, elastin is insoluble and has a strong tendency to calcify, making purification even more difficult.[28]

1.2.2. Collagen and gelatin

Most of the collagens are fibrous proteins, responsible for important mechanical functions throughout the body. Collagens are particularly present in articular and bone tissues, where they provide most of the biochemical properties essential for proper functioning. Furthermore, collagens can bind and release cellular mediators such as cytokines and growth factors.[29] The structural element of collagen is the triple helix, consisting of a -Gly-Xaa-Yaa- repeat. The amino acids Xaa and Yaa are usually proline and hydroxyproline (Hyp).[30] Collagen is widely used as biomaterial in tissue engineering. It is used in its native fibrillar form, as well as after denaturation. Denaturation offers the possibility to fabricate several collagen forms, including sheets, tablets, pellets and sponges.[31] Collagen has for example been used to repair tendon defects in rabbits[32], for curing of chronic wounds caused by diabetes[33] and as delivery system for proteins, drugs and genes.[34] When the triple-helix structure of collagen is broken into single-strand molecules,

gelatin is obtained. Gelation of a gelatin solution occurs easily by a change in temperature. Gelatin gels have shown to be non-immunogenic, biodegradable and biocompatible, making them suitable candidates for biomedical applications. However, the thermal and mechanical stability of the gelatin gels is rather low. For long term biomedical applications, the stability of gelatin gels is improved by chemical modifications such as cross-linking.[7,35] Gelatin-based materials have already been used in several tissue engineering applications, for example in adipose tissue repair[36] and as bone tissue engineering material.[37]

1.2.3. Silk fibroin

Silks are natural structural proteins produced by insects such as spiders and worms. Silk produced by the silkworm *Bombyx mori* is called silk fibroin. This fibrous protein contains two protein components: fibroin and sericin. Fibroin consists of light (~26 kDa) and heavy chain (~390 kDa) polypeptides, which are present in a 1:1 ratio and are connected by a disulfide bridge. Silk fibroin forms β-sheets, due to the presence of the highly repetitive amino acid motif GAGAGS (**Figure 1.2**).[38,39]

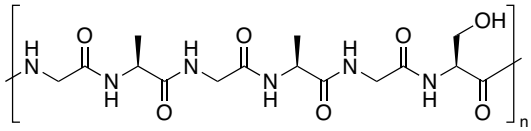

Figure 1.2. The ubiquitous GAGAGS motif present in silk fibroin induces the formation of β-sheets.

These β-sheets are responsible for the formation of silk fibroin hydrogels. Due to the formation of the β-sheets, the silk fibroin becomes insoluble in water. Hydrophobic interactions among the protein chains in fibroin lead to the assembly of the material into hydrogels. Gelation can be enhanced by an increase in temperature or fibroin concentration. Furthermore, gelation can be promoted by a decrease in pH or by addition of a hydrophilic polymer. Both factors stimulate desorption of water and decrease the repulsion between the protein chains. Addition of Ca^{2+} ions also accelerates the formation of hydrophobic interactions, presumably because the pH is lowered by ionic interactions with the COO^- ions of the amino acid side chains.[40] Silk fibroin hydrogels are biocompatible, have unique mechanical properties, are biodegradable and display cellular interactions.[41] For example, *in vitro* and *in vivo* tests on rabbits with cancellous bone defects showed bone healing and stimulated cell proliferation.[42]

1.2.4. Globular proteins

Many studies have been performed on the gelation processes of globular proteins such as bovine serum albumin, β-lactoglobulin and ovalbumin. From these proteins, β-lactoglobulin is the one most intensively studied. This protein, with a molecular mass of 18.6 kDa, is widely used in the food industry. This globular protein denatures when heated, leading to either large linear

aggregates or small primary aggregates, both consisting of peptide fragments.[43,44] The small aggregates can further grow into larger aggregates and at a certain concentration self-assemble into gels. Alternatively, the large linear aggregates can phase separate, leading to protein-rich domains. These can also further aggregate and form gels.[43]

1.3. Biosynthetic polypeptide-based hydrogels

Natural protein-based hydrogels also display some disadvantages for use as biomaterials. As outlined above, their purification and low stability might be problematic. Furthermore, when using samples from natural sources, it is difficult to obtain identical compositions. As an alternative, synthetic polypeptide-based hydrogels have been investigated. These materials are prepared using methods such as gene expression in bacteria, via recombinant technology and solid phase peptide synthesis. Synthetic hydrogels can contain sequences mimicking those of natural proteins. Functionalities to increase the biological or mechanical properties of the hydrogels can easily be incorporated. Moreover, modifications in the peptide sequences can simply be made, in order to improve the features of the hydrogels. The following part of this chapter gives an overview of biosynthetic polypeptide-based hydrogels.

1.3.1. Collagen-based synthetic hydrogels

Hydrogels based on collagen have been designed for the purpose of tissue engineering. As an example of the solid phase peptide synthesis approach, a small library of Nap-Gly-Phe-Phe-Tyr-Gly-Gly-Xaa-Hyp was synthesized (**Figure 1.3**). The repeating collagen sequence Gly-Xaa-Hyp was used, in which amino acid Xaa was Lys, Glu, Ser, Ala or Pro. This sequence was connected to Nap-Gly-Phe-Phe-Tyr, a peptide with an N-terminal naphthyl (Nap) moiety that is able to form gels.

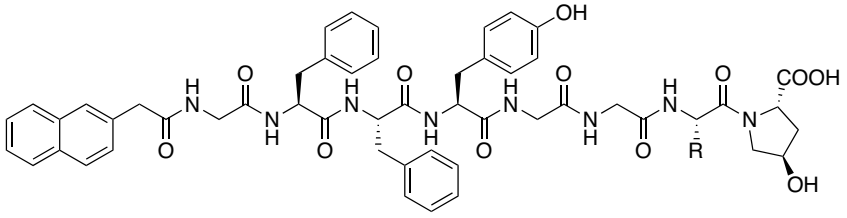

Figure 1.3. Nap-Gly-Phe-Phe-Tyr-Gly-Gly-Xaa-Hyp. Residue Xaa can be Lys, Glu, Ser, Ala or Pro. Due to the naphthyl moiety (Nap), all 5 members are capable of forming hydrogels.

All five members were capable of forming hydrogels in phosphate buffered saline. The construct with lysine proved to give the strongest hydrogel. A construct without the collagen domain Gly-Xaa-Hyp was also prepared. This compound also formed a hydrogel, but more extensive

hydrogen bonds between the peptides were found in the other, collagen-based constructs. In order to test the biocompatibility of the gels, in vitro cell culture experiments were performed. Mouse embryonic fibroblast cells (3T3) were placed on top of the hydrogels. After 72 h, most cells on the surface of the Lys-, Glu- and Ser-containing constructs were still alive. Fewer 3T3 cells were observed on the surface of Ala- and Pro-containing hydrogels and, if present, many of them were dead. These two hydrogels are thus not suitable for 3T3 cell culture, possibly due to the less polar side chains of Ala and Pro. The gel with lysine proved to be the most suitable in these tests, probably because the positively charged lysine increases the binding to the negative cell surface.[45]

E. coli cannot be used for the synthesis of hydroxyproline containing collagens, since this bacterial host lacks the ability to perform the post-translational modification of proline to hydroxyproline. In order to broaden the applications of collagen as injectable biomaterial, hydroxyproline-free collagen mimetic peptides (CMP) were synthesized. An example is the $(GPP)_3$ GPR GEK GER GPR $(GPP)_3$ GPCCG peptide, containing a $(GPP)_3$ triplet, that stabilizes the formation of a triple-helix. Analysis of the CMP indeed revealed the formation of stable triple helices, the important structural feature of collagen. The observed assembly behaviour suggests that these hydroxyproline-free peptides can be used as collagen mimetics, with the advantageous possibility to use *E. coli* for their production.[46] An application of collagen-based hydrogels as delivery system was recently reported. CMPs were used to create DNA polyplex-modified collagens. The release of the DNA polyplexes was demonstrated and could also be tuned by varying the CMP content.[47] In another example, the release of green fluorescent protein and human epidermal growth factor was shown from a highly cross-linked CMP-based 3-D matrix. After release of the growth factor, it remained active, which was shown by its ability to stimulate cell growth. When cell binding motif RGDS was incorporated in the CMP constructs, encapsulated epithelial cells formed spheroid structures. This result shows the potential of collagen-based hydrogels for mimicking the ECM.[48]

Collagen was also taken as a basis for the preparation of triblock thermo-reversible gels as shown by Skrzeszewska and co-workers via a protein engineering approach.[49] The end blocks consisted of the $(Pro\text{-}Gly\text{-}Pro)_9$ sequence, which forms collagen-like triple helices. The middle block was a 399 amino acid long sequence containing the $(Gly\text{-}Xaa\text{-}Yaa)_n$ structure and, besides proline, only hydrophilic residues such as asparagine and glutamine.[49,50] This highly hydrophilic sequence is not able to form secondary structures and hence maintains a random coil conformation. Stable gels were only obtained when three of the collagen-like sequences form a triple helix, since double helices are not stable. The triblock construct was present as a viscous solution at temperatures above 50°C, but formed a gel at room temperature. This thermo-responsive behaviour was shown to be reversible, hence an increase in temperature

led to the soluble form. The gelation process of the triblock construct was used to develop a theoretical model that is able to predict the viscoelastic behaviour of polymer gels.[49] In a later study rheology, light scattering and atomic force microscopy were conducted to investigate the pH-dependent fibre- and gel formation of the triblock constructs. Monomers were found at low pH, but with a pH value above 6, these self-assembled into fibres and then hydrogels. At physiological pH, gels appeared to have the highest moduli, although gel strength was found to be dependent on the purification and preparation method of the gels.[51] As a first test, rat bone marrow cells were cultured in the presence of the triblock hydrogels. These cells remained viable, but comparison with collagen controls showed lower cell proliferation and mineralization.[52] Possibly these results could be employed in the design of novel collagen-based gels with predictable and controllable properties.[49]

1.3.2. Elastin-like polypeptides

As indicated above, elastin has important biological functions but is very difficult to be used in biomedical applications. Therefore, elastin-like polypeptides (ELPs) have been designed, inspired by natural elastin. These ELPs contain a pentapeptide repeat VPGXG, in which X can be any natural amino acid, except proline (**Figure 1.4**).[53]

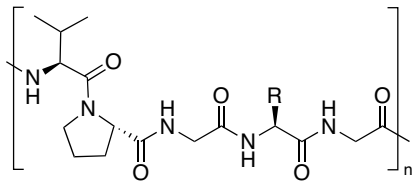

Figure 1.4. The ELP pentapeptide repeat VPGXG. Residue X can be every natural amino acid, except proline.

The gelation behaviour of ELPs is temperature-dependent. At low temperatures, the hydrophobic residues are surrounded by ordered water from hydrophobic hydration, resulting in a soluble aqueous ELP. Above a certain transition temperature, the surrounding water becomes less-ordered and bulky, leading to the collapse of the polymer. This gives rise to folding and self-assembly of the ELP, hence gelation occurs.[54] The stimulus responsive behaviour of ELPs has extensively been described by the Chilkoti and the Urry groups.[55-58]

Since the immune system does not differentiate between ELPs and natural elastin, these materials hold great promise as drug deliverers or in tissue engineering. Additionally, the degradation products of ELPs only contain natural amino acids, making them perfectly biocompatible. Poly(VPAVG) is a member of the elastin-like polymers, in which the central glycine has been replaced by an alanine. Poly(VPAVG) shows a similar self-assembly process. It has been studied

whether poly(VPAVG) is suitable as carrier for the delivery of bone morphogenetic proteins (BMPs). These BMPs are responsible for triggering the differentiation of stem cells during bone formation. BMP-2 and BMP-14 were successfully released from the elastin-like polymers and proved to increase the mineralization of C2C12 cells. Poly(VPAVG) thus has potential to be used in tissue engineering applications in bone.[53]

Apart from changes in temperature, the ordering of ELPs into hydrogels can also be initiated by performing chemical cross-linking. A variety of cross-linking strategies is known, but in order to use the ELPs for tissue engineering, the choice is limited. Many methods cannot be used because the cross-linking reagents are toxic to cells. Cross-linking reactions that require organic solvents are also not suitable, since this eliminates the possibility of encapsulating cells before cross-linking.[56] Lim et al. therefore developed a new cross-linking strategy for ELPs.[59] Lysine-containing ELPs in aqueous solution were reacted with the amine reactive cross-linker β[tris(hydroxymethyl) phosphino] propionic acid (THPP), resulting in the rapid formation of hydrogels (**Figure 1.5**). The mechanical properties of the cross-linked ELP gels can be controlled by the number of lysine residues and by the pH at which the cross-linking reaction takes place. Cell viability studies after encapsulation of mouse fibroblasts in these ELP hydrogels revealed that cross-linking with THPP is not cytotoxic.[59]

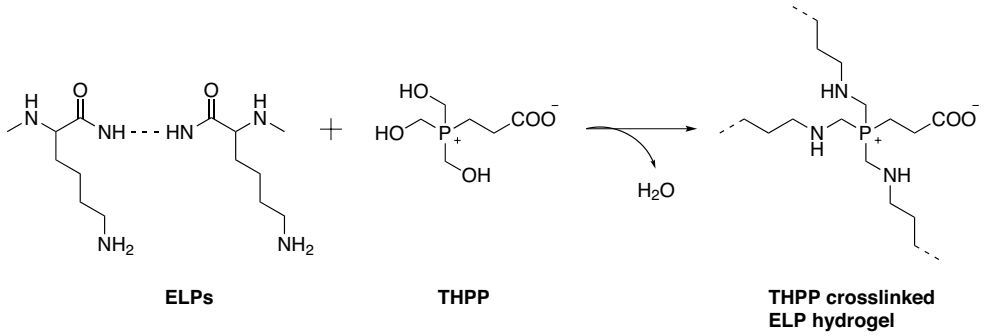

Figure 1.5. Hydrogel formation by the cross-linking between the ELP Lys-residues and THPP.

The THPP cross-linking strategy has been used by Nettles et al. to develop an ELP hydrogel for repair of the cartilage matrix in goats.[60] For this purpose, the knees of goats with osteochondral defects were filled by injecting the THPP-cross-linked ELP gel. After 3 months, a significant increase in integration was observed for the ELP filled knees, compared to the unfilled knees. However, after 6 months this increase was not maintained, due to degradation of the ELP-hydrogel. Optimizations of these hydrogels should make them useful for long-term benefits in cartilage repair applications.[60] Lim et al. further optimized ELP gels for biological applications.[61] ELP triblock copolymers were synthesized with an ABA structure. The central B-block was hydrophilic and surrounded by hydrophobic cross-linkable A domains. Gel formation occurred

rapidly with THPP as cross-linking agent. It was shown that the presence of the non-cross-linkable B block and the variation of its length influenced the swelling, structure and mechanical properties of the gels. Cell viability of fibroblasts was also proven; it was actually found that the ELP triblock copolymers led to a greater cell proliferation than a monoblock ELP hydrogel (containing only the A block). Since the mechanical properties of ELP hydrogels can be tuned, gels can be designed in such a way that they support cell viability and that they are suitable for tissue repair applications.[61]

Another chemical cross-linking method used in combination with ELPs is the formation of disulfide linkages. Asai et al. used this method to form hydrogels via intramolecular disulfide cross-links between cysteine containing ELPs. Hydrogen peroxide (0.3%) was used to accelerate the gelation process, leading to gels formed within 2.5 min.[62] Cysteine containing ELPs were also used by the Chaikof group for functionalization with an RGD peptide utilizing maleimide-thiol chemistry.[63] The properties of ELPs can furthermore be modified with chemical cross-linkers. Genipin, glutaraldehyde and disulfide formation can all be used to cross-link ELP polymer films. Varying the cross-linking method and strategy enables tailoring of mechanical and physical properties as well as drug release profiles of ELP hydrogels.[64] The porous ELP materials offer space for transplanted cells to grow in, to generate their own extracellular matrix. Rodríguez-Cabello and co-workers developed a method to synthesize macroporous ELP hydrogels as polymeric scaffolds, because they anticipated that materials containing $(VPGIG)_n$ would display elastin-like properties such as elasticity and biocompatibility.[65] Some lysine residues were incorporated in the elastin blocks for cross-linking purposes. The second block contained the cell adhesive motive REDV, specific for endothelial cells. The final block consisted of a hexapeptide sequence for elastase-proteolytic action. Cross-linking of this ELP triblock material was performed using a so-called salt-leaching/gas-foaming technique, in which the amount of salt and the particle size control porosity and pore size of the material. This technique allowed the authors to prepare macroporous ELP hydrogels with tuneable pore size. It was found that HUVEC cells were present both on the surface and in the inner layers of the ELP hydrogel, showing that this type of ELP hydrogels indeed has potential for use as an artificial extracellular matrix.[65]

1.3.3. Silk-like polypeptides

Schacht et al. examined hydrogels made from β-sheet forming silk proteins.[66] To this purpose, a spider silk protein called eADF4 (C16) was produced, consisting of 16 repeats of molecule C. Its sequence is GSSAAAAAAAASGPGGYGPENQGPSGPGGYGPGGP and mimics the silk protein ADF4 of the garden cross spider. Hydrogelation of the eADF4 (C16) protein took place at increasing concentration, invoked by dialysis. Gelation occurred via the transition of random coil conformations and α-helices into β-sheets. In order to increase the stability, the hydrogels

that formed were chemically cross-linked. The tyrosine residue side chains of the eADF4 (C16) protein were connected using ammonium peroxodisulfate and tris(2,2'-bipyridyl)dichloro-ruthenium(II). The cross-linking resulted in a higher mechanical strength for the hydrogels. The mechanical properties of the eADF4 (C16) hydrogels were furthermore influenced by addition of fluorescein. This interfered with the assembly into β-sheets resulting in less stable gels.[66]

1.3.4. Silk-elastin-like polypeptides

Silk-elastin-like polypeptides (SELPs) are composed of elastin-like and silk-like peptide components. The silk-like blocks provide chemical and thermal stability, since they have the ability to form hydrogen-bonded β-sheet crystals. The degree of crystallization is reduced by the elastin-like blocks, thereby introducing flexibility and aqueous solubility to the SELPs. These silk-elastin-like materials are liquid at room temperature, but form gels at elevated temperature. It appeared that the gel formation was caused by the crystallization of the silk-like components. This hypothesis was tested by the addition of urea, which prevents the formation of hydrogen bonding. Gelation was indeed not observed, since the silk-like blocks were unable to form the hydrogen-bonded β-sheet crystals. The addition of seed crystals enhanced the rate of gelation, further proving that the crystal formation of the silk-like blocks is responsible for the gelation. In a further study, the gelation of SELPs was found to be a two-step process. In the first step, it indeed is the hydrogen bonding between the silk blocks which causes spontaneous self-assembly. In this first step, micellar-like particles are formed. In the second step, the SELP molecules are ordered by hydrophobic interactions between the elastin blocks, leading to hydrogel or nanoparticle formation. [67-69] The ratio of elastin-like and silk-like components can be varied, as well as the block lengths and the sequence. This influences the biological, physicochemical and material properties of the formed hydrogels.[67] Successful diffusion out of the SELP hydrogels was demonstrated for small molecules like vitamin B_{12}, cytochrome c and theophylline[70], for DNA[71] and for adenoviruses.[72] This shows that SELP hydrogels are already applied as biomaterials. Since their gelation is dependent on both elastin-like and silk-like proteins, a high level of control is possible. This makes SELP hydrogels very suitable for more applications in the controlled release of therapeutics.

By introducing stimulus sensitivity, more applications of SELPs are foreseen, including use as sensors and drug delivery devices. Nagarsekar et al. synthesized protein polymers, aiming for pH and temperature sensitivity.[73,74] These SELPs were composed of repeating silk-like (GAGAGS) and elastin-like (VPGVG) sequences. The general structure of the synthesized SELPs is $[(\text{Gly-Val-Gly-Val-Pro})_4\text{-Gly-X-Gly-Val-Pro-}(\text{Gly-Val-Gly-Val-Pro})_4\text{-Gly-Ala-Gly-Ala-Gly-Ser}]_{11}$, in which residue X can be either glutamic acid or valine. A transition from a solution state to a turbid state was observed for these protein polymers upon increasing temperature. Increasing ionic strength leads to less hydration of the polymer by water molecules, meaning that precipitation

of the polymer occurs at lower temperatures. Furthermore, a decrease in transition values was also shown with increasing protein polymer concentrations. Altogether, these results show that mutations of neutral into ionic residues and changes in polymer length, gives the possibility to control the sensitivity of SELPs towards pH, temperature and ionic strength.[73,74]

1.3.5. Hydrogels based on a coiled-coil motif

A natural way of self-assembly of biological systems is the formation of an α-helical coiled-coil. Most of these coiled-coil sequences contain the characteristic heptad repeat abcdefg, with hydrophobic residues at positions a and d and with charged amino acids usually located at positions e and g (**Figure 1.6**). These peptides form a helical conformation, with the hydrophobic amino acids located at one side of the helix. The hydrophobic interhelical interfaces thus obtained, promote the aggregation into coiled-coil dimers. These aggregates are stabilized by the pH-dependent interactions between the charged residues.[75] In the Woolfson group, two 28-residue peptides were designed to yield hydrogel materials. To ensure the formation of coiled-coil dimers, each peptide contained heptad repeats with isoleucines at position a and leucines at position d. To form a dimer with sticky ends, oppositely charged glutamate and lysine residues were placed on positions e and g. The complementary sticky ends promoted the assembly of the two peptides in α-helical coiled-coil fibrils.[76]

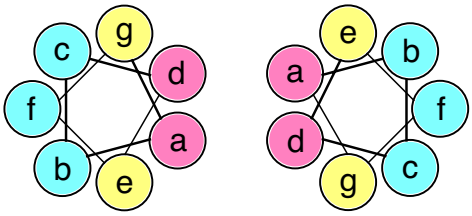

Figure 1.6. The coiled-coil dimer based on the heptad repeat (abcdefg). Positions a and d are usually occupied by hydrophobic amino acids, whereas charged residues are often found at positions e and g. The residues located at positions b, c and f are exposed on the surface of the coiled coil.

By choosing the right amino acids for position b, c and f, the interactions between the fibres might increase, resulting in a further assembly into hydrogels. It was chosen to make combinations of alanine and glutamine, since alanine can enhance the weak hydrophobic interactions between the fibrils and glutamine has the tendency to make hydrogen bonds. The constructs containing three alanines and the one with three glutamines on positions b,c and f were shown to form a gel. The possibility to use the three alanine- containing hydrogels as a substrate for cell growth was tested using rat adrenal pheochromocytoma cells. It was shown that the two peptide component hydrogel supports cell differentiation and cell growth.[77]

In another study, the coiled-coil domain of the cartilage oligomeric matrix protein was used to design hydrogels. This polypeptide is able to self-assemble into pentamers. After functionalization

with a cysteine residue, linkage to polymer PEGDA was performed using a Michael-type addition reaction. These polypeptide-polymers formed hydrogels upon exposure with UV-light. Fibroblasts encapsulated in the hydrogels showed spreading and migration, making these materials suitable for tissue engineering applications.[78]

The Tirrell group studied a protein containing six heptad repeats to make up a leucine zipper helix.[75] The design of the peptide was based on the sequence of the *Jun* oncogene product and on a database containing naturally occurring coiled-coil proteins. A triblock copolymer was designed with the leucine zipper domains flanking the central polyelectrolyte domain. This central region was based on the Ala-Gly-rich sequence $[(AG)_3PEG]_{10}$ and was water soluble. The triblock copolymer formed a switchable hydrogel. Gelation was lost at pH values above 9.5 and at temperatures above 55°C, due to dissociation of the coiled-coil domains. The biosynthetic approach allowed controlling the characteristics of both the leucine zipper domains and the polyelectrolyte region. This gives the possibility to design hydrogels with specific features, aiming at the controlled release of therapeutics.[75]

Another series of triblock polypeptides were designed by Xu and co-workers based on the coiled-coil domain.[79] Polypeptides ABA, CBA, ABC and CBC all contained two terminal coiled-coil motifs, A and C. The sequence of block A was $(VSSLESK)_6$ and the C block sequence was $(VSSLESK)_2$-VSKLESK-KSKLESK-VSKLESK-VSSLESK. Block C was obtained by changing one valine and three serine residues from block A in lysine residues. The central B block was the water-soluble random coil polyelectrolyte segment $[(AG)_3PEG]_{10}$. The balance between oligomerisation of blocks A and C and the swelling of block B should result in self-assembly of the triblocks. The thermal stability of the four triblocks was measured. The difference between the constructs containing block C, is the presence of four more lysine residues compared to block A. The introduced lysine amino acids disrupted hydrophobic interactions and introduced electrostatic repulsive forces. As a consequence, the thermal stability decreased, resulting in a lower temperature needed for coiled coil association. Triblock CBC indeed gave the lowest temperature (45°C) for unfolding of the polymer, whereas ABA was thermally stable even at temperatures as high as 95°C. All four constructs formed viscoelastic hydrogels at sufficiently high concentrations. The concentration to obtain elastic gels was the lowest for triblock CBC. When the same concentration range was taken for all constructs, it was found that the solution of ABA only contained monomers and dimers. In contrast, dimer to tetramer association was shown for triblock CBC. This explains why lower concentrations of CBC already form gels and furthermore indicates that gelation is related to the association of the coiled coil blocks. The triblocks were also shown to be pH sensitive. Finally, the reversibility of secondary structure formation was tested for polymer CBC. Addition of denaturant GdnHCl resulted in unfolding of the α-helical structure. After removal of the denaturant, the polymer folded back to its

original structure and hydrogels were formed again. Since these triblocks are stimuli responsive and hydrogelation is reversible, applications in the biomedical field are foreseen.[79]

In contrast to these examples where the coiled-coil motif was essential for hydrogel formation, Mehl et al. designed a protein hydrogel not forming a coiled-coil. This gel was based on the four-helix bundle of the *E. coli* protein GrpE. This protein contained an amphipathic helix at each end and a random coil as the middle domain. The domain in between these two was an α-helix, not able to form a coiled coil structure. The amphipathic helices of the protein dimer were able to form a four-helix bundle. Instead of coiled-coil driven gelation, hydrogels were formed by simple hydrophilic and hydrophobic interactions forming the four-helix bundle.[80]

1.3.6. Two-component hydrogels

Two-component protein-engineered hydrogels have been designed by the Heilshorn group.[81] For the synthesis of the two components, two protein association domains were chosen. The first was domain WW, consisting of conserved tryptophan residues. This WW domain is known to fold into antiparallel β-sheets. Secondly, a proline-rich protein domain was chosen. The first component consisted of multiple WW domains, linked together by hydrophilic spacers containing the cell adhesion motif RGDS. These spacers were designed to introduce flexibility and biofunctionality. The second component contained the proline-rich proteins, also linked by hydrophilic spacers. Upon mixing of the two components, physical cross-linking occurred, leading to the formation of a hydrogel. This type of material is therefore called a mixing-induced two-component hydrogel (MITCH). The viscoelasticity of the hydrogels can be altered, by adjusting the binding strength between the two domains and by changing the frequency of the repeated domains per component. This type of gels could be advantageous for use in the encapsulation of cells and proteins. Since gelation is not induced upon a change in temperature, pH or ionic strength, these cells and proteins can be kept under constant physiological conditions. The three cell types PC-12, HUVEC and NSC were encapsulated in these hydrogels. In all cases, the cells were distributed throughout the gels and were highly viable. Moreover, the two-component hydrogels showed complete self-healing after shear-thinning and can thus be useful as injectable materials for clinical use.[81] In a follow-up study, the proline-rich protein was linked to 8-armed PEG. Upon mixing with the WW domain, a MITCH-PEG construct was obtained. In this way, multiple weak interactions were combined to get a stronger binding. This system allows altering the cross-linking density of hydrogels both by changing the PEG content as well as by peptide avidity. When endothelial cells were cultured in the MITCH-PEG hydrogels, a well-spread morphology was found.[82]

Two-component hydrogels were also investigated by Kiick et al.[83] In their research, a PEG star polymer was modified with heparin (PEG-LMWH), since this is known to sequester and stabilize growth factors. The second component consisted of the heparin-binding growth factor VEGF. Hydrogels were formed by mixing the PEG-LMWH and the VEGF component in phosphate buffered saline. Gelation was induced by the effective cross-linking between VEGF and LMWH. VEGF-receptors were shown to selectively remove VEGF, which thereby causes gel erosion (**Figure 1.7**). These results demonstrate that therapeutically relevant growth factors can be used as cross-linkers in hydrogel formation and can afterwards selectively be released in the body upon action of receptors.[83] Another two-component hydrogel with heparin was studied by Wieduwild and co-workers. Star-PEG was functionalized with several heparin-binding peptide motifs. These peptides form α-helices upon interaction with heparin, leading to assembly and thus hydrogel formation. The peptide-star-PEG / heparin hydrogels could encapsulate cells which remained metabolically active.[84]

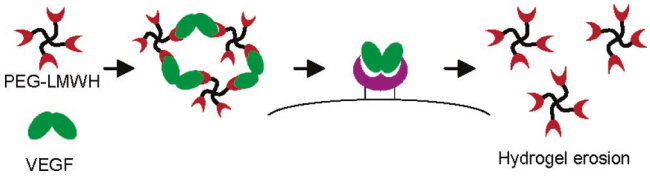

Figure 1.7. The two-component hydrogel PEG-LMWH/VEGF and the receptor-mediated gel erosion. Reproduced with permission from ref 83.[83]

1.4. Oligopeptides

1.4.1. Hydrogels based on β-sheet forming peptides

Another type of hydrogels is based on the β-sheet motif of peptides. The peptides used to make this type of hydrogels are designed to be soluble in aqueous solutions, displaying a random coil conformation. Only after addition of an external stimulus, the peptides form a β-hairpin conformation. After rapid self-assembly, a cross-linked, β-sheet rich hydrogel is obtained. External stimuli used to induce gel formation include heat, light and changes in pH or ionic strength.[85] In the Messersmith group, the 16 residues containing peptide $(FEFEFKFK)_2$ (FEK16) was studied.[86] This peptide consists of alternating hydrophilic and hydrophobic amino acids and is able to self-assemble into β-sheet structures. The self-assembly was induced by the addition of salts. This resulted in shielding of the repulsive electrostatic interactions, thereby favouring attractive hydrophobic and Van der Waals forces. Peptide FEK16 is fully soluble in water and was shown to form β-sheets when the salts NaCl, $CaCl_2$ and KCl were added in mM concentrations. It was investigated whether this assembly could be triggered by the addition of stimuli-responsive liposomes. Both temperature- and light-sensitive liposomes containing $CaCl_2$ were prepared

and added to a FEK16 solution. $CaCl_2$ was released after applying the thermal or photochemical trigger, resulting in the formation of highly cross-linked β-sheet hydrogels. This peptide hydrogel was suggested to have potential in drug delivery, tissue engineering and wound healing.[86]

In the Schneider and Pochan groups, the 20 amino acid containing peptide MAX1 was synthesized.[87] This peptide (VKVKVKVK-V^{D}PPT-KVKVKVKV-NH_2) contains a tetra-peptide surrounded by hydrophobic valine and hydrophilic lysine residues. MAX1 formed an amphiphilic β-hairpin at high pH (9.0) or after addition of salt at physiological pH. Addition of the cell culture growth media DMEM (Dulbecco's Modified Eagle Medium) to the aqueous peptide solution resulted in β-hairpin folding, followed by self-assembly into a gel (**Figure 1.8**). Studies performed on model fibroblasts revealed that MAX1 hydrogels are cytocompatible and maintain their rigidity during cell proliferation.[87]

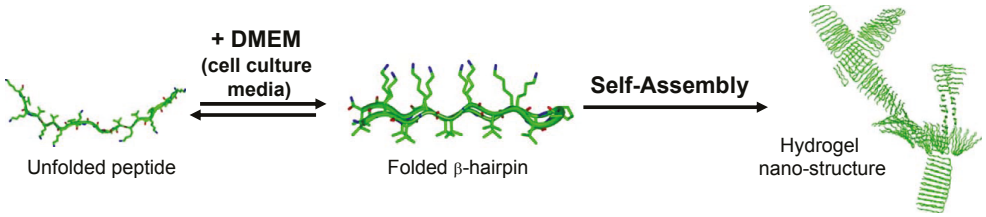

Figure 1.8. Hydrogelation of the MAX1 peptide. Addition of cell culture medium results in folding of the peptide in a β-hairpin, followed by self-assembly into a gel. Reproduced with permission from ref 87.[87]

The same researchers also synthesized peptide MAX8, in which one lysine was replaced by a glutamic acid (VKVKVKVK-V^{D}PPT-KV<u>E</u>VKVKV-NH_2). This lowered the overall positive charge of the peptide, which should make folding and self-assembly faster in the same cell culture conditions. It was indeed shown that the MAX8 hydrogel was formed faster than MAX1, thereby maintaining the way of folding and self-assembly. The MAX8 hydrogels were used for the encapsulation of C3H10t1/2 mesenchymal stem cells, resulting in a homogeneous distribution. To be able to deliver the gel-cell constructs by syringe, the gels must show shear-thinning behaviour. The MAX8 hydrogel became a low-viscosity gel after shear stress was applied. When the stress was no longer applied, the gel quickly recovered its initial rigidity. These properties make MAX8 hydrogels useful for the delivery of cells in tissue-regeneration applications.[85] MAX8 hydrogels are more rigid and contain more cross-links than MAX1 gels, leading to smaller mesh sizes. Dextran macromolecules and protein probes encapsulated in the MAX gels were released in rates varying from days till a month. Fastest release rates were recorded for MAX1, due to the larger mesh size.[88] An additional study further demonstrated that electrostatic interactions have an influence on the release rate. Positively charged proteins encapsulated in the MAX8 hydrogel experience repulsive electrostatic interactions, which enhanced the protein release

from the gel. On the other hand, less than 10% of the initially loaded amount of negatively charged proteins is released from these gels. Since the peptide hydrogel is positively charged, the strong attraction with the negatively charged proteins reduces the release.[89] Furthermore, electrostatic interactions are also known to play a role in cell adhesion, cell viability and cell proliferation. Therefore, the MAX8 alternative HLT2 was designed, with a lower overall charge state (+5 compared to +7) and thus a less electropositive character. These constructs showed comparable gel formation and could both be used for cell encapsulation and syringe delivery of cells. However, when primary bovine chondrocytes were encapsulated, the less electropositive HLT2 showed higher cell viability and better supported maintenance of morphology.[90] Further research on MAX1 and the more hydrophobic analogue MAX35 focussed on the lytic behaviour. Both constructs bound to negatively charged liposomes and induced release of their content by pore formation.[91]

1.4.2. Short aromatic peptides

Short aromatic peptide derivatives also have the ability to form hydrogels.[92,93] Dipeptides protected with the fluorenylmethoxycarbonyl (Fmoc) group can self-assemble through the formation of hydrogen bonds and π-π interactions. The latter involves the attractions between the π-electrons in the aromatic fluorenyl rings of Fmoc. The gel formation of dipeptide Fmoc-Phe_2 was tested, by dissolving the peptide in a basic solution (pH > 8.0). The drop wise addition of hydrochloric acid, to lower the pH, resulted in gel formation (**Figure 1.9**).[94] Gelation of the dipeptide was also possible in cell culture medium DMEM. Fmoc-Phe_2 dipeptides were also mixed in a 1:1 ratio with Fmoc-Ser, Fmoc-Lys and Fmoc-Asp. All four resulting hydrogels were shown to support the viability of chondrocytes. Cell viability of human dermal fibroblasts was increased by the Fmoc-Phe_2/Ser and Fmoc-Phe_2/Asp gels. The Fmoc-Phe_2/Ser gels furthermore also supported viability of 3T3 fibroblasts and retention of cell morphology of chondrocytes.[95] In another study, the effect of Fmoc-Phe_2 and Fmoc-RGD gels on dermal fibroblasts was further investigated. The fibroblasts were encapsulated in a gel containing both Fmoc-Phe_2 and Fmoc-RGD. Adhesion of the fibroblasts was promoted and cell spreading was observed, through specific binding of the RGD-motif to integrins. These results show that short aromatic peptide derivatives might be used as scaffolds for *in vitro* tissue regeneration.[96] Inspired by the results obtained for the natural amino acid phenylalanine, a short peptide sequence containing the non-proteinogenic amino acid taurine was developed. This motif also proved to be a hydrogelator, resulting in gels containing up to 98% water.[97]

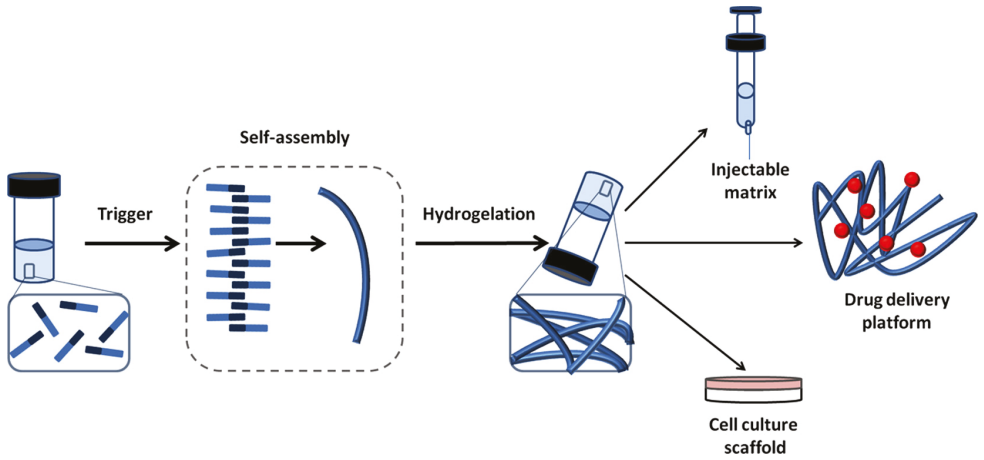

Figure 1.9. Hydrogelation of short aromatic peptides. Upon applying an external trigger, the peptides associate with each other, leading to self-assembly into hydrogels. Adapted from ref. 92.[92]

The gelation of short peptide sequences was further investigated by utilizing different aromatic capping groups. Peptide sequence Gly-Phe-Phe-Tyr was capped with naphthalene, phenothiazine, benzyloxycarbonyl (Cbz) and with Fmoc. All constructs formed nanofibres, which entangled with each other to form the hydrogel network. The peptide with capping group phenothiazine was the most efficient gelator, as it already could form hydrogels at a very low concentration (0.01 wt%).[98] Analogous to this, pyrene and Fmoc were used as capping group for tyrosine-leucine hydrogelators. Both constructs were assembled and co-assembled with serine surfactants, also capped with both pyrene and Fmoc. This allows variation in peptide and aromatic content. In all cases self-assembly behaviour was found, caused by aromatic interactions as wells as by β-sheet-type arrangements.[99] In another research, the Phe-Phe sequence was capped with indole, resulting in gels with a high storage modulus.[100] Constructs with only one amino acid were also able to form hydrogels, for example Fmoc-Phe-OH[101,102] and Fmoc-Tyr-OH.[102] Even without the Fmoc group, but with the aromatic pyrene moiety as capping group, gelation of the single amino acid Phe was possible.[103]

1.4.3. Peptide amphiphiles

An important driving force for self-assembly is amphiphilicity. There are three types of amphiphilic peptides distinguished in literature.[104] One type of peptide-amphiphiles is composed of a hydrophobic aliphatic tail and a hydrophilic peptide sequence, linked to each other via an amide bond. Amphiphiles have the ability to self-assemble in aqueous solution, in such a way that the hydrophilic domains are exposed to the water, while the hydrophobic regions are hidden from the aqueous environment. Amphiphiles can self-assemble in several organizations, including spheres, rods, disks, channels and sheets. With the introduction of peptide elements

in amphiphilic molecules, chemical functionalities can be introduced. Peptide amphiphiles often self-assemble in cylindrical micelles, called nanofibres. The core of these nanofibres is formed by the aliphatic tail, while the peptide sequence is displayed on the outer surface. This self-assembly can be controlled by adjustment of the pH or by addition of divalent cations such as Ca^{2+} and Mg^{2+}. When the peptide-amphiphile concentration is sufficient, the nanofibres further assemble into a gel.[15,105] Since the pioneering work of Stupp et al., peptide amphiphile nanofibre gels have been applied in the field of tissue engineering.[106] One example is the use of peptide-amphiphiles containing the cell adhesion motif RGDS. These constructs were tested as scaffolds for the delivery of bone marrow derived stem and progenitor cells. *In vitro* tests showed that the cells are viable and proliferative. *In vivo* tests revealed an increase in the relative bioluminescent signal intensity coming from viable cells, indicating cell proliferation. Furthermore, the nanofibre gel showed only a mild tissue reaction, suggesting biocompatibility and biodegradability of the peptide amphiphiles. These results demonstrate the use of peptide-amphiphiles as injectable materials for bone marrow cell therapies.[107]

Another application of peptide-amphiphiles has been demonstrated by the Kokkoli group.[108] They developed a fibronectin-mimetic peptide amphiphile containing the peptide sequences GRGDSP and PHSRN. The sequence GRGDSP contains the tripeptide RGD, which is naturally present in the cell binding domain of natural extracellular matrix (ECM) proteins, like fibronectin. Peptide sequence PHSRN was incorporated to enhance the activity and specificity of the fibronectin-mimetic. These two peptide domains were connected by a linker to mimic the natural distance between the respective domains and the overall hydrophobicity/hydrophilicity. The thus designed PR_b peptide [KSSPHSRN$(SG)_5$RGDSP] was linked to a C_{16} double hydrocarbon tail, to form the peptide-amphiphile.[108] This construct showed excellent cell adhesion properties compared to other fibronectin-mimetic peptides, but was unable to form hydrogels.[108,109] For this purpose, peptide PR_g [GGGSSPHSRN$(SG)_5$RGDSP] was synthesized, containing the spacer GGGSS. In contrast to KSS, this spacer was able to promote nanofibre formation. Peptide-amphiphiles were created by linkage of peptide PR_g to a C_{16} hydrocarbon tail. The PR_g construct self-assembled into nanofibres, followed by a further aggregation into hydrogels. In order to test their biological properties, HUVECs (human umbilical vein endothelial cells) were adhered on the surface on the gels. A comparison with PEG gels, fibronectin-functionalized PEG and commercially available peptide hydrogels (PuraMatrix) showed that PR_g hydrogels support cell adhesion and proliferation and thereby outperforms the comparison gels. Peptide-amphiphile nanofibre hydrogels are therefore promising as ECM mimetic scaffolds in tissue engineering.[109]

Several small peptides have been synthesized by the Zhang group as another kind of amphiphilic biomaterials.[110] These peptides contain alternating hydrophobic and hydrophilic amino acids. The charged residues used have an alternating positive or negative charge. Solutions of these

peptides in deionized water formed stable β-sheets. After exposure to electrolytes, self-assembly into nanofibres took place. These fibres further self-assembled into stable hydrogels. Peptide concentrations of 0.1-1% were sufficient for gelation to occur. Oligopeptide KLD-12 was synthesized, aiming for cartilage tissue repair (**Figure 1.10**).

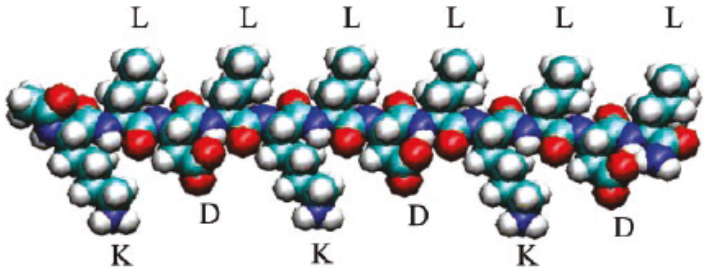

Figure 1.10. Oligopeptide KLD-12. The peptide contains alternating positive and negative charges, leading to the formation of ß-sheets and assembly into nanofibres and gels. Reproduced with permission from ref 110.[110]

An efficient encapsulation of chondrocytes into the hydrogels was achieved. It was shown that the chondrocytes were evenly distributed over the hydrogel and maintained a high cell viability (>80%). Furthermore, the chondrocytes retained their morphology. The peptide hydrogels formed a cartilage-like ECM, showing their potential as scaffold for cartilage tissue repair.[110] Apart from the chondrocytes, other cell interactions with these hydrogels have also been investigated, including osteoblasts,[111] neural cells[112] and endothelial cells.[113]

Another example of a small amphiphilic peptide for hydrogel formation was recently given by the Arosio group. Model peptide RADA 16-1 (RADARADARADARADA) was chosen as it is known to self-assemble into fibrils and higher ordered structures. The peptide first formed short rigid fibrils with a length of approximately 100 nm. Strong hydrophobic interactions led to the formation of longer fibrils and aggregates. At higher peptide concentrations hydrogels were formed, which were broken down upon dilution.[114]

Also peptide-based amphiphilic block copolymers have been designed for hydrogel formation. This category contains polymers prepared entirely from amino acids, as well as hybrid systems in which polypeptides are combined with synthetic polymers.[104] The hydrogelation of diblock copolypeptide amphiphiles was investigated by Deming and coworkers. One part of these amphiphiles was built up from the polyelectrolytes (poly-L-lysine) or poly(L-glutamate). Both of these polyelectrolytes are soluble in water and are highly charged at pH 7. The other part of the diblock amphiphiles contained the hydrophobic domains poly(L-leucine) or poly(L-valine), which adopt an α-helical or a β-sheet conformation, respectively. Rigid hydrogels were formed

at low concentrations of the diblock amphiphiles in water. These hydrogels were thermally stable, even at temperatures as high as 90°C. When the hydrophobic part was short in length, hydrogels could not be formed. This is caused by the fact that the peptides are unable to adopt their desired conformation. A slightly better gelation was found for amphiphiles with the α-helical conformation. Gelation was furthermore influenced by the balance between the hydrophobic and the hydrophilic blocks. The hydrophobic interactions need to be strong enough, to stop the swelling caused by the electrostatic repulsion in the polyelectrolyte part of the gel. The hydrogels were broken down by applying large-amplitude oscillations, to test their shear thinning behaviour. An 80-90% recovery of the mechanical strength was observed within the short time period of 10 s. A slower reorganization process then led to the complete recovery of hydrogel strength.[115] Several variations in the compositions of the diblock amphiphiles have been made, to optimize the hydrogel strength in ionic media. This type of hydrogels has shown to be stable in cell growth media, salt concentrations up to 0.5 M and in aqueous media of varying pH. These features, together with the ability to rapidly recover after shear thinning, make these hydrogels promising candidates in biomedical applications such as drug delivery and tissue regeneration.[116]

1.4.4. Multidomain peptides

Besides relatively simple peptide amphiphiles, coiled-coil and β-sheet forming peptides, also multidomain peptides have been designed to form gels. In these peptides, factors favouring assembly and factors disfavouring assembly are both present. Mostly, these multidomain peptides have an ABA structure. The central B domain contains both hydrophilic and hydrophobic amino acids, creating an amphiphile that has the ability to self-assemble. The A domains surrounding the B domain consist of charged residues, causing electrostatic repulsion at neutral pH, thereby working against the assembly. When these forces are properly balanced, multidomain peptides self-assemble into nanofibres and further into hydrogels. Several multidomain peptides have been synthesized and compared with respect to their ability to control gelation. Peptides containing the positively charged lysine in domain A, self-assemble in the presence of negatively charged ions such as phosphate. On the other hand, positively charged ions are required for gelation of peptides with glutamic acid in domain A. When hydrophilic glutamines in domain B were replaced for serines, a large increase in mechanical strength of the gels was obtained. More importantly, these serine-containing peptides were able to undergo shear-thinning and recovery of their mechanical strength after shear. Peptides containing both serine and cysteine residues in domain B showed a further increase in strength, due to the possibility to make cysteine disulfide bonds.[117] In a follow-up study, the aromatic residues phenylalanine, tryptophan and tyrosine were incorporated in domain B. All multidomain peptides retained their ability to form nanofibres, but the presence of aromatic residues influenced the ability to form hydrogels. Constructs containing the motif QFQL or QF in the B-block still formed good hydrogels, while

constructs with QW or QY only formed short fibres and therefore also poor hydrogels.[118] These results show that gelation of multidomain peptides can be controlled through changes in chemical functionalities.[117,118] As mentioned, an important goal in tissue engineering is to generate materials providing an ECM-like environment for cells. Matrix metalloproteinases (MMPs) are used by cells to degrade the matrix, so that it can be replaced by newly synthesized ECM proteins. With this in mind, a peptide was synthesized containing the MMP specific cleavage motif LRG in domain B and the adhesion motif RGD in one of the A domains. Compared to a multidomain peptide without these motifs, increased cell viability, cell spreading and an improved cell migration into the hydrogel was observed.[14]

Peptide-based photo-responsive hydrogels have been synthesized by Huang and co-workers.[119] Their materials contained an azobenzene moiety, which was used as a conformational switch. Upon UV-irradiation, a conformational change from (*E*) to (*Z*) took place, which changed the position of the phenylalanine residues and thereby led to less effective π-π stacking (**Figure 1.11**). The azobenzene moiety was coupled to the N-terminus of dipeptides using (*E*)-2-(4-(phenyldiazenyl)phenyl) acetic acid. Self-assembly of these azo-dipeptides was thought to occur via intermolecular π-π stacking of the phenyl rings from azobenzene and via hydrogen bonding of the peptides. A series of azo-dipeptides was synthesized. Constructs containing aromatic residues such as phenylalanine and tyrosine easily formed hydrogels. Poor gelation behaviour was observed for dipeptides with the cationic residues Arg and Lys. Insertion of phenylalanine or tyrosine into these dipeptides (azo-Arg-Ala, azo-Lys-Ala) facilitated gelation. Salt concentration and pH also had an effect on the hydrogelation behaviour. Azo-dipeptide hydrogels collapsed upon UV-irradiation, due to the expected less effective π-π stacking. The gel reformed after an average of two days under ambient visible light. To test the biological applications of these gels, vitamin B12 was trapped into azo-Gln-Phe-Ala. Release of B12 took more than two days, but was greatly enhanced upon UV-irradiation (4h).[119] Velema et al. incorporated the azobenzene moiety into the structure of dichromyl molecules. Upon triggering with light, these compounds self-assembled into fibres, resulting in gel formation. Another trigger for assembly was NaCl, addition of this salt enhanced aggregate formation.[120] Recently, constructs were synthesized containing an azobenzene motif, as well as alkyl chains and a polyether moiety. These constructs readily formed nanofibres in water and displayed multistimuli responsive behaviour. Apart from light, changes in temperature, pH and mechanical stress also initiated hydrogel formation.[121]

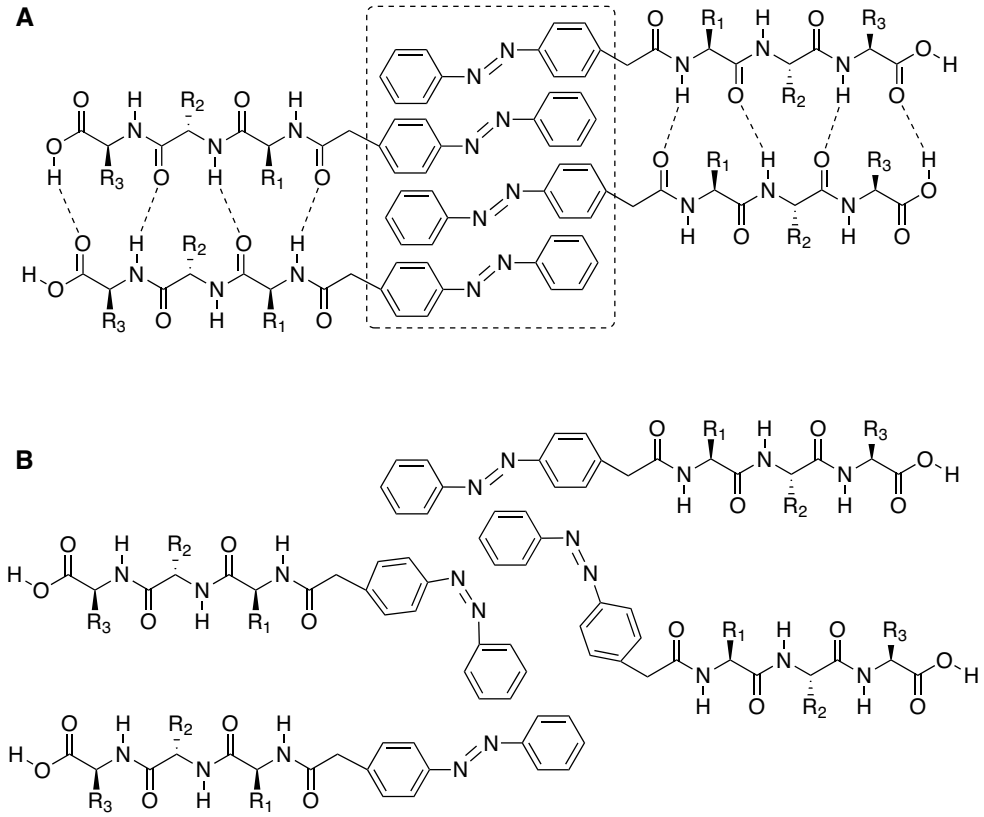

Figure 1.11. Balanced (A) and disturbed (B) interactions between the azo-dipeptides. Conformation A leads to the formation of hydrogels. Adapted from ref 119.[119]

1.5. Hybrid hydrogels with a polymeric scaffold

Poly(ethylene glycol) (PEG) has widely been used as a component in the synthesis of biomaterials. This polymer has good water solubility, lacks toxicity and has a low immunogenicity.[122] The conjugation of PEG to proteins, known as PEGylation, increases the protein solubility and stability. Immunogenicity caused by proteins is reduced by incorporation of the PEG polymer. PEGylation prevents receptor-mediated protein uptake by the reticuloendothelial system and avoids the rapid renal clearance of small proteins. Therefore, PEGylation can be used as a method to prolong the plasma half-life of proteins.[123] Furthermore, the PEG chain is flexible and is able to associate with water molecules.[124] Due to its interesting features, PEG has attracted much attention for use in biomedical applications. In 1990, this led to the first FDA approval of the PEG-based compound ADAGEN. This compound is used for the treatment of severe combined immunodeficiency disease.[125-127] Altogether, PEG is very suitable for use as basis in the design of hydrogels.

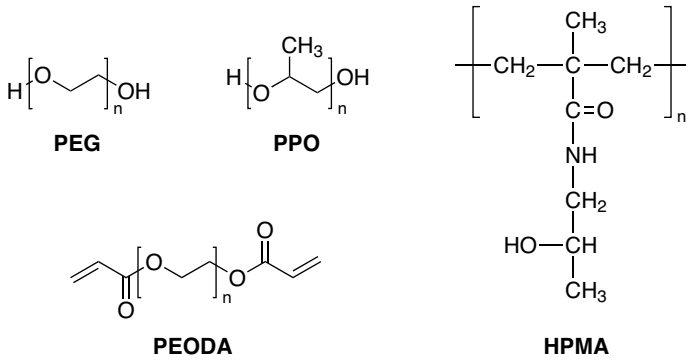

Figure 1.12. Structures of the commonly used polymeric scaffolds for hydrogel formation. In this thesis, the focus will be on poly(ethylene)glycol (PEG) based hydrogels, as this polymer has good water solubility, lacks toxicity, has low immunogenicity and is widely used for the preparation of hydrogels.

Apart from PEG, several other polymers can be used, including poly(propylene oxide) (PPO), poly(ethylene oxide) diacrylate (PEODA) and *N*-(2-hydroxypropyl)methacrylamide (HPMA) (**Figure 1.12**). This section will focus on peptide-based hydrogels with synthetic polymeric building blocks.

In the Kiick and Jia group, the synthetic polymer PEG was used in the synthesis of elastin-based hydrogels.[124] PEG was used to replace the dynamic, entropic peptide segments of elastin. In order to maintain the cross-linking properties of natural elastin, a peptide sequence was coupled to the polymer using copper (I) catalyzed azide-alkyne cycloaddition (aka 'click reaction'). For this purpose, PEG was functionalized with azides. Based on the hydrophilic cross-linking domains of elastin, peptide [X(AKAAAKA)$_2$X] was prepared. X stands for the non-natural amino acid L-propargylglycine, containing the desired alkyne functionality. The peptide-PEG multiblock contained three to five repeats of PEG and the peptide. A cross-linking procedure with hexamethylene diisocyanate was carried out to form urea linkages through the lysine side chains of the peptide domain (**Figure 1.13**).

Hydrogels were afforded, which showed softening behaviour after hydration, similar to natural elastin. In vitro toxicity studies with the soluble peptide-PEG product showed some toxicity to primary porcine vocal fold fibroblasts. After cross-linking, however, the hydrogel allowed fibroblasts to grow and proliferate, showing that the gel does not leach toxic impurities during cell culture. The elastin-based PEG-hydrogels are thus promising for use as elastomeric scaffolds in tissue engineering applications.[124] Further studies performed by the same researchers focused on a more straightforward approach to synthesize the (AKAAAKA)$_2$ containing hydrogels. For this purpose, PEG was replaced by Pluronics: a PEG- poly(propylene oxide) (PPO)-PEG block copolymer. This polymer self-assembles into micelles. To be able to couple the copolymer to

the peptide, a vinyl sulfone end group was incorporated in Pluronics. The lysine amines in the $(AKAAAKA)_2$ peptide showed a high reactivity towards vinyl sulfones, when deprotonated. The peptide and copolymer were coupled at a temperature of 60°C, under formation of stable, viscoelastic hydrogels.[128]

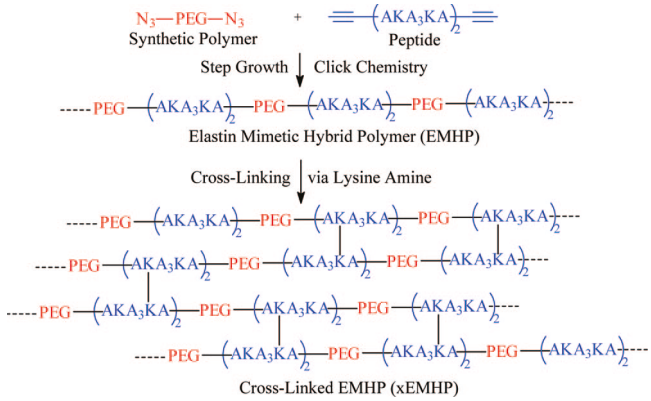

Figure 1.13. Synthesis of the elastin-based polymeric hydrogels. Adapted from ref 124.[124]

1.5.1. Collagen-based hydrogels with a polymeric scaffold

Lee et al. combined collagen with poly(ethylene glycol) (PEG) for tissue engineering applications.[129] In their study, poly(ethylene oxide) diacrylate (PEODA) was used. This compound polymerizes after exposure with UV light to form a cross-linked PEG gel. The collagen mimetic peptide (CMP) $(Pro–Hyp–Gly)_7$–Tyr was incorporated in the backbone of PEODA. The utility of these CMP/PEODA hydrogels as tissue engineering scaffolds was examined by the encapsulation of chondrocytes. Since the extracellular matrix of chondrocytes is mainly composed of fibrous type II collagen, the collagen content in the hydrogels was measured. A 103% increase in collagen content was observed compared to non-CMP containing hydrogels, showing that CMP enhanced the tissue production of encapsulated cells.[129]

1.5.2. Fibroin- and collagen-based hydrogels

Rizzi and co-workers developed a PEG-based material containing protein polymers to support tissue repair.[130,131] The monomers of the protein polymers were built up from several components. One of them was a 15-amino acid sequence based on human fibrinogen, containing a plasmin degradation site and the cell adhesion motif RGD. The second component was adopted from human collagen and was a matrix metalloproteinase (MMP) cleavage sequence. A block of negatively charged amino acids (glutamic acid) was also present, in order to improve the solubility of the protein. Finally, the end termini of the proteins contained cysteine residues, used as cross-linking sites for the linkage to PEG. The PEG molecule used was functionalized with

vinyl sulfone groups, able to react with the cysteine thiol groups. After polymerization of the protein monomers, the protein solution was mixed with the PEG solution, resulting in hydrogel formation.[130] Biochemical analysis revealed that the hydrogels promote cellular adhesion. The RGD motif proved to be responsible for this binding, since the mutant with the RGG sequence did not support cellular adhesion.[131] In another research, fibrinogen was PEGylated in order to prepare hydrogels by making use of free radical polymerization. These gels were implanted into segmental rat defects to promote new bone formation. After 5 weeks, histology and X-ray studies confirmed the formation of new bone tissue.[132,133]

1.5.3. Coiled coil based hydrogels

The coiled coil motif has been used by the Kopeček group as cross-links for synthetic polymers to create hybrid hydrogels.[134] A linear copolymer was synthesized by radical copolymerization of N-(2-hydroxypropyl)-methacrylamide (HPMA) and the metal-chelating monomer N-(N',N'-dicarboxymethylaminopropyl)-methacrylamide (DAMA). The produced polymer had iminodiacetate groups in its side-chains. Two His-tagged peptides (CC1 and CC2) containing the characteristic coiled-coil motif were also synthesized (**Figure 1.14**). Peptides CC1 and CC2 were separately mixed with the HPMA-DAMA polymer, in the presence of Ni^{2+}. The iminodiacetate groups formed complexes with Ni^{2+}, to which the histidines of the coiled-coil peptides were attached. This process leads to the formation of temperature-responsive hydrogels.[134,135]

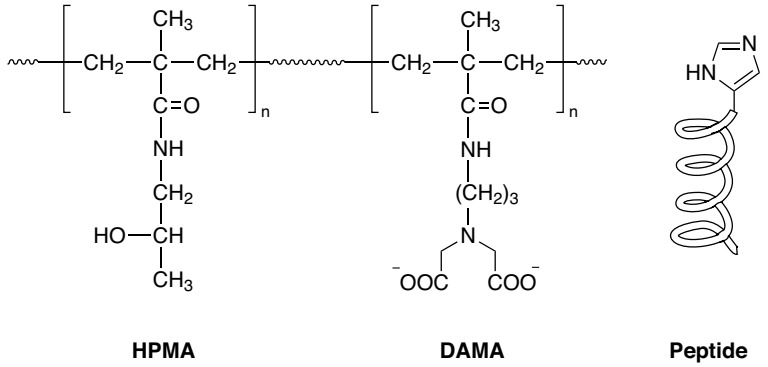

Figure 1.14. A schematic representation of the HPMA-DAMA copolymer and the His-tagged coiled-coil peptides. In the presence of Ni^{2+}, complexes with the iminodiacetate groups are formed, to which the His-tag is attached. This process leads to hydrogel formation.

Further research by the Kopeček group focussed on two pentaheptad peptides (CCE and CCK), that were grafted onto a maleimide-functionalized *N*-(2-hydroxypropyl) methacrylamide (HPMA) polymer.[136] It was found that the peptide should contain at least four heptad repeats to ascertain gelation of the HPMA-peptide copolymer.[137] The two peptides CCE and CCK were

built up from valine and leucine residues at positions a and d of the heptad repeat (**Figure 1.6**). The charged amino acid glutamic acid occupied positions e and g for CCE, while CCK contained lysine residues at these places. These oppositely charged peptides were designed, to act as cross-linkers in the hydrogel formation. In order to improve the solubility of the peptides, CCE contained a lysine residue at position f, whereas this was a glutamic acid for CCK. The uncharged amino acids serine and alanine occupied the remaining b and c positions. Both peptides were functionalized with the tetrapeptide Cys-Tyr-Gly-Gly on the N-terminus. The peptides were attached to HPMA via a thioether linkage formed between the N-terminal Cys and the maleimide groups of HPMA. Gelation was observed when solutions of CCE-HPMA and CCK-HPMA were mixed in a 1:1 ratio. Circular dichroism spectroscopy confirmed the formation of the expected two-stranded α-helical coiled-coil between CCE and CCK, which appeared to be reversible.[136] To investigate the role of the coiled-coil motif in the hydrogel formation, mutants of CCE and CCK were synthesized. In both mutants, a single amino acid modification resulted in a random coil conformation, showing the importance of the coiled-coil motif for gelation.[138]

A more native design using the coiled coil motif was described by Jing and co-workers.[139] The peptide used in their peptide-polymer system was based on the coiled-coil region of human fibrin. The solvent-exposed amino acids b, c and f of the heptad repeat were kept intact. Substitutions of the residues at positions a, d and g were made, in order to design a peptide that readily oligomerises. Their designed peptide $\gamma_{52\text{-}88}$KI was functionalized with a terminal cysteine residue, to conjugate it to maleimide-containing PEG and thereby create a PEG-peptide diblock and a peptide-PEG-peptide triblock. CD analysis showed that PEG did not influence the secondary structure, since both constructs still formed coiled-coils. The triblock formed transparent, elastic hydrogels, in contrast to the diblock which formed nonviscous solutions. This suggests that gelation occurs via the cross-linking of PEG by the coiled-coil motifs.[139] In a more recent study, the immunogenicity of these triblocks was investigated. Since these tests use mouse models, a new triblock was synthesized, in which the peptide (γ-KEI) was based on mouse fibrin rather than on human fibrin. The newly synthesized γ-KEI – PEG - γ-KEI triblock formed coiled-coil bundles as well as higher-order supramolecular structures such as 12-, 18-, 30- and 50-mers. This construct did not cause peptide-specific T-cell responses, which was shown by the absence of the cytokines IL-2 and interferon-gamma. The triblock provoked moderate antibody response in mice, while this was not observed for the native mouse fibrin peptide or γ-KEI. The question arises whether the measured moderate antibody response in mice influences the application of self-assembling materials for biomedical applications.[140]

1.5.4. β-sheet based hydrogels

Tzokova et al. used the oligomer PEO_7 functionalized with a terminal azide.[141] Tetraphenylalanine was coupled to 4-pentynoic acid in order to introduce an alkyne functionality. Click chemistry was then performed to obtain the peptide-polymer construct $mPEO_7$-Phe_4-OEt (**Figure 1.15**). Self-assembly of this diblock in water was not possible due to its low solubility. Instead water was added to solutions of the construct in THF to prepare a series of varying $mPEO_7$-Phe_4-OEt concentrations. After removal of THF by dialysis against water, viscous solutions were obtained at low polymer-peptide concentrations. At higher concentrations, transparent hydrogels were formed. After addition of water, π-π-stacking became dominant, providing a platform for self-assembly. The self-assembly was also driven by the formation of antiparallel β-sheets. The formed hydrogels were shown to be sufficiently strong to make biomedical applications possible.[141]

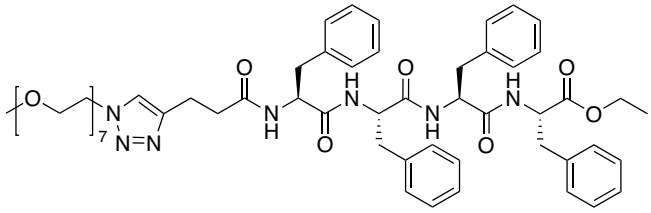

Figure 1.15. The $mPEO_7$-F4-OEt construct, in which click chemistry was used to link the peptide and the polymer. Self-assembly was triggered by addition of THF to aqueous solutions, after which dialysis resulted in transparent hydrogels.

In a further study, the effect of mPEO length on the self-assembly behaviour was investigated. Circular dichroism spectroscopy was used to measure the amount of π-π-stacking for constructs with mPEO molecular weights of 350, 1200 and 1800 Da. For the shortest mPEO length, some π-π-stacking was observed as well as β-sheet formation. For the largest mPEO-Phe_4-OEt construct, π-π-stacking was clearly dominant. This indicates that a longer polymer length disrupts the formation of the preferred β-sheet conformation of the peptide. The structures that were obtained for the mPEO-Phe_4-OEt constructs varied from nanotubes and fibres to micelles for the longer mPEO blocks. Apart from tetra-phenylalanine, tetra-valine was also clicked to the mPEO polymers of the three different lengths. For all these three mPEO-Val_4-OEt constructs, a mixture of β-sheets and random coils was observed. Valine is more hydrophobic than phenylalanine and has a great tendency to form β-sheets. These valine-containing diblocks formed wide, plank-like structures after dialysis. Due to the dominance of β-sheet formation, self-assembled structures were obtained that closely resemble those formed by the peptides alone. The length of the PEO polymer did not seem to influence this self-assembly behaviour. These results show that both the choice of peptides and the length of the polymer influences the self-assembly behaviour of these peptide-PEO constructs.[142] The β-sheet forming principle was also used by Castelletto and co-workers. Peptide DGRFFF was chosen as it has a β-sheet

secondary structure and contains the cell-binding motif RGD. This peptide was linked to PEG and at sufficiently high concentrations β-sheet aggregates were formed. Films of the peptide-polymer construct were prepared on tissue culture plate. Fibroblasts cultured on these films remained viable and showed cell proliferation.[143]

1.6. Chemical cross-linking methods

As described before, hydrogels retain their stability through cross-links between the polymeric constituents. These cross-links are chemical or physical in nature and prevent the uncontrolled dissolution of the polymer chains in an aqueous environment. Chemical cross-linking allows control over the cross-linking density, as well as over the final mechanical properties of the hydrogel. Numerous chemical cross-linking methods have been utilized for gel formation. Many of these methods are termed 'click' reactions. Requirements to be classified as click reaction are a near quantitative conversion, biological compatibility and limited by-products.[144] In the last part of this chapter, a number of prominent examples of chemical cross-linking methods for hydrogel formation are mentioned, all with PEG as the polymeric basis. Except for radical polymerization, they can all be classified as click reactions. For a more extensive overview of click reactions for hydrogel formation and other conjugates, one is referred to excellent recent reviews by Tang et al. and Jiang et al.[144,145]

1.6.1. Radical polymerization

Radical polymerization involves the formation of free radicals by means of UV-light, visible light, redox reactions or temperature. Photopolymerization is a type of radical polymerization that mainly uses UV light.[146] This chemistry was used by the Hubbell group for hydrogel formation using PEG as the central domain. PEG was modified with oligomeric α-hydroxy acid. After addition of a photoinitiator to the polymeric solution, UV irradiation resulted in the formation of hydrogels. These gels appeared to be useful for the controlled release of proteins.[147] In another research, redox initiated free radical polymerization was used to make photodegradable PEG-based gels. For this purpose, a photolabile nitrobenzyl ether-derived moiety was first linked to PDA (photodegradable acrylate). Hydrogels were formed after copolymerization of the photolabile acrylate to PEG. These hydrogels are degradable, as the PEG monomers are released upon irradiation. Complete degradation also releases the (poly)acrylate chains. Incorporation of cell-binding domain RGD allowed cell migration and differentiation.[148] A disadvantage of using radical polymerization for hydrogel formation is the presence of free radicals. These radicals can be transferred to proteins, which might lead to degradation or a reduced bioactivity.[146]

1.6.2. CuAAC

The Cu(I)-catalyzed azide-alkyne cycloaddition (CuAAC) as introduced by Meldal and Sharpless, is commonly known as the first click reaction (**Figure 1.16**). CuAAC has been widely used for many applications. A huge advantage of this chemistry is the orthogonality, since both the azide and alkyne are unreactive towards biological molecules.[149-151] Hydrogels were also prepared with CuAAC as cross-linking method. Azide-functionalized 4-armed PEG and diacetylene-functionalized PEG gave a well-defined hydrogel network upon catalysis by copper.[152] Enzyme degradable CuAAC hydrogels were also prepared by cross-linking 4-armed alkyne-functionalized PEG to a protease-sensitive bis-azido peptide.[153]

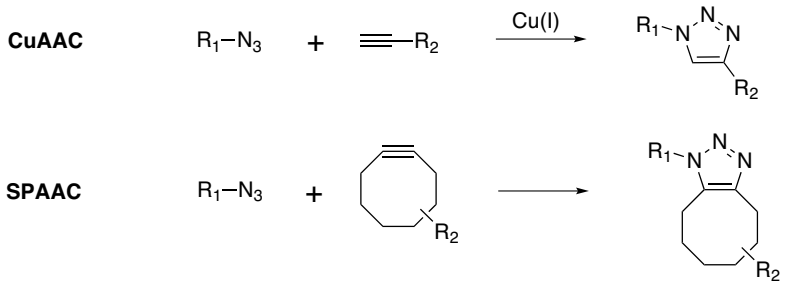

Figure 1.16. CuAAC and SPAAC reaction

1.6.3. SPAAC

A disadvantage of CuAAC as cross-linking method is the need of the heavy metal catalyst. This hampers its use for *in vivo* applications as copper is cytotoxic to both bacterial and mammalian cells. As a solution to this problem, ring strain was introduced to activate alkynes for their reaction with azides. This copper-free click chemistry between a ring-strained alkyne and azide is named SPAAC (strain-promoted azide-alkyne cycloaddition) (**Figure 1.16**). Except from being orthogonal and efficient, the SPAAC reaction can also be applied in living sytems.[154-156] The use of SPAAC for hydrogel formation was demonstrated by DeForest and coworkers, who cross-linked azide-functionalized star-shaped PEG to cyclooctyne-containing peptides. This peptide sequence was composed of an enzyme degradable motif, which allowed the cells to spread and migrate through the hydrogel material. High cell viability (>90% after 24h) was observed after encapsulating fibroblasts, showing the potential of SPAAC cross-linked gels for biological applications. Moreover, by incorporation of the orthogonal thiol-ene photochemistry, the gels could be used for 3D patterning of biological functionalities.[157] In other examples where SPAAC was utilized, high viability of human mesenchymal stem cells and bone marrow derived stromal cells was demonstrated.[158,159] The tethering and tunable release of drugs from SPAAC cross-linked PEG-gels has also been shown.[160] Furthermore, the incorporation of labile ester linkages near the SPAAC cross-links gave rise to controlled degradation of the hydrogels.[161]

1.6.4. Diels-Alder conjugation

Diels-Alder chemistry is the [4+2] cycloaddition between a diene and a dienophile (**Figure 1.17**). Since this reaction is highly accelerated in water and chemoselective, it is a useful cross-linking method for gelation.[162] Wei et al. demonstrated the formation of hydrogels using Diels-Alder by coupling poly(N,N-dimethylacrylamide-co-furfuryl methacrylate (dienes) to maleimide-functionalized PEG.[163] Nimmo et al. used the same chemistry to make hydrogels containing hyaluronic acid (HA), a natural polymer highly abundant in the extracellular matrix. HA was modified with furan groups and then cross-linked to bis-maleimide PEG. Hydrogels were formed with tuneable mechanical and degradation properties and were shown to be cytocompatible.[164] The inverse electron demand Diel-Alder reaction between tetrazines and norbornene was used by the Anseth group to make cytocompatible hydrogels (**Figure 1.17**). Cross-linking of 4-armed PEG tetrazine to an ECM mimetic cell degradable dinorbornene peptide quickly resulted in hydrogel formation. Gels were shown to be suitable for cellular encapsulation as human mesenchymal stem cells retained high cell viability after being encapsulated for 72 h.[165]

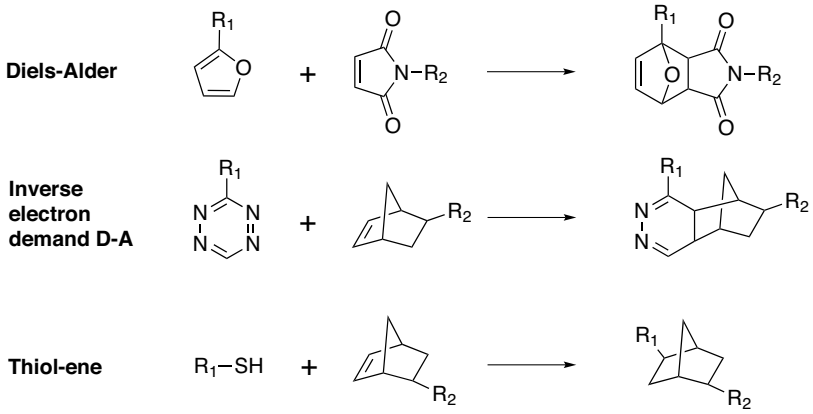

Figure 1.17. Diels-Alder and thiol-ene chemistry.

1.6.5. Thiol-ene chemistry

Thiol-ene chemistry is the reaction between a thiol and unsaturated functional groups such as alkenes or norbornene (**Figure 1.17**). The orthogonality as well as high efficiency of this coupling procedure makes it suitable for hydrogel formation.[151,166] Aimetti et al. showed that norbornene-functionalised four-armed PEG can form hydrogels with thiol-functionalised enzyme sensitive peptides (human neutrophil elastase) upon photo irradiation. The obtained hydrogels are degradable, which was shown through release of the model protein bovine serum albumin (BSA).[167] The thiol-norbornene photopolymerization was also utilized to make hydrogels with matrix metalloproteinase (MMP) or chymotrypsin degradable cross-

linkers. Human mesenchymal stem cells retained high cell viability upon encapsulation in these hydrogels.[168] In another example, pancreatic β-cells were encapsulated in the hydrogel network and could be regained via chymotrypsin-mediated gel erosion.[169] Further studies on hydrogels formed by thiol-ene chemistry revealed that degradation of the network is primarily caused by ester bond hydrolysis. Degradation was accelerated when network formation was less ideal, which allows tuning of the degradation process.[170]

1.6.6. Michael-type additions

Michael-type additions are widely used as cross-linking method for hydrogel formation (**Figure 1.18**). Vinyl sulfone functionalized multi-armed PEG was reacted with bis-cysteine peptides, yielding elastic hydrogels. When the RGD or MMP sequence was chosen as the peptide cross-linker, cell adhesive and degradation properties were introduced, respectively.[171] The same cross-linking approach was also used to incorporate resilin-like polypeptides to mimic the elastomeric properties of natural resilin. Fibroblasts encapsulated in the formed hydrogels remained viable, thereby making these resilin-functionalized gels promising in cardiovascular tissue engineering.[172] Another Michael-type addition is the reaction between a maleimide and a thiol moiety. Phelps and co-workers prepared a maleimide-functionalized 4-armed PEG molecule, which was reacted with a thiol-modified RGD-containing peptide. The resulting hydrogels were efficiently formed, even at low polymer concentrations.[173] Another type of Michael addition was recently reported between acrylate and amine groups. Eight-armed PEG molecules with acrylate end-groups were reacted with different amounts of cross-linker NH_3 to yield a range of hydrogels. The excess of the small ammonia cross-linker could easily be removed by evaporation. By changing the amounts of NH_3 the cross-linking density and thereby the final mechanical properties of the gels could be tuned.[174]

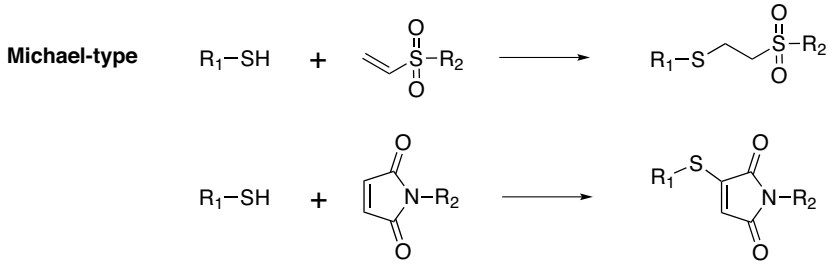

Figure 1.18. Michael type additions.

1.6.7. Native chemical ligation

Native chemical ligation is the reaction between an N-terminal cysteine and a thioester. An *S*-acyl covalent intermediate is formed, which rapidly undergoes *S*- to *N*-acyl migration, thereby forming a new amide bond (**Figure 1.19**). The reaction can be performed in mild

aqueous conditions and is highly efficient. Native chemical ligation was used for cross-linking by the Messersmith group. For this purpose several dipeptides were synthesized containing an N-terminal cysteine. Polymer 4-armed PEG was modified with either a dipeptide or a thioester moiety. Mixing of aqueous solutions of both polymers (10 – 20 wt%) resulted in hydrogel formation within minutes.[175]

1.6.8. Oxime chemistry

Recently, oxime chemistry was introduced as a novel hydrogel cross-linking method. Oxime chemistry is the reaction between an aminooxy group and an aldehyde or ketone (**Figure 1.19**). Grover et al. demonstrated that this chemistry is suitable for gel formation as it allows control over the reaction kinetics and efficiency. Hydrogels were prepared using eight armed aminooxy functionalized PEG and glutaraldehyde. Introduction of cell binding domain RGD revealed that the oxime-formed gels supported mesenchymal stem cell incorporation.[176] The Becker group further investigated oxime cross-linked hydrogels. The gelation time and mechanical properties of the gels can be tuned by pH and by addition of a catalyst. Gels formed faster and appeared to be much stiffer at pH 4.5 than at pH 7.6. Addition of catalyst aniline resulted in stronger gels, with shorter gelation times.[177]

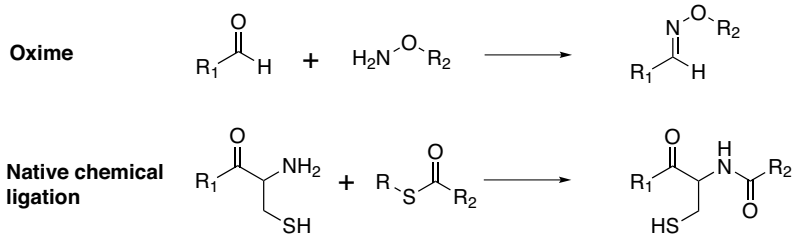

Figure 1.19. Oxime chemistry and native chemical ligation.

1.6.9. Combined click reactions

This paragraph clearly showed the potential of click reactions for hydrogel formation. Recently, the Dove group decided to combine two click reactions to create a double network gel. A dual cross-linking method was developed in which simultaneously a loose and a dense network were formed. The loose network was prepared by Diels-Alder norbornene-tetrazine chemistry. The nucleophilic thiol-alkyne addition was utilized for formation of the dense network. The hydrogels were formed rapidly under physiological conditions. Rheological analysis showed that gels had a high mechanical strength. Due to the bioorthogonality of the two click reactions, the gels were also suitable for encapsulation of human cells.[178]

1.7. Outline

This introductory chapter showed that there are multiple ways to develop hydrogels, aiming for use in biomedical applications. Hydrogels show distinctly different properties when cross-linked via physical or via chemical methods. The way in which cross-linking occurs determines the mechanical properties of the gel, the biocompatibility and has an influence on hydrogel administration. With control over the cross-linking method, the gel properties can also be controlled, which facilitates their clinical use. In this thesis, several bio-inspired cross-linking methods for hydrogel formation are studied, with the aim to develop adaptive scaffolds for bone tissue engineering. In **Chapter 2**, we investigate the possibilities to construct physically cross-linked hydrogels by adopting calcium-binding peptide motifs found in nature. These domains were conjugated to star shaped poly(ethylene)glycol (star-PEG). The hydrogel forming capacity was studied by addition of calcium ions, to induce ionic cross-links between the polymeric constituents. After studying this physical cross-linking method, we switched our focus to chemically cross-linked hydrogels. We employed the copper-free click reaction between a ring-strained alkyne (BCN) and an azide (SPAAC) for the formation of soft PEG hydrogels. The biocompatibility of these gels was investigated, by performing several cell adhesion studies (**Chapter 3**). A new type of chemical cross-linking method is reported in **Chapter 4**, in which we used the oxidation controlled reaction between alkyne BCN and a catechol (SPOCQ). The novelty of this method lies in the fact that for the first time a fast and activatable click chemistry approach is obtained. Both chemical cross-linking methods SPAAC and SPOCQ were further used in **Chapter 5**, where hydrogels were combined with peptide amphiphile fibres. By magnetic alignment of the fibres and entrapment of the aligned structures in a hydrogel matrix, we aimed for creating a scaffold to direct the growth of neuronal cells. In the final chapter, we focus on combining physical and chemical cross-linking methods to make dual cross-linked gels. For this purpose, we explored bisphosphonate moieties, which efficiently interact with Ca^{2+} to yield physically cross-linked gels and combined this methodology with chemical SPOCQ cross-linked gels (**Chapter 6**).

1.8. References

(1) Hoffman, A. S. *Adv. Drug Deliv. Rev.* **2002**, *54*, 3-12.
(2) Peppas, N. A.; Bures, P.; Leobandung, W.; Ichikawa, H. *Eur. J. Pharm. Biopharm.* **2000**, *50*, 27-46.
(3) Wichterle, O.; Lim, D. *Nature* **1960**, *185*, 117-118.
(4) Van Vlierberghe, S.; Dubruel, P.; Schacht, E. *Biomacromolecules* **2011**, *12*, 1387-1408.
(5) Kharkar, P. M.; Kiick, K. L.; Kloxin, A. M. *Chem. Soc. Rev.* **2013**, *42*, 7335-7372.
(6) Minh, K. N.; Lee, D. S. *Macromol. Biosci.* **2010**, *10*, 563-579.
(7) Lee, K. Y.; Mooney, D. J. *Chem. Rev.* **2001**, *101*, 1869-1879.
(8) Shin, H.; Jo, S.; Mikos, A. G. *Biomaterials* **2003**, *24*, 4353-4364.
(9) Marler, J. J.; Upton, J.; Langer, R.; Vacanti, J. P. *Adv. Drug Deliv. Rev.* **1998**, *33*, 165-182.
(10) Putnam, A. J.; Mooney, D. J. *Nat. Med.* **1996**, *2*, 824-826.
(11) Drury, J. L.; Mooney, D. J. *Biomaterials* **2003**, *24*, 4337-4351.
(12) Augst, A. D.; Kong, H. J.; Mooney, D. J. *Macromol. Biosci.* **2006**, *6*, 623-633.
(13) Slaughter, B. V.; Khurshid, S. S.; Fisher, O. Z.; Khademhosseini, A.; Peppas, N. A. *Adv. Mater.* **2009**, *21*, 3307-3329.
(14) Galler, K. M.; Aulisa, L.; Regan, K. R.; D'Souza, R. N.; Hartgerink, J. D. *J. Am. Chem. Soc.* **2010**, *132*, 3217-3223.
(15) Jun, H. W.; Paramonov, S. E.; Hartgerink, J. D. *Soft Matter* **2006**, *2*, 177-181.
(16) Collier, J. H.; Segura, T. *Biomaterials* **2011**, *32*, 4198-4204.
(17) Ruoslahti, E. *Annu. Rev. Cell Dev. Biol.* **1996**, *12*, 697-715.
(18) Perlin, L.; MacNeil, S.; Rimmer, S. *Soft Matter* **2008**, *4*, 2331-2349.
(19) Hersel, U.; Dahmen, C.; Kessler, H. *Biomaterials* **2003**, *24*, 4385-4415.
(20) Krishna, O. D.; Kiick, K. L. *Biopolymers* **2010**, *94*, 32-48.
(21) Van Hest, J. C. M. *Polym. Rev.* **2007**, *47*, 63-92.
(22) Yan, C. Q.; Pochan, D. J. *Chem. Soc. Rev.* **2010**, *39*, 3528-3540.
(23) Daamen, W. F.; Veerkamp, J. H.; van Hest, J. C. M.; van Kuppevelt, T. H. *Biomaterials* **2007**, *28*, 4378-4398.
(24) Annabi, N.; Mithieux, S. M.; Camci-Unal, G.; Dokmeci, M. R.; Weiss, A. S.; Khademhosseini, A. *Biochem. Eng. J.* **2013**, *77*, 110-118.
(25) Li, Y.; Rodrigues, J.; Tomás, H. *Chem. Soc. Rev.* **2012**, *41*, 2193-2221.
(26) Ferreira, A. M.; Gentile, P.; Chiono, V.; Ciardelli, G. *Acta Biomater.* **2012**, *8*, 3191-3200.
(27) Jia, X. Q.; Kiick, K. L. *Macromol. Biosci.* **2009**, *9*, 140-156.
(28) Daamen, W. F.; Hafmans, T.; Veerkamp, J. H.; van Kuppevelt, T. H. *Biomaterials* **2001**, *22*, 1997-2005.
(29) Aigner, T.; Stove, J. *Adv. Drug Deliv. Rev.* **2003**, *55*, 1569-1593.
(30) Engel, J.; Bächinger, H. P. *Top. Curr. Chem.* **2005**, *247*, 7-33.
(31) Cen, L.; Liu, W.; Cui, L.; Zhang, W. J.; Cao, Y. L. *Pediatr. Res.* **2008**, *63*, 492-496.
(32) Juncosa-Melvin, N.; Shearn, J. T.; Boivin, G. P.; Gooch, C.; Galloway, M. T.; West, J. R.; Nirmalanandhan, V. S.; Bradica, G.; Butler, D. L. *Tissue Eng.* **2006**, *12*, 2291-2300.
(33) Boyce, S. T. *Med. Biol. Eng. Comput.* **1998**, *36*, 791-800.
(34) Lee, C. H.; Singla, A.; Lee, Y. *Int. J. Pharm.* **2001**, *221*, 1-22.
(35) Kuijpers, A. J.; Engbers, G. H. M.; Krijgsveld, J.; Zaat, S. A. J.; Dankert, J.; Feijen, J. *J. Biomater. Sci.-Polym. Ed.* **2000**, *11*, 225-243.
(36) Masuda, T.; Furue, M.; Matsuda, T. *Tissue Eng.* **2004**, *10*, 523-535.

(37) Liu, X.; Smith, L. A.; Hu, J.; Ma, P. X. *Biomaterials* **2009**, *30*, 2252-2258.
(38) Vepari, C.; Kaplan, D. L. *Prog. Polym. Sci.* **2007**, *32*, 991-1007.
(39) Gong, Z. G.; Yang, Y. H.; Huang, L.; Chen, X.; Shao, Z. Z. *Soft Matter* **2010**, *6*, 1217-1223.
(40) Kim, U. J.; Park, J. Y.; Li, C. M.; Jin, H. J.; Valluzzi, R.; Kaplan, D. L. *Biomacromolecules* **2004**, *5*, 786-792.
(41) Altman, G. H.; Diaz, F.; Jakuba, C.; Calabro, T.; Horan, R. L.; Chen, J. S.; Lu, H.; Richmond, J.; Kaplan, D. L. *Biomaterials* **2003**, *24*, 401-416.
(42) Fini, M.; Motta, A.; Torricelli, P.; Glavaresi, G.; Aldini, N. N.; Tschon, M.; Giardino, R.; Migliaresi, C. *Biomaterials* **2005**, *26*, 3527-3536.
(43) Durand, D.; Gimel, J. C.; Nicolai, T. *Physica A* **2002**, *304*, 253-265.
(44) Akkermans, C.; Venema, P.; van der Goot, A. J.; Gruppen, H.; Bakx, E. J.; Boom, R. M.; van der Linden, E. *Biomacromolecules* **2008**, *9*, 1474-1479.
(45) Hu, Y. H.; Wang, H. M.; Wang, J. Y.; Wang, S. B.; Liao, W.; Yang, Y. G.; Zhang, Y. J.; Kong, D. L.; Yang, Z. M. *Org. Biomol. Chem.* **2010**, *8*, 3267-3271.
(46) Krishna, O. D.; Kiick, K. L. *Biomacromolecules* **2009**, *10*, 2626-2631.
(47) Urello, M. A.; Kiick, K. L.; Sullivan, M. O. *J. Mater. Chem. B* **2014**, *2*, 8174–8185.
(48) Hernandez-Gordillo, V.; Chmielewski, J. *Biomaterials* **2014**, *35*, 7363-7373.
(49) Skrzeszewska, P. J.; de Wolf, F. A.; Werten, M. W. T.; Moers, A.; Stuart, M. A. C.; van der Gucht, J. *Soft Matter* **2009**, *5*, 2057-2062.
(50) Werten, M. W. T.; Wisselink, W. H.; van den Bosch, T. J. J.; de Bruin, E. C.; de Wolf, F. A. *Protein Eng.* **2001**, *14*, 447-454.
(51) Golinska, M. D.; Włodarczyk-Biegun, M. K.; Werten, M. W. T.; Stuart, M. A. C.; de Wolf, F. A.; de Vries, R. *Biomacromolecules* **2014**, *15*, 699-706.
(52) Włodarczyk-Biegun, M. K.; Werten, M. W. T.; de Wolf, F. A.; van den Beucken, J. J. J. P.; Leeuwenburgh, S. C. G.; Kamperman, M.; Cohen Stuart, M. A. *Acta Biomater.* **2014**, *10*, 3620-3629.
(53) Bessa, P. C.; Machado, R.; Nurnberger, S.; Dopler, D.; Banerjee, A.; Cunha, A. M.; Rodriguez-Cabello, J. C.; Redl, H.; van Griensven, M.; Reis, R. L.; Casal, M. *J. Control. Release* **2010**, *142*, 312-318.
(54) Haider, M.; Megeed, Z.; Ghandehari, H. *J. Control. Release* **2004**, *95*, 1-26.
(55) Chow, D.; Nunalee, M. L.; Lim, D. W.; Simnick, A. J.; Chilkoti, A. *Mater. Sci. Eng. R-Rep.* **2008**, *62*, 125-155.
(56) MacEwan, S. R.; Chilkoti, A. *Biopolymers* **2010**, *94*, 60-77.
(57) Urry, D. W.; Luan, C. H.; Parker, T. M.; Gowda, D. C.; Prasad, K. U.; Reid, M. C.; Safavy, A. *J. Am. Chem. Soc.* **1991**, *113*, 4346-4348.
(58) Urry, D. W. *J. Phys. Chem. B* **1997**, *101*, 11007-11028.
(59) Lim, D. W.; Nettles, D. L.; Setton, L. A.; Chilkoti, A. *Biomacromolecules* **2007**, *8*, 1463-1470.
(60) Nettles, D. L.; Kitaoka, K.; Hanson, N. A.; Flahiff, C. M.; Mata, B. A.; Hsu, E. W.; Chilkoti, A.; Setton, L. A. *Tissue Eng. Part A* **2008**, *14*, 1133-1140.
(61) Lim, D. W.; Nettles, D. L.; Setton, L. A.; Chilkoti, A. *Biomacromolecules* **2008**, *9*, 222-230.
(62) Asai, D.; Xu, D.; Liu, W.; Garcia Quiroz, F.; Callahan, D. J.; Zalutsky, M. R.; Craig, S. L.; Chilkoti, A. *Biomaterials* **2012**, *33*, 5451-5458.
(63) Ravi, S.; Krishnamurthy, V. R.; Caves, J. M.; Haller, C. A.; Chaikof, E. L. *Acta Biomater.* **2012**, *8*, 627-635.
(64) Martinez, A. W.; Caves, J. M.; Ravi, S.; Li, W.; Chaikof, E. L. *Acta Biomater.* **2014**, *10*, 26-33.
(65) Martin, L.; Alonso, M.; Girotti, A.; Arias, F. J.; Rodriguez-Cabello, J. C. *Biomacromolecules* **2009**, *10*, 3015-3022.
(66) Schacht, K.; Scheibel, T. *Biomacromolecules* **2011**, *12*, 2488-2495.
(67) Megeed, Z.; Cappello, J.; Ghandehari, H. *Adv. Drug Deliv. Rev.* **2002**, *54*, 1075-1091.

(68) Cappello, J.; Crissman, J. W.; Crissman, M.; Ferrari, F. A.; Textor, G.; Wallis, O.; Whitledge, J. R.; Zhou, X.; Burman, D.; Aukerman, L.; Stedronsky, E. R. *J. Control. Release* **1998**, *53*, 105-117.

(69) Xia, X.-X.; Xu, Q.; Hu, X.; Qin, G.; Kaplan, D. L. *Biomacromolecules* **2011**, *12*, 3844−3850.

(70) Dinerman, A. A.; Cappello, J.; Ghandehari, H.; Hoag, S. W. *J. Control. Release* **2002**, *82*, 277-287.

(71) Megeed, Z.; Haider, M.; Li, D. Q.; O'Malley, B. W.; Cappello, J.; Ghandehari, H. *J. Control. Release* **2004**, *94*, 433-445.

(72) Hatefi, A.; Cappello, J.; Ghandehari, H. *Pharm. Res.* **2007**, *24*, 773-779.

(73) Nagarsekar, A.; Crissman, J.; Crissman, M.; Ferrari, F.; Cappello, J.; Ghandehari, H. *J. Biomed. Mater. Res.* **2002**, *62*, 195-203.

(74) Nagarsekar, A.; Crissman, J.; Crissman, M.; Ferrari, F.; Cappello, J.; Ghandehari, H. *Biomacromolecules* **2003**, *4*, 602-607.

(75) Petka, W. A.; Harden, J. L.; McGrath, K. P.; Wirtz, D.; Tirrell, D. A. *Science* **1998**, *281*, 389-392.

(76) Pandya, M. J.; Spooner, G. M.; Sunde, M.; Thorpe, J. R.; Rodger, A.; Woolfson, D. N. *Biochemistry* **2000**, *39*, 8728-8734.

(77) Banwell, E. F.; Abelardo, E. S.; Adams, D. J.; Birchall, M. A.; Corrigan, A.; Donald, A. M.; Kirkland, M.; Serpell, L. C.; Butler, M. F.; Woolfson, D. N. *Nat. Mater.* **2009**, *8*, 596-600.

(78) Yao, M.-H.; Yang, J.; Du, M.-S.; Song, J.-T.; Yu, Y.; Chen, W.; Zhao, Y.-D.; Liu, B. *J. Mater. Chem. B* **2014**, *2*, 3123.

(79) Xu, C. Y.; Breedveld, V.; Kopecek, J. *Biomacromolecules* **2005**, *6*, 1739-1749.

(80) Mehl, A. F.; Feer, S. P.; Cusimano, J. S. *Biomacromolecules* **2012**, *13*, 1244-1249.

(81) Foo, C.; Lee, J. S.; Mulyasasmita, W.; Parisi-Amon, A.; Heilshorn, S. C. *Proc. Natl. Acad. Sci. U. S. A.* **2009**, *106*, 22067-22072.

(82) Mulyasasmita, W.; Cai, L.; Dewi, R. E.; Jha, A.; Ullmann, S. D.; Luong, R. H.; Huang, N. F.; Heilshorn, S. C. *J. Control. Release* **2014**, *191*, 71-81.

(83) Yamaguchi, N.; Zhang, L.; Chae, B. S.; Palla, C. S.; Furst, E. M.; Kiick, K. L. *J. Am. Chem. Soc.* **2007**, *129*, 3040-3041.

(84) Wieduwild, R.; Tsurkan, M.; Chwalek, K.; Murawala, P.; Nowak, M.; Freudenberg, U.; Neinhuis, C.; Werner, C.; Zhang, Y. *J. Am. Chem. Soc.* **2013**, *135*, 2919-2922.

(85) Haines-Butterick, L.; Rajagopal, K.; Branco, M.; Salick, D.; Rughani, R.; Pilarz, M.; Lamm, M. S.; Pochan, D. J.; Schneider, J. P. *Proc. Natl. Acad. Sci. U. S. A.* **2007**, *104*, 7791-7796.

(86) Collier, J. H.; Hu, B. H.; Ruberti, J. W.; Zhang, J.; Shum, P.; Thompson, D. H.; Messersmith, P. B. *J. Am. Chem. Soc.* **2001**, *123*, 9463-9464.

(87) Kretsinger, J. K.; Haines, L. A.; Ozbas, B.; Pochan, D. J.; Schneider, J. P. *Biomaterials* **2005**, *26*, 5177-5186.

(88) Branco, M. C.; Pochan, D. J.; Wagner, N. J.; Schneider, J. P. *Biomaterials* **2009**, *30*, 1339-1347.

(89) Branco, M. C.; Pochan, D. J.; Wagner, N. J.; Schneider, J. P. *Biomaterials* **2010**, *31*, 9527-9534.

(90) Sinthuvanich, C.; Haines-Butterick, L. A.; Nagy, K. J.; Schneider, J. P. *Biomaterials* **2012**, *33*, 7478-7488.

(91) Gupta, K.; Jang, H.; Harlen, K.; Puri, A.; Nussinov, R.; Schneider, J. P.; Blumenthal, R. *Biophys. J.* **2013**, *105*, 2093-2103.

(92) Fichman, G.; Gazit, E. *Acta Biomater.* **2014**, *10*, 1671-1682.

(93) Babu, S. S.; Praveen, V. K.; Ajayaghosh, A. *Chem. Rev.* **2014**, *114*, 1973-2129.

(94) Jayawarna, V.; Ali, M.; Jowitt, T. A.; Miller, A. E.; Saiani, A.; Gough, J. E.; Ulijn, R. V. *Adv. Mater.* **2006**, *18*, 611-614.

(95) Jayawarna, V.; Richardson, S. M.; Hirst, A. R.; Hodson, N. W.; Saiani, A.; Gough, J. E.; Ulijn, R. V. *Acta Biomater.* **2009**, *5*, 934-943.

(96) Zhou, M.; Smith, A. M.; Das, A. K.; Hodson, N. W.; Collins, R. F.; Ulijn, R. V.; Gough, J. E. *Biomaterials* **2009**, *30*, 2523-2530.

(97) Kuang, Y.; Gao, Y.; Shi, J.; Li, J.; Xu, B. *Chem. Comm.* **2014**, *50*, 2772.

(98) Ou, C.; Zhang, J.; Zhang, X.; Yang, Z.; Chen, M. *Chem. Comm.* **2013**, *49*, 1853.
(99) Fleming, S.; Ulijn, R. V. *Chemical Society Reviews* **2014**, *43*, 8150-8177.
(100) Martin, A. D.; Robinson, A. B.; Mason, A. F.; Wojciechowski, J. P.; Thordarson, P. *Chemical Communications* **2014**, *50*, 15541-15544.
(101) Roy, S.; Banerjee, A. *Soft Matter* **2011**, *7*, 5300–5308.
(102) Sutton, S.; Campbell, N. L.; Cooper, A. I.; Kirkland, M.; Frith, W. J.; Adams, D. J. *Langmuir* **2009**, *25*, 10285–10291.
(103) Nanda, J.; Biswas, A.; Banerjee, A. *Soft Matter* **2013**, *9*, 4198.
(104) Löwik, D. W. P. M.; van Hest, J. C. M. *Chem. Soc. Rev.* **2004**, *33*, 234-245.
(105) Paramonov, S. E.; Jun, H. W.; Hartgerink, J. D. *J. Am. Chem. Soc.* **2006**, *128*, 7291-7298.
(106) Hartgerink, J. D.; Beniash, E.; Stupp, S. I. *Science* **2001**, *294*, 1684-1688.
(107) Webber, M. J.; Tongers, J.; Renault, M. A.; Roncalli, J. G.; Losordo, D. W.; Stupp, S. I. *Acta Biomater.* **2010**, *6*, 3-11.
(108) Mardilovich, A.; Craig, J. A.; McCammon, M. Q.; Garg, A.; Kokkoli, E. *Langmuir* **2006**, *22*, 3259-3264.
(109) Shroff, K.; Rexeisen, E. L.; Arunagirinathan, M. A.; Kokkoli, E. *Soft Matter* **2010**, *6*, 5064-5072.
(110) Kisiday, J.; Jin, M.; Kurz, B.; Hung, H.; Semino, C.; Zhang, S.; Grodzinsky, A. J. *Proc. Natl. Acad. Sci. U. S. A.* **2002**, *99*, 9996-10001.
(111) Bokhari, M. A.; Akay, G.; Zhang, S. G.; Birch, M. A. *Biomaterials* **2005**, *26*, 5198-5208.
(112) Semino, C. E.; Kasahara, J.; Hayashi, Y.; Zhang, S. G. *Tissue Eng.* **2004**, *10*, 643-655.
(113) Davis, M. E.; Motion, J. P. M.; Narmoneva, D. A.; Takahashi, T.; Hakuno, D.; Kamm, R. D.; Zhang, S. G.; Lee, R. T. *Circulation* **2005**, *111*, 442-450.
(114) Owczarz, M.; Bolisetty, S.; Mezzenga, R.; Arosio, P. *J. Colloid Interf. Sci.* **2015**, *437*, 244-251.
(115) Nowak, A. P.; Breedveld, V.; Pakstis, L.; Ozbas, B.; Pine, D. J.; Pochan, D.; Deming, T. J. *Nature* **2002**, *417*, 424-428.
(116) Nowak, A. P.; Breedveld, V.; Pine, D. J.; Deming, T. J. *J. Am. Chem. Soc.* **2003**, *125*, 15666-15670.
(117) Aulisa, L.; Dong, H.; Hartgerink, J. D. *Biomacromolecules* **2009**, *10*, 2694-2698.
(118) Bakota, E. L.; Sensoy, O.; Ozgur, B.; Sayar, M.; Hartgerink, J. D. *Biomacromolecules* **2013**, *14*, 1370-1378.
(119) Huang, Y. C.; Qiu, Z. J.; Xu, Y. M.; Shi, J. F.; Lin, H. K.; Zhang, Y. *Org. Biomol. Chem.* **2011**, *9*, 2149-2155.
(120) Velema, W. A.; Stuart, M. C. A.; Szymanski, W.; Feringa, B. L. *Chem. Comm.* **2013**, *49*, 5001.
(121) Yang, R.; Peng, S.; Wan, W.; Hughes, T. C. *J. Mater. Chem. C* **2014**, *2*, 9122–9131.
(122) Sanborn, T. J.; Messersmith, P. B.; Barron, A. E. *Biomaterials* **2002**, *23*, 2703-2710.
(123) Duncan, R. *Nat. Rev. Drug Discov.* **2003**, *2*, 347-360.
(124) Grieshaber, S. E.; Farran, A. J. E.; Lin-Gibson, S.; Kiick, K. L.; Jia, X. Q. *Macromolecules* **2009**, *42*, 2532-2541.
(125) Veronese, F. M.; Pasut, G. *Drug Discov. Today* **2005**, *10*, 1451-1458.
(126) Levy, Y.; Hershfield, M. S.; Fernandezmejia, C.; Polmar, S. H.; Scudiery, D.; Berger, M.; Sorensen, R. U. *J. Pediatr.* **1988**, *113*, 312-317.
(127) Canalle, L. A.; Löwik, D. W. P. M.; van Hest, J. C. M. *Chem. Soc. Rev.* **2010**, *39*, 329-353.
(128) Grieshaber, S. E.; Nie, T.; Yan, C. Q.; Zhong, S.; Teller, S. S.; Clifton, R. J.; Pochan, D. J.; Kiick, K. L.; Jia, X. Q. *Macromol. Chem. Phys.* **2011**, *212*, 229-239.
(129) Lee, H. J.; Lee, J. S.; Chansakul, T.; Yu, C.; Elisseeff, J. H.; Yu, S. M. *Biomaterials* **2006**, *27*, 5268-5276.
(130) Rizzi, S. C.; Hubbell, J. A. *Biomacromolecules* **2005**, *6*, 1226-1238.
(131) Rizzi, S. C.; Ehrbar, M.; Halstenberg, S.; Raeber, G. P.; Schmoekel, H. G.; Hagenmuller, H.; Muller, R.; Weber, F. E.; Hubbell, J. A. *Biomacromolecules* **2006**, *7*, 3019-3029.
(132) Dikovsky, D.; Bianco-Peled, H.; Seliktar, D. *Biomaterials* **2006**, *27*, 1496-1506.

(133) Peled, E.; Boss, J.; Bejar, J.; Zinman, C.; Seliktar, D. *J. Biomed. Mater. Res. A* **2007**, *80A*, 874-884.
(134) Wang, C.; Stewart, R. J.; Kopecek, J. *Nature* **1999**, *397*, 417-420.
(135) Wang, C.; Kopecek, J.; Stewart, R. J. *Biomacromolecules* **2001**, *2*, 912-920.
(136) Yang, J. Y.; Xu, C. Y.; Wang, C.; Kopecek, J. *Biomacromolecules* **2006**, *7*, 1187-1195.
(137) Yang, J. Y.; Xu, C. Y.; Kopeckova, P.; Kopecek, J. *Macromol. Biosci.* **2006**, *6*, 201-209.
(138) Yang, J.; Wu, K.; Konak, C.; Kopecek, J. *Biomacromolecules* **2008**, *9*, 510-517.
(139) Jing, P.; Rudra, J. S.; Herr, A. B.; Collier, J. H. *Biomacromolecules* **2008**, *9*, 2438-2446.
(140) Rudra, J. S.; Tripathi, P. K.; Hildeman, D. A.; Jung, J. P.; Collier, J. H. *Biomaterials* **2010**, *31*, 8475-8483.
(141) Tzokova, N.; Fernyhough, C. M.; Topham, P. D.; Sandon, N.; Adams, D. J.; Butler, M. F.; Armes, S. P.; Ryan, A. J. *Langmuir* **2009**, *25*, 2479-2485.
(142) Tzokova, N.; Fernyhough, C. M.; Butler, M. F.; Armes, S. P.; Ryan, A. J.; Topham, P. D.; Adams, D. J. *Langmuir* **2009**, *25*, 11082-11089.
(143) Castelletto, V.; Gouveia, R. J.; Connon, C. J.; Hamley, I. W. *Eur. Polym. J.* **2013**, *49*, 2961-2967.
(144) Tang, W.; Becker, M. L. *Chem. Soc. Rev.* **2014**, *43*, 7013-7039.
(145) Jiang, Y.; Chen, J.; Deng, C.; Suuronen, E. J.; Zhong, Z. *Biomaterials* **2014**, *35*, 4969-4985.
(146) Vermonden, T.; Censi, R.; Hennink, W. E. *Chem. Rev.* **2012**, *112*, 2853-2888.
(147) Sawhney, A. S.; Pathak, C. P.; Hubbell, J. A. *Macromolecules* **1993**, *26*, 581-587.
(148) Kloxin, A. M.; Kasko, A. M.; Salinas, C. N.; Anseth, K. S. *Science* **2009**, *324*, 59-63.
(149) Tornoe, C. W.; Christensen, C.; Meldal, M. *J. Org. Chem.* **2002**, *67*, 3057-3064.
(150) Rostovtsev, V. V.; Green, L. G.; Fokin, V. V.; Sharpless, K. B. *Angew. Chem. Int. Edit.* **2002**, *41*, 2596-2599.
(151) Iha, R. K.; Wooley, K. L.; Nyström, A. M.; Burke, D. J.; Kade, M. J.; Hawker, C. J. *Chem. Rev.* **2009**, *109*, 5620–5686.
(152) Malkoch, M.; Vestberg, R.; Gupta, N.; Mespouille, L.; Dubois, P.; Mason, A. F.; Hedrick, J. L.; Liao, Q.; Frank, C. W.; Kingsbury, K.; Hawker, C. J. *Chem. Comm.* **2006**, 2774.
(153) Dijk, M. v.; Nostrum, C. F. v.; Hennink, W. E.; Rijkers, D. T. S.; Liskamp, R. M. J. *Biomacromolecules* **2010**, *11*, 1608-1614.
(154) Agard, N. J.; Prescher, J. A.; Bertozzi, C. R. *J. Am. Chem. Soc.* **2004**, *126*, 15046-15047.
(155) Jewett, J. C.; Bertozzi, C. R. *Chem. Soc. Rev.* **2010**, *39*, 1272-1279.
(156) Codelli, J. A.; Baskin, J. M.; Agard, N. J.; Bertozzi, C. R. *J. Am. Chem. Soc.* **2008**, *130*, 11486-11493.
(157) DeForest, C. A.; Polizzotti, B. D.; Anseth, K. S. *Nat. Mater.* **2009**, *8*, 659-664.
(158) Xu, J.; Filion, T. M.; Prifti, F.; Song, J. *Chem.-Asian J.* **2011**, *6*, 2730-2737.
(159) Zheng, J.; Smith Callahan, L. A.; Hao, J.; Guo, K.; Wesdemiotis, C.; Weiss, R. A.; Becker, M. L. *ACS Macro Letters* **2012**, *1*, 1071-1073.
(160) Ashley, G. W.; Henise, J.; Reid, R.; Santi, D. V. *PNAS* **2013**, *110*, 2318–2323.
(161) Xu, J.; Feng, E.; Song, J. *J. Am. Chem. Soc.* **2014**, *136*, 4105-4108.
(162) Rideout, D. C.; Breslow, R. *J. Am. Chem. Soc.* **1980**, *102*, 7817-7818.
(163) Wei, H.-L.; Yang, Z.; Zheng, L.-M.; Shen, Y.-M. *Polymer* **2009**, *50*, 2836-2840.
(164) Nimmo, C. M.; Owen, S. C.; Shoichet, M. S. *Biomacromolecules* **2011**, *12*, 824-830.
(165) Alge, D. L.; Azagarsamy, M. A.; Donohue, D. F.; Anseth, K. S. *Biomacromolecules* **2013**, *14*, 949-953.
(166) Hoyle, C. E.; Bowman, C. N. *Angew. Chem. Int. Edit.* **2010**, *49*, 1540-1573.
(167) Aimetti, A. A.; Machen, A. J.; Anseth, K. S. *Biomaterials* **2009**, *30*, 6048-6054.
(168) Fairbanks, B. D.; Schwartz, M. P.; Halevi, A. E.; Nuttelman, C. R.; Bowman, C. N.; Anseth, K. S. *Adv. Mater.* **2009**, *21*, 5005-5010.
(169) Lin, C.-C.; Raza, A.; Shih, H. *Biomaterials* **2011**, *32*, 9685-9695.

(170) Shih, H.; Lin, C.-C. *Biomacromolecules* **2012**, *13*, 2003-2012.

(171) Lutolf, M. P.; Raeber, G. P.; Zisch, A. H.; Tirelli, N.; Hubbell, J. A. *Adv. Mater.* **2003**, *15*, 888-892.

(172) McGann, C. L.; Levenson, E. A.; Kiick, K. L. *Macromol. Chem. Phys.* **2013**, *214*, 203-213.

(173) Phelps, E. A.; Enemchukwu, N. O.; Fiore, V. F.; Sy, J. C.; Murthy, N.; Sulchek, T. A.; Barker, T. H.; García, A. J. *Adv. Mater.* **2012**, *24*, 64-70.

(174) Zhang, Z.; Loebus, A.; de Vicente, G.; Ren, F.; Arafeh, M.; Ouyang, Z.; Lensen, M. C. *Chem. of Mater.* **2014**, *26*, 3624-3630.

(175) Hu, B.-H.; Su, J.; Messersmith, P. B. *Biomacromolecules* **2009**, *10*, 2194–2200.

(176) Grover, G. N.; Lam, J.; Nguyen, T. H.; Segura, T.; Maynard, H. D. *Biomacromolecules* **2012**, *13*, 3013-3017.

(177) Lin, F.; Yu, J.; Tang, W.; Zheng, J.; Defante, A.; Guo, K.; Wesdemiotis, C.; Becker, M. L. *Biomacromolecules* **2013**, *14*, 3749-3758.

(178) Truong, V. X.; Ablett, M. P.; Richardson, S. M.; Hoyland, J. A.; Dove, A. P. *J. Am. Chem. Soc.* **2015**, *137*, 1618-1622.

Chapter 2

Physical cross-linking of star-PEG polymers using calcium-binding peptides

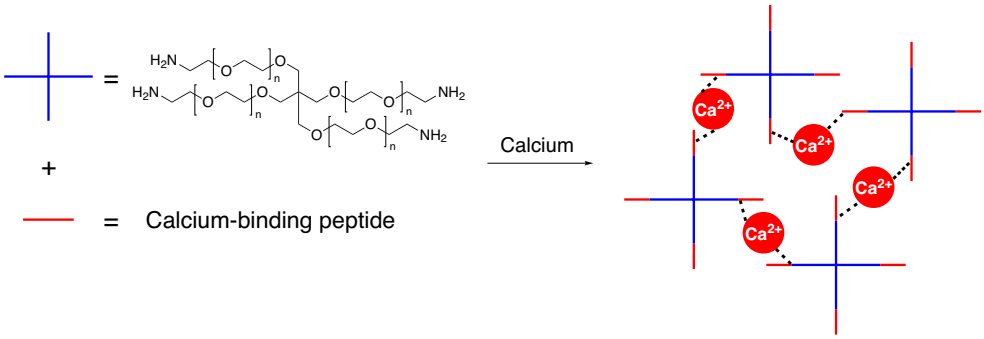

2.1. Introduction

Bone tissue is composed of the two cell types osteoblasts and osteoclasts, responsible for bone mineralization and bone resorption, respectively. These cells are embedded in an organic matrix composed of collagen and hydroxyapatite. Collagen is the main structural component, which gives the bone its tensile strength. The inorganic part of bone tissue is made up of the calcium and phosphate-containing mineral hydroxyapatite: $Ca_5(PO_4)_3OH$. Much research has been carried out in the field of bone tissue engineering, in order to find scaffolds for bone repair. Two important criteria in the development of these scaffolds are degradability and the ability to induce apatite formation.[1] Materials that mineralize bone tissue are usually non-collagenous proteins, with strong calcium-binding features.[1,2] These calcium-binding motifs are abundantly present in nature.

An important class of proteins with mineralizing capacity and strong calcium-binding features are the bone sialoproteins. These highly glycosylated proteins contain two glutamic acid-rich domains and a C-terminal RGD-integrin binding sequence. Sialoproteins can promote cell adhesion and provide hydroxyapatite nucleation. Important in the nucleating activity is the first glutamic acid-rich domain, in which 16 of the 46 residues are glutamic acid (Glu) amino acids. Apart from a block containing 8 glutamic acid residues in a row, this domain also contains a number of serine residues. The second glutamic acid-rich domain also has nucleating activity, but needs posttranslational modifications in order to be active.[3] Another example of an apatite-binding protein is osteonectin. This glycoprotein contains 4 domains and a total of 287 amino acids. N-terminal domain I is again rich in Glu, and appears to be responsible for hydroxyapatite binding, due to its high glutamic acid content, whereas domain II is rich in cysteine and contains N-glycosylation sites. Domains III and IV are made up of EF-hand motifs, which are helix-loop-helix structural domains responsible for binding of calcium ions.[4] A different type of apatite binder is the non-collagenous bone protein osteocalcin. Characteristic about this protein are the three γ-carboxyglutamic acid residues, formed by the posttranslational modification of glutamic acid. These modified Glu-residues are responsible for hydroxyapatite binding. The γ-carboxyglutamic acid binding motif is not capable of binding to amorphous calcium phosphate, which implies that the protein specifically binds to the surface of hydroxyapatite.[2,5] The role of the Glu domains in hydroxyapatite binding was further supported by studies with Glu_6 peptides as a model system. Moreover, studies with peptides containing fewer Glu residues showed lower binding affinity to hydroxyapatite.[4]

In contrast to the previous examples, glutamic acid (or related) residues are not responsible for apatite binding in the last class of proteins, the phosphophoryns. This protein is mainly composed of phosphorylated serines and aspartic acid residues. Phosphophoryns precipitate upon binding

to calcium, but this feature is lost after dephosphorylation of the serine residues. Additionally, blocking of the acidic side chain of aspartic acid also results in loss of the calcium binding ability. Both residues are therefore important for binding to calcium as well as to hydroxyapatite.[6,7]

As described above, calcium is important in the mineralization of bone tissue, but it also has a function in many other biological processes. Calcium is essential for the cell as it regulates several cellular processes, including cell metabolism, cell death, cell cycle, signal transduction and neurotransmission. A large number of calcium-binding proteins have been identified in nature. An important class of these are the EF-hand calcium-binding proteins, consisting of calcium-buffering and calcium-sensing members. The difference between these two is that calcium-sensing proteins undergo a conformational change upon Ca^{2+} binding, which does not occur for calcium-buffering proteins. The most prominent member of the calcium-sensing proteins is calmodulin, which is expressed in all eukaryotic cells. The important structural motif, the EF-hand domain, consists of an N-terminal and C-terminal helix (named E and F). The central Ca^{2+} coordinating loop is located between the two helices. Calmodulin consists of four EF-hand motifs, able to bind four calcium ions. Seven carboxylate ligands are responsible for coordinating Ca^{2+} in each binding loop. A conformational change occurs upon calcium binding leading to a more open conformation of calmodulin. As a result the hydrophobic methionine residues are exposed to the solvent, leading to release of free energy. This conformational change is the basis of action of calmodulin, as the released energy is used to transduce calcium signals (**Figure 2.1**).[8,9]

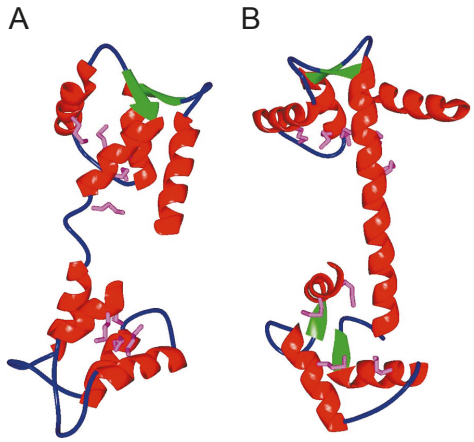

Figure 2.1. The conformational change of calmodulin (A) upon interaction with calcium (B). Calcium binding leads to a more open conformation, resulting in the exposure of hydrophobic residues (methionine, shown in purple).[8]

Apart from proteins with calcium-binding properties, there are also natural polysaccharides with this ability. Alginate is the most commonly known calcium-binding polysaccharide, which is present in the cell wall of brown algae. It is composed of the two monomers α-L-guluronic acid (G) and β-D-mannuronic acid (M) (**Figure 2.2**). In the polymer, blocks of one of the monomers are present, as wells as regions with alternating units. Alginates from different natural sources are different in their proportion of M and G blocks. An important feature of alginate is its ability to form gels with divalent cations such as Ca^{2+}, Ba^{2+} and Sr^{2+}. Gelation is not induced by monovalent cations and by Mg^{2+}.[10-12] Gelation is mainly achieved by binding of the cation to the guluronic acid regions of alginate. A strong binding to calcium was observed in a cooperative manner for polyguluronic acid segments of at least 20 monomers. A similar polymannuronic acid segment of alternating MG blocks did not show cooperative binding to calcium. This suggests a mechanism in which binding of one ion facilitates binding of the next. The mode of gelation of alginate is called the egg-box model. The guluronic acid segments form two chains with a buckled shape, with cavities in between which can accommodate a calcium ion. This model also explains why alginate gels with a higher guluronic acid content have better mechanical properties.[13]

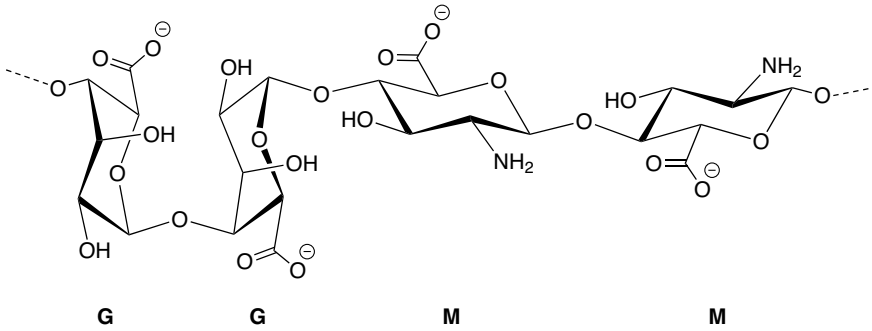

Figure 2.2. Alginate; G = guluronic acid, M = mannuronic acid.

In summary, nature has developed many calcium-binding motifs in different proteins, like bone sialoproteins and EF-hand proteins, but also in polysaccharides like alginate. Interestingly, calcium-binding in all of these examples depends on the electrostatic interactions between the positively charged calcium and negatively charged carboxylate groups, such as glutamic acid, aspartic acid or related residues. Only in the alginate example, calcium-binding has been utilized for hydrogel formation. Surprisingly, the strong calcium binding properties found in nature hardly have been translated to synthetic polymers. Our goal therefore is to develop synthetic calcium-cross-linkable polymers (**Figure 2.3**). For this purpose, we first synthesized several bio-inspired peptides and explored their calcium-binding features (**Paragraph 2.2**). The next step was the conjugation of these calcium-binding peptides to poly(ethylene)glycol

(PEG), to obtain peptide-polymer constructs (**Paragraph 2.3**). It was envisaged that addition of calcium to these constructs should lead to physical cross-links between the polymers; hence the propensity to hydrogel formation of the constructs was investigated.

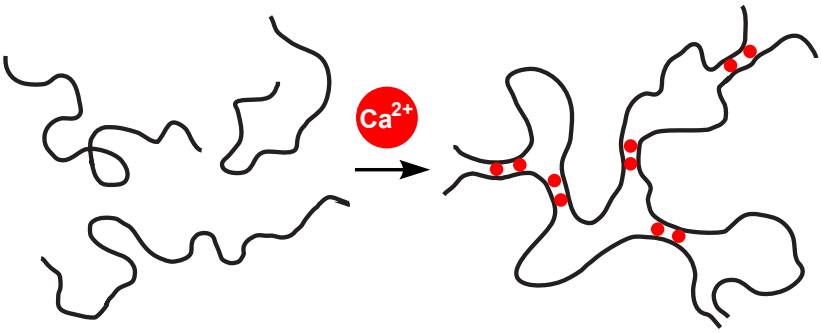

Figure 2.3. Formation of a polymeric network, a hydrogel, upon addition of calcium (red) to calcium-binding polymers (black)

2.2. Synthesis and analysis of Ca^{2+} binding peptides

2.2.1. GE_7G

As explained in the introduction, glutamate domains are responsible in most proteins for Ca^{2+} binding ability, as was for example seen for osteonectin. Our first choice for a calcium-binding peptide therefore was an oligo-glutamate to induce Ca^{2+} binding (**Figure 2.4**).[14]

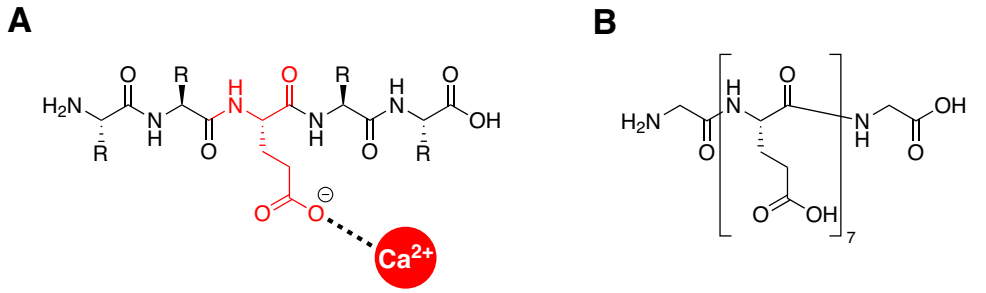

Figure 2.4. Calcium binding peptides. A) Binding principle, physical interaction between anionic residue and positively charged calcium. B) Peptide GE_7G (**2**).

Solid phase peptide synthesis (SPPS) was utilized as method for peptide synthesis. This method easily allows us to control the number of acidic moieties in the peptide. A 2-chlorotrityl resin was utilized for the synthesis of oligo-glutamates Glu_6, Glu_7 and Glu_8. Although synthesis of all

three oligo-glutamates was successful, some solubility issues were encountered for Glu_8, as it was hardly soluble in water. We therefore decided to continue our research with oligo-glutamate Glu_7 (E_7). In order to prevent racemization when either the N-terminus or C-terminus was utilized for further modifications, the Glu_7 part was flanked by glycine residues yielding peptide GE_7G (**2**). The next step was to investigate the calcium-binding features of the oligo-glutamate. As it was expected that Ca binding would lead to a conformational change in the peptide, circular dichroism (CD) spectroscopy was employed.

A CD spectrometer measures the difference in absorbance between counter-clockwise rotating (left-handed, L) and clockwise rotating (right-handed, R) circularly polarized light. A CD signal will only be recorded if there is a chromophore which is optically active (chiral). In case of peptides, measurements will occur in the far UV region (190-250 nm), as the peptide bond functions as the chromophore. CD can be used as an analysis method for peptides to determine their secondary structure and also to determine whether ligand binding changes the conformation.[15] CD spectra were recorded for a solution of peptide GE_7G (**2**; 0.4 mg/mL) in Tris buffer (pH 8.9). The peptide adopted a random coil, indicated by the characteristic negative signal around 198 nm. Based on the number of carboxylic acid moieties in the peptide, up to 16 equivalents $CaCl_2$ were added, but this did not change the conformation of the peptide (**Figure 2.5**).

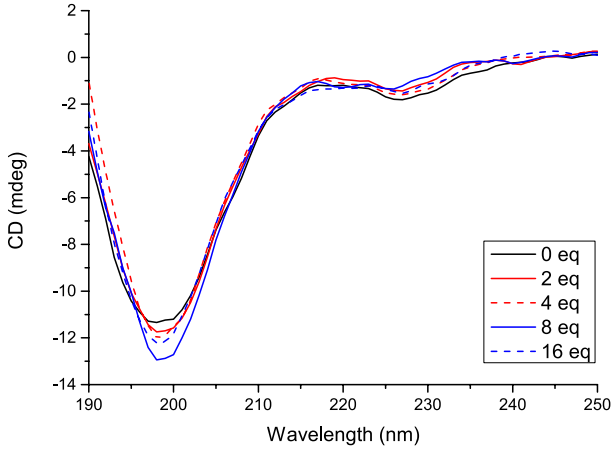

Figure 2.5. Circular dichroism (CD) spectra of peptide GE_7G (**2**) with several equivalents of Ca^{2+}. A random coil conformation was measured prior and after addition of calcium.

However, this does not necessarily imply that Ca^{2+} binding to GE_7G (**2**) does not occur. We therefore turned to isothermal calorimetry (ITC) analysis. This technique measures the heat generated or consumed upon interaction of two molecules. One of the molecules is loaded in the sample cell, which is maintained at a constant temperature. The other molecule, the ligand,

is loaded in the syringe. Small volumes of the ligand are titrated into the sample solution. The heat of the binding process (enthalpy ΔH) is measured for each injection. The heat is integrated as a function of the molar ratio between the two molecules to yield a titration curve. Since the binding sites become more saturated with the ligand over time, the heat signal diminishes progressively. The titration curve can be fitted in various binding models in order to obtain binding constants such as the stoichiometry of the interaction, the affinity constant (K), Gibbs free energy (ΔG) and entropy (ΔS) (**Figure 2.6**).[16]

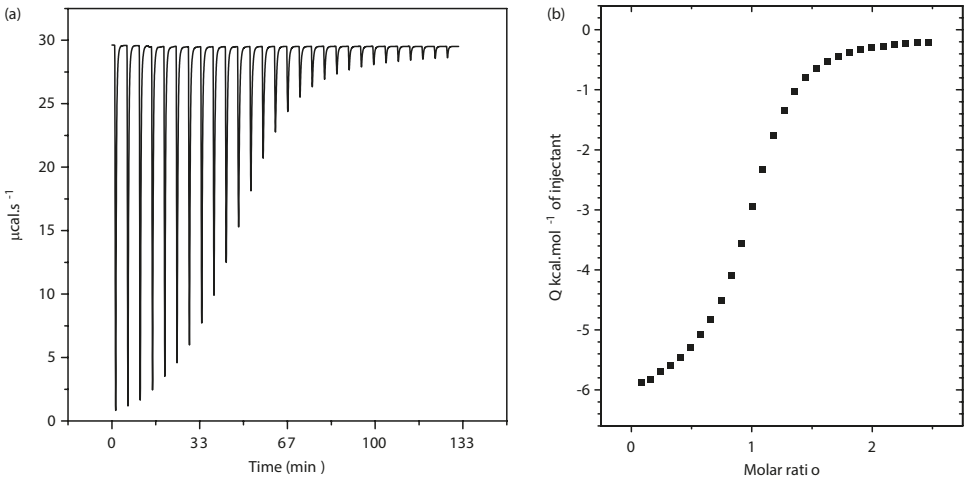

Figure 2.6. A typical isothermal calorimetry (ITC) spectrum, showing the binding of 1-adamantylamine to β-cyclodextrin. A) Plot showing the exothermic heat release upon injection of the syringe solution into the cell solution. B). Plot showing the integrated heat data. A typical S-shaped differential binding curve is obtained, which can be fitted into a binding model to obtain the binding parameters.[16]

In order to estimate the calcium-binding features of the oligo-glutamate, a solution of GE_7G (**2**; 100 µM) in HEPES buffer was loaded in the sample cell. A solution of ligand $CaCl_2$ in HEPES buffer was added to the syringe and titrated in the peptide solution. ITC analysis revealed an endothermic reaction, since the injection peaks were positive in value (**Figure 2.7 A-C**). A range of calcium concentrations (1.25, 2.5 and 5 mM) were added to the peptide (**2**), in order to get more insight in the binding process. The value for the heat generated per injection appeared to be twice as high when the calcium concentration was doubled from 1.25 mM to 2.5 mM. Furthermore, the peptide reached its saturation point at an earlier stage. These effects were more pronounced when a 5 mM calcium solution was titrated. We thus observed an injection pattern, but the high calcium concentrations used might lead to background heat signals, caused by the solubility effect. We therefore conducted a control experiment in which $CaCl_2$ (5 mM) was titrated into HEPES buffer (**Figure 2.7 D**).

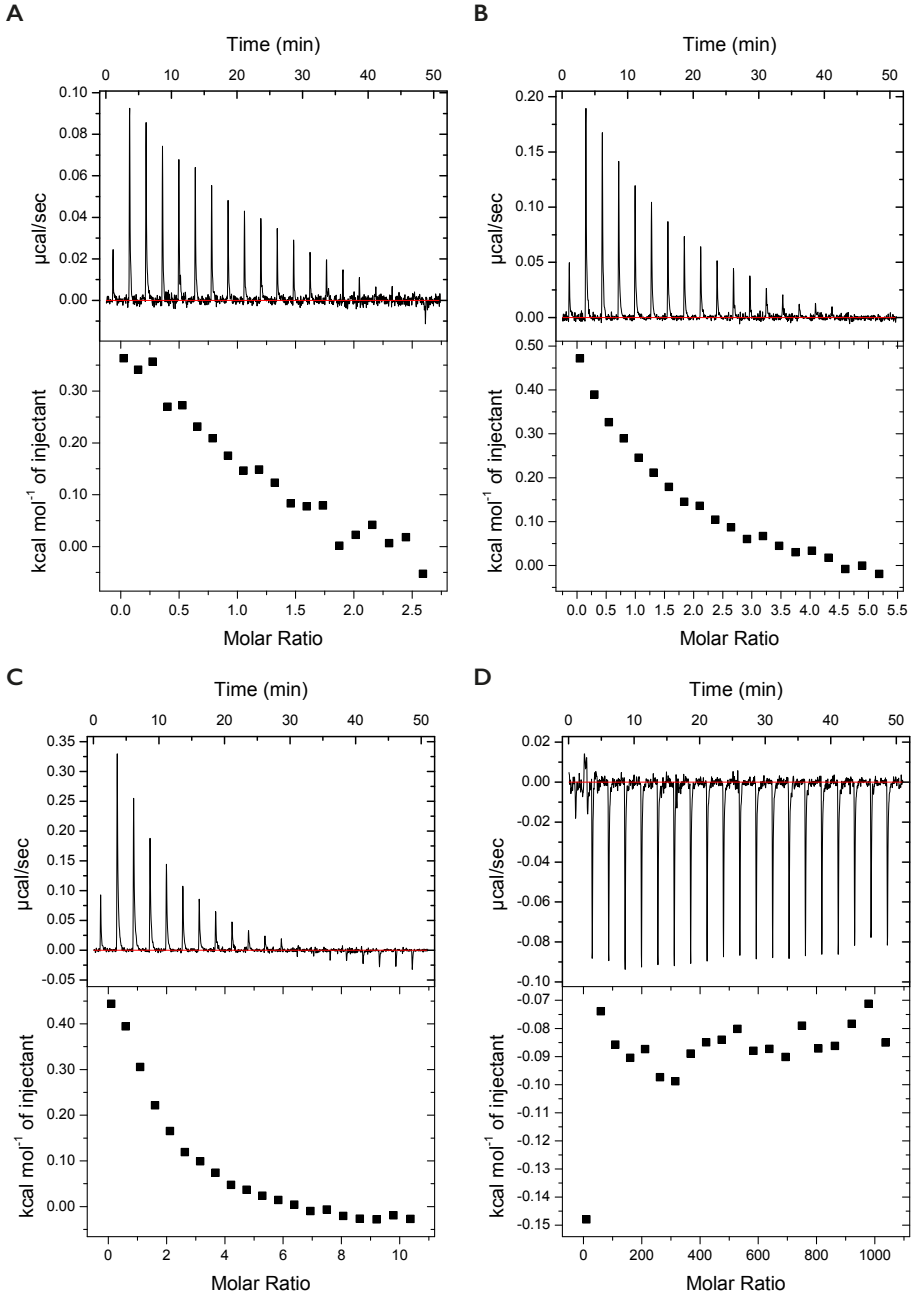

Figure 2.7. ITC spectra for the interaction between peptide GE_7G (**2**; 100 µM) and varying amounts of $CaCl_2$ (A-C) A) 1.25 mM $CaCl_2$ B) 2.5 mM $CaCl_2$ C) 5.0 mM $CaCl_2$ D) Background spectrum of $CaCl_2$ (5 mM) in HEPES buffer.

A typical background spectrum was recorded, lacking the progressive change in heat signals upon injection. The plot of the enthalpy change (ΔH) against the molar ratio also gave randomly distributed signals. Now that we confirmed that the observed injection peaks for peptide GE_7G (**2**) are not background signals, we attempted to estimate the binding parameters from the recorded ΔH spectrum. The data points did not follow the typical S-curve, usually seen in ITC graphs (compare **Figure 2.6** with **2.7**). We tried to fit the data but unfortunately, we were not able to find a model to fit all obtained data points. This might be caused by the large number of possible dependent binding sites (8) present in the peptide (7 Glu side chains and the C terminus), which might give rise to a more complicated binding event. As a consequence of the lack of a suitable binding model, we could not reliably estimate binding parameters for calcium to GE_7G (**2**). An important point to mention is that the effect of binding of calcium to GE_7G seems to be small. Values for the heat released upon interaction are significantly lower than for calcium-binding examples found in literature (for example: EDTA). A comparison with the example ITC curve (compare **Figure 2.6** with **2.7**) also shows this, which indicates that the binding between the peptide and calcium is weak.[16-20]

Our next step was to examine the interaction of peptide **2** with Ca^{2+} using dynamic light scattering (DLS). This analysis technique is based on the principle that molecules in solution experience Brownian motion. When light is passed through the solution, it will be scattered by the molecules. DLS measures the fluctuations in scattering intensity due to the Brownian motion. The scattering intensity will change faster, if particles move faster. Temperature, viscosity of the solvent and size can have an effect on the diffusion rate of molecules. In DLS, both temperature and solvent are constant, meaning that variation in scattering intensity can directly be related to the size of the molecule. DLS was used as a technique to measure calcium binding, since we expected calcium to make cross-links between peptides, leading to aggregation. DLS was performed on peptide GE_7G (**2**) prior and after addition of several equivalents of calcium (**Figure 2.8**). In the presence of calcium, a small shift was observed towards molecules with a larger size, indicating the formation of small aggregates. In conclusion, it is likely that binding of calcium to peptide GE_7G (**2**) takes places. This is based on the measured shift in DLS and on ITC analysis showing typical progressively decreasing signals of generated heat, and the fact that these signals change with changing calcium concentration. Although quantification of the effects and the mode of binding remained elusive, we still decided to continue with peptide GE_7G in further steps in reaching our goal to develop peptide-polymer based calcium cross-linked hydrogels (see **Paragraph 2.3.2**).

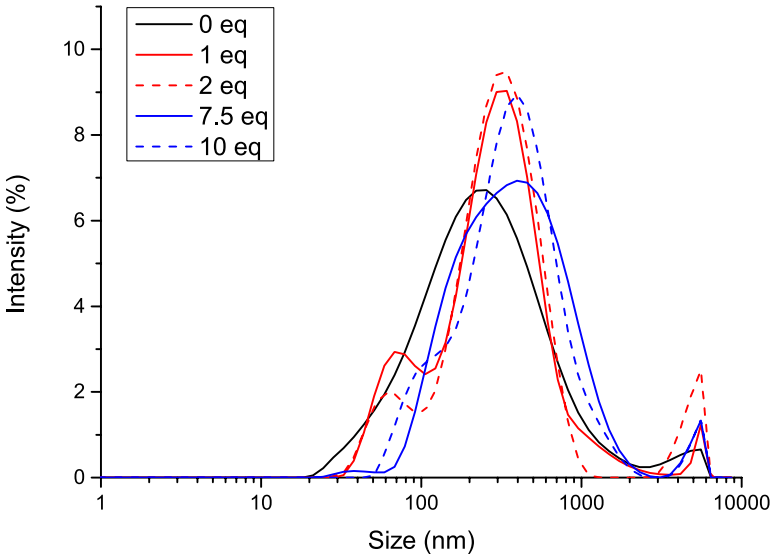

Figure 2.8. Dynamic light scattering (DLS) spectra of peptide GE_7G (**2**) with several equivalents of calcium.

2.2.2. Calmodulin binding domains

As a second binding motif, we focused on calmodulin, which, as described in the introduction, is a well-known calcium-binding protein, containing 4 EF-hand domains. The Ca^{2+} binding loop of these domains is composed of 12 amino acids. We decided to synthesize these four peptide segments by SPPS, whereby each fragment was flanked by an N-terminal and/or C-terminal glycine. Calmodulin domain 4 has the sequence DIDGDGQVNYEE (residues 130-141) and was obtained in high purity, but did contain a small fraction with an amino acid deletion (~10%). The same result was obtained for domain 1, peptide DKDGDGTITTKE (residues 21-32). Both domain 2 (**4**; DADGNGTIDFPE, residues 57-68) and domain 3 (**6**; DKDGNGYISAAE, residues 94-105) were obtained in a pure form employing SPPS. Since these two peptides could directly be used without further purification, we decided to start with these for analysing the calcium-binding features. ITC analysis was conducted on calmodulin domain 3 (**6**). When the sample cell was loaded with the peptide (**6**) in a concentration of 100 μM, spectra were obtained which very much resembled the background spectrum of Ca^{2+} in water (**Figure 2.7 D, Figure 2.9 A**). The same measuring conditions were utilized for domain 2 (**4**), which also hardly gave any heat signals. We decided to increase the peptide concentration for domain 2 (**4**) to 500 μM and measured ITC again (**Figure 2.9 B**). For low calcium concentrations (1.25 mM and 2.5 mM) the same background resembling binding isotherms were obtained. We measured a certain trend with a further increased calcium concentration (5 mM), since the measured heat signals showed a progressive decrease. However, the intensity of these signals was very low, despite the high

peptide concentration. Moreover, the plot of ΔH showed a random distribution. The absence of the S-shaped binding curve can be caused by a buffer mismatch, the existence of more than one binding event or by the fact that binding does not occur. Since the buffer was kept constant in the experiment and only calcium binding was analysed, it is likely that the observed heat of injection (ΔH) is due to absence of binding.

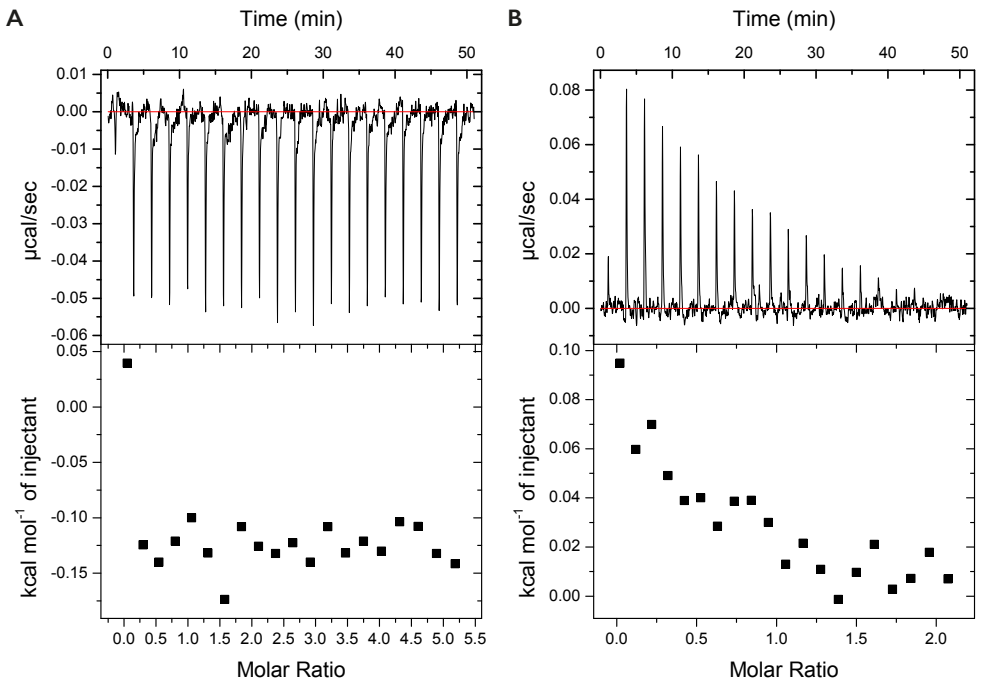

Figure 2.9. ITC spectra of the interaction between the calmodulin domains and $CaCl_2$, in HEPES buffer. A) Calmodulin domain 3 (**6**; GDKDGNGYISAAEG, 100 µM) and 2.5 mM $CaCl_2$. B) Calmodulin domain 2 (**4**; GDADGNGTIDFPEG, 500 µM) and 5.0 mM $CaCl_2$.

Based on the ITC results obtained for calmodulin domain 2 and 3 (**4,6**), we concluded that binding of Ca^{2+} to these peptides does not occur, or at least cannot be measured properly using ITC. As an alternative characterization technique, we performed DLS analysis on calmodulin domain 2 (**4**; 100 µM) with an excess of calcium (2.5 mM) (**Figure 2.10**).

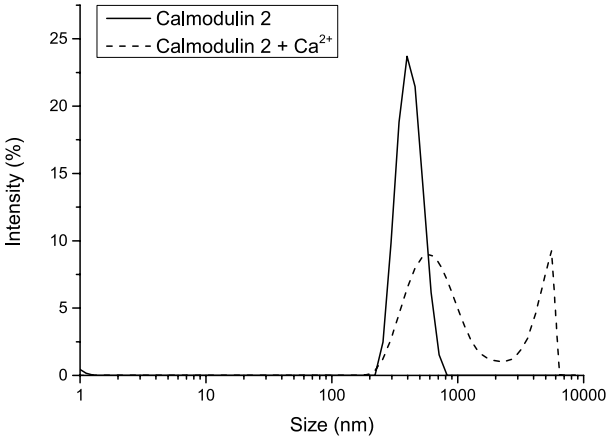

Figure 2.10. DLS spectra of peptide calmodulin domain 2 (**4**; GDADGNGTIDFPE, 100 μM) prior and after addition of calcium (2.5 mM).

Upon addition of Ca^{2+} a shift in particle size was observed, indicating the formation of peptide aggregates. This result indicates that calmodulin domain 2 (**4**) has calcium-binding properties, which is therefore in contrast to the ITC analysis. Since these two analysis techniques did not lead to conclusive results, we decided not to discard these sequences, but still consider them as potential binding motifs in peptide-polymer constructs which can be physically cross-linked with Ca^{2+} (**Paragraph 2.3.3**). Analysis of another nature-inspired calcium-binding peptide sequence was less ambiguous. One of the two calcium binding domains of the intracellular calcium-binding protein parvalbumin (residues 52 – 63) was synthesized. Although solid phase synthesis of peptide DKDKSGFIEEDEG was successful, we did not find any effect upon addition of calcium ions with CD and DLS analysis (data not shown).

2.2.3. G[LEELLEE]$_2$G

Several metal ions have the ability to induce the assembly of peptides into α-helical coiled-coils.[21] An example was given for a peptide derived from a marine snail, which showed α-helix formation upon addition of calcium.[18] As also outlined in **Chapter 1,** most of these coiled-coil sequences contain the characteristic heptad repeat abcdefg, with hydrophobic residues located at one side of the helix (positions a and d). The thus obtained hydrophobic interhelical interfaces promote the aggregation into coiled-coil dimers. Recently, the Börner group utilized these design rules to develop a peptide with a calcium-dependent self-assembly into an α-helix.[22] These researchers investigated peptide sequence LLEELLEELEELLEEFG and showed a clear shift from a random coil to an α-helix with CD spectroscopy upon addition of Ca^{2+}. The abundance of glutamates in the peptide clearly indicates calcium-binding features. This inspired us to synthesize the closely resembling peptide G[LEELLEE]$_2$G (**8**). Solid phase peptide synthesis

using the 2-chlorotrityl resin afforded the peptide in good purity. We adopted the measuring conditions of the Börner group to measure CD of peptide G[LEELLEE]$_2$G (**8**) (**Figure 2.11**).[22] As seen for the characteristic minima around 208 nm and 220 nm, the peptide indeed adopts an α-helical conformation. Surprisingly, this secondary structure was already obtained prior to calcium addition. A calcium-induced assembly of the peptide was not measured.

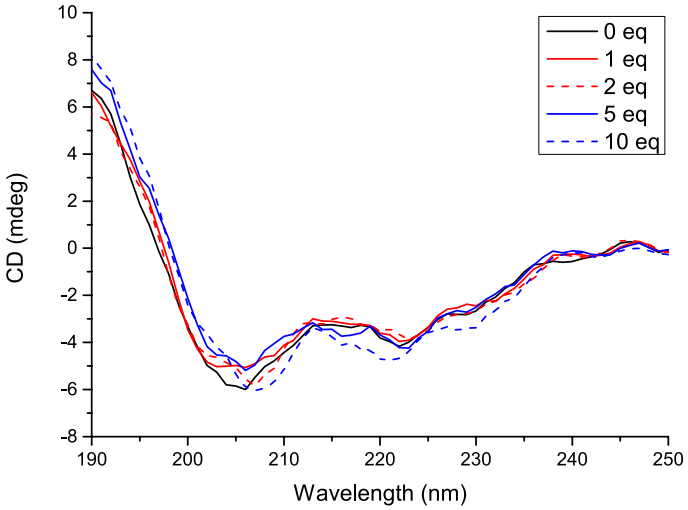

Figure 2.11. CD spectra of peptide G[LEELLEE]$_2$G (**8**) with several equivalents of calcium, showing an α-helical conformation in all cases.

Our peptide sequence only differed in the N-terminal amino acid, being a glycine instead of a leucine and in the absence of the phenylalanine residue. The latter one was added for spectroscopic purposes and the leucine was introduced to increase hydrophobicity. Both were not expected to have an influence on the secondary structure of the peptide. However, the authors indicate that there is a fragile balance between the two secondary structures. This might explain why we could not measure the conformational shift for our peptide. Since CD analysis did not answer the question whether peptide G[LEELLEE]$_2$G (**8**) has calcium-binding properties, we continued our analysis with ITC. The sample cell was loaded with 100 μM peptide G[LEELLEE]$_2$G (**8**) and the syringe was loaded with 1.25 mM calcium chloride. ITC analysis showed an exothermic reaction, as negative heat signals were measured. As expected, the intensity of these signals decreased over time. An almost straight line was seen in the plot of the enthalpy change ΔH which was impossible to fit into a model to obtain the binding parameters. Nevertheless, a trend was visible when looking at the heat signals, which indicates that calcium binding to G[LEELLEE]$_2$G (**8**) occurs (**Figure 2.12**).

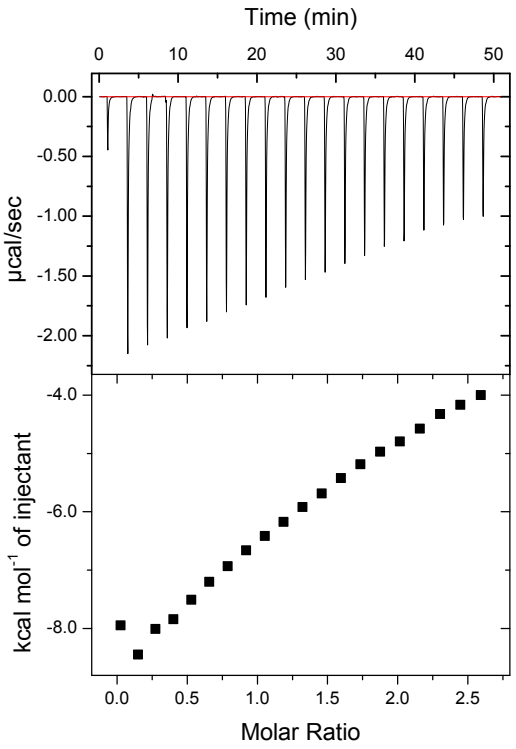

Figure 2.12. ITC spectrum of G[LEELLEE]$_2$G (**8**; 100 µM) and $CaCl_2$ (1.25 mM).

We continued our analysis by performing DLS with a calcium concentration range (0 - 10 eq). Upon addition of 7.5 eq Ca^{2+} or more a clear shift towards larger size molecules was observed (**Figure 2.13**). This shows that addition of calcium to the peptide results in aggregate formation. In conclusion, both ITC and DLS analysis of G[LEELLEE]$_2$G (**8**) indicate that the peptide is a promising candidate for the synthesis of peptide-polymer constructs (see **Paragraph 2.3.4**).

In order to improve the self-assembly properties and the stability of the peptide, we decided to modify the peptide by linkage of an alkyl tail to create a peptide amphiphile. Alkyl functionalized [LEELLEE]$_2$G was obtained by coupling of palmitic acid to the C-terminus via SPPS. CD analysis showed an α-helical structure for peptide $C_{15}H_{31}C(O)$-[LEELLEE]$_2$G (**10**), prior and after addition of calcium (data not shown). Addition of the alkyl tail did not significantly change the calcium-binding properties of the peptide. As for the unmodified peptide, ITC analysis gave negative heat signals (data not shown) and DLS showed aggregate formation upon addition of calcium ions (**Figure 2.14**).

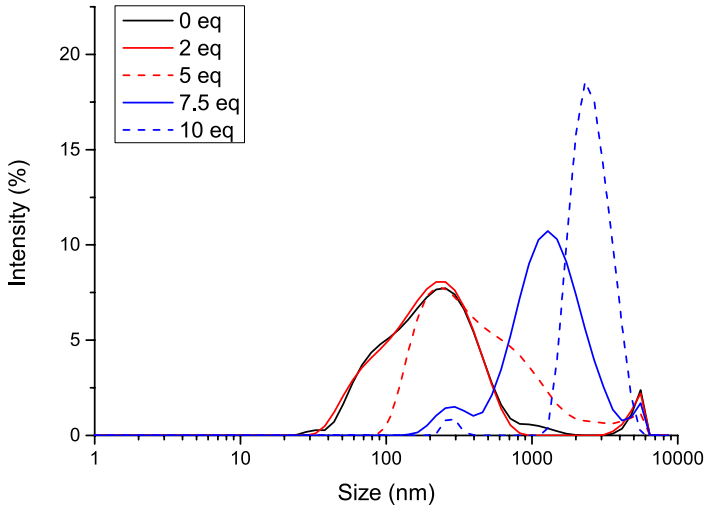

Figure 2.13. DLS spectra of peptide G[LEELLEE]$_2$G (**8**) and $CaCl_2$, showing the formation of aggregates.

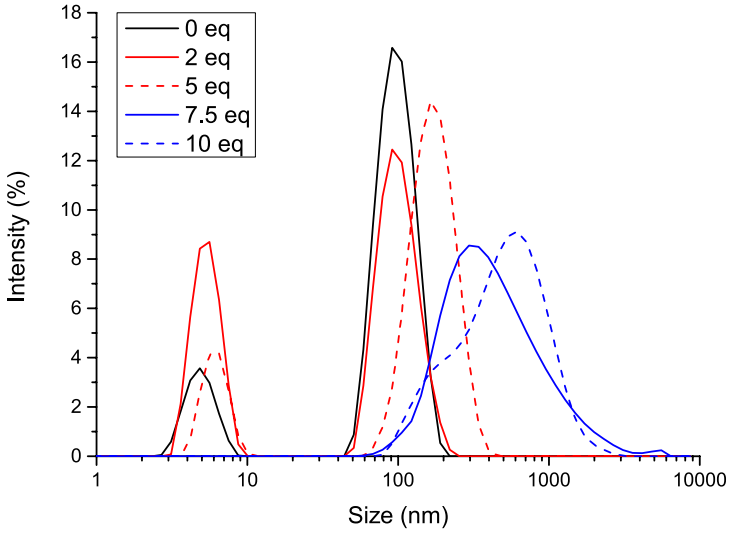

Figure 2.14. DLS spectra of peptide $C_{15}H_{31}C(O)$-[LEELLEE]$_2$G (**10**), showing an increase in size (aggregate formation) after calcium addition.

To verify that the observed aggregate formation was caused by binding of calcium to the peptide, we decided to add the strong calcium binder ethylenediaminetetraacetic acid (EDTA). DLS measurements were performed on a solution of peptide $C_{15}H_{31}C(O)$-[LEELLEE]$_2$G (**10**) with $CaCl_2$ and EDTA. Upon addition of EDTA aggregate formation was not measured anymore, as the size shifted to values comparable to when the peptide solution without calcium was measured. This result confirms that Ca^{2+} actually causes aggregate formation of peptide $C_{15}H_{31}C(O)$-[LEELLEE]$_2$G (**10**) (**Figure 2.15**).

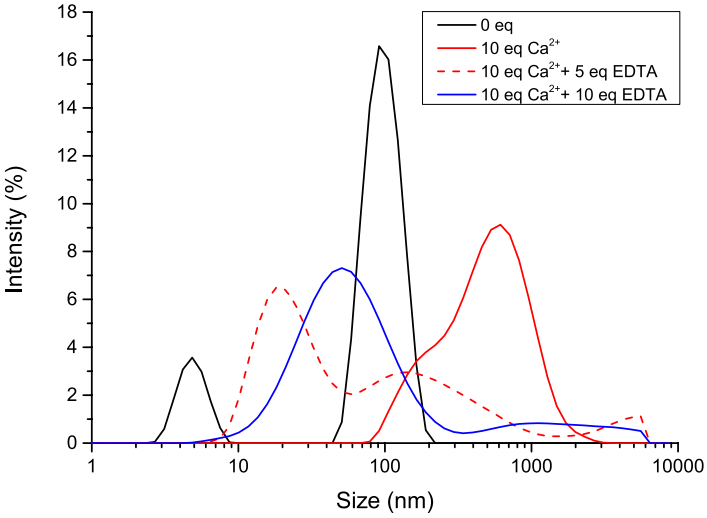

Figure 2.15. DLS spectra of peptide $C_{15}H_{31}C(O)$-[LEELLEE]$_2$G (**10**) after addition of calcium and EDTA. Addition of strong calcium binder EDTA diminishes aggregate formation, giving sizes comparable to peptide only (0 eq).

Table 2.1. Overview of all calcium-binding peptides. Prot. stands for protected, meaning that the peptide is side-chain and N-terminally protected, leaving the C-terminus as the only functional group. Peptides **11-19** will be discussed in **Paragraph 2.4**.

No.	Peptide	Full name
1	GE_7G (protected)	Boc-Gly-[Glu(OtBu)]$_7$-Gly-OH
2	GE_7G	H-Gly-Glu$_7$-Gly-OH
3	Calmodulin domain 2 (prot.) GDADGNGTIDFPE	Boc-Gly-Asp(OtBu)-Ala-Asp(OtBu)-Gly-Asn(Trt)-Gly-Thr(tBu)-Ile-Asp(OtBu)-Phe-Pro-Glu(OtBu)-OH
4	Calmodulin domain 2 GDADGNGTIDFPE	H-Gly-Asp-Ala-Asp-Gly-Asn-Gly-Thr-Ile-Asp-Phe-Pro-Glu-OH
5	Calmodulin domain 3 (prot.) GDKDGNGYISAAEG	Boc-Gly-Asp(OtBu)-Lys(Boc)-Asp(OtBu)-Gly-Asn(Trt)-Gly-Tyr(tBu)-Ile-Ser(tBu)-Ala-Ala-Glu(OtBu)-Gly-OH
6	Calmodulin domain 3 GDKDGNGYISAAEG	Boc-Gly-Asp-Lys-Asp-Gly-Asn-Gly-Tyr-Ile-Ser-Ala-Ala-Glu-Gly-OH
7	G[LEELLEE]$_2$G (prot.)	Boc-Gly-[Leu-Glu(OtBu)-Glu(OtBu)-Leu-Leu-Glu(OtBu)-Glu(OtBu)]$_2$-Gly-OH
8	G[LEELLEE]$_2$G	H-Gly-Leu-Glu-Glu-Leu-Leu-Glu-Glu-Leu-Glu-Glu-Leu-Leu-Glu-Glu-Gly-OH
9	$C_{15}H_{31}$-G[LEELLEE]$_2$G (prot.)	$C_{15}H_{31}C(O)$-Gly-[Leu-Glu(OtBu)-Glu(OtBu)-Leu-Leu-Glu(OtBu)-Glu(OtBu)]$_2$-Gly-OH
10	$C_{15}H_{31}$-G[LEELLEE]$_2$G	$C_{15}H_{31}C(O)$-Gly-Leu-Glu-Glu-Leu-Leu-Glu-Glu-Leu-Glu-Glu-Leu-Leu-Glu-Glu-Gly-OH
11	GEG (prot.)	Boc-Gly-Glu(OtBu)-Gly-OH
12	GEG	H-Gly-Glu-Gly-OH
13	LEL (prot.)	Boc-Leu-Glu(OtBu)-Leu-OH
14	LEL	H-Leu-Glu-Leu-OH
15	AEA (prot.)	Boc-Ala-Glu(OtBu)-Ala-OH
16	AEA	H-Ala-Glu-Ala-OH
17	FFE (prot.)	Boc-Phe-Phe-Glu(OtBu)-OH
18	FEF (prot.)	Boc-Phe-Glu(OtBu)-Phe-OH
19	EFF (prot.)	Boc-Glu(OtBu)-Phe-Phe-OH

2.3. Synthesis and gelation of peptide-polymer constructs

2.3.1. General protocol for the synthesis of peptide-polymer constructs

Now that we analysed the binding properties of several peptides towards calcium (**Table 2.1**), we decided to continue with the synthesis of calcium cross-linkable hydrogels. Since hydrogels are polymeric networks, the next step was to couple the peptides to polymers. The addition of Ca^{2+} should then lead to physically cross-linked peptide-polymer constructs, and hence a hydrogel (**Figure 2.16**).

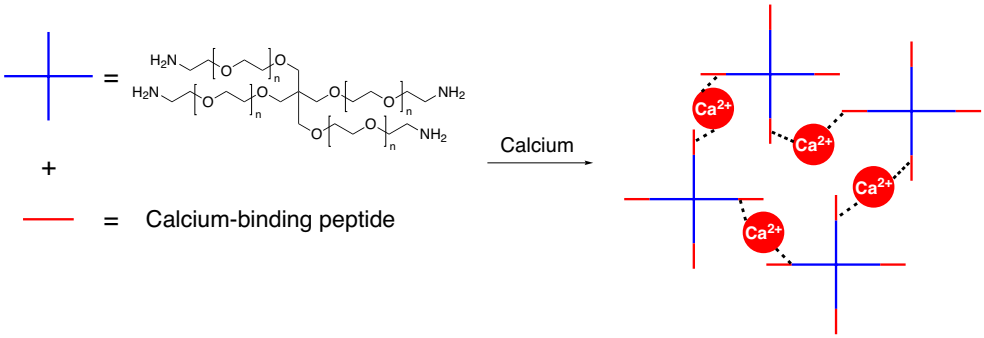

Figure 2.16. Hydrogel formation of a calcium-binding peptide-polymer construct using calcium as cross-linker.

We chose poly(ethylene)glycol (PEG) as the polymeric basis, because of its good water solubility, low immunogenicity and its lack of toxicity (see **Chapter 1**). Our starting compound was a star-shaped 4-armed PEG (star-PEG), each arm end functionalized with an amino group. In order to obtain control over the site of coupling (namely the C-terminus of the peptide) peptide synthesis was performed on a 2-chlorotrityl resin, which enabled us to apply a mild procedure for cleavage. Treatment of the 2-chlorotrityl resin with a mixture of DCM: TFE: HOAc (6:1:1) only cleaves the peptide from the resin, but does not remove any other acid-labile groups. Hence, this mild cleavage procedure afforded a fully side-chain protected peptide. The peptide was also N-terminally modified with a Boc-group, resulting in the C-terminal carboxylic acid as the only available functional group. Linkage of the C-terminus to the amino-groups of star-PEG was performed with coupling reagents BOP and D*i*PEA as a base, forming the native amide bond (**Figure 2.17**). An excess of peptide was used in the coupling reaction, which was easily removed by column chromatography on basic aluminium oxide. The final step in obtaining the peptide-polymer construct was the deprotection of the amino-acid side-chain and the N-terminal Boc-group. This was easily done in one step by treatment of the construct with TFA (**Figure 2.17**).

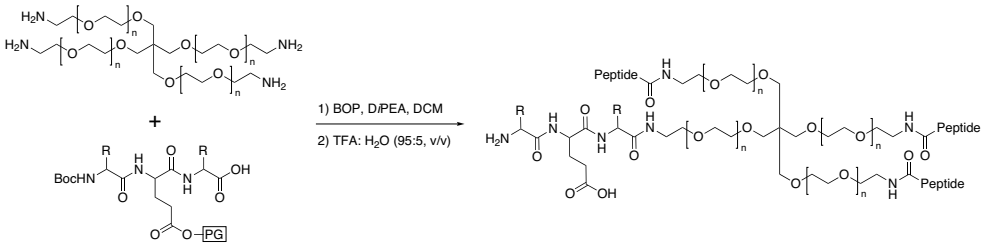

Figure 2.17. Synthesis of peptide-polymer constructs. A fully protected peptide (PG = protecting group) is coupled via an amide bond to star-PEG-NH_2 using BOP and D*i*PEA. TFA cleavage affords the final deprotected peptide-polymer construct.

2.3.2. GE_7G-star-PEG

The coupling procedure was first followed to connect protected peptide Boc-Gly-$[Glu(OtBu)]_7$-Gly-OH (**1**) to star-PEG-NH_2. Completion of the reaction was monitored with TLC analysis; staining with ninhydrin showed disappearance of the free amino groups. Analysis of the Boc-Gly-$[Glu(OtBu)]_7$-Gly-star-PEG construct (**20**) was performed with NMR and MALDI-TOF. The same techniques were used after TFA treatment and confirmed the synthesis of the final (unprotected) peptide-polymer construct (**21**). The next step was to add calcium to star-PEG-GE_7G (**21**) to investigate if a polymeric network could be formed, hence whether calcium functions as physical cross-linker. First, a 5 mg/mL solution of GE_7G-star-PEG (**21**) was used in MilliQ. A cloudy solution was obtained which disrupted the visual analysis of the effect of calcium addition. Attempts to improve the solubility of construct **21** by changing the solvent to Tris buffer (pH 8.9), HEPES buffer (pH 7.1) or basic H_2O (pH 10) failed. Finally, GE_7G-star-PEG (**21**) appeared to be soluble in a 1M NaOH solution and also remained soluble upon further dilution in HEPES buffer. Via this method, a 1 wt% (10 mg/mL) clear solution was prepared to which stepwise increasing equivalents of calcium (0.5 – 10 eq) were added. Since gel formation was not observed after two days, we increased the concentration of peptide-polymer construct **21** to 5 wt%. Addition of calcium ions quickly caused formation of a precipitate. Calcium was added up to 20 equivalents, but despite precipitate formation, we did not observe any gelation. These experiments were also performed at a temperature of 37°C and with 10 wt% GE_7G-star-PEG (**21**), but this gave the same results. Probably, precipitation is caused by the formation of $Ca(OH)_2$. As a final attempt, a 10 wt% solution was prepared in concentrated ammonia (25%). A clear solution remained after addition of an aqueous solution of calcium. Unfortunately, addition of increasing amounts of calcium still did not result in gel formation.

2.3.3. Calmodulin-star-PEG-constructs

The second series of peptide-polymer constructs were based on the calmodulin domains 2 and 3 (GDADGNGTIDFPE and GDKDGNGYISAAEG) as these peptides were obtained in a pure form by solid phase peptide synthesis. The standard coupling procedure was used for linkage of protected domain 2 (**3**) to star-PEG-NH_2. Problems were encountered during the work-up, as the construct appeared to be hardly soluble in DCM. Due to this solubility problem, purification of the peptide-polymer (**22**) conjugate via column chromatography on basic Al_2O_3 did not work, also not via pre-adsorption of the compound on celite. Unfortunately, these solubility problems also occurred for the polymer with calmodulin domain 3 (**23**). Since deprotection of the amino-acid side chains changes the solubility of the calmodulin 3-star-PEG construct (**23**), a cleavage procedure with TFA was carried out. After evaporation of TFA, dialysis was performed using a dialysis bag with a molecular weight cut off of 3500 Da. Unbound peptide has a lower molecular weight and was therefore expected to be removed from the sample. To check whether the pure material was obtained after dialysis, size-exclusion chromatography (SEC)

was performed. In order to be able to analyse the spectra, first the deprotected calmodulin domain 3 (**6**) was analysed on SEC, which gave a clear peak at Rt = 9.05 min. As a reference, also the starting material star-PEG-NH_2 was measured on SEC. Due to the absence of any UV-active groups; it could not be visualized on SEC. A solution to this problem was found by linkage of the UV-active benzoyl chloride. Analysis of star-PEG-benzoyl gave a peak with Rt = 8.10 min. This retention time was used as reference point, as the larger peptide-polymer construct should have a faster elution.

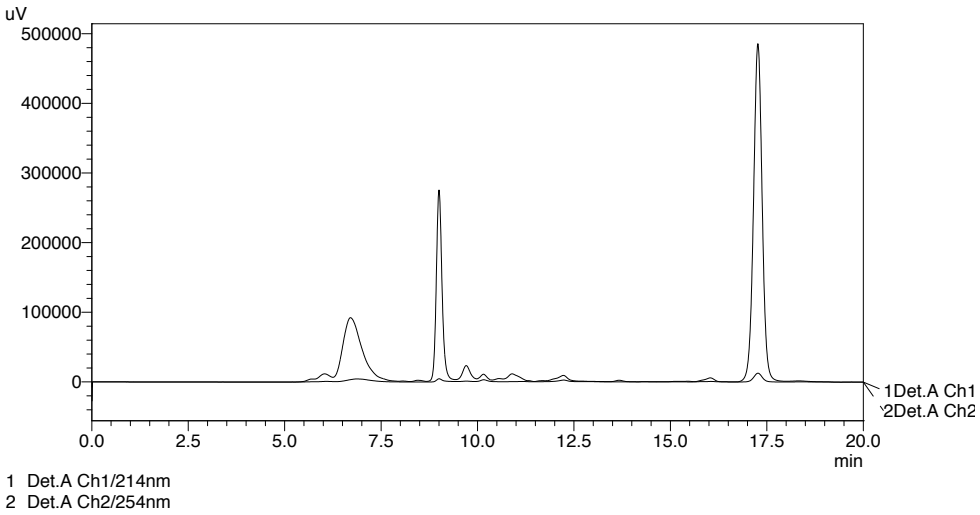

Figure 2.18. Analytical size exclusion (SEC) chromatogram of the peptide-polymer construct with calmodulin domain 3. The product (**23**; Rt = 6.70 min) is contaminated with the excess of peptide (**6**; Rt = 9.00 min). Ch1 is the spectrum recorded at 214 nm, channel 2 is obtained at 254 nm.

Analytical SEC of the dialysed calmodulin 3-star-PEG (**23**) gave peaks at 6.70, 9.00 and 17.264 min (**Figure 2.18**). This clearly shows that dialysis was not successful for removal of the excess peptide. SEC also indicated formation of the product, as the peak at 6.70 min belongs to a compound that is larger in size than starting material star-PEG-NH_2. Preparative use of the SEC column afforded the isolation of polymer-peptide construct **23** (**Figure 2.19**). MALDI-TOF analysis of this product resulted in a broad peak with a mass lower than calculated. This indicates that coupling of the peptide was less efficient than expected. Despite the lower mass, a gelation test was performed with calmodulin 3-star-PEG (**23**). Since the purification method afforded only little amounts of material, a 2 wt% solution was tested. The construct was readily soluble in water, but unfortunately addition of calcium did not result in gelation. Because purification of the calmodulin polymers was found to be tedious and time-consuming, we decided to abandon this approach.

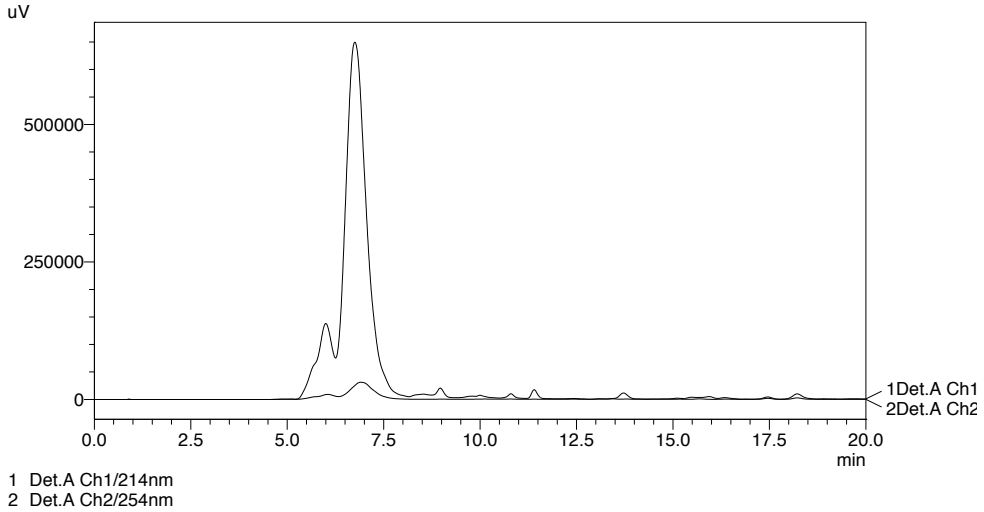

Figure 2.19. Preparative size exclusion (SEC) chromatography afforded the pure peptide-polymer construct with calmodulin domain 3 (**23;** Rt = 6.75 min). Ch1 is the spectrum recorded at 214 nm, channel 2 is obtained at 254 nm.

2.3.4. G[LEELLEE]$_2$G-star-PEG

Protected peptide Boc-G[LEELLEE]$_2$G (**7**) was coupled to star-PEG-NH_2 using the standard coupling reagents BOP and D*i*PEA in DMF. TLC analysis confirmed conversion to the peptide-polymer construct (**24**). As for the calmodulin peptides, the obtained product was insoluble in DCM. The compound was therefore first deprotected using TFA. Dialysis was then carried out to try to remove the excess of peptide **8**. SEC analysis revealed peaks at Rt = 7.09 min and Rt = 10.74 min. The deprotected peptide (**8**) gave the same retention time around 10.7 min, implying that dialysis was not successful for purification. SEC analysis was performed using an isocratic flow composed of 55% MilliQ and 45% acetonitrile. In order to be able to use this method preparatively, the construct needs to soluble in the H_2O/MeCN mixture. Polymer G[LEELLEE]$_2$G-star-PEG (**24**) had very low solubility in the solvent mixture, making purification using preparative SEC impossible. Since peptide G[LEELLEE]$_2$G (**8**) was found to have promising calcium binding properties, it was disappointing to see that the peptide-polymer construct (**24**) could not be purified and therefore gelation studies could not be carried out. Due to the severe solubility and purification problems with G[LEELLEE]$_2$G, we decided not to continue with the synthesis of the polymer construct with alkyl functionalized peptide $C_{15}H_{31}C(O)$-[LEELLEE]$_2$G (**10**).

2.3.5. Discussion

A range of calcium-binding peptides were selected based on motifs found in Ca^{2+}-binding proteins (**Table 2.1**). The synthesis of these peptides was successfully accomplished. The calcium binding properties were measured using ITC, DLS and CD analysis. For some peptides, it was difficult to be conclusive about the ability to bind calcium, based on contradictory results obtained by the used techniques. On the other hand, for some peptides both aggregation upon calcium addition was measured (DLS) and Ca^{2+}-binding was established via ITC. We decided to evaluate all peptides of which at least one technique showed interaction with Ca^{2+} for their ability to form Ca^{2+} cross-linked hydrogels. For this purpose, we started with the synthesis of peptide-polymer constructs. GE_7G-star-PEG (**21**) was successfully obtained and was therefore used in gelation studies. Unfortunately, its solubility in aqueous solutions was problematic, and in the end addition of calcium did not result in gel formation. Synthesis of the peptide-polymer constructs with the calmodulin peptides (**22, 23**) and with $G[LEELLEE]_2G$ (**24**) was troublesome. These constructs appeared to have a very low solubility, making purification difficult or even impossible. In conclusion, only the synthesis and purification of GE_7G-star-PEG (**21**) was successful, but gelation did not occur. A possible explanation for the lack of gelation could be that calcium binding can occur both intermolecularly as well as intramolecularly. Gelation can only occur when a polymeric network is formed, hence when calcium makes intermolecular connections. A problem occurs when calcium makes intramolecular bonds, between the anionic groups within a peptide, or between peptides connected to two arms of one star-PEG molecule. In both cases, calcium binding occurs, but calcium does not provide the physical connection between two polymers. A second explanation for the lack of gelation could be that the tested conditions are not ideal, in terms of pH or polymer concentration. The final reason to explain that addition of calcium to GE_7G-star-PEG (**21**) did not give a hydrogel, is that binding simply is not efficient enough to make sufficient physical cross-links to form a polymeric network. This seems to be the most likely explanation, since ITC data of peptide GE_7G (**2**) with calcium indicated weak binding and only a small shift was recorded with DLS analysis. To confirm this hypothesis, we decided to gain further information on the gelation process, by studying short anionic peptides, aiming to prevent intramolecular cross-linking (see **Paragraph 2.4**).

2.4. Short anionic peptides

A new approach was taken by using short anionic peptides. This idea was inspired on research by the Ulijn group, who showed the gelation of the short aromatic peptide Fmoc-Phe_2 (see **Chapter 1**).[23,24] Despite the fact that intramolecular calcium binding between two arms of a star-PEG molecule cannot be prevented, this new approach eliminates the intramolecular

binding within a peptide. Hopefully, this approach forces intermolecular calcium binding, and thus the formation of a network. Moreover, solubility and purification problems are less likely to occur with smaller peptides. Based on the previous GE_7G peptide (**2**), we first decided to synthesize short peptide Boc-Gly-Glu(OtBu)Gly (**11**; GEG). Since synthesis of these small peptides was easy using SPPS, protected analogues LEL and AEA (**13, 15**) were also prepared (**Figure 2.20**). This allows investigating whether introducing less or more hydrophobicity has an influence on the ability to bind calcium. Inspired by work of the Ulijn group, peptides containing both anionic and aromatic peptides were synthesized. Peptides Boc-Phe-Phe-Glu(OtBu) (**17**; FFE) and protected analogues FEF (**18**) and EFF (**19**) were afforded pure after SPPS (**Figure 2.20**).

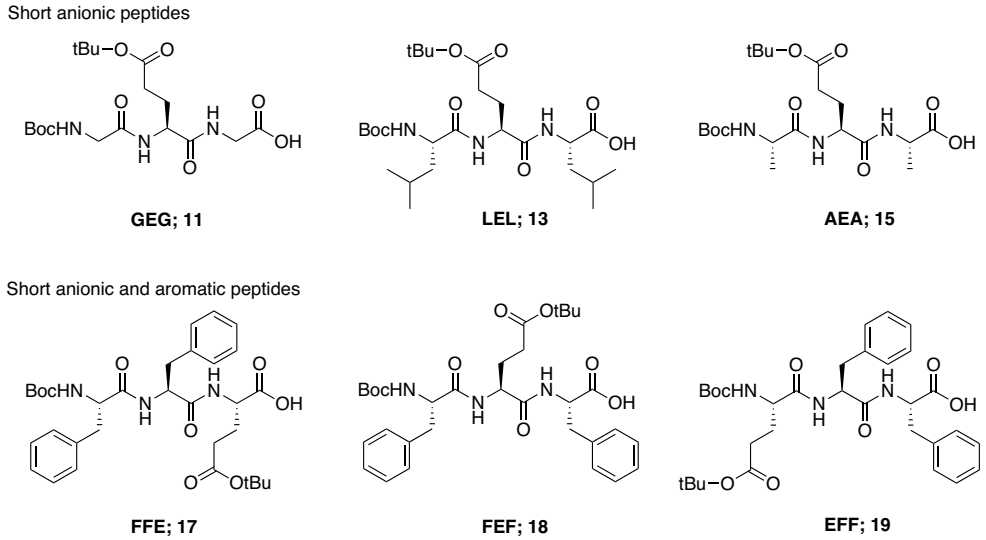

Figure 2.20. Overview of the protected short anionic (and aromatic) peptides.

The calcium binding properties of the first set of peptides GEG, LEL and AEA (**12, 14, 16**) was determined using ITC analysis. For all three peptides, the obtained spectra looked random, as if they were background samples (data not shown). Since these short peptides do not have a secondary structure and aggregation is not likely to occur, we did not measure CD and DLS, but instead directly continued with the synthesis of the peptide-polymer construct. All the protected short anionic (and aromatic) peptides (**11, 13, 15, 17, 18** and **19**) were linked to star-PEG-NH_2 using standard coupling reagents (Py)BOP and D*i*PEA. Purification was readily performed using column chromatography, after which TFA treatment gave the final deprotected peptide-polymer constructs (**26, 28, 30, 32, 34** and **36**). Gelation studies with calcium were first performed for solutions of GEG-star-PEG (**26**), LEL-star-PEG (**28**) and AEA-star-PEG (**30**) in water. A high total polymer content, 15 wt%, was tested. Addition of calcium was performed

stepwise, first 1 equivalent $CaCl_2$ and then stepwise to a total of 4 eq. With an excess of calcium (4 eq) precipitate formation was seen, however, the viscosity of the solution did not change. The same procedure was used for gelation studies with FFE-star-PEG (**32**), FEF-star-PEG (**34**) and EFF-star-PEG (**36**), and apart from MilliQ a 15 wt% solution was also prepared in Tris buffer (pH 9.0). In all cases, no effects were seen after addition of up to 5 eq calcium. Gelation mediated by short (and aromatic) peptide polymers could therefore not be demonstrated using calcium as cross-linker.

2.5. Conclusion

In this chapter, we aimed for the development of synthetic calcium-cross-linkable polymers. Several bio-inspired peptides were successfully synthesized and then analysed with circular dichroism (CD) spectroscopy, isothermal calorimetry (ITC) and dynamic light scattering (DLS) to determine their calcium-binding properties. Although it was difficult to be conclusive about the binding with Ca^{2+}, we evaluated all peptides of which at least one technique showed interaction. These peptides were coupled to polymer star-poly(ethylene)glycol (PEG) to obtain peptide-polymer constructs. The constructs with the calmodulin peptide (**22, 23**) and with peptide $G[LEELLEE]_2G$ (**24**) could not be used in gelation studies due to purification problems. The peptide-polymers with oligo-glutamate GE_7G (**21**) and with short anionic peptides (GEG **26**, LEL **28**, AEA **30**, FFE **32**, EFF **34** and FEF **36**) were successfully obtained. Their ability to make a physically cross-linked hydrogel was tested by addition of $CaCl_2$ to a solution of the peptide-polymers in water or in a basic solvent. None of the tested constructs formed a hydrogel. Based on our observations and the data obtained with CD, ITC and DLS analysis, we draw the conclusion that the interaction of calcium with GE_7G (**2**) or with the short anionic peptides is not strong enough to make physical connections between the polymers. The calcium-binding ability of the peptide-polymer constructs is too weak to make a calcium cross-linked hydrogel. Therefore, we first decided to focus on chemically cross-linked hydrogels, as will be described in **Chapters 3, 4** and **5**. New insights in the field of hydrogels gave us reason to return to physically cross-linked systems, as explored in **Chapter 6**.

2.6. Acknowledgement

Lindsey Lelieveld is acknowledged for her help with the calcium-binding studies.

2.7. Materials and methods

The 2-chlorotrityl resin was purchased from Bachem (Bubendorf, Switzerland) and Fmoc-L-amino acids were purchased from Novabiochem (EMD Chemicals, Gibbstown, USA) or Bachem. 4-Armed poly(ethylene glycol)-NH_2 (10 kDa) salt was obtained from JenKem Technology (USA). All other chemicals were purchased from Sigma-Aldrich, Baker or Fluka and utilized as received. Column chromatography was performed with Silica gel 60 (particle size 0.040 – 0.063 mm Merck) or aluminum oxide (basic activated, pore size 58 Å, Sigma-Aldrich). Thin-layer chromatography (TLC) was performed on silica gel coated plates (Merck 60, F-254). Visualization was accomplished with UV-light and/or ninhydrin or permanganate staining. MilliQ water was purified using a WaterPro PS Polisher (Labconco), set to 18.2 MΩ/cm.

^{1}H NMR spectra were recorded on a Varian Mercury (400 MHz). As a solvent shift reference, we used $CDCl_3$ (δ = 7.26 ppm), and D_2O (δ = 4.79 ppm). Mass spectra were recorded on a Thermo Finnigan LCQ-Advantage MAX or on a Bruker Biflex MALDI-TOF (Bruker Daltronik, Bremen, Germany). As matrix, α-cyano-4-hydroxycinnamic acid or dithranol were used. LC-MS was performed on a Thermo Finnigan LCQ-Fleet ESI-ion trap (Thermo Fischer, Breda, The Netherlands) equipped with a Phenomenex C18 column, 50 x 2.0 mm, particle size 3 µM (Phenomenex, Utrecht, The Netherlands). An acetonitrile/water gradient containing 0.1% formic acid was used for elution (5-100%, 1-10 min, flow 0.2 mL/min).

Analytic HPLC was performed on a Shimadzu LC-20A Prominence system (Shimadzu, 's Hertogenbosch, The Netherlands) equipped with a C18 Reprosil column, 150 x 3 mm, particle size 3 µm (Dr. Maisch GmbH, Screening Devices, Amersfoort, The Netherlands). Elution of the peptides was achieved using an acetonitrile/water gradient containing 0.1% trifluoroacetic acid (5-100% MeCN, 1-31 min, flow 0.4 mL/min). Preparative HPLC was performed on a Shimadzu LC-20A system equipped with a Reprosil C18 column, 250 x 20 mm (particle size: 10 µm) or 250 x 10 mm (particle size: 5 µm) (both: Dr. Maisch GmbH). Elution was achieved using an acetonitrile/water gradient containing 0.1% trifluoroacetic acid (5-100% MeCN, 5-55 min, flow 8 mL/min or 4 mL/min). Analytical and preparative SEC were performed on the Shimadzu HPLC systems, using a BioSep SEC-s2000 column (particle size 5 µm, pore size 150 Å, Phenomenex). An isocratic elution was performed for 20 min with 45% acetonitrile and 55% water (containing 0.1% TFA).

CD spectra were recorded on a Jasco J-815 spectropolarimeter equipped with a Jasco PFD-425S Peltier type temperature control system. ITC experiments were performed on a fully automated isothermal titration calorimeter (Microcal Auto-iTC200, GE Healthcare). DLS measurements were carried out on a Malvern instruments Zetasizer Nano-S (ZEN 1600). Lyophilization was achieved using an ilShin Freeze Dryer (ilShin, Ede, The Netherlands).

General procedure 1: Peptide synthesis (SPPS)

Peptides were synthesized from 1.0 g 2-chloro-trityl resin using Fmoc solid-phase peptide synthesis (SPPS). The resin was swollen in DCM for 20 min prior to use. Functionalization of the resin with the first amino acid was performed for 60 min with 2.0 eq of the required amino acid and 3.0 eq N,N-diisoproylethylamine (D*i*PEA). After the coupling reaction, capping of the resin was performed with 2.0 eq D*i*PEA in methanol. Deprotection of the Fmoc-groups was carried out with piperidine in DMF (20%, v/v) for 20 min. Subsequent couplings were performed for 45 min with 3.0 eq of the required amino acid, 3.3 eq of *N,N'*-diisopropylcarbodiimide (DIPCDI) and 3.6 eq of *N*-hydroxybenzotriazole (HOBt) in DMF. After each coupling and deprotection step, a Kaiser test was done to ensure completion of the reaction.[25] Two different cleavage protocols were applied to remove peptides from the resin, a mild procedure using acetic acid and a TFA-cleavage protocol. The mild cleavage was performed in order to ensure that the acid-labile protecting groups remained intact. Mild cleavage was performed by treatment of the resin with a mixture of dichloromethane (DCM), trifluoroethanol (TFE) and acetic acid (HOAc) (6:1:1) for 3 h. The solvents were evaporated under reduced pressure and co-evaporation was performed with chloroform (3 x 40 mL). Peptides were afforded as white solids after freeze-drying from dioxane. For the TFA-cleavage protocol, the resin was treated with a mixture of TFA: triisopropylsilane (TIS): H_2O (95: 2.5: 2.5) for 3h at r.t. Peptides were afforded by precipitation in Et_2O, followed by freeze-drying from water.

General procedure 2A: Synthesis peptide-polymer constructs (column chromatography)

To star-poly(ethylene glycol)-NH_2 HCl salt (200 mg, 20 µmol) in DCM (20 mL) was added subsequently BOP (53 mg, 6 eq, 120 µmol), protected peptide (6 eq, 120 µmol), and D*i*PEA 82 µL, 24 eq, 0.48 mmol). The reaction mixture was stirred overnight at r.t. Extraction was performed with 1 M $KHSO_4$ (3 x 40 mL) and brine (1 x 40 mL), after which the organic layer was dried over Na_2SO_4. Column chromatography on basic aluminum oxide (MeOH: DCM; 10:90) afforded the protected peptide-polymer construct as a white powder after freeze-drying from dioxane.

General procedure 2B: Deprotection peptide-polymer constructs

Deprotection of the peptide-polymer construct (200 mg) was performed by treatment with TFA: H_2O (95:5; 10 mL) for 4 h at r.t. The reaction mixture was concentrated and co-evaporated with toluene (3 x 30 mL). The product was dialysed against water using a membrane with a MW cut-off of 3500 Da. Dialysis was performed for 3 days under regular exchange of the water (twice a day). Freeze drying afforded the product as a white solid.

General procedure 3: Synthesis peptide-polymer constructs (SEC)

To star-poly(ethylene glycol)-NH_2 HCl salt (75 mg, 7.5 µmol) in DMF (10 mL) was added subsequently PyBrOP (21 mg, 6 eq, 45 µmol), protected peptide (6 eq, 45 µmol), and D*i*PEA 31 µL, 24 eq, 180 µmol). The reaction mixture was stirred overnight at r.t. Evaporation of the DMF was performed under reduced pressure at 50°C. The residue was directly treated with a mixture of TFA: TIS: H_2O (95: 2.5: 2.5; 5 mL) for 4 h at r.t. The product was dissolved in water: MeOH (1:1) and dialysed against 800 mL water using dialysis membranes with a MW cut-off of 3500 Da. Dialysis was performed for 2 days under regular exchange of the water/MeOH mixture (twice a day). After dialysis, the products were obtained as white solids by freeze-drying. Analytical SEC was performed to check the purity of the peptide-polymer construct. If possible, purification was performed by preparative SEC using an isocratic elution (45% MeCN; 55% H_2O, containing 0.1% TFA). Samples were prepared in the same solvent mixture (20 mg in 5 mL).

CD measurements

CD spectra were measured from 250 – 190 nm at 20°C using a 1 mm quartz cuvette. Peptide solutions were prepared in Tris buffer (0.17 mM, pH 8.9) at final concentrations of 0.2 mg/mL. To the peptide solution, varying amounts of calcium chloride were added. For peptide GE_7G, a $CaCl_2$ concentration range of 0 – 16 eq was added. For peptides $[LEELLEE]_2G$ and $C_{15}H_{31}C(O)$-$[LEELLEE]_2G$, 0 – 10 eq $CaCl_2$ were added. Final spectra were obtained by subtracting the background spectrum obtained for the buffer.

ITC measurements

Prior to the ITC measurements, peptides were purified using preparative HPLC. All ITC experiments were carried out in HEPES buffer (20 mM, pH 7.1). Peptide solutions were loaded in the cell (400 µL), $CaCl_2$ solutions in the syringe (200 µL) and the HEPES buffer was added to the reference cell. ITC measurements were carried out using a temperature of 25°C, a reference power of 10 µCal/sec, a scanning time of 150 s and a rotation speed of 1000 rpm. Titrations comprising 19 injections (2 µL) were carried out from the syringe into the cell. For peptides GE_7G and calmodulin domain 3, a peptide solution of 100 µM was measured with $CaCl_2$ concentrations of 1.25, 2.5 and 5.0 mM. Calmodulin domain 2 was measured in a concentration of 500 µM with 1.25, 2.5, 5.0 and 10 mM $CaCl_2$. Peptide $G[LEELLEE]_2G$ was measured at 100 µM with 1.25 mM $CaCl_2$. For the short anionic peptides GEG, LEL and AEA, peptide concentrations of 100 µM were measured with a $CaCl_2$ range of 0.5, 1.0, 2.0 and 5.0 mM.

DLS measurements

DLS measurements were performed in a 1 mL cuvette in HEPES buffer (20 mM, pH 7.1). Peptide solutions of 1 mM were measured with a calcium concentration range of 0 – 10 eq. For each experiment, three runs were performed with 10 measurements of 10 sec each. Final graphs were created based on the average of the three runs. For peptide $C_{15}H_{31}$-[LEELLEE]$_2$G, EDTA was added to the peptide/calcium solution (5 eq, 10 eq). For peptide calmodulin domain 2, a concentration of 100 µM was measured, with 2.5 mM $CaCl_2$.

Synthesis of the peptides

Boc-Gly-[Glu(OtBu)]$_7$-Gly-OH (1)

The peptide was synthesized according to general procedure 1 using 4.60 g 2-chlorotrityl resin. Cleavage from the resin was performed using the mild procedure and afforded the peptide (**1**) as white powder after freeze-drying.

LCQ: m/z: 1528.3 $[M + H]^+$ (calculated $[M + H]^+$ = 1528.8)

LC-MS: m/z: 1528.1 $[M + H]^+$, Rt = 12.50 min

HPLC: Rt = 20.74 min

^{1}H-NMR (400 MHz, $CDCl_3$): δ = 1.24 – 1.50 (m, 72H, C$\underline{H}_3$), 1.94 – 2.63 (m, 28H, (C$\underline{H}_2$)$_2$ OtBu), 3.74 – 4.50 (m, 11H, 7 C$\underline{H}$ (Cα), BocHN-C$\underline{H}_2$, C$\underline{H}_2$COOH).

H-Gly-Glu$_7$-Gly-OH (2)

The peptide was synthesized using general procedure 1 and cleaved from the resin using a mixture of TFA: H_2O (95:5) for 3h. The peptide could also be afforded by TFA-treatment of the protected peptide (Boc-Gly-[Glu(OtBu)]$_7$-Gly-OH) (**1**). In both cases, precipitation in ether followed by freeze-drying from water provided the deprotected peptide (**2**).

LCQ: m/z: 1036.3$[M + H]^+$ (calculated $[M + H]^+$ = 1036.4)

LC-MS: m/z: 1036.28 $[M + H]^+$, Rt = 2.55 min

LC-MS (MS/MS): MS^2 m/z: 961.13 $[M – G – H_2O]^+$; 832.05 $[M – EG – H_2O]^+$; 702.99 $[M – EEG – H_2O]^+$. MS^3 m/z: 574.00 $[M – EEEG – H_2O]^+$; 427.03 $[M – EEEEG – 2H_2O]^+$; 316.03 $[M – EEEEEG – H_2O]^+$

HPLC: Rt = 2.48 min

Calmodulin binding domain 2 – GDADGNGTIDFPE (protected) (3)

Boc-Gly-Asp(OtBu)-Ala-Asp(OtBu)-Gly-Asn(Trt)-Gly-Thr(tBu)-Ile-Asp(OtBu)-Phe-Pro-Glu(OtBu)-OH

General procedure 1 was followed for synthesis of calmodulin binding domain 2, using the mild cleavage procedure.

LCQ: m/z: 1952.6 $[M + Na]^+$ (calculated $[M + H]^+$ = 1930.01)
LC-MS: m/z: 1930.00 $[M + H]^+$, Rt = 12.44 min HPLC: Rt = 27.12 min
MALDI-TOF (dithranol): m/z: 1952.0 $[M + Na]^+$
HPLC: Rt = 27.12 min

Calmodulin binding domain 2 – GDADGNGTIDFPE (4)
H-Gly-Asp-Ala-Asp-Gly-Asn-Gly-Thr-Ile-Asp-Phe-Pro-Glu-OH
Protected calmodulin domain 2 (**3**) was treated with a mixture of TFA: TIS: H_2O (95: 2.5: 2.5) for 4h at r.t. The peptide was precipitated in diethyl ether and obtained as a white solid after drying (air).
LCQ: m/z: 1307.6 $[M + H]^+$ (calculated $[M + H]^+$ = 1307.53)
LC-MS: m/z: 1308.08 $[M + H]^+$, Rt = 6.44 min
HPLC: Rt = 14.52 min
SEC: Rt = 9.71min

Calmodulin binding domain 3 – GDKDGNGYISAAEG (protected) (5)
Boc-Gly-Asp(OtBu)-Lys(Boc)-Asp(OtBu)-Gly-Asn(Trt)-Gly-Tyr(tBu)-Ile-Ser(tBu)-Ala-Ala-Glu(OtBu)-Gly-OH
General procedure 1 was followed for synthesis of calmodulin binding domain 3, using the mild cleavage procedure.
LCQ: m/z: 1038.8 $[M + H]^{2+}$ (calculated $[M + H]^+$ = 2076.11, $[M + H]^{2+}$ = 1038.56)
LC-MS: m/z: 1038.84 $[M + H]^{2+}$, Rt = 12.68 min
HPLC: Rt = 25.52 min

Calmodulin binding domain 3 – GDKDGNGYISAAEG (6)
Boc-Gly-Asp-Lys-Asp-Gly-Asn-Gly-Tyr-Ile-Ser-Ala-Ala-Glu-Gly-OH
Protected calmodulin domain 3 (**5**) was treated with a mixture of TFA: TIS: H_2O (95: 2.5: 2.5) for 4h at r.t. The peptide was precipitated in diethyl ether and obtained as a white solid after drying (air).
LCQ: m/z: 1353.5 $[M + H]^+$ (calculated $[M + H]^+$ = 1353.58)
LC-MS: m/z: 1353.76 $[M + H]^+$, Rt = 3.14 min
HPLC: Rt = 12.15 min
SEC: Rt = 9.05 min

Boc-Gly-[Leu-Glu(OtBu)-Glu(OtBu)-Leu-Leu-Glu(OtBu)-Glu(OtBu)]$_2$-Gly-OH (protected) (7)
General procedure 1 was followed using 1.5 g 2-chlorotrityl resin. Cleavage was performed using the mild procedure.

LCQ: m/z: 1196.9 $[M + H]^{2+}$, calculated $[M + H]^{2+}$ = 1196.73)
MALDI-TOF (dithranol): m/z: 2414.8 $[M + Na]^{+}$, calculated $[M + Na]^{+}$ = 2414.45
HPLC: Rt = 33.88 min

H-G[LEELLEE]$_2$G-OH (8)
H-Gly-Leu-Glu-Glu-Leu-Leu-Glu-Glu-Leu-Glu-Glu-Leu-Leu-Glu-Glu-Gly-OH
General procedure I was used for peptide synthesis, followed by TFA cleavage. After precipitation, the peptide was further purified by prep-HPLC.
LCQ: m/z: 1844.5 $[M + H]^{+}$ (calculated $[M + H]^{+}$ = 1843.90)
LC-MS: m/z: 1844.52 $[M + H]^{+}$, 922.68 $[M + H]^{2+}$, Rt = 9.11 min
HPLC: Rt = 22.01 min

$C_{15}H_{31}C(O)$-Gly-[Leu-Glu(OtBu)-Glu(OtBu)-Leu-Leu-Glu(OtBu)-Glu(OtBu)]$_2$-Gly-OH (protected) (9)
General procedure I was followed using 1.5 g 2-chlorotrityl resin. In the final step, palmitic acid (3.0 eq) was coupled using DIPCDI (3.3 eq) and HOBt (3.6 eq). Cleavage was performed using the mild procedure.
LCQ: m/z: 1237.5 $[M + H]^{2+}$, 1260.4 $[M + Na]^{2+}$ (calculated $[M + H]^{2+}$ = 1237.31)
MALDI-TOF (dithranol): m/z: 2496.1 $[M + Na]^{+}$, calculated $[M + Na]^{+}$ = 2495.61

$C_{15}H_{31}C(O)$-Gly-[Leu-Glu-Glu-Leu-Leu-Glu-Glu]$_2$-Gly-OH (10)
General procedure I was used for peptide synthesis. In the final step, palmitic acid (3.0 eq) was coupled using DIPCDI (3.3 eq) and HOBt (3.6 eq). Cleavage was performed using TFA.
LCQ: m/z: 1013.4 $[M + H]^{2+}$ (calculated $[M + H]^{2+}$ = 1013.06)
HPLC: Rt = 31.69 min

Boc-Gly-Glu(OtBu)-Gly-OH (protected) (11)
General procedure I (1.0 g resin), followed by the mild cleavage procedure.
LCQ: m/z: 417.9 $[M + H]^{+}$; 857.0 $[2M + Na]^{+}$ (calculated $[M + H]^{+}$ = 418.21)
LC-MS: m/z: 417.88 $[M + H]^{+}$, 834.92 $[2M + H]^{+}$, Rt = 7.92 min
HPLC: Rt = 17.11 min
^{1}H-NMR (400 MHz, CD_3OD): δ = 1.42 – 1.52 (m, 18H, CH_3), 1.92 & 2.16 (2m, 2H, Cα-C$\underline{H}_2$-CH_2), 2.37 (m, 2H, Cα-CH_2-C$\underline{H}_2$), 3.74 (s, 2H, BocHN-C$\underline{H}_2$), 3.92 (s, 2H, C$\underline{H}_2$COOH), 4.49 (m, 1H, Cα)

H-Gly-Glu-Gly-OH (12)
General procedure I (1.0 g resin), followed by the TFA-cleavage procedure.
LCQ: m/z: 261.9 $[M + H]^{+}$, 522.9 $[2M + H]^{+}$ (calculated $[M + H]^{+}$ =262.10)
HPLC: Rt = 2.53 min

Boc-Leu-Glu(OtBu)-Leu-OH (protected) (13)

General procedure I (1.0 g resin), followed by the mild cleavage procedure.
LCQ: m/z: 529.9 $[M + H]^+$, 1081.2 $[2M + Na]^+$ (calculated $[M + H]^+ = 530.34$)
LC-MS: m/z: 530.00 $[M + H]^+$, 1059.08 $[2M + H]^+$, Rt = 9.90 min
HPLC: Rt = 22.66 min
^{1}H-NMR (400 MHz, $CDCl_3$): δ = 0.84 – 1.00 (m, 12H, CH_3 (Leu)), 1.36 – 1.53 (s, 18H, CH_3 (Boc, OtBu)), 1.56 – 1.79 (m, 6H, CH_2, CH (Leu)), 1.96 & 2.08 (2m, 2H, Cα-C$\underline{H}_2$-CH_2 (Glu)), 2.40 (m, 2H, Cα-CH_2-C$\underline{H}_2$ (Glu)), 4.40 – 4.55 (m, 3H, 3 Cα).

H-Leu-Glu-Leu-OH (14)

General procedure I (1.0 g resin), followed by the TFA-cleavage procedure.
LCQ: m/z: 374.1 $[M + H]^+$, 747.1 $[2M + H]^+$ (calculated $[M + H]^+ = 374.22$)
HPLC: Rt = 12.95 min

Boc-Ala-Glu(OtBu)-Ala-OH (protected) (15)

General procedure I (1.0 g resin), followed by the mild cleavage procedure.
LCQ: m/z: 445.9 $[M + H]^+$, 913.1 $[2M + Na]^+$ (calculated $[M + H]^+ = 446.24$)
LC-MS: m/z: 445.96 $[M + H]^+$, 890.92 $[2M + H]^+$ Rt = 8.18 min
HPLC: Rt = 17.88 min
^{1}H-NMR (400 MHz, $CDCl_3$): δ = 1.26 – 1.57 (m, 24H, CH_3), 1.92 & 2.10 (2m, 2H, Cα-C$\underline{H}_2$-CH_2), 2.38 (m, 2H, Cα-CH_2-C$\underline{H}_2$), 4.07 (m, 1H, Cα), 4.33 – 4.46 (m, 2H, 2 Cα).

H-Ala-Glu-Ala-OH (16)

General procedure I (1.0 g resin), followed by the TFA-cleavage procedure.
LCQ: m/z: 289.9 $[M + H]^+$, 579.0 $[2M + H]^+$ (calculated $[M + H]^+ = 290.13$)
HPLC: Rt = 2.66 min

Boc-Phe-Phe-Glu(OtBu)-OH (protected) (17)

General procedure I (1.0 g resin), followed by the mild cleavage procedure.
LCQ: m/z: 597.9 $[M + H]^+$, 1194.9 $[2M + H]^+$ (calculated $[M + H]^+ = 598.31$)
LC-MS: m/z: 598.08 $[M + H]^+$, 1195.24 $[2M + H]^+$, Rt = 10.02 min
HPLC: Rt = 22.69 min

Boc-Phe-Glu(OtBu)-Phe-OH (protected) (18)

General procedure I (1.0 g resin), followed by the mild cleavage procedure.
LCQ: m/z: 598.1 $[M + H]^+$, 1194.9 $[2M + H]^+$ (calculated $[M + H]^+ = 598.31$)
LC-MS: m/z: 598.08 $[M + H]^+$, 1195.20 $[2M + H]^+$, Rt = 10.02 min
HPLC: Rt = 22.67 min

Boc-Glu(OtBu)-Phe-Phe-OH (protected) (19)
General procedure 1 (1.0 g resin), followed by the mild cleavage procedure.
LCQ: m/z: 597.9 $[M + H]^+$, 1194.8 $[2M + H]^+$ (calculated $[M + H]^+ = 598.31$)
LC-MS: m/z: 598.04 $[M + H]^+$, 1195.20 $[2M + H]^+$, Rt = 10.05 min
HPLC: Rt = 22.70 min

Synthesis of the peptide-polymer constructs

Boc-Gly-[Glu(OtBu)]$_7$-Gly-star-PEG (protected) (20)
General procedure 2A was followed with star-PEG-NH_2 HCl salt (200 mg, 20 µmol) and peptide Boc-Gly[Glu(OtBu)]$_7$-Gly (**1**; 183 mg, 120 µmol).
^{1}H-NMR (400 MHz, $CDCl_3$): δ = 1.38 – 1.51 (m, CH_3), 1.95 – 2.62 (m), 3.59 – 3.68 (m, $[CH_2CH_2O]_n$), 3.72 – 4.38 (m).
MALDI-TOF (dithranol): m/z: 15894, calculated m/z: 15911 for 217 ethylene glycol units.

H-Gly-[Glu]$_7$-Gly-star-PEG (21)
Deprotection was performed via general procedure 2B, without the dialysis step.
^{1}H-NMR (400 MHz, D_2O): δ = 1.81 – 2.08 (m, Cα-C$\underline{H}_2$-CH_2), 2.28 – 2.43 (m, Cα-CH_2-C$\underline{H}_2$), 3.43 – 3.82 (m, $[CH_2CH_2O]_n$, CH_2(Gly)), 4.17 – 4.31 (m, Cα).
MALDI-TOF (dithranol): m/z: 14071, calculated m/z: 14072 for 220 ethylene glycol units.

Calmodulin 2 – star-PEG (22)
General procedure 3 was followed using star-PEG-NH_2 (75 mg, 7.5 µmol) and protected peptide GDADGNGTIDFPE (**3**; 87 mg, 45 µmol). After dialysis, SEC analysis resulted in peaks at Rt = 6.909 min (product), Rt = 9.705 min (peptide) and Rt = 17.506 min. The construct calmodulin 2 –star-PEG was not obtained in pure form.

Calmodulin 3 – star-PEG (23)
General procedure 3 was followed using star-PEG-NH_2 (75 mg, 7.5 µmol) and protected peptide GDKDGNGYISAAEG (**5**; 93 mg, 45 µmol). After dialysis, SEC analysis resulted in peaks at Rt = 6.703 min (product), Rt = 8.997 min (peptide) and Rt = 17.264 min. The construct (20 mg) was dissolved in 5 mL MeCN: H_2O (45:55) for purification using preparative SEC (isocratic, MeCN: H_2O 45:55). The purified product was analysed by MALDI-TOF mass spectrometry.
SEC: Rt = 6.748 min
MALDI-TOF (alpha-cyano): m/z: 12706, calculated m/z: 15341 for 220 ethylene glycol units.

H-G[LEELLEE]$_2$G-star-PEG (24)

General procedure 3 was followed using star-PEG-NH_2 (75 mg, 7.5 µmol) and protected peptide Boc-Gly-[Leu-Glu(OtBu)-Glu(OtBu)-Leu-Leu-Glu(OtBu)-Glu(OtBu)]$_2$-Gly-OH (**7**; 108 mg, 45 µmol). After dialysis, SEC analysis resulted in peaks at Rt = 7.093 min (product), Rt = 10.74 min (peptide **8**). The construct was hardly soluble in a mixture of MeCN: H_2O (45:55), making purification using preparative SEC impossible.

Boc-Gly-Glu(OtBu)-Gly-star-PEG (protected) (25)

General procedure 2A was followed using star-PEG-NH_2 (75 mg, 7.5 µmol), PyBrOP (28 mg, 8 eq, 60 µmol), peptide Boc-Gly-Glu(OtBu)-Gly (**11**; 25 mg, 8 eq, 60 µmol) and D*i*PEA (31 µL, 24 eq, 180 µmol).

^{1}H-NMR (400 MHz, $CDCl_3$): δ = 1.40 – 1.48 (m, CH_3), 1.91 – 2.47 (m, Cα-C$\underline{H}_2$-C$\underline{H}_2$), 3.35 – 3.99 (m, $[CH_2CH_2O]_n$, CH_2(Gly)), 4.34 – 4.56 (m, Cα).

MALDI-TOF (alpha cyano): m/z: 11575, calculated m/z: 11554 for 219 ethylene glycol units.

H-Gly-Glu-Gly-star-PEG (26)

Deprotection was performed according to general procedure 2B.

^{1}H-NMR (400 MHz, D_2O): δ = 1.71 – 1.99 (m, Cα-C$\underline{H}_2$-CH_2), 2.08 – 2.17 (m, Cα-CH_2-C$\underline{H}_2$), 3.21 – 3.78 (m, $[CH_2CH_2O]_n$, CH_2(Gly)), 4.21(m, Cα).

MALDI-TOF (alpha cyano): m/z: 11188, calculated m/z: 11193 for 225 ethylene glycol units.

Boc-Leu-Glu(OtBu)-Leu-star-PEG (protected) (27)

General procedure 2A was followed using star-PEG-NH_2 (75 mg, 7.5 µmol), PyBrOP (28 mg, 8 eq, 60 µmol), peptide Boc-Leu-Glu(OtBu)-Leu (**13**; 24 mg, 8 eq, 60 µmol) and D*i*PEA (31 µL, 24 eq, 180 µmol).

^{1}H-NMR (400 MHz, $CDCl_3$): δ = 0.82 – 1.00 (m, CH_3 (Leu)), 1.41 – 1.52 (m, CH_3 (Boc, OtBu)), 1.60 – 2.18 (m), 3.38 – 3.87 (m, $[CH_2CH_2O]_n$), 4.40 (m, Cα).

MALDI-TOF (alpha cyano): m/z: 11905, calculated m/z: 11914 for 217 ethylene glycol units.

H-Leu-Glu-Leu-star-PEG (28)

Deprotection was performed according to general procedure 2B.

^{1}H-NMR (400 MHz, D_2O): δ = 0.82 – 1.04 (m, CH_3 (Leu)), 1.23 – 1.85 (m, CH_2, CH (Leu)) 1.89 – 2.36 (m, Cα-C$\underline{H}_2$-C$\underline{H}_2$), 3.33 – 3.97 (m, $[CH_2CH_2O]_n$), 4.34 (m, Cα).

MALDI-TOF (alpha cyano): m/z: 11556, calculated m/z: 11554 for 223 ethylene glycol units.

Boc-Ala-Glu(OtBu)-Ala-star-PEG (protected) (29)

General procedure 2A was followed using star-PEG-NH_2 (75 mg, 7.5 µmol), PyBrOP (28 mg, 8 eq, 60 µmol), peptide Boc-Ala-Glu(OtBu)-Ala (**15**; 27 mg, 8 eq, 60 µmol) and D*i*PEA (31 µL, 24 eq, 180 µmol).

^{1}H-NMR (400 MHz, $CDCl_3$): δ = 1.24 – 1.50 (m, CH_3 (Ala, Boc, OtBu)), 1.87 – 2.48 (m, Cα-$C\underline{H}_2$-$C\underline{H}_2$), 3.37 – 3.73 (m, $[CH_2CH_2O]_n$), 3.99 – 4.67 (m, Cα).
MALDI-TOF (alpha cyano): m/z: 11755, calculated m/z: 11754 for 221 ethylene glycol units.

H-Ala-Glu-Ala-star-PEG (30)
Deprotection was performed according to general procedure 2B.
^{1}H-NMR (400 MHz, D_2O): δ = 1.26 – 1.38 (m, CH_3 (Ala)), 1.81 – 2.30 (m, Cα-$C\underline{H}_2$-$C\underline{H}_2$), 3.27 – 3.86 (m, $[CH_2CH_2O]_n$), 4.23 (m, Cα).
MALDI-TOF (alpha cyano): m/z: 11321, calculated m/z: 11305 for 225 ethylene glycol units.

Boc-Phe-Phe-Glu(OtBu)-star-PEG (protected) (31)
General procedure 2A was followed using star-PEG-NH_2 (250 mg, 25 μmol), PyBOP (78 mg, 6 eq, 150 μmol), peptide Boc-Phe-Phe-Glu(OtBu) (**17**; 90 mg, 6 eq, 150 μmol) and D*i*PEA (104 μL, 24 eq, 600 μmol).
^{1}H-NMR (400 MHz, $CDCl_3$): δ = 1.23 – 1.46 (m, CH_3), 1.88 – 2.32 (m, Cα-$C\underline{H}_2$-$C\underline{H}_2$), 2.85 – 3.12 (m, CH_2 (Phe)), 3.38 – 3.85 (m, $[CH_2CH_2O]_n$), 4.18 – 4.57 (m, Cα), 6.99 – 7.38 (m, Ar-CH)
MALDI-TOF (alpha cyano): m/z: 12286, calculated m/z: 12275 for 219 ethylene glycol units.

H-Phe-Phe-Glu-star-PEG (32)
Deprotection was performed according to general procedure 2B.
^{1}H-NMR (400 MHz, D_2O): δ = 1.80 – 1.96 (m, Cα-$C\underline{H}_2$-CH_2), 2.15 – 2.22 (m, Cα-CH_2-$C\underline{H}_2$), 2.96 – 3.13 (m, CH_2 (Phe)), 3.29 – 3.90 (m, $[CH_2CH_2O]_n$), 4.13 (m, Cα), 7.17 – 7.40 (m, Ar-CH)
MALDI-TOF (alpha cyano): m/z: 11740, calculated m/z: 11738 for 221 ethylene glycol units.

Boc-Phe-Glu(OtBu)-Phe-star-PEG (protected) (33)
General procedure 2A was followed using star-PEG-NH_2 (250 mg, 25 μmol), PyBOP (78 mg, 6 eq, 150 μmol), peptide Boc-Phe-Glu(OtBu)-Phe (**18**; 90 mg, 6 eq, 150 μmol) and D*i*PEA (104 μL, 24 eq, 600 μmol).
^{1}H-NMR (400 MHz, $CDCl_3$): δ = 1.23 – 1.48 (m, CH_3), 1.98 – 2.28 (m, Cα-$C\underline{H}_2$-$C\underline{H}_2$), 2.82 – 3.10 (m, CH_2 (Phe)), 3.38 – 3.87 (m, $[CH_2CH_2O]_n$), 4.29 (m, Cα), 7.13 – 7.34 (m, Ar-CH).
MALDI-TOF (alpha cyano): m/z: 12228, calculated m/z: 12230 for 218 ethylene glycol units.

H-Phe-Glu-Phe-star-PEG (34)
Deprotection was performed according to general procedure 2B.
^{1}H-NMR (400 MHz, D_2O): δ = 1.73 – 1.98 (m, Cα-$C\underline{H}_2$-CH_2), 2.05- 2.18 (m, Cα-CH_2-$C\underline{H}_2$), 2.95 – 3.16 (m, CH_2 (Phe)), 3.37 – 3.89 (m, $[CH_2CH_2O]_n$), 4.32 (m, Cα), 7.11 – 7.40 (m, Ar-CH)
MALDI-TOF (alpha cyano): m/z: 11778, calculated m/z: 11782 for 222 ethylene glycol units.

Boc-Glu(OtBu)-Phe-Phe-star-PEG (protected) (35)

General procedure 2A was followed using star-PEG-NH_2 (250 mg, 25 μmol), PyBOP (78 mg, 6 eq, 150 μmol), peptide Boc-Glu(OtBu)-Phe-Phe (**19**; 90 mg, 6 eq, 150 μmol) and D*i*PEA (104 μL, 24 eq, 600 μmol).

^{1}H-NMR (400 MHz, $CDCl_3$): δ = 1.23 – 1.48 (m, CH_3), 2.12 - 2.44 (m, Cα-C$\underline{H}_2$-C$\underline{H}_2$), 2.92 – 3.08 (m, CH_2 (Phe)), 3.15 – 3.98 (m, $[CH_2CH_2O]_n$), 4.48 – 4.71 (m, Cα), 7.09 – 7.29 (m, Ar-CH); MALDI-TOF (alpha cyano): m/z: 12107, calculated m/z: 12099 for 215 ethylene glycol units.

H-Glu-Phe-Phe-star-PEG (36)

Deprotection was performed according to general procedure 2B.

^{1}H-NMR (400 MHz, D_2O): δ = 1.86 – 2.08 ((m, Cα-C$\underline{H}_2$-C$\underline{H}_2$), 2.85 – 3.03 (m, CH_2 (Phe)), 3.21 – 3.96 (m, $[CH_2CH_2O]_n$), 4.47 (m, Cα), 7.17 – 7.36 (m, Ar-CH).

MALDI-TOF (alpha cyano): m/z: 11682, calculated m/z: 11694 for 220 ethylene glycol units.

Gelation studies

Gelation GE_7G-star-PEG (21)

A 1 wt% solution of GE_7G-star-PEG (**21**) was prepared by dissolving 5 mg in 50 μL 1 M NaOH, which was further diluted by addition of 450 μL HEPES buffer (20 mM, pH7.1). Aliquots of $CaCl_2$ (2 μL = 1 eq) were added, resulting in final additions of 0.5 – 10 eq (1 eq $CaCl_2$ corresponds to 1 eq per peptide, hence 4 eq based on the total construct). Gelation was tested at r.t. via the inverted vial test. A 5 wt% solution of **21** was tested at r.t. and at 37°C by dissolving 5 mg GE_7G-star-PEG (**21**) in 50 μL 1 M NaOH and 50 μL HEPES buffer, and addition of $CaCl_2$ aliquots (0.5 – 20 eq). Gelation of 10 wt% solutions in NaOH (10 mg in 100 μL 1 M NaOH) and in ammonia (10 mg in 40 μL 25% ammonia and 55 μL H_2O) was investigated by addition of $CaCl_2$ aliquots (2 – 20 eq).

Gelation Calmodulin 3-star-PEG (23)

A 2 wt% solution of Calmodulin 3-star-PEG (**23**) was prepared by dissolving 2 mg in 100 μL MilliQ. Aliquots of $CaCl_2$ (2 μL = 1 eq) were added, resulting in final additions of 0.5 – 10 eq (1 eq $CaCl_2$ corresponds to 1 eq per peptide, hence 4 eq based on the total construct). Gelation was tested at r.t. via the inverted vial test.

Gelation GEG-star-PEG (26), LEL-star-PEG (28) and AEA-star-PEG (30)

Gel formation was studied with 15 wt% solution of GEG-star-PEG (**26**), LEL-star-PEG (**28**) and AEA-star-PEG (**30**) (15 mg in 100 μL MilliQ). Aliquots of $CaCl_2$ (5 μL = 1 eq) were added, resulting in final additions of 1 – 4 eq (1 eq $CaCl_2$ corresponds to 1 eq per peptide, hence 4 eq based on the total construct). Gelation was tested at r.t. via the inverted vial test.

Gelation FFE-star-PEG (32), FEF-star-PEG (34) and EFF-star-PEG (36)

Gel formation was studied with 15 wt% solution of FFE-star-PEG (**32**), FEF-star-PEG (**34**) and EFF-star-PEG (**36**) (15 mg in 100 µL MilliQ and 15 mg in 100 mM Tris buffer, pH 9.0). Aliquots of $CaCl_2$ (5 µL = 1 eq) were added, resulting in final additions of 1 – 4 eq (1 eq $CaCl_2$ corresponds to 1 eq per peptide, hence 4 eq based on the total construct). Gelation was tested at r.t. via the inverted vial test.

2.8. References

(1) Benesch, J.; Mano, J. F.; Reis, R. L. *Tissue Eng Pt B* **2008**, *14*, 433-445.

(2) Romberg, R. W.; Werness, P. G.; Riggs, B. L.; Mann, K. G. *Biochemistry* **1986**, *25*, 1176-1180.

(3) Harris, N. L.; Rattray, K. R.; Tye, C. E.; Underhill, T. M.; Somerman, M. J.; D'Errico, J. A.; Chambers, A. F.; Hunter, G. K.; Goldberg, H. A. *Bone Vol.* **2000**, *27*, 795-802.

(4) Fujisawa, R.; Wada, Y.; Nodasaka, Y.; Kuboki, Y. *Biochim. Biophys. Acta* **1996**, *1292*, 53-60.

(5) Price, P. A.; Otsuka, A. S.; Poser, J. W.; Kristaponis, J.; Raman, N. *Proc. Natl. Acad. Sci. USA* **1976**, *73*, 1447-1451.

(6) Fujisawa, R.; Kuboki, Y.; Sasaki, S. *Calcif. Tissue Int.* **1986**, *39*, 248-251.

(7) George, A.; Bannon, L.; Sabsay, B.; Dillon, J. W.; Malone, J.; Veis, A.; Jenkins, N. A.; Gilbert, D. J.; Copeland, N. G. *J. Biol. Chem.* **1996**, *271*, 32869–32873.

(8) Chin, D.; Means, A. R. *Trends Cell Biol.* **2000**, *10*, 322-328.

(9) Braunewell, K.-H.; Gundelfinger, E. D. *Cell Tissue Res.* **1999**, *295*, 1-12.

(10) Pina, S.; Oliveira, J. M.; Reis, R. L. *Adv. Mater.* **2015**, *27*, 1143-1169.

(11) Tønnesen, H. H.; Karlsen, J. *Drug. Dev. Ind. Pharm.* **2002**, *28*, 621-630.

(12) George, M.; Abraham, T. E. *J. Control. Release* **2006**, *114*, 1-14.

(13) Rees, D. A.; Welsh, E. J. *Angew. Chem. Int. Ed. Engl.* **1977**, *16*, 214-224.

(14) Nagano, A.; Sato, H.; Tanioka, Y.; Nakazawa, Y.; Knight, D.; Asakura, T. *Soft Matter* **2012**, *8*, 741-748.

(15) Kelly, S. M.; Jess, T. J.; Price, N. C. *BBA-Proteins Proteom.* **2005**, *1751*, 119-139.

(16) Bouchemal, K.; Mazzaferro, S. *Drug Discov. Today* **2012**, *17*, 623-629.

(17) Christensen, T.; Gooden, D. M.; Kung, J. E.; Toone, E. J. *J. Am. Chem. Soc.* **2003**, *125*, 7357-7366.

(18) Dai, Q.; Prorok, M.; Castellino, F. J. *J. Mol. Biol.* **2004**, *336*, 731-744.

(19) Dai, Q.; Dong, M.; Liu, Z.; Prorok, M.; Castellino, F. J. *J. Inorg. Biochem.* **2011**, *105*, 52-57.

(20) Henzl, M. T.; Larson, J. D.; Agah, S. *Anal. Biochem.* **2003**, *319*, 216-233.

(21) Suzuki, K.; Hiroaki, H.; Kohda, D.; Nakamura, H.; Tanaka, T. *J. Am. Chem. Soc.* **1998**, *120*, 13008-13015.

(22) Kühnle, R. I.; Gebauer, D.; Börner, H. G. *Soft Matter* **2011**, *7*, 9616-9619.

(23) Jayawarna, V.; Ali, M.; Jowitt, T. A.; Miller, A. E.; Saiani, A.; Gough, J. E.; Ulijn, R. V. *Adv. Mater.* **2006**, *18*, 611-614.

(24) Jayawarna, V.; Richardson, S. M.; Hirst, A. R.; Hodson, N. W.; Saiani, A.; Gough, J. E.; Ulijn, R. V. *Acta Biomater.* **2009**, *5*, 934-943.

(25) Kaiser, E.; Colescott, R. L.; Bossinger, C. D.; Cook, P. I. *Anal. Biochem.* **1970**, *34*, 595-598.

Chapter 3

Soft PEG-hydrogels with independently tunable stiffness and RGDS-content for cell adhesion studies


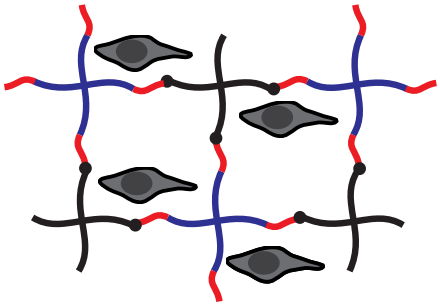
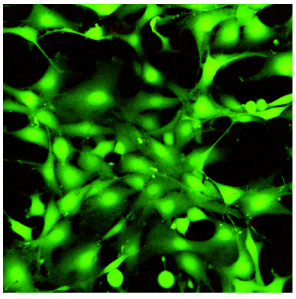

This chapter has been published as:
Jonker, A.M.; Bode, S.A.; Kusters, A.H.; van Hest, J.C.M.; Löwik, D.W.P.M.
Macromol. Biosci. **2015**, *15*, 1338-1347

3.1. Introduction

Hydrogels are water-swollen cross-linked polymeric networks. Due to their high water content, biocompatibility and mechanical properties, hydrogels are promising biomaterials for mimicking the extracellular matrix (ECM).[1-4] Poly(ethylene glycol) (PEG) is a common choice as the polymeric basis for synthetic hydrogels. PEG is hydrophilic, has excellent biocompatibility, low toxicity and is non-adhesive towards proteins and cells.[5-7] PEG-based hydrogels can be formed by physical or chemical cross-links.[8] Among the chemical cross-linking procedures, the copper-catalyzed "click" reaction between an azide and alkyne (CuAAC) is widely used as it is fast, high-yielding and modular, but most importantly orthogonal.[9,10] In order to circumvent the necessity of applying cytotoxic copper ions, recently copper-free strain promoted azide-alkyne cycloaddition (SPAAC)[11-14], thiol-ene chemistry[15-18], Diels-Alder cycloadditions[19-22] and the SPOCQ reaction (strain-promoted oxidation-controlled cyclooctyne–1,2-quinone cycloaddition) between a catechol and a ring-strained alkyne[23,24] have emerged as efficient alternative cross-linking reactions.[25,26] Among others, the SPAAC method has shown its validity in constructing hydrogels which promote cellular adhesion via the incorporation of synthetic adhesion peptides, such as the RGDS sequence.[27-29] DeForest *et al.*[30] demonstrated that star-shaped PEG functionalized with azide moieties can be clicked to cyclooctyne-containing peptides, leading to hydrogel formation. Also enzymatically cleavable peptide sequences were efficiently incorporated, making the hydrogels biodegradable.[30] The bio-orthogonal character of these coupling chemistries ensures the functional integrity of the biological motifs in the final hydrogel structure. The broad applicability of these materials was demonstrated by successful cell culturing of a range of cells, such as fibroblasts, human mesenchymal stem cells and bone marrow derived stromal cells.[30-33]

When culturing cells on hydrogels, it is important to understand how they interact with their surroundings. It has been stated that cells are able to feel the substrate they are attached to and that they will respond based on these external mechanical signals.[34,35] For example it has been shown that the differentiation of mesenchymal stem cells is dependent on substrate stiffness. Culturing on soft gels (0.1 – 1 kPa) led to neurons, but myoblasts were formed on stiffer substrates (8 – 17 kPa) and cells differentiated into osteoblasts on rigid matrices (25 – 40 kPa).[36] Recent research indicates that these stem cells retain their phenotype on a non-fouling zwitterionic hydrogel, independent of stiffness.[37] In general, most cell lines seem to have a preference to adhere to and grow on stiffer substrates.[35,38-45] However, there remains some debate about the influence of matrix stiffness on cell adhesion, differentiation and migration. Recently, Trappmann and co-workers[46] demonstrated that human mesenchymal cells were able to spread and differentiate on collagen-coated polydimethylsiloxane (PDMS) hydrogel surfaces (0.1 kPa – 2.3 MPa) independent of their stiffness. Cells on collagen-coated

polyacrylamide (PAAm) gels (0.5 – 740 kPa) on the other hand could only spread on stiff surfaces and differentiated on soft surfaces due to their inability to form focal adhesions. This was confirmed by the fact that decreasing the number of anchoring points on stiff gels resulted in cellular behavior as if there were on soft gels. The authors therefore stated that cells apply a mechanical force on substrate-bound ECM and need the feedback to make cell-fate decisions. These results thus show that is it not the stiffness, but the mechanical feedback of the ECM that influences cell behavior.[46] On the other hand, Missirlis and Spatz[47] studied the effect of substrate elasticity on fibroblast adhesion using PEG hydrogels (5.5 – 65 kPa). They found that cells respond to differences in substrate elasticity and were unlikely to respond to differences in ligand tethering. Fibroblasts were found to spread increasingly better on stiffer substrates. These results thereby support the general idea that most cells prefer stiffer substrates.[47] However, there are also studies that reported different cellular responses to hydrogel stiffness. The Caruso group revealed that HeLa cell adhesion on soft poly(methacrylic acid) PMA_{SH} hydrogels (2.5 kPa) decreased with increasing film stiffness. They found negligible differences in the hydrogel film roughness, hydrophobicity and charge and stated that the differences in cell adhesion are caused by the mechanical properties of the gel.[48] Robinson *et al.* found that proliferation of NIH 3T3 cells and HUVECs was larger on gels with a lower strength. On the other hand, human vascular smooth muscle cells and adventitial fibroblasts showed enhanced growth on stiffer surfaces.[49] All together, these examples highlight the need to further study the influence of the synthetic matrix on cellular adhesion, migration and differentiation.[3]

So far, most cellular adhesion studies have been performed with stiff substrates, usually exceeding the stiffness range of most mammalian organs, which have elastic moduli (G') between 100 – 10.000 Pa.[43,44,46,47,50] In this study, we aim to investigate how different cell lines respond to various soft hydrogels. For this purpose, we fabricated soft hydrogels with PEG as the polymeric basis, using bicyclo[6.1.0]nonyne (BCN) based copper-free click chemistry.[13] In order to promote cellular adhesion of our PEG hydrogels, an RGDS peptide motif was incorporated in the polymeric network (**Figure 3.1**). These clickable hydrogels constitute a platform that allows us to vary both the RGDS content and the polymer density independently of each other. In this way, we intend to get insight on the influence of the stiffness of soft hydrogels in combination with the amount of adhesion motifs on the cell viability of three different cell types.

3.2. Hydrogel design

Hydrogels were fabricated using 4-armed poly(ethylene glycol) (M_n = 10 kDa, star-PEG) as the polymeric basis. As cross-linking methodology, we used copper-free strain-promoted click (SPAAC) chemistry, with a bicyclo[6.1.0]nonyne (BCN) derivative as the ring-strained

alkyne.[13] Star-PEG-amine was functionalized with either an azide or BCN moiety, by coupling of azido acetic acid and BCN-OSu, respectively (**Figure 3.1**). Additionally, we also synthesized the corresponding di-functionalized PEG analogues. Hydrogels were formed by combining equimolar amounts of star-PEG-BCN and star-PEG-N_3, or by replacing one of the star-polymer components by di-functionalized PEG. Upon mixing the components in water, the click reaction commenced, leading to the formation of a polymeric network. Cross-linking took place without the need of additional chemicals or further processing. Gel formation was qualitatively examined via the inverted vial test. We investigated the minimal polymer concentration required for gelation to occur, by varying the total polymer content from 5 up to 30 mg/mL. Very soft hydrogels were formed overnight for the combination of star-PEG-BCN with star-PEG-N_3 at a total polymer concentration of 10 mg/mL (1 wt%). This appeared to be the minimum gelation concentration, since only viscous solutions were obtained at 5 mg/mL. Increasing polymer concentration resulted in faster gelation times. Hydrogels could also be obtained when combining star-PEG polymers with di-functionalized PEG, but gelation times were significantly longer. When star-shaped polymers are used for gelation, more branching points are available, so a denser network is formed, leading to faster gelation. We therefore decided to continue with the star-shaped polymers for further studies.

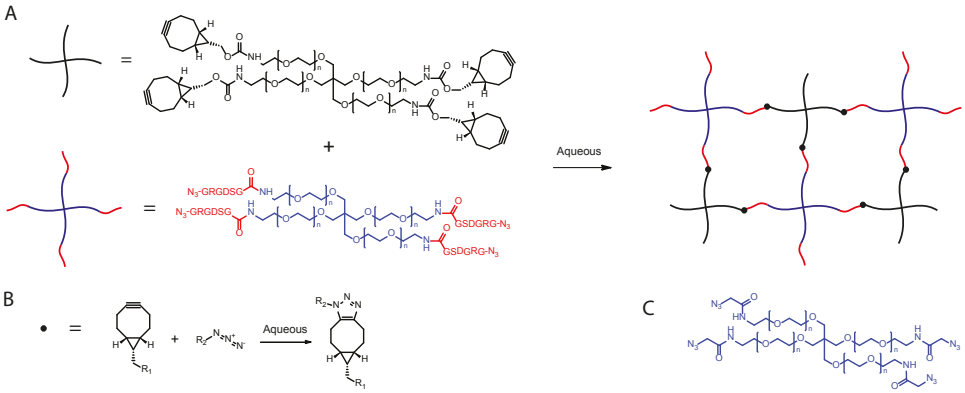

Figure 3.1. Hydrogel formation. A: Mixing of star-PEG-BCN with star-PEG-RGDS-N_3 yields a stable hydrogel network (containing 100% RGDS). B: Cross-links are formed by copper-free click chemistry. C: The composition of the hydrogel network can be adjusted by mixing in certain amounts of star-PEG-N_3, and thereby changing the total RGDS content. Furthermore, the RGDS-polymer can also be replaced by a RDGS-containing star-PEG (star-PEG-scrambled (structure not shown)).

Next, IR-spectroscopy was performed on 30 mg/mL gels to confirm that gelation concurred via the click reaction. When equimolar amounts of azide and BCN were used, the typical azide-signal around 2100 cm^{-1} could not be detected after hydrogel formation, while it was clearly present before cross-linking. When an excess of star-PEG-N_3 was utilized, the azide-signal did not fully disappear after gelation had occurred (**Figure 3.2**).

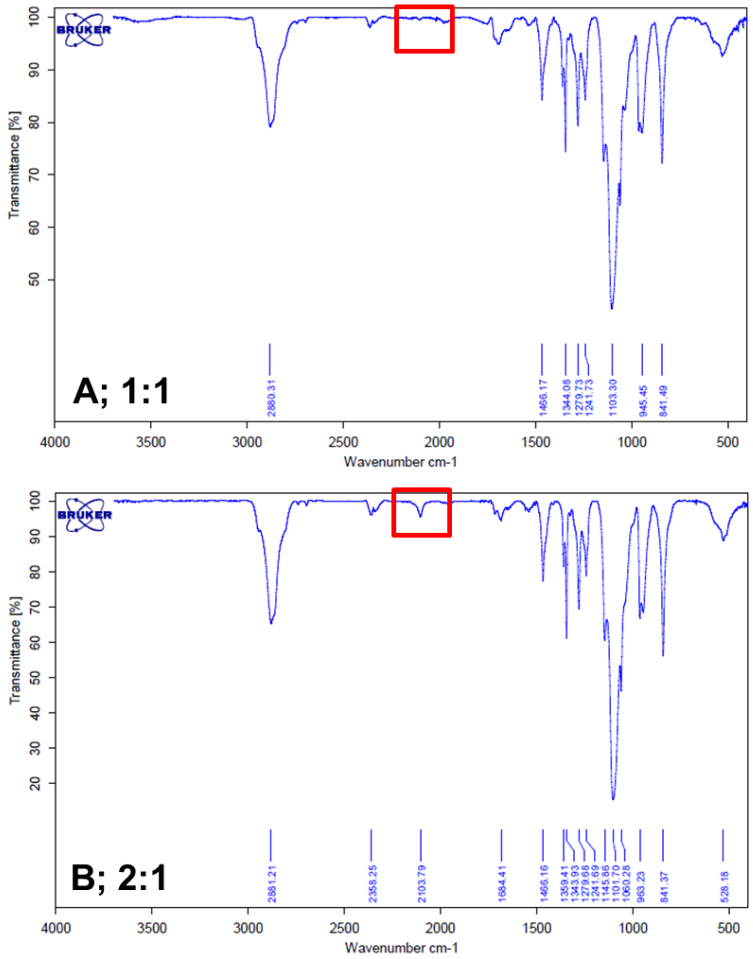

Figure 3.2. IR spectroscopy of 30 mg/mL PEG-hydrogels. **A:** ratio azide:alkyne 1:1, the azide-signal could not be detected after gelation had occurred. **B:** ratio azide: alkyne 2:1; when using an excess of azide in the hydrogels, the N_3-signal was present (2103.79 cm^{-1}).

Now that we confirmed that copper-free azide-BCN cycloaddition chemistry is suitable as a cross-linking method for soft hydrogel formation, we aimed to introduce peptide functionalities in the PEG polymer network (**Figure 3.1**). To be able to investigate the cellular adhesion properties of the hydrogels, we incorporated the well-known RGDS adhesion domain.[27-29] First, this peptide was synthesized using standard Fmoc solid phase peptide synthesis, with coupling of azido-acetic acid as the final residue. The employed Barlos solid phase resin allowed mild resin cleavage to keep all acid-labile side-chain protecting groups in place. Coupling of the peptide to star-PEG-NH_2 could therefore be performed selectively at the C-terminus. This method allowed us to easily obtain azidoGly-Arg-Gly-Asp-Ser-Gly functionalized star-PEG, which is

further referred to as star-PEG-RGDS-N_3 (**Figure 3.3, Chapter 2.3.1**). We also synthesized the scrambled peptide (azidoGly-Arg-Asp-Gly-Ser-Gly) polymer construct star-PEG-scrambled, which was not expected to be able to induce cell adhesion. With these building blocks in hand, we were able to fabricate various soft hydrogels. Our modular approach allows us to vary both the polymer density and RGDS-content independently of each other. We could adjust the polymer density by varying the total polymer content. Hydrogels were prepared in the concentration range 10 – 30 mg/mL. Furthermore, we tuned the RGDS content by mixing in both star-PEG-RGDS-N_3 and star-PEG-N_3, for cross-linking to star-PEG-BCN.

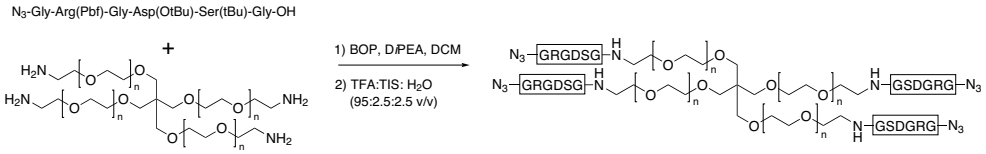

Figure 3.3. Synthesis of star-PEG-RGDS-N_3.

3.3. Rheology

The mechanical properties of the PEG- and PEG-RGDS-hydrogels were determined using rheology. The storage (G') and loss modulus (G'') were measured using an oscillatory time sweep test. Hydrogels were prepared with varying total polymer concentration (10 – 30 mg/mL) using a molar ratio of 1:1 between the azide and alkyne groups. The cross-over point at which G' exceeds G'' was determined as an estimate of the point of gelation. With increasing polymer concentration, the time to reach this point of gelation decreased. Gel formation started after 22 min for the 30 mg/mL PEG-only hydrogel, where the gelation time increased to 47 min for 20 mg/mL and 338 min for 10 mg/mL (**Table 3.1**).

Table 3.1. Cross-over points (G' exceeds G'') in minutes for 10, 20 and 30 mg/mL hydrogels containing 0, 50 and 100% RGDS. Gelation time increases with incorporation of the peptide moiety. * = Single measurement, the other 10 mg/mL gels were not constantly measured during the gelation process.

RGDS	Gelation point 10 mg/mL (min)	Gelation point 20 mg/mL (min)	Gelation point 30 mg/mL (min)
0%	338 ± 25	47 ± 2	22 ± 1
50%	423*	53 ± 1	25 ± 2
100%	478*	63 ± 2	29 ± 1

After reaching the cross-over point, G' steadily increased for all hydrogels and reached a final value which was much larger than G'' (**Figure 3.4**). Typically, G'' values in the background range were obtained (0 ± 5 Pa). A significant increase in final G' was found after set time points with

increasing polymer content. Hydrogels of 10 mg/mL showed a G' of 25 Pa (16 h), while values for 20 mg/mL and 30 mg/mL were 1192 Pa (5.5 h) and 2298 Pa (2.5 h), respectively (**Table 3.2**). Frequency sweep measurements were conducted on all cured hydrogels and G' and G'' were found to be independent of frequency. This corresponds to a predominantly elastic composition of the PEG gels (**Figure 3.4**).

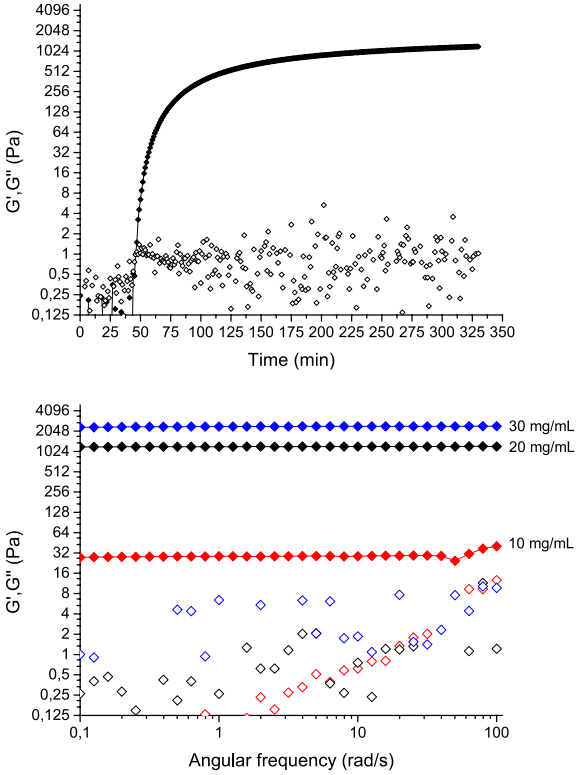

Figure 3.4. Rheology data of the PEG-hydrogels, G' is represented by closed symbols, G'' by open symbols. Top: time sweep measurement of the 20 mg/mL PEG-hydrogel. After reaching the gelation point (47 min), G' steadily increases and reaches a final value (1192 Pa) which is much larger than G''. Bottom: frequency sweep measurements of the 10, 20 and 30 mg/mL, showing that hydrogels have a predominantly elastic composition.

Table 3.2. Hydrogel strength G' (Pa) measured by rheology. Values were recorded after set time points of 16h, 5.5h and 2.5h for 10 mg/mL, 20 mg/mL and 30 mg/mL, respectively. All measurements performed with n = 3 or n = 4. Hydrogel strength increases with increasing polymer density. Incorporation of the RGDS-peptide results in lower moduli.

RGDS	G' 10 mg/mL	G' 20 mg/mL	G' 30 mg/mL
0%	25 ± 3	1192 ± 23	2298 ± 67
50%	18 ± 16	841 ± 21	2094 ± 64
100%	12 ± 1	611 ± 56	1496 ± 77

These results indicate that the PEG materials show typical hydrogel behaviour (G' >> G''); the obtained hydrogels are highly elastic and, as expected, stronger gels are obtained with increasing polymer content.[51] Importantly, as intended, we obtained PEG hydrogels with relatively low stiffness. Our hydrogels have elastic moduli in the soft tissue range, comparable to that of most mammalian organs (G' = 100 – 10.000 Pa) and are softer than most materials reported thus far.[50] Swelling ratios of the 10, 20 and 30 mg/mL hydrogels were determined to be 1.032 ± 0.004, 1.008 ± 0,004 and 1.013 ± 0.011, respectively (**Table 3.5**) Due to the low polymer content (1-3 wt%), these gels have a high water content, resulting in hardly any swelling. The polymer density of the hydrogels can thus only be varied effectively by appyling different concentrations of star-PEG polymers during hydrogel preparation. Next, we studied the mechanical properties of RGDS-containing hydrogels. We measured hydrogels containing 50 and 100% RGDS for all three polymer concentrations. Lower G' values were obtained than for PEG-only hydrogels after set time points (**Table 3.2**). Since the cross-over point was observed at a later time-point (**Table 3.1**), we estimated that gelation was likely to occur more slowly in RGDS-containing hydrogels. To rule out the possibility that this pattern is sequence dependent, we also tested hydrogels containing the scrambled peptide sequence and found the same effect (G' = 1355 Pa ± 65, 100% Scrambled, 30 mg/mL) (**Figure 3.5**). To test our hypothesis that gelation occurs slower with peptide-containing hydrogels, we measured the 30 mg/mL hydrogels overnight (16h). We measured star-PEG, star-PEG-RGDS-N_3 (100%) and star-PEG-scrambled (100%) and found G' values of 3186 Pa, 2863 Pa and 3086 Pa, respectively (**Table 3.4**). Comparable G' values were obtained with or without peptide for fully cured gels. We can therefore conclude that incorporation of peptide sequences does not hinder network formation, and thus, albeit slower, yields stable hydrogels.

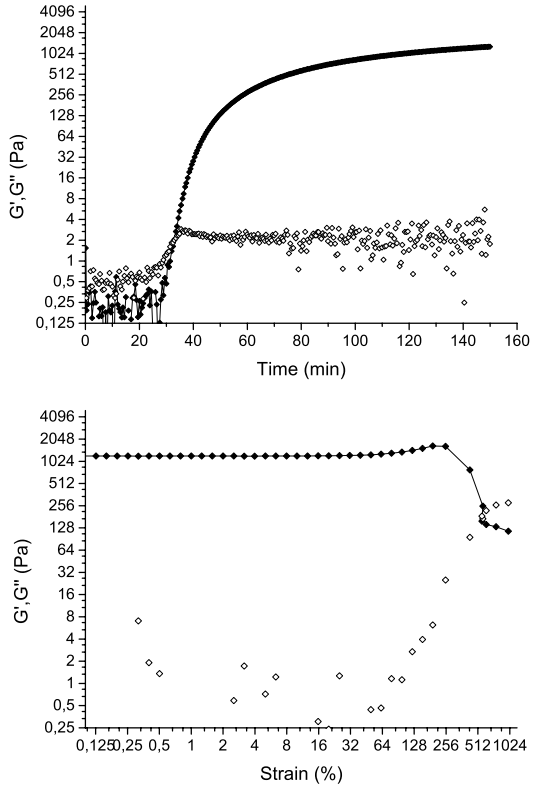

Figure 3.5. Top: Representative time sweep measurement (2.5 h) of a 30 mg/mL 100% Scrambled hydrogel. G' is represented by closed symbols, G'' by open symbols. Final G' value: 1355 ± 64 Pa (n = 3). Bottom: Strain sweep measurement of a 20 mg/mL PEG-only hydrogel to determine the linear viscoelastic region. Strain sweeps were measured for all other hydrogels compositions, giving the same results. Rheology measurements were conducted with 1% strain.

3.4. Cell adhesion studies

3.4.1. Total cell count (WST-8 assay)

After synthesizing and studying the mechanical properties of our RGDS-containing PEG-based gels, we set out to investigate the cell adhesion properties of these soft hydrogels. Since our hydrogel formation method easily allows us to vary the amount of RGDS present in the network, an RGDS concentration range was studied. We prepared hydrogels in the three polymer concentrations (10, 20 and 30 mg/mL) containing 1, 5, 10, 25, 50, 75 and 100% RGDS, in order to investigate how much RGDS is required to give cellular adhesion. This corresponds to a concentration range of RGDS clusters from 5 μM (1% RGDS, 10 mg/mL) up to 1500 μM (100% RGDS, 30 mg/mL). If we assume that clusters of four peptides are homogeneously

distributed throughout the polymeric network, and that cells are able to interact with these peptides within 5 nm from the surface, we can calculate the amount of RGDS clusters in the top surface layer of the hydrogels.[47,52] We calculated this range to be between 15 and 4500 RGDS clusters/μm^2. Massia and Hubbell demonstrated that a peptide spacing of 140 nm is sufficient for focal contact formation, which corresponds to 60 peptides/μm^2.[53] In the weakest hydrogel (10 mg/mL) with 1% RGDS (15 clusters/μm^2), the adhesion points might thus be too far from each other for decent cellular adhesion, although each cluster already contains 4 RGDS moieties. Apart from the lowest RGDS concentrations, the range used here corresponds to previous studies on cell adhesion.[47,54]

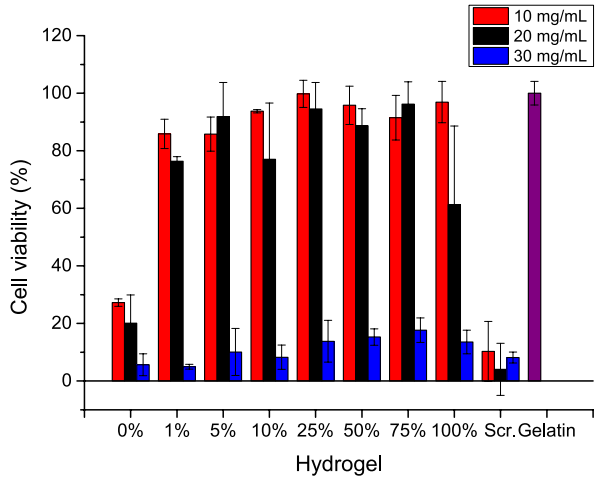

Figure 3.6. WST-8 assay with NIH 3T3 fibroblasts, the x-axis shows the different hydrogel compositions, the y-axis shows the cell viability calculated based on the positive gelatin control (set to 100%). Varying of the RGDS content does not have an influence on total cell count. The 10 and 20 mg/mL hydrogels have a high cell count, in contrast to the stiffest hydrogel of 30 mg/mL which shows a remarkable decrease in the total amount of living cells.

To investigate the influence of RGDS-content on cell adhesion, gels with an RGDS concentration range (1, 5, 10, 25, 50, 75 and 100%) were tested in a WST-8 assay to measure the number of viable cells. Upon cellular reduction, the cell-permeable WST-8 is converted into the water soluble formazan, of which the absorbance can be measured.[55] As a negative control, PEG-only hydrogels were tested. Since PEG is known to be non-adhesive, cellular adherence to these hydrogels is unlikely to occur.[5-7] As a second negative control we also tested the star-PEG-scrambled (RDGS) hydrogels. Based on the rheology studies, we left the gels overnight to allow them to cure fully. The next day, NIH 3T3 fibroblasts were seeded on each hydrogel. Gelatin-coated wells were used as positive control; the total number of viable cells in these wells was set to 100%. The total cell count of the hydrogel samples was calculated as a percentage of the gelatin control. The WST-8 assay performed with the RGDS concentration range revealed

that changing the RGDS content did not have an influence on the total amount of viable cells (**Figure 3.6**). Within one hydrogel stiffness similar viability percentages were obtained for all different RGDS concentrations. Interestingly, clear differences in total cell count were observed between gels with varying stiffness (10, 20 and 30 mg/mL). The amount of viable cells on the 10 and 20 mg/mL resembled the gelatin control, but their number clearly decreased on the 30 mg/mL gels (**Figure 3.6**). Since the amount of RGDS did not show to have an influence on the total cell count, we decided to only study the influence of hydrogel stiffness on cell adhesion in further experiments.

3.4.2. Confocal microscopy – Live/dead assay

Apart from the NIH 3T3 fibroblasts, we chose to study HeLa and human osteosarcoma (HOS) cells. We were interested in these cell lines, since they originate from different tissue. HOS cells originate from human bone tumor and might be more likely to adhere to stiffer surfaces. HeLa cells and NIH 3T3 fibroblasts are both derived from softer tissues, and are therefore interesting to compare to HOS cells. We studied the hydrogels with confocal laser scanning microscopy (CLSM) using a live/dead assay to assess viability. This assay consists of two dyes, one to color living cells (calcein-AM) and one for dead cells (ethidium homodimer-1, EthD-1). Calcein-AM is cell-permeable and is converted to the green fluorescent calcein by intracellular esterase activity of live cells. Ethidium homodimer-1 can only enter cells with a damaged membrane, and then binds to nucleic acids, leading to a bright red fluorescence. We first investigated whether cell adhesion is specific for the RGDS sequence by performing the live/dead assay with HeLa cells seeded on 20 mg/mL PEG-only, RGDS-containing and scrambled hydrogels (**Figure 3.7**).

Since we found that varying the RGDS content does not have an influence, we decided to perform further studies with gels containing 50% RGDS. The live/dead assay showed red fluorescent cells for PEG-only and scrambled hydrogels, showing that cells do not remain viable. Furthermore, their transmission images revealed that these cells have a round morphology. As expected, gels lacking a cell adhesion motif are not suitable substrates for cellular adherence (**Figure 3.19**). Incorporation of the RGDS-motif turned the hydrogels into an appropriate substrate for cellular adhesion, as seen by the large number of green fluorescent cells and their spread morphology (**Figure 3.7**).

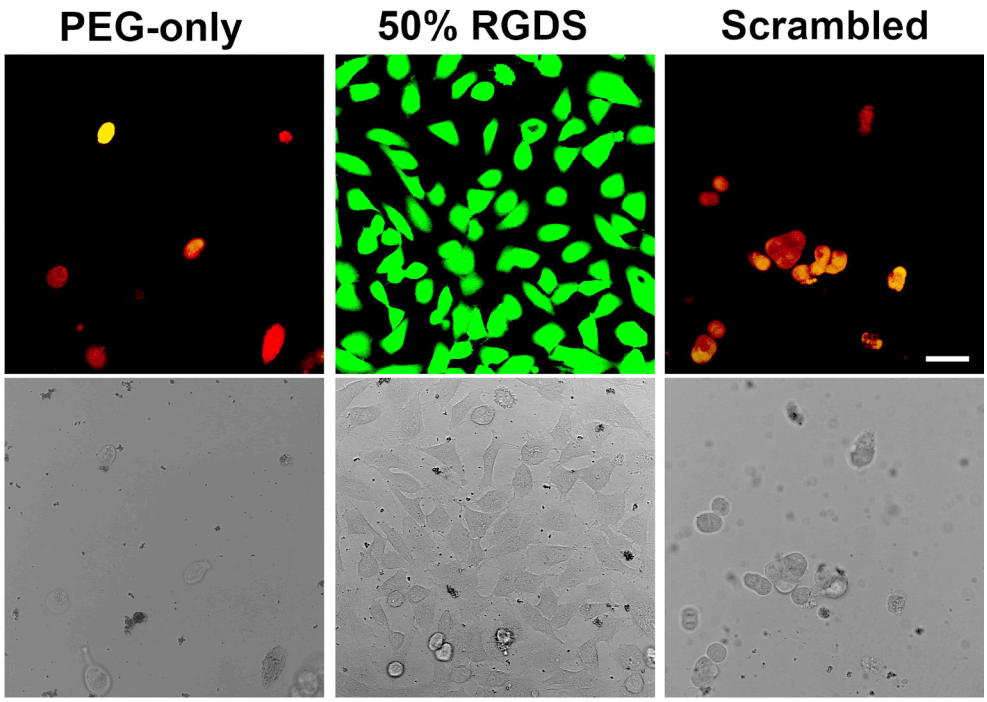

Figure 3.7. Cell viability images for the live/dead assay on 20 mg/mL hydrogels. Images are composed from overlays of the calcein-AM (green) and ethidium homodimer-1 (EthD-1, red) channels. Dead cells (red) were observed on PEG-only (left) and scrambled hydrogels (right), live cells (green) were found on RGDS-containing hydrogels (center). Cell spreading is thus specific for the RGDS sequence. Upper picture: confocal fluorescence, lower picture: transmission image. Scale bar represents 50 µm for all micrographs.

Next, the live/dead assay was performed on the RGDS-containing hydrogels with the three cell types (HeLa, NIH 3T3 and HOS) (**Figure 3.8, Figures 3.16-3.18**). All hydrogel coatings were prepared in the same manner, containing 50% RGDS. Hydrogels only differed in the total polymer content (10, 20, 30 mg/mL) and thus in gel stiffness. Many live cells with a spread morphology were observed for HOS cells on all hydrogels, indicating that these bone marrow-derived cells were able to spread on RGDS-hydrogels, independent of their stiffness (**Figures 3.8** and **3.9, Figure 3.18**). The live/dead assay performed with HeLa cells and NIH 3T3 fibroblasts revealed many live cells for the 10 and 20 mg/mL hydrogels, which nicely adhered in a spread morphology (**Figure 3.8, Figures 3.16** and **3.17**). Interestingly, cell adherence on the stiffest hydrogel (30 mg/mL) was clearly diminished for both HeLa cells and NIH 3T3 fibroblasts. The assay revealed a lower amount of adhered cells in both samples; however these cells were still viable as seen by the green fluorescent signals. NIH 3T3 fibroblasts on the 30 mg/mL gel showed a mixture of cells with a spread and round morphology, whereas HeLa cells mainly had a round morphology. Differences in cell adhesion between 10 or 20 mg/mL and 30 mg/mL were significant, as determined by counting the total number of adhered cells (**Figure 3.9,**

Table 3.3). Both HeLa cells and NIH3T3 fibroblasts are derived from softer tissues than HOS cells and experience difficulties with adherence to the stiffest hydrogel (30 mg/mL) (**Figures 3.8** and **3.9; Figures 3.16** and **3.17**)

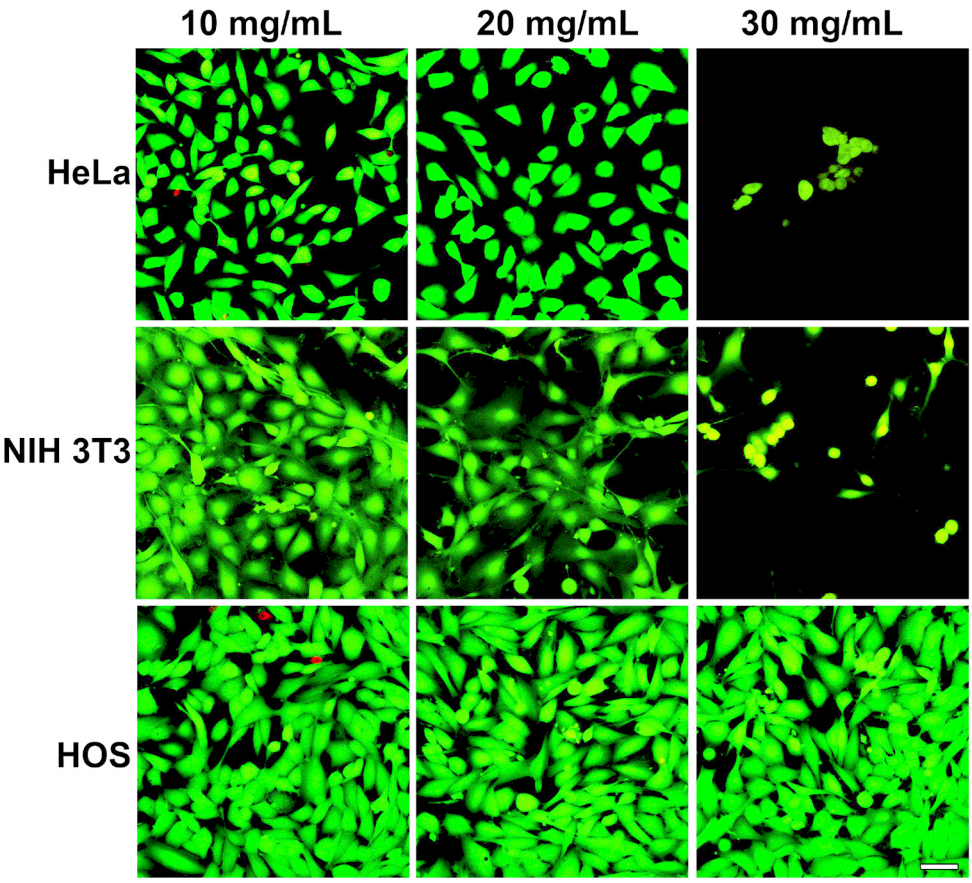

Figure 3.8. Representative confocal fluorescence micrographs for HeLa, NIH 3T3 fibroblasts and HOS cells seeded on RGDS-containing hydrogels with different polymer densities. Cells are stained with calcein (green) and EthD-1 (red). Pictures are obtained from overlay images of the calcein and EthD-1 channels. From left to right: 10, 20 and 30 mg/mL hydrogels, all containing 50% RGDS. Scale bar corresponds to 50 μm for all micrographs (for cell count, see **Figure 3.9**) (for transmission images, see **Figures 3.16-3.18**).

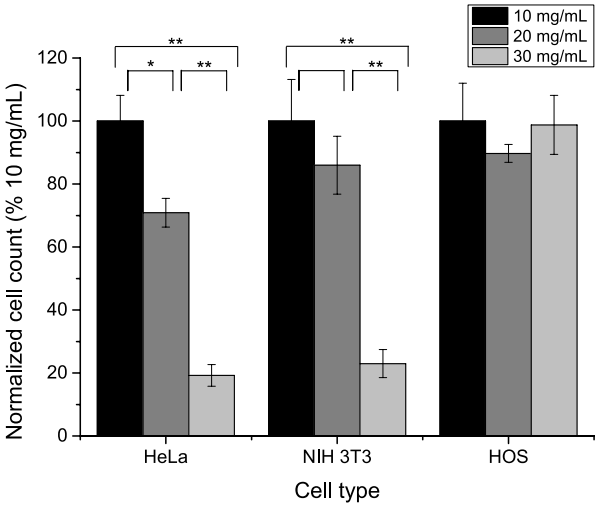

Figure 3.9. Cell count, based on live-dead assay confocal images (n = 3, **Figure 3.8**). The amount of counted cells on 10 mg/mL hydrogels was set to 100%. HeLa and NIH 3T3 showed significant differences in the number of cells adhered to 10 or 20 mg/mL and the amount on 30 mg/mL gels. HOS cells did not show significant differences with varying hydrogel stiffness (for p-values, see **Table 3.3,** * means: $p < 0.05$; ** means: $p < 0.01$, no star: not significant).

Table 3.3. P-values for cell count based on live/dead confocal images (**Figure 3.9**). Values were obtained via an unpaired T-test based on a confidence interval of 95%.

	p-values HeLa	p-values NIH 3T3	p-values HOS
10 vs 20 mg/mL	0.0399	0.4307	0.4560
10 vs 30 mg/mL	0.0008	0.0076	0.9315
20 vs 30 mg/mL	0.0009	0.0056	0.4143

3.5. Discussion

The live/dead assay revealed that 10 and 20 mg/mL RGDS-containing hydrogels are suitable substrates for cell adhesion for all cell-types tested. Many live HOS cells with a spread morphology were also found for the stiffest hydrogel of 30 mg/mL, in contrast to the results for HeLa cells and NIH 3T3 fibroblasts for which the amount of spread cells was clearly decreased. Because we found that the RGDS concentration does not have an influence, the only difference with the 30 mg/mL hydrogels is the increased total polymer concentration, which affects the mechanical properties of the gel. Swelling of the gels was not taken into account, since none of the gels absorbed water due to their high water content. Based on literature results, we assume that the surface chemistry of the hydrogels is not affected by the increased polymer density.[41,48] Hence, the increased stiffness is likely to be the reason for the decreased cellular adhesion

properties of the 30 mg/mL hydrogels. These results are in contrast to the general consensus from literature that most cells seem to have a preference for stiffer substrates. There is, however, still debate on the influence of the mechanical properties on cellular adhesion. Several studies indicate that stiffness is an important factor to determine cell adhesion, whereas others state that it is the mechanical feedback of the ECM.[35,38-47,50] Important to note in this discussion is that most hydrogels studied thus far have elastic moduli (G') in the order of magnitude of kPa, or even MPa. The high stiffness of these gels might also influence the adhesion behavior of cells. The Caruso group investigated this effect by developing soft PMA_{SH} hydrogel films with a strength up to 2500 Pa, thus in the same range as our PEG-hydrogels.[48] They found the same pattern as we did and thus opposite to what others have reported; decreasing cell adhesion was observed with increasing hydrogel stiffness. Negligible differences were seen in the surface chemistry of hydrogel films with various strengths, showing that cells respond to substrate elasticity. The authors postulated that this effect was due to the enhanced cell-film contact area for softer hydrogels. Additionally, the Heilshorn group studied spreading of fibroblasts on soft ELP-PEG gels. Many fibroblasts (~ 60%) spread on gels with a modulus of 1300 Pa, whereas only 3% of the cells showed a spread morphology on the stiffer hydrogel (2500 Pa).[56] Moreover, the same effect was found by the Anseth group for human mesenschymal stem cells adhered to thiol-ene photopolymerized PEG-gels. Gels with a low G' modulus (110 Pa) showed greater cell spreading than stiffer gels (1180 Pa).[57] Results from the Caruso, Heilshorn and Anseth group are thus in good agreement with our data using SPAAC cross-linked PEG-hydrogels and were all performed on soft hydrogels (up to 2500 Pa).[48,56,57] Taken together, this indicates that stiffness seems to have an influence on the cellular adhesion of *soft hydrogels* and results in decreased cellular adhesion with increasing hydrogel stiffness.

3.6. Conclusion

We used bio-orthogonal copper-free azide-BCN cycloaddition chemistry (SPAAC) for the construction of soft PEG-based hydrogels. Hydrogels with different polymer densities were obtained by varying the total polymer content. From rheology studies to determine stiffness, storage moduli (G') in the range of 25 Pa (10 mg/mL) till 2298 Pa (30 mg/mL) were obtained. The cellular adhesion motif RGDS could easily be incorporated in the hydrogel network. Gels containing the peptide moiety formed slower, but still yielded stable networks. The RGDS content and polymer density could be varied independently of each other. Live/dead assay studies revealed that HOS cells are viable and well-spread on all RGDS-containing hydrogels, independent of their stiffness. For both HeLa cells and NIH 3T3 fibroblasts many live cells were found on the 10 mg/mL (25 Pa) and 20 mg/mL (1192 Pa) gels. With increased hydrogel stiffness (30 mg/mL, 2298 Pa), cellular adhesion decreased. For hydrogels in the very soft regime we

studied, hydrogel stiffness seems to be a determining factor in cellular adhesion of HeLa cells and NIH 3T3 fibroblasts.

3.7. Acknowledgements

Saskia Bode is gratefully acknowledged for carrying out all the microscopy experiments, her expertise on the cell studies, all useful discussions and for co-authoring the manuscript. Addie Kusters is thanked for starting this research during his internship. Sander Leeuwenburgh is acknowlegded for fruitful discussions. The department of General Instruments of the Radboud University Nijmegen, especially Liesbeth Pierson, is thanked for providing light microscopy services.

3.8. Materials and methods

The 2-chlorotrityl resin was purchased from Bachem (Bubendorf, Switzerland) and Fmoc-L-amino acids were purchased from Novabiochem (EMD Chemicals, Gibbstown, USA) or Bachem. 4-Armed poly(ethylene glycol)-NH_2 (10 kDa) salt was obtained from JenKem Technology (USA). (1*R*,8*S*,9*S*)-Bicyclo[6.1.0]non-4-yn-9-ylmethyl succinimidyl carbonate was purchased from Synaffix (Oss, The Netherlands). Fetal bovine serum (FBS) was from Integro (Zaandam, The Netherlands) and plain Dulbecco's Modified Eagle Medium (DMEM) and trypsin/EDTA were both from PAA Laboratories (Pasching, Austria). The WST-8 dye was obtained from Dojindo Molecular Technologies (Rockville, USA). The Live/Dead® viability reagents were obtained from Life Technologies (Thermo Fisher Scientific Inc., Waltham, U.S.A.). All other chemicals were purchased from Sigma-Aldrich, Baker or Fluka and utilized as received. Human epithelial ovarian carcinoma (HeLa), human osteosarcoma (HOS) cells and NIH 3T3 fibroblasts were obtained from ATCC (Rockville, USA).

^{1}H NMR spectra were recorded on a Varian Mercury (400 MHz). As a solvent shift reference, we used $CDCl_3$ (δ = 7.26 ppm), and D_2O (δ = 4.79 ppm). Mass spectra were recorded on a Thermo Finnigan LCQ-Advantage MAX or on a Bruker Biflex MALDI-TOF (Bruker Daltronik, Bremen, Germany). As matrix, α-cyano-4-hydroxycinnamic acid was used. IR-spectra were recorded on a Bruker Tensor 27 FTIR spectrometer. Column chromatography was performed with Silica gel 60 (particle size 0.040 – 0.063 mm Merck) or aluminum oxide (basic activated, pore size 58 Å, Sigma-Aldrich). Thin-layer chromatography (TLC) was performed on silica gel coated plates (Merck 60, F-254). Visualization was accomplished with UV-light and/or ninhydrin or permanganate staining. Lyophilization was achieved using an ilShin Freeze Dryer (ilShin, Ede,

The Netherlands). Analytic HPLC was performed on a Shimadzu LC-20A Prominence system (Shimadzu, 's Hertogenbosch, The Netherlands) equipped with a C18 ReproSil column, 150 x 3 mm, particle size 3 µm (Dr. Maisch GmbH, Screening Devices, Amersfoort, The Netherlands). Elution of the peptides was achieved using an acetonitrile/water gradient containing 0.1% trifluoroacetic acid (5-100%, 1-31 min, flow 0.4 mL/min). LC-MS was performed on a Thermo Finnigan LCQ-Fleet ESI-ion trap (Thermo Fischer, Breda, The Netherlands) equipped with a Phenomenex C18 column, 50 x 2.0 mm, particle size 3 µm (Phenomenex, Utrecht, The Netherlands). An acetonitrile/water gradient containing 0.1% formic acid was used for elution (5-100%, 1-10 min, flow 0.2 mL/min). Rheology measurements were performed on an AR2000ex rheometer (TA instruments, New Castle, USA). Absorbance was measured at 450 nm using a Tecan Infinite M200 Pro plate reader. Confocal laser scanning microscopy (CLSM) studies were performed on a Leica-microsystems (Mannheim, Germany) TCS SP2 AOBS system, installed on an inverted motorized DM IRE2 microscope and equipped with a 40 x water immersion HCX apo long distance lens.

Star-PEG-BCN

To a dry reaction flask was added 10 kDa 4-armed poly(ethylene glycol)-NH_2 HCl salt (600 mg, 0.06 mmol), (1*R*,8*S*,9*S*)-bicyclo[6.1.0]non-4-yn-9-ylmethyl succinimidyl carbonate (BCN-OSu; 87.4 mg, 0.30 mmol) and 100 µL triethylamine (100 µL, 0.72 mmol) in dry DCM (25 mL). The reaction mixture was stirred at r.t. overnight under N_2 atmosphere. Extraction was performed with 2M NaOH (3 x 25 mL). The organic layer was dried over $MgSO_4$ and concentrated in vacuo. The residue was purified by column chromatography on silica gel (MeOH:DCM 2:98, followed by 10:90). The product was afforded as a white powder after freeze-drying from dioxane (406 mg, 63%).

R_f = 0.36 (MeOH:DCM, 10:90)

^{1}H-NMR (400 MHz, $CDCl_3$): δ = 0.86 – 1.01 (m, 4H), 1.25 – 1.43 (m, 8H), 1.52 – 1.66 (m, 8H), 2.18 – 2.34 (m, 16H), 3.38 (m, 16H), 3.51 – 3.86 (m, $[CH_2CH_2O]_n$), 4.15 (d, J = 8.0 Hz, 8H).

MALDI-TOF (α-cyano-4-hydroxycinnamic acid): **Figure 3.10**

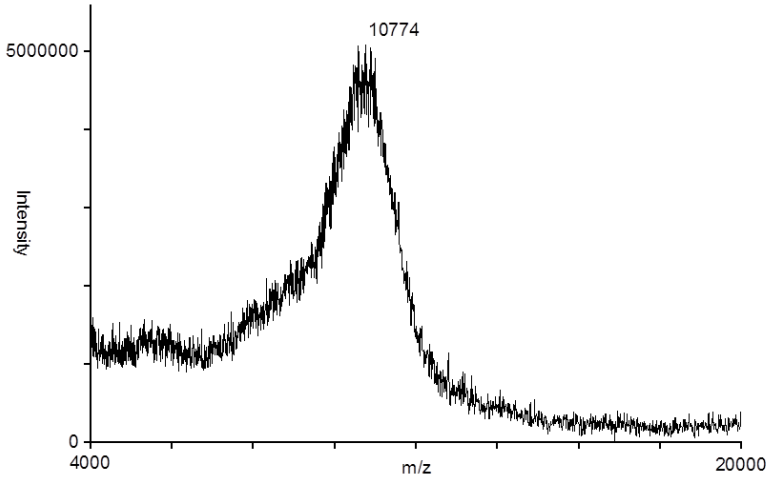

Figure 3.10. MALDI –TOF spectrum star-PEG-BCN, calculated m/z: 10791 for 222 ethylene glycol units.

Azido-acetic acid[58]

Bromoacetic acid (13.9 g, 100 mmol) and sodium azide (13.0 g, 200 mmol) were dissolved in water (60 mL) and stirred for 48 h at r.t. Concentrated hydrochloric acid (50 mL) was added to the reaction mixture after which extraction was performed with diethylether (4 x 100 mL). The combined organic phases were dried over $MgSO_4$ and evaporated in vacuo. The product was obtained as yellow oil and was dried under vacuum (9.86 g, 98%).

^{1}H-NMR (400 MHz, $CDCl_3$): δ = 3.98 (s, 2H)

LCQ: m/z: 138.7 $[M + K]^+$ (calculated $[M + K]^+$ = 139.15)

IR: 2115.73 cm^{-1} (N_3)

Star-PEG-N_3

To 4-armed poly(ethylene glycol)-NH_2 HCl salt (800 mg, 80 µmol) in DCM (25 mL) was added subsequently benzotriazol-1-yl-oxy-tris dimethylaminophosphonium hexafluorophosphate (BOP; 283 mg, 0.64 mmol), azido acetic acid (65 mg, 0.64 mmol) and D*i*PEA (328 µL 1.92 mmol). The reaction mixture was stirred overnight at r.t and extracted with 1 M $KHSO_4$ (5 x 50 mL) and brine (1 x 50 mL). The organic layer was dried over $MgSO_4$ and concentrated in vacuo. The compound was purified by column chromatography on basic aluminum oxide, using MeOH:DCM (10:90) as eluent. Freeze-drying from dioxane afforded the product as a white powder (760 mg, 92%).

R_f = 0.38 (MeOH:DCM, 10:90)

^{1}H-NMR (400 MHz, $CDCl_3$): δ = 3.41 (s, 8H), 3.45 – 3.55 (m, 16H), 3.57 – 3.70 (m, $[CH_2CH_2O]_n$), 3.96 (s, 8H).

MALDI-TOF (α-cyano-4-hydroxycinnamic acid): **Figure 3.11**

IR = 2103.52 cm^{-1} (N_3)

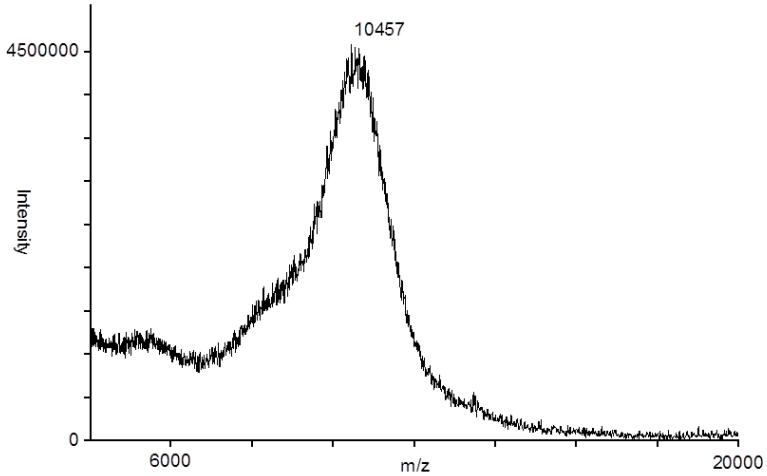

Figure 3.11. MALDI-TOF spectrum star-PEG-N_3, calculated m/z: 10463 for 223 ethylene glycol units.

Peptide synthesis

The peptides were synthesized from 2.0 g 2-chloro-trityl resin using Fmoc solid-phase peptide synthesis (SPPS). The resin was swollen in DCM for 20 min prior to use. Functionalization of the resin with the first amino acid was performed for 30 min with 2.0 eq of the required amino acid and 3.0 eq D*i*PEA. This procedure was repeated with a coupling time of 60 min, after which capping was performed with 2.0 eq D*i*PEA in methanol. Deprotection of the Fmoc-groups was carried out with piperidine in DMF (20%, v/v) for 20 min. Subsequent couplings were performed with 3.0 eq of the required amino acid, 3.3 eq of *N,N'*-diisopropylcarbodiimide (DIPCDI) and 3.6 eq of *N*-hydroxybenzotriazole (HOBt) in DMF. After each coupling and deprotection step, a Kaiser test[59] was done to ensure completion of the reaction. In the final step, azido acetic acid (3.0 eq) was coupled using DIPCDI (3.3 eq) and HOBt (3.6 eq). The peptides were cleaved from the resin with mild cleaving reagents, to ensure that the acid-labile protecting groups remained intact. Cleavage was performed by treatment of the resin with a mixture of dichloromethane (DCM), trifluoroethanol (TFE) and acetic acid (HOAc) (6:1:1) for 3 h. The solvents were evaporated under reduced pressure and co-evaporation was performed with chloroform (3 x 40 mL). The peptides were afforded as white solids after freeze-drying from dioxane.

Azidoacetyl-Arg(Pbf)-Gly-Asp(OtBu)-Ser(tBu)-Gly-OH (azidoGly-Arg-Gly-Asp-Ser-Gly-OH)
LCQ: m/z: 938.3 $[M + H]^+$ (calculated $[M + H]^+$ = 938.4)
LC-MS: m/z: 938.5 $[M + H]^+$, Rt = 9.21 min
HPLC: Rt = 21.56 min
IR: 2107.08 cm^{-1} (N_3)

Azidoacetyl-Arg(Pbf)-Asp(OtBu)-Gly-Ser(tBu)-Gly-OH (azidoGly-Arg-Asp-Gly-Ser-Gly-OH (scrambled))
LCQ: m/z: 938.3 $[M + H]^+$ (calculated $[M + H]^+ = 938.4$)
LC-MS: m/z: 938.8 $[M + H]^+$, Rt = 9.09 min
HPLC: Rt = 19.96 min
IR: 2102.76 cm^{-1} (N_3)

Star-PEG-RGDS-N_3 and star-PEG-scrambled

To star-poly(ethylene glycol)-NH_2 HCl salt (750 mg, 75 µmol) in DCM (20 mL) was added subsequently BOP (199 mg, 0.45 mmol), protected peptide (azidoGly-Arg-Gly-Asp-Ser-Gly-OH or azidoGly-Arg-Asp-Gly-Ser-Gly-OH 422 mg, 0.45 mmol), and D*i*PEA (314 µL, 1.8 mmol). The reaction mixture was stirred overnight at r.t. Extraction was performed with 1 M $KHSO_4$ (4 x 60 mL) and brine (1 x 60 mL), after which the organic layer was dried over $MgSO_4$. Column chromatography on basic aluminum oxide (MeOH: DCM; 10:90) afforded white powders after freeze-drying from dioxane (RGDS: 885 mg, 86%; Scrambled: 896 mg, 87%).

Star-PEG-RGDS-N_3 (Azidoacetyl-Arg(Pbf)-Gly-Asp(OtBu)- Ser(tBu)-Gly-star-PEG)
R_f = 0.30 (MeOH:DCM 10:90)
^{1}H-NMR (400 MHz, $CDCl_3$): δ = 1.15 (s, 36H), 1.42 (s, 36H), 1.46 (s, 32H), 2.09 (s), 2.53 - 3.07 (m), 3.48 – 3.70 (m, $[CH_2CH_2O]_n$), 3.99 (m), 4.35 (m), 4.67 (m).
MALDI-TOF (α-cyano-4-hydroxycinnamic acid): **Figure 3.12**

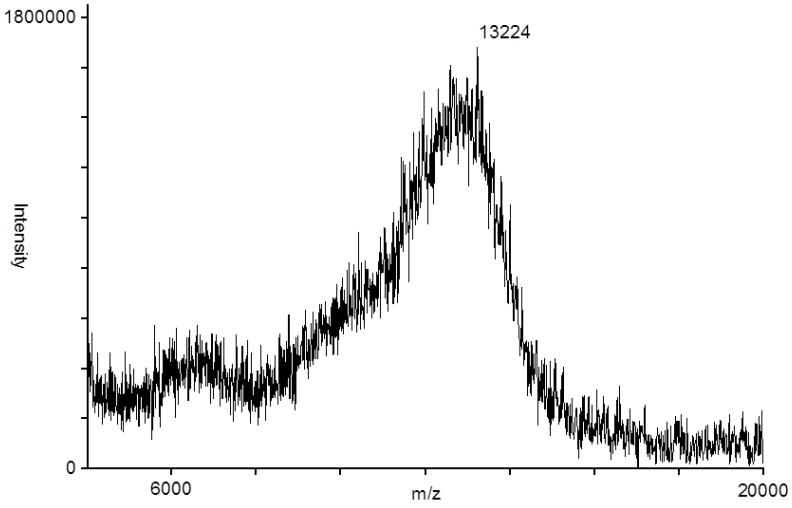

Figure 3.12. MALDI-TOF spectrum star-PEG-RGDS-N_3 (Azidoacetyl-Arg(Pbf)-Gly-Asp(OtBu)- Ser(tBu)-Gly-star-PEG), calculated m/z: 13239 for 210 polyethylene glycol units.

Star-PEG-scrambled (Azidoacetyl-Arg(Pbf)-Asp(OtBu)-Gly-Ser(tBu)-Gly-star-PEG)

R_f = 0.30 (MeOH:DCM 10:90)

^{1}H-NMR (400 MHz, $CDCl_3$): δ = 1.18 (s, 36H), 1.42 (s, 36H), 1.46 (s, 32H), 2.09 (s), 2.52 - 3.00 (m), 3.50 – 3.69 (m, $[CH_2CH_2O]_n$), 3.95 (m), 4.49 (m), 4.75 (m).

MALDI-TOF (α-cyano-4-hydroxycinnamic acid): **Figure 3.13**

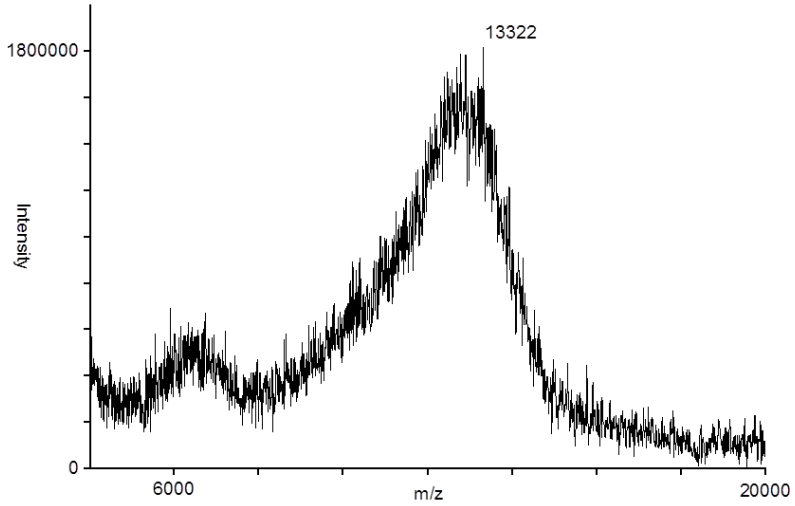

Figure 3.13. MALDI-TOF spectrum star-PEG-scrambled (Azidoacetyl- Arg(Pbf)-Asp(OtBu)-Gly-Ser(tBu)-Gly-star-PEG), calculated m/z: 13327 for 212 polyethylene glycol units.

Deprotection star-PEG-RGDS-N_3 and star-PEG-scrambled

The protected peptide-star-PEG construct (350 mg; 25.6 µmol) was treated with TFA:TIS: H_2O (95:2.5:2.5; 8 mL) for 4 h at r.t. The reaction mixture was concentrated and co-evaporated with toluene (4 x 30 mL). The product was dissolved in water and dialysed against 800 mL water using dialysis membranes with a MW cut-off of 3500 Da. Dialysis was performed for 5 days under regular exchange of the water (twice a day). After dialysis, the products were obtained as white solids by freeze-drying (RGDS: 289 mg, 92%; Scrambled: 298 mg, 95%).

Star-PEG-RGDS-N_3

^{1}H-NMR (400 MHz, D_2O): δ = 1.60 – 1.99 (m), 2.68 (m), 3.36 – 3.75 (m, $[CH_2CH_2O]_n$), 3.84 – 4.10 (m), 4.41 (m).

MALDI-TOF (α-cyano-4-hydroxycinnamic acid): **Figure 3.14**

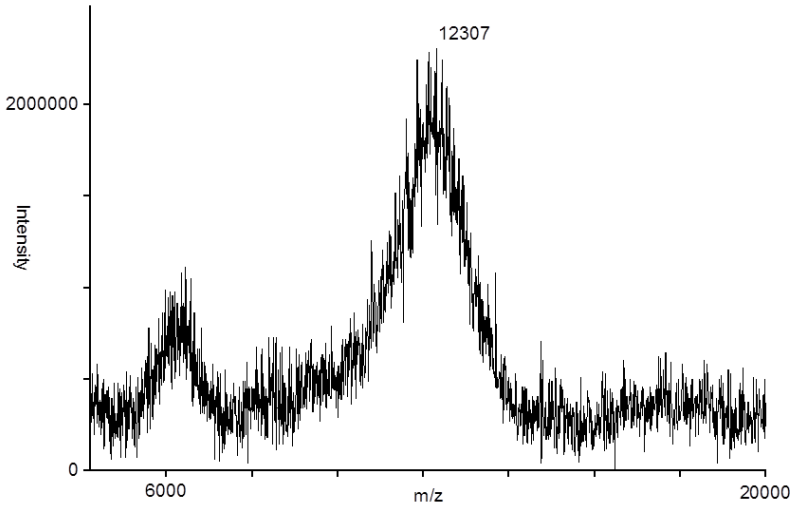

Figure 3.14. MALDI-TOF spectrum star-PEG-RGDS-N_3, calculated m/z: 12310 for 222 ethylene glycol units.

Star-PEG-scrambled

^{1}H-NMR (400 MHz, D_2O): δ = 1.57 – 1.98 (m), 2.69 (m), 3.35 – 3.74 (m, $[CH_2CH_2O]_n$), 3.83 – 4.10 (m), 4.38 (m).

MALDI-TOF (α-cyano-4-hydroxycinnamic acid): **Figure 3.15**

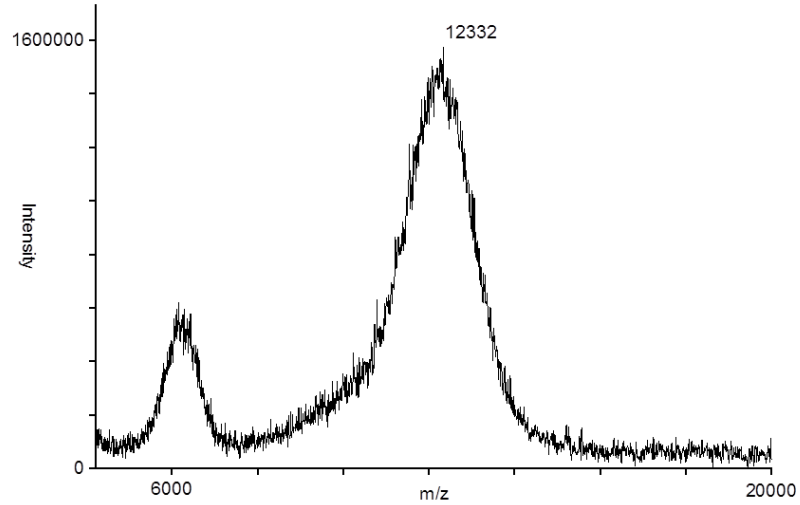

Figure 3.15. MALDI-TOF spectrum star-PEG-scrambled, calculated m/z: 12353 for 223 ethylene glycol units.

Hydrogel formation

Hydrogels were prepared by weighing off equal amounts of star-PEG-BCN and star-PEG-N_3 with a total polymer concentration of 10, 20 or 30 mg/mL. For example, a typical 30 mg/mL PEG hydrogel was obtained by dissolving 3.00 mg star-PEG-BCN in 100 µL MilliQ. To this solution was added 100 µL star-PEG-N_3 (30 mg/mL, in MilliQ). The two hydrogel components were mixed by vortexing and left at room temperature to allow gel formation. For a peptide-containing hydrogel, stock solutions of star-PEG-N_3 and star-PEG-RGDS/star-PEG-RDGS were added to star-PEG-BCN. For example, a 50% RGDS-containing gel (20 mg/mL) was prepared by adding 50 µL star-PEG-N_3 and 50 µL star-PEG-RGDS (each 20 mg/mL in MilliQ) to a star-PEG-BCN solution (2 mg in 100 µL MilliQ).

Rheology

The storage (G') and loss modulus (G'') of the hydrogels were measured using an AR2000ex rheometer (TA instruments). All measurements were performed using a flat steel plate geometry (20 mm, gap size 500 µm) and were performed at a temperature of 20°C. Hydrogel solutions were prepared at different polymer concentrations and RGDS-content. A molar ratio of 1:1 between the alkyne and azide groups was used to ensure complete cross-linking. Hydrogel solutions were loaded on the rheometer as liquid (200 µL) and were measured during the gelation process. To minimize evaporation, a solvent trap was utilized which was filled with water. Initially, a strain sweep measurement was conducted on cured gels to determine the linear viscoelastic range, by measuring between 0.1 and 1000% strain at an angular frequency of 10 rad/s. Within this range, a strain percentage (1%) was chosen to perform further measurements (**Figure 3.5**). Oscillatory time sweep measurements were measured at a constant strain of 1% and an angular frequency of 10 rad/s and were continued until stable values of G' were obtained. Typically, time sweep tests were conducted for 2.5 h (30 mg/mL), 5.5 h (20 mg/mL) and 16 h (10 mg/mL). Additionally, overnight time sweep measurements (16 h) were performed for 30 mg/mL hydrogels containing 0% peptide, 100% RGDS and 100% Scrambled peptide (**Table 3.4**, n = 2). All other rheology measurements were performed with n = 3 or n = 4.

Table 3.4. G' values for overnight time sweep measurements (16 h) for 30 mg/mL gels (n = 2)

Peptide	**Overnight 30 mg/mL (16h)**
0%	3186 ± 110
100 % RGDS	2863 ± 107
100% Scrambled	3086 ± 501

Swelling

Hydrogels (250 µL) were prepared from star-PEG-BCN and star-PEG-N_3 following the general protocol using total polymer concentrations of 10, 20 and 30 mg/mL. Gels were allowed to

cross-link overnight, after which they were weighed to obtain the mass after gelation (Mg). After swelling for 24 h in MilliQ water, gels were weighed again, yielding the mass after swelling (Ms). The swelling ratio was given as Q = Ms/Mg. Samples were made with n = 5 for each polymer concentration (**Table 3.5**).

Table 3.5. Swelling ratios (Q) for star-PEG-BCN / star-PEG-N_3 hydrogels as determined by dividing the mass after swelling (Ms) through the mass after gelation (Mg) (n = 5).

Hydrogel	Swelling ratio Q
10 mg/mL	1.032 ± 0.004
20 mg/mL	1.008 + 0.004
30 mg/mL	1.013 ± 0.011

Cell culture

NIH 3T3 fibroblasts and HeLa cells were maintained in sterile conditions in Dulbecco's Modified Eagle's medium (DMEM) supplemented with 10% heat-inactivated fetal bovine serum (FBS). For Human Osteosarcoma (HOS) cells, DF medium (DMEM: Ham's F-12 nutrient mixture 1:1) containing 10% heat-inactivated FBS was used. Cells were maintained on tissue culture plastic and kept at 37°C in a humidified atmosphere of 7.5% CO_2. Cells were passaged every 2-3 days. Prior to cell studies, cells within a confluent layer were detached by trypsinisation (using trypsin/EDTA). Cells were resuspended in media and the number of cells was counted using an inverted microscope and a cell counting chamber (Fuchs-Rosenthal).

WST-8 assay[55]

Hydrogels were formed in a 96-well plate; to each well 75 µL hydrogel solution (see hydrogel formation) was added. The plate was wrapped with parafilm and gels were allowed to form overnight (24 h). All samples were measured in triplo. As a positive control, a number of wells were coated with 1% gelatin to obtain 100% viable cells. NIH 3T3 fibroblasts were plated at a density of 18000 cells in 100 µL per hydrogel-containing well. Cells cultured on the hydrogels were incubated for 18 h (37°C, 7.5% CO_2). Cells were examined under a standard inverted microscopy (Olympus CK2) prior to WST-8 addition, to evaluate the total cell count visually. Media were replaced by 100 µL WST-8 (1:10 in DMEM) and incubation was performed for 4-6 h. The absorbance of the WST-8 solution was measured at 450 nm using a Tecan Infinite M200 Pro plate reader. For all samples and the gelatin control, the background absorbance was subtracted, which was the absorbance measured in wells that only contained the WST-8 dye in medium. Total cell count for all hydrogels was calculated as a percentage of the positive gelatin control, which was set to 100% viable cells.

Confocal microscopy

Hydrogel solutions were prepared, following the general protocol of hydrogel formation. All RGDS-hydrogels contained 50% of the cell adhesion domain. An 8-chambered coverslip (Nunc, Wiesbaden, Germany) was coated with gel by addition of a small layer of hydrogel solution. The coverslip was wrapped with parafilm and gels were allowed to cure for 24 h at r.t. In each well, 40.000 cells in 250 µL medium were seeded. Wells coated with gelatin were used as positive control. Cells were incubated overnight (37°C, 7.5% CO_2). After this incubation period, the cells were treated with the live/dead staining, which was prepared by diluting calcein-AM and ethidium homodimer-1 (EthD-1) in PBS to obtain a concentration of 4 mM calcein-AM and 8 mM EthD-1 for HeLa and HOS cells, the concentration was lowered to 1.33 mM calcein-AM and 2.67 mM EthD-1 for NIH 3T3 fibroblasts. The samples were allowed to rest for 10 minutes, after which they were immediately analysed by confocal laser scanning microscopy. Calcein was excited with the 488 nm line of an argon ion laser, and emission was collected between 494 and 515 nm. EthD-1 was excited with the 561 nm line of a yellow diode laser and emission was collected between 600 and 625 nm. Using the ImageJ software, overlay images of the calcein and EthD-1 signals were produced (**Figures 3.7, 3.8** and **3.16-3.18**).

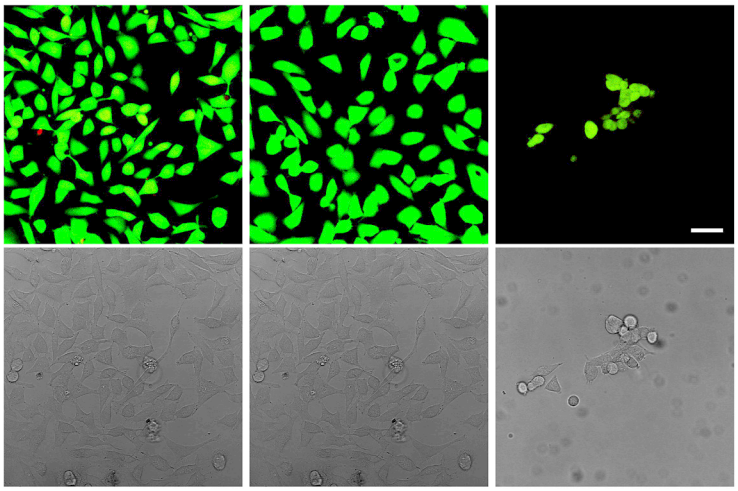

Figure 3.16. Live dead assay with HeLa cells, showing fluorescent overlay images of the calcein (green) and EthD-1 (red) channel and transmission images. HeLa cells were seeded on RGDS-containing hydrogels (50%) with varying stiffness (10, 20 and 30 mg/mL, left to right). Scale bar corresponds to 50 µm for all pictures.

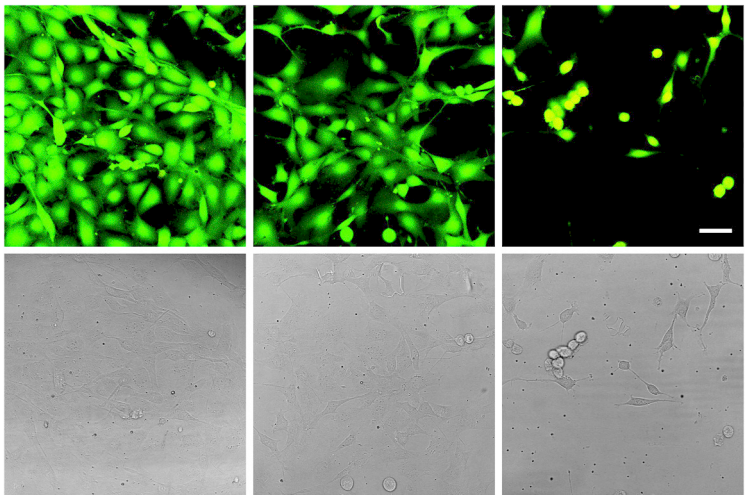

Figure 3.17. Live dead assay with NIH 3T3 fibroblasts, showing fluorescent overlay images of the calcein (green) and EthD-1 (red) channel and transmission images. Fibroblasts were seeded on RGDS-containing hydrogels (50%) with varying stiffness (10, 20 and 30 mg/mL, left to right). Scale bar corresponds to 50 µm for all pictures.

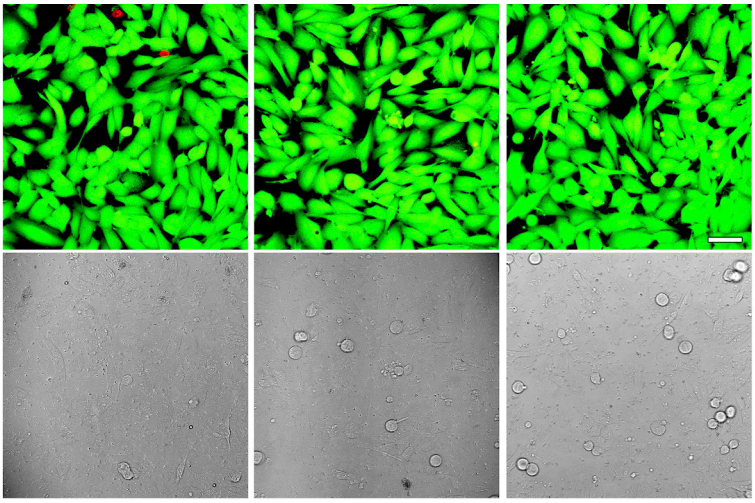

Figure 3.18. Live dead assay with HOS cells, showing fluorescent overlay images of the calcein (green) and EthD-1 (red) channel and transmission images. HOS cells were seeded on RGDS-containing hydrogels (50%) with varying stiffness (10, 20 and 30 mg/mL, left to right). Scale bar corresponds to 50 µm for all pictures.

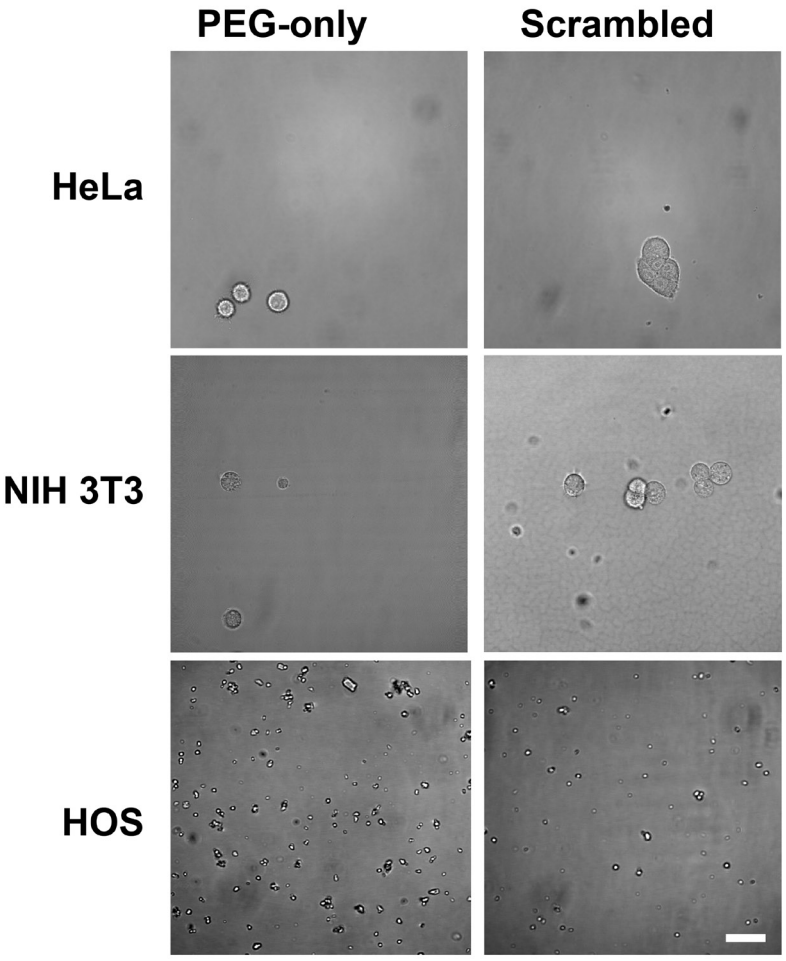

Figure 3.19. Representative transmission images of both negative controls for all cell types. Hydrogels stiffness did not have an influence, no living cells were found for all PEG-only and scrambled hydrogels. Scale bar corresponds to 50 μm for all pictures.

3.9. References

(1) Van Vlierberghe, S.; Dubruel, P.; Schacht, E. *Biomacromolecules* **2011**, *12*, 1387-1408.

(2) Peppas, N. A.; Hilt, J. Z.; Khademhosseini, A.; Langer, R. *Adv. Mater.* **2006**, *18*, 1345-1360.

(3) Kharkar, P. M.; Kiick, K. L.; Kloxin, A. M. *Chem. Soc. Rev.* **2013**, *42*, 7335-7372.

(4) Jonker, A. M.; Löwik, D. W. P. M.; van Hest, J. C. M. *Chem. Mater.* **2012**, *24*, 759-773.

(5) Zhu, J. *Biomaterials* **2010**, *31*, 4639-4656.

(6) Lin, C.-C.; Anseth, K. S. *Pharm. Res.* **2008**, *26*, 631-643.

(7) Peppas, N. A.; Keys, K. B.; Torres-Lugo, M.; Lowman, A. M. *J. Control. Release* **1999**, *62*, 81-87.

(8) Peppas, N. A.; Bures, P.; Leobandung, W.; Ichikawa, H. *Eur. J. Pharm. Biopharm.* **2000**, *50*, 27-46.

(9) Tornoe, C. W.; Christensen, C.; Meldal, M. *J. Org. Chem.* **2002**, *67*, 3057-3064.

(10) Rostovtsev, V. V.; Green, L. G.; Fokin, V. V.; Sharpless, K. B. *Angew. Chem. Int. Ed.* **2002**, *41*, 2596-2599.

(11) Jewett, J. C.; Bertozzi, C. R. *Chem. Soc. Rev.* **2010**, *39*, 1272-1279.

(12) Codelli, J. A.; Baskin, J. M.; Agard, N. J.; Bertozzi, C. R. *J. Am. Chem. Soc.* **2008**, *130*, 11486-11493.

(13) Dommerholt, J.; Schmidt, S.; Temming, R.; Hendriks, L. J. A.; Rutjes, F. P. J. T.; van Hest, J. C. M.; Lefeber, D. J.; Friedl, P.; van Delft, F. L. *Angew. Chem. Int. Ed.* **2010**, *49*, 9422-9425.

(14) Thirumurugan, P.; Matosiuk, D.; Jozwiak, K. *Chem. Rev.* **2013**, *113*, 4905-4979.

(15) Lowe, A. B. *Polym. Chem.* **2010**, *1*, 17-36.

(16) Hoyle, C. E.; Bowman, C. N. *Angew. Chem. Int. Ed.* **2010**, *49*, 1540-1573.

(17) Aimetti, A. A.; Machen, A. J.; Anseth, K. S. *Biomaterials* **2009**, *30*, 6048-6054.

(18) Shih, H.; Lin, C.-C. *Biomacromolecules* **2012**, *13*, 2003-2012.

(19) Devaraj, N. K.; Weissleder, R.; Hilderbrand, S. A. *Bioconjugate Chem.* **2008**, *19*, 2297-2299.

(20) Alge, D. L.; Azagarsamy, M. A.; Donohue, D. F.; Anseth, K. S. *Biomacromolecules* **2013**, *14*, 949-953.

(21) Wei, H.-L.; Yang, Z.; Zheng, L.-M.; Shen, Y.-M. *Polymer* **2009**, *50*, 2836-2840.

(22) Nimmo, C. M.; Owen, S. C.; Shoichet, M. S. *Biomacromolecules* **2011**, *12*, 824-830.

(23) Borrmann, A.; Fatunsin, O.; Dommerholt, J.; Jonker, A. M.; Löwik, D. W. P. M.; van Hest, J. C. M.; van Delft, F. L. *Bioconjugate Chem.* **2015**, *26*, 257-261.

(24) Jonker, A. M.; Borrmann, A.; van Eck, E. R. H.; van Delft, F. L.; Löwik, D. W. P. M.; van Hest, J. C. M. *Adv. Mater.* **2015**, *27*, 1235-1240.

(25) Altintas, O.; Vogt, A. P.; Barner-Kowollik, C.; Tunca, U. *Polym. Chem.* **2012**, *3*, 34-45.

(26) Debets, M. F.; Van Berkel, S. S.; Dommerholt, J.; Dirks, A. J.; Rutjes, F.; Van Delft, F. L. *Accounts Chem. Res.* **2011**, *44*, 805-815.

(27) Burdick, J. A.; Anseth, K. S. *Biomaterials* **2002**, *23*, 4315-4323.

(28) Ruoslahti, E. *Annu. Rev. Cell Dev. Biol.* **1996**, *12*, 697-715.

(29) Hern, D. L.; Hubbell, J. A. *J. Biomed. Mater. Res.* **1998**, *39*, 266-276.

(30) DeForest, C. A.; Polizzotti, B. D.; Anseth, K. S. *Nat. Mater.* **2009**, *8*, 659-664.

(31) Zheng, J.; Smith Callahan, L. A.; Hao, J.; Guo, K.; Wesdemiotis, C.; Weiss, R. A.; Becker, M. L. *ACS Macro Letters* **2012**, *1*, 1071-1073.

(32) Xu, J.; Filion, T. M.; Prifti, F.; Song, J. *Chem.-Asian J.* **2011**, *6*, 2730-2737.

(33) Steinhilber, D.; Rossow, T.; Wedepohl, S.; Paulus, F.; Seiffert, S.; Haag, R. *Angew. Chem. Int. Ed.* **2013**, *52*, 13538-13543.

(34) Discher, D. E. *Science* **2005**, *310*, 1139-1143.

(35) Georges, P. C. *J. Appl. Physiol.* **2005**, *98*, 1547-1553.

(36) Engler, A. J.; Sen, S.; Sweeney, H. L.; Discher, D. E. *Cell* **2006**, *126*, 677-689.

(37) Bai, T.; Sun, F.; Zhang, L.; Sinclair, A.; Liu, S.; Ella-Menye, J.-R.; Zheng, Y.; Jiang, S. *Angew. Chem. Int. Ed.* **2014**, *53*, 12729-12734.

(38) Pelham, R. J.; Wang, Y. L. *Proc. Natl. Acad. Sci. U. S. A.* **1997**, *94*, 13661-13665.

(39) Richert, L.; Engler, A. J.; Discher, D. E.; Picart, C. *Biomacromolecules* **2004**, *5*, 1908-1916.

(40) Diederich, V. E. G.; Studer, P.; Kern, A.; Lattuada, M.; Storti, G.; Sharma, R. I.; Snedeker, J. G.; Morbidelli, M. *Biotechnol. Bioeng.* **2013**, *110*, 1508-1519.

(41) Peyton, S. R.; Raub, C. B.; Keschrumrus, V. P.; Putnam, A. J. *Biomaterials* **2006**, *27*, 4881-4893.

(42) Lo, C. M.; Wang, H. B.; Dembo, M.; Wang, Y. L. *Biophys. J.* **2000**, *79*, 144-152.

(43) Engler, A. J.; Richert, L.; Wong, J. Y.; Picart, C.; Discher, D. E. *Surf. Sci.* **2004**, *570*, 142-154.

(44) Schneider, A.; Francius, G.; Obeid, R.; Schwinte, P.; Hemmerle, J.; Frisch, B.; Schaaf, P.; Voegel, J. C.; Senger, B.; Picart, C. *Langmuir* **2006**, *22*, 1193-1200.

(45) Li, Z.; Gong, Y.; Sun, S.; Du, Y.; Lü, D.; Liu, X.; Long, M. *Biomaterials* **2013**, *34*, 7616-7625.

(46) Trappmann, B.; Gautrot, J. E.; Connelly, J. T.; Strange, D. G. T.; Li, Y.; Oyen, M. L.; Stuart, M. A. C.; Boehm, H.; Li, B. J.; Vogel, V.; Spatz, J. P.; Watt, F. M.; Huck, W. T. S. *Nat. Mater.* **2012**, *11*, 642-649.

(47) Missirlis, D.; Spatz, J. P. *Biomacromolecules* **2014**, *15*, 195-205.

(48) Best, J. P.; Javed, S.; Richardson, J. J.; Cho, K. L.; Kamphuis, M. M. J.; Caruso, F. *Soft Matter* **2013**, *9*, 4580-4584.

(49) Robinson, K. G.; Nie, T.; Baldwin, A. D.; Yang, E. C.; Kiick, K. L.; Akins, R. E. *J. Biomed. Mater. Res. A* **2012**, *100A*, 1356-1367.

(50) Levental, I.; Georges, P. C.; Janmey, P. A. *Soft Matter* **2007**, *3*, 299-306.

(51) Yan, C.; Pochan, D. J. *Chem. Soc. Rev.* **2010**, *39*, 3528-3540.

(52) Arnold, M.; Cavalcanti-Adam, E. A.; Glass, R.; Blümmel, J.; Eck, W.; Kantlehner, M.; Kessler, H.; Spatz, J. P. *ChemPhysChem* **2004**, *5*, 383-388.

(53) Massia, S. P.; Hubbell, J. A. *J. Cell Biol.* **1991**, *114*, 1089-1100.

(54) Koo, L. Y.; Irvine, D. J.; Mayes, A. M.; Lauffenburger, D. A.; Griffith, L. G. *J. Cell Sci.* **2002**, *115*, 1423-1433.

(55) Tominaga, H.; Ishiyama, M.; Ohseto, F.; Sasamoto, K.; Hamamoto, T.; Suzuki, K.; Watanabe, M. *Anal. Commun.* **1999**, *36*, 47-50.

(56) Wang, H.; Cai, L.; Paul, A.; Enejder, A.; Heilshorn, S. C. *Biomacromolecules* **2014**, *15*, 3421-3428.

(57) Kyburz, K. A.; Anseth, K. S. *Acta Biomater.* **2013**, *9*, 6381-6392.

(58) Pfeiffer, H.; Rojas, A.; Niesel, J.; Schatzschneider, U. *Dalton T.* **2009**, 4292-4298.

(59) Kaiser, E.; Colescott, R. L.; Bossinger, C. D.; Cook, P. I. *Anal. Biochem.* **1970**, *34*, 595-598.

Chapter 4

A fast and activatable cross-linking strategy for hydrogel formation

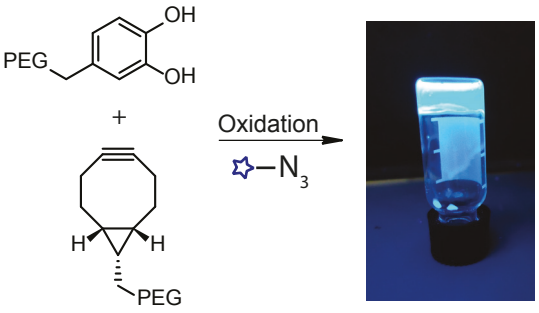

This chapter has been published as:
Jonker, A. M.; Borrmann, A.; van Eck, E. R. H.; van Delft, F. L.; Löwik, D. W. P. M.; van Hest, J. C. M.
Adv. Mater. **2015**, 27, 1235-1240

4.1. Introduction

Hydrogels are water-swollen networks, formed by cross-links between the polymeric constituents. In the past years, they have received increasing attention as injectable drug deliverables, as scaffolds for the immobilization of biomolecules and as matrix materials in regenerative medicine. Poly(ethylene)glycol (PEG) is often applied as the polymeric basis, because it has excellent biocompatibility, is hydrophilic, shows low toxicity and is non-adhesive towards proteins and cells. Typically, the PEG-based polymers contain terminal mutually reactive groups that form a cross-linked network upon reaction.[1-7] A variety of reactions have been successfully used to form gels via chemical cross-linking.[8,9] The Cu(I)-catalysed azide-alkyne cycloaddition (CuAAC, commonly known as click chemistry), as introduced by Meldal and Sharpless[10,11], has proven to be very promising to form PEG-based hydrogels as it is fast, high-yielding and modular, but most importantly orthogonal.[12,13] However, the cytotoxicity associated with the Cu(I)-catalyst limits the usage of CuAAC for the preparation of hydrogels for biomedical applications. Other conjugation strategies have also been reported for hydrogel formation such as thiol-ene photoclick reactions[14-16], Michael-type additions[17,18], thiol-norbornene reactions[19], oxime chemistry[20], Diels-Alder cycloadditions[21-23] and strain-promoted azide-alkyne cycloadditions (SPAAC).[24-26] Especially, Diels-Alder reactions and SPAAC form viable alternatives to CuAAC as cross-linking method due to their bio-orthogonal character and spontaneous reactivity.[27-30] The Anseth group was the first to exploit SPAAC for hydrogel formation by using star-shaped PEG-azide and cyclooctyne-containing peptides. By incorporation of a photocleavable group, hydrogels could be post-modified with thiol-containing compounds using UV-light.[24] However, an important aspect the abovementioned crosslinking methods are all lacking is a coupling strategy which is both fast and which can be activated. This is a highly desired property for injectable hydrogels and for other biomedical applications where spatiotemporal control of hydrogel formation is demanded. An interesting activatable and bio-inspired cross-linking method has been reported by Messersmith and co-workers. They functionalized four-armed PEG (M_n = 10.000 Da) with the unnatural amino acid 3,4-dihydroxyphenylalanine (DOPA). Subsequent oxidation of the DOPA groups with sodium periodate resulted in hydrogel formation.[31] In recent years, more groups have developed DOPA-inspired hydrogels with potential as adhesive materials in tissue engineering.[32-34] Apart from covalent cross-linking methods, the catechol moiety is also capable of forming strong complexes with metal ions like Fe^{3+}. This property was recently used as a non-covalent cross-linking method to rapidly form pH-induced reversible hydrogels.[35,36] However, strategies to form covalently cross-linked hydrogels are still hampered by slow reaction kinetics.

In this chapter, we report a fast and activatable cross-linking method for hydrogel formation using a strain-promoted oxidation-controlled cyclooctyne–1,2-quinone cycloaddition (SPOCQ).[37] We show that the formation of hydrogels out of four-armed star PEG functionalized with cyclooctyne derivative bicyclo[6.1.0]non-4-yne (BCN) and catechol DHPA (3,4 dihydroxy phenylacetic acid), proceeds extremely fast after oxidation of the catechol to the quinone, which can be triggered both chemically (**Paragraph 4.2.1**) and enzymatically (**Paragraph 4.2.2**; **Figure 4.1**). Moreover, both BCN and DHPA are readily accessible, making this a user-friendly cross-linking method for hydrogel formation. Furthermore, we demonstrate that the SPOCQ and SPAAC reactions can be used in concert, due to the large difference in reaction rates (**Paragraph 4.3, Figure 4.1**). The SPOCQ reaction thus offers a versatile, fast and activatable alternative to current hydrogel cross-linking strategies.

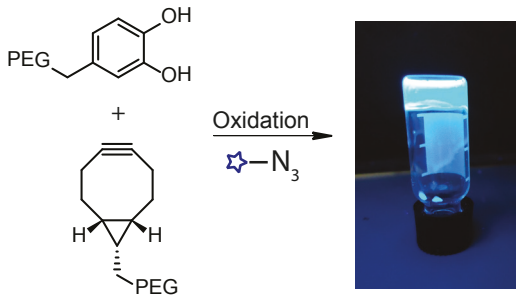

Figure 4.1. Schematic overview of the SPOCQ reaction between catechol- and cyclooctyne-functionalized PEG, resulting in hydrogel formation upon oxidation. SPOCQ and SPAAC can be used as an orthogonal reaction pair, as demonstrated with an azide-functionalized fluorescent dye.

4.2. Hydrogel synthesis using SPOCQ

4.2.1. Sodium periodate as oxidizing agent

To form hydrogels with four-armed poly(ethylene) glycol (M_n = 10.000 Da, star-PEG), we first had to functionalize PEG with cyclooctyne derivative bicyclo[6.1.0]non-4-yne (BCN) and with DOPA derivative 3,4 dihydroxy phenylacetic acid (DHPA). This could simply be performed in one step by coupling of respectively BCN-succinimidyl ester (**Chapter 3**) or 3,4 dihydroxy phenylacetic acid to star-PEG-amine. Hydrogel formation was studied at polymer concentrations of 10, 20 and 30 mg/mL (1-3 wt%). Sodium periodate was used to oxidize the catechol moieties. The oxidizing agent (1 eq) was added to an equimolar mixture of polymers star-PEG-BCN and star-PEG-DHPA. Hydrogels were formed almost instantaneously, due to the fast reaction kinetics of the SPOCQ reaction (**Figure 4.2**).[37]

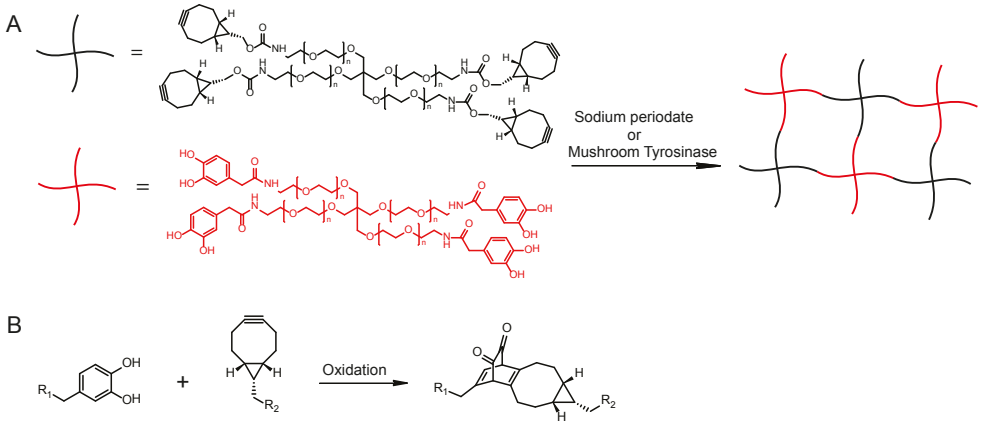

Figure 4.2. Hydrogel formation using the SPOCQ reaction. A: A mixture of star-PEG-BCN and star-PEG-DHPA is oxidized with sodium periodate or mushroom tyrosinase, to yield a stable hydrogel network. B. SPOCQ cross-linking between BCN and DHPA upon oxidization.

Varying the polymer concentration (10, 20 or 30 mg/mL) did not influence the gelation time. The mechanical properties of the hydrogels were measured using rheology. The storage (G') and loss modulus (G'') were determined with an oscillatory time sweep test. Due to fast gelation of our periodate-induced hydrogels, the gelation point (where G' exceeds G'') could not be determined. Stable G' and G'' values were already found from the start of the measurement and remained constant in an overnight time sweep study showing that gels very quickly obtained their final strength (**Figure 4.3A**).

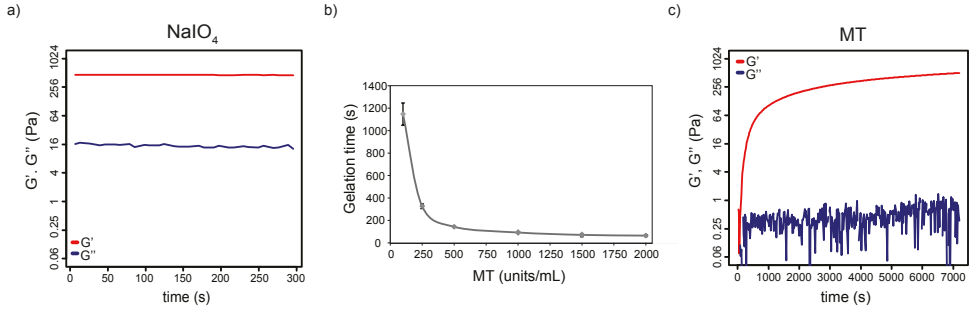

Figure 4.3. Rheological analysis of SPOCQ cross-linked hydrogels. a) Representative time sweep measurement (t = 5 min) of a $NaIO_4$ oxidized hydrogel. Gels directly obtained their final G' (red line) and G'' (blue line) values. b). Gelation time of mushroom tyrosinase cross-linked hydrogels as estimated via the inverted vial test. The gelation time was approximately 1 min with 2000 units/mL and increased with decreasing enzyme concentration. c). Representative time sweep measurement (t = 2 h) of enzyme cross-linked hydrogels (500 units/mL).

Gels were found to be soft for all studied polymer concentrations (10, 20 and 30 mg/mL), as expected at these low weight percentages. Stronger gels were formed with increasing polymer content. G' values of 65 Pa (10 mg/mL), 454 Pa (20 mg/mL) and 1375 Pa (30 mg/mL) were obtained for the periodate-induced gels. The PEG material displayed typical hydrogel behaviour, as G' values were much larger than G'' values. Frequency sweep measurements were conducted on all cured hydrogels and G' and G'' values were found to be independent of frequency (**Figure 4.4**). This corresponds to a predominantly elastic composition of the hydrogels.

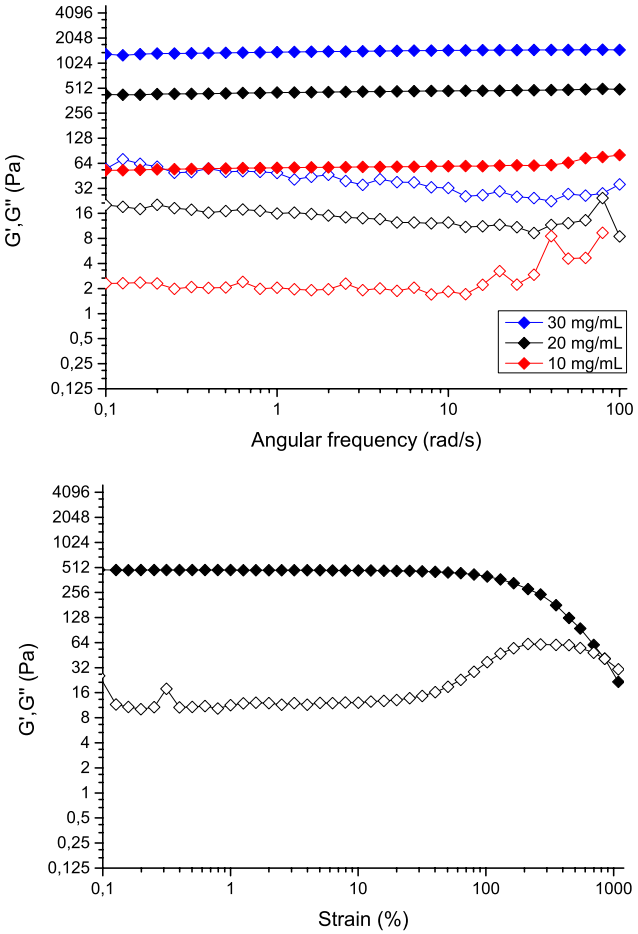

Figure 4.4. Rheological analysis of periodate-induced gels. G' is represented by closed symbols, G'' by open symbols. Top: Representative frequency sweeps of 10, 20 and 30 mg/mL hydrogels oxidized by sodium periodate. Bottom: Strain sweep measurement of a 20 mg/mL hydrogel to determine the linear viscoelastic region.

Magic-angle spinning (MAS) ^{1}H-NMR was performed on 30 mg/mL hydrogels with an equimolar polymer ratio in order to study cross-linking efficiency. We focused on the peak at δ = 2.2 ppm, from the protons next to the alkyne, which shifts upon reaction with the quinone. As expected, a small peak was still detectable in the gel, revealing the presence of dangling ends in the network (**Figure 4.5**). Next, we investigated the stability of star-PEG-BCN and star-PEG-DHPA upon storage. Solutions of both polymers were stored at room temperature and at 4°C for 1 week. Hydrogels could still be formed in both cases; however, gels made with polymers stored at room temperature appeared to be less stiff. Time sweep measurements of hydrogels formed with polymers stored at 4°C for 1 week resulted in comparable moduli (G' = 468 ± 26 Pa, n = 3) as obtained for freshly prepared gels (G' = 454 ± 19 Pa, **Table 4.2**). Hydrogels prepared with polymers left at room temperature were less stiff, resulting in slightly lower G' values (G' = 361 ± 16 Pa, n = 2).

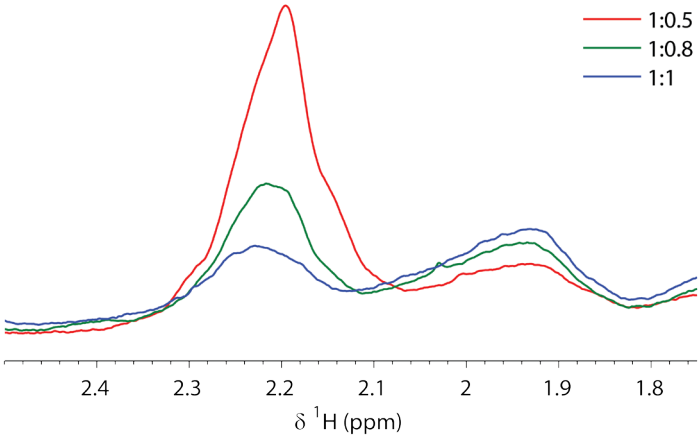

Figure 4.5. MAS ^{1}H NMR spectrum showing the region where the alkyne signal resonates (δ = 2.2 ppm, protons next to the triple bond). Three different ratios of star-PEG-BCN: star-PEG-DHPA were measured. With an excess of star-PEG-BCN, more unreacted alkyne is present, with the most intense signal for the 1:0.5 mixture.

4.2.2. Mushroom tyrosinase as oxidizing agent

Besides chemical activation of the catechol moiety, it can also be oxidized by enzymes such as mushroom tyrosinase.[31] Also other gelation systems have been described in previous reports that utilize an enzymatic reaction for gel formation, like horseradish peroxidase[31,38], phosphatase[39] and transglutamidase[40,41]. Enzymatic cross-linking is advantageous due to the high substrate specificity of the enzyme. Furthermore, by tuning the enzyme concentration, the overall cross-linking rate can be controlled.[42] We set out to investigate enzymatically induced gel formation with the SPOCQ reaction. To this end, we studied gelation of an equimolar mixture of star-PEG-DHPA and star-PEG-BCN with the enzyme mushroom tyrosinase. We

first investigated 20 mg/mL solutions at different enzyme concentrations (100 – 2000 units/mL) (**Figure 4.3B**). Gelation times of the resulting enzymatically cross-linked hydrogels were estimated using the inverted vial test. Gelation was found to be fast and the time to gelation decreased, as expected, with increasing enzyme concentration. Samples of 20 mg/mL already gelled in approximately 1 min using an enzyme concentration of 2000 units/mL. Lowering the enzyme concentration to 100 units/mL still resulted in gel formation after approximately 20 min (**Figure 4.3B, Table 4.1**).

Table 4.1. Gelation time of enzymatically (mushroom tyrosinase) cross-linked hydrogels, determined using the inverted vial test (n = 3).

MT (units/mL)	Gelation time (s)
100	1147 ± 100
250	326 ± 21
500	143 ± 4
1000	92 ± 6
1500	71 ± 9
2000	65 ± 8

The gelation time of the hydrogels can thus easily be controlled by adjusting the enzyme concentration. In order to follow the gelation using rheology, we decided to perform these measurements with an enzyme concentration of 500 units/mL on hydrogel solutions with a total polymer content of 10, 20 and 30 mg/mL. Time sweep measurements were carried out for 2 h and showed that G' began to increase rapidly after addition of the enzyme (**Figure 4.3C**). The mechanical properties of enzymatically cross-linked hydrogels were comparable to periodate-induced gels. G' values of 35 Pa (10 mg/mL), 476 Pa (20 mg/mL) and 921 Pa (30 mg/mL) were acquired (**Table 4.2**). Hydrogels induced by tyrosinase also mainly had an elastic composition (**Figure 4.6)**.

Table 4.2. Hydrogel strength G' (Pa) measured by rheology. Values were recorded after 5 min for sodium periodate (n = 5) and after 2 h for mushroom tyrosinase (MT, n = 3).

	10 mg/mL	20 mg/mL	30 mg/mL
$NaIO_4$	65 Pa ± 10	454 Pa ± 19	1375 Pa ± 21
MT	35 ± 3	476 Pa ± 28	921 Pa ± 37

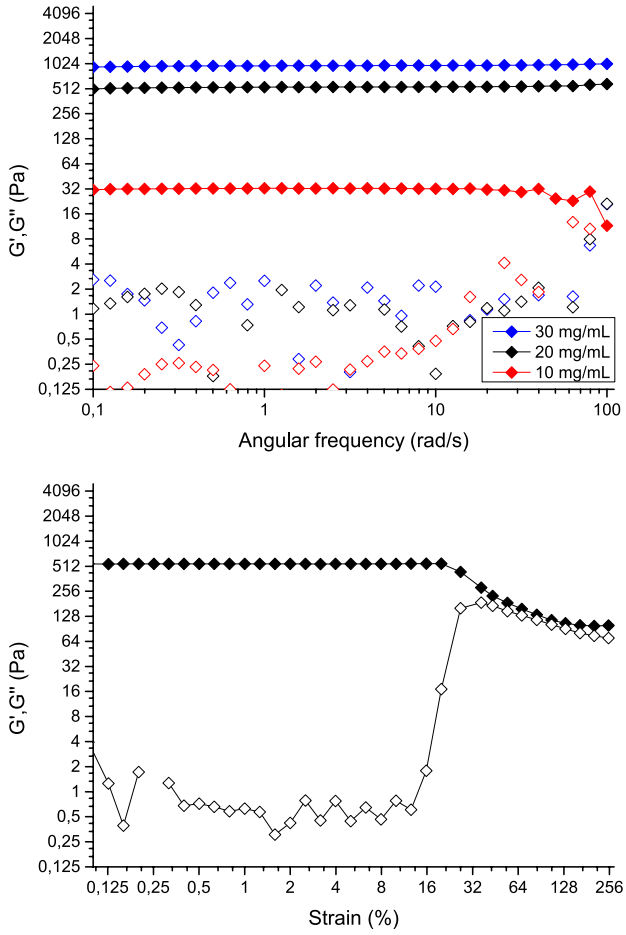

Figure 4.6. Rheological analysis of enzymatically oxidized gels. G' is represented by closed symbols, G'' by open symbols. Top: Representative frequency sweeps of 10, 20 and 30 mg/mL hydrogels oxidized by mushroom tyrosinase (500 units/mL). Bottom: Strain sweep measurement of a 20 mg/mL hydrogel to determine the linear viscoelastic region.

These data show that the high reaction rate constant of the SPOCQ reaction also translates into fast hydrogel formation after enzymatic or chemical oxidation of the DHPA groups. A similar study that solely used four-armed PEG-DOPA constructs for gelation reported slower kinetics. Gelation of four-armed PEG-DOPA (130 mg/mL) occurred at a minimum of 18 min with $NaIO_4$. Enzymatic cross-linking with 25.000 units/mL mushroom tyrosinase resulted in hydrogel formation after 2 days.[31] Another study that used the SPAAC reaction for cross-linking obtained a gelation point (G' > G'') within 5 min, using a polymer concentration of 13.5 wt% (135 mg/mL).[24]

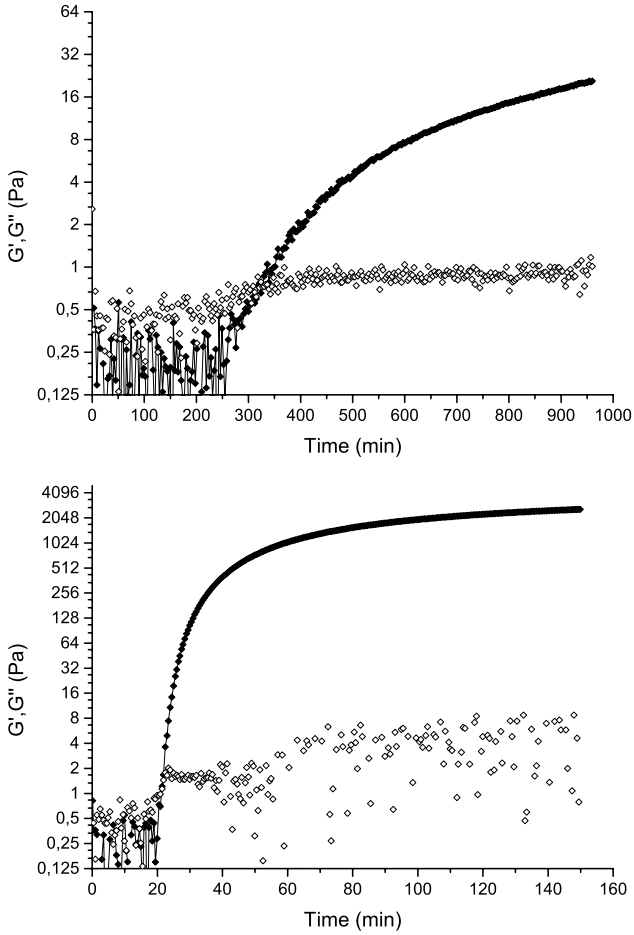

Figure 4.7. Rheology of SPAAC-cross-linked hydrogels; composed of star-PEG-BCN and star-PEG-N_3. G' is represented by closed symbols, G'' by open symbols. Top: time sweep measurement (16 h) for a 10 mg/mL, with the gelation point after approximately 6 h. Bottom: time sweep measurement (2.5 h) for a 30 mg/mL hydrogel, with the gelation point after approximately 20 min (see **Chapter 3.3**).

To be able to make a direct comparison with SPOCQ, we also performed the SPAAC reaction with our low polymer concentrations. For this purpose, star-PEG-N_3 was first synthesized by coupling of azido-acetic acid to star-PEG-amine. Cross-linking of star-PEG-BCN and star-PEG-N_3 with SPAAC resulted in gelation points of 20 min for 30 mg/mL up to 6 h for the 10 mg/mL hydrogel (**Figure 4.7; Chapter 3.3**). This clearly shows the high reaction rate of SPOCQ for hydrogel formation compared to the SPAAC reaction. Furthermore, the mechanical properties of SPOCQ formed PEG-hydrogels are also comparable to other previously reported PEG-hydrogels. For instance, measured moduli of 10 wt % SPOCQ gels (G' = 11.7 ± 0.6 kPa,

(**Figure 4.8**)) were similar to the reported moduli for 13.5 wt % SPAAC cross-linked gels (G' = 12.0 ± 0.6 kPa)[24] and to 13 wt% DOPA-DOPA cross-linked gels (G' = 13 kPa).[31] Moreover, Waite and co-workers recently introduced non-covalently cross-linked hydrogels with a more stable catechol analogue (3-hydroxy 4-pyridinone, HOPO). Gels formed via the coordination of Fe^{3+} to HOPO appeared to have similar mechanical properties (10 wt%, G' = 12 kPa) as our SPOCQ formed hydrogels.[43]

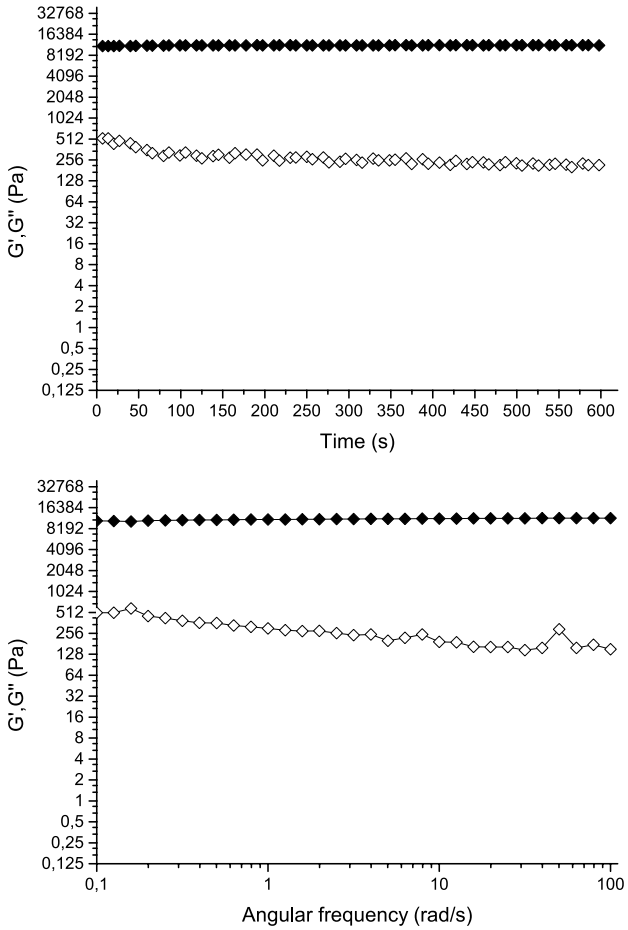

Figure 4.8. Rheological analysis of 100 mg/mL (10 wt%) SPOCQ cross-linked hydrogels, oxidized by periodate. G' is represented by closed symbols, G'' by open symbols. Gels obtained a G' value of 11.7 ± 0.6 kPa. Top: representative time sweep test (10 min). Bottom: frequency sweep measurement.

4.3. SPOCQ and SPAAC as an orthogonal reaction pair

Now that we showed that the SPOCQ reaction can be applied as an efficient, activatable and fast cross-linking method for hydrogel formation, we wanted to further explore the possibilities to functionalize these hydrogels. In our previous research, we demonstrated that the 1,2-quinone and the azide moieties can be utilized as an orthogonal reaction pair due to their large difference in reactivity towards BCN.[37] In this respect, we hypothesized that we could utilize this property to post-functionalize our SPOCQ-formed hydrogels using the SPAAC reaction. To this end, we first tested if gels could be formed with non-equimolar amounts of star-PEG-DHPA and star-PEG-BCN. We chose to study gels with a final polymer concentration of 20 mg/mL (2 wt%) containing star-PEG-DHPA and star-PEG-BCN in a ratio of 0.8: 1.0. Oxidation with sodium periodate still resulted in rapid gelation, corroborated by the inverted vial test. For subsequent functionalization, we utilized 3-azido-7-coumarin, a dye that shows a strong increase in fluorescence upon cycloaddition to an alkyne. We added azido-coumarin to already formed hydrogels containing an excess of BCN-groups. Illumination with UV-light showed fluorescence at the site of addition, proving that the BCN-groups are accessible for the SPAAC reaction with azido-coumarin (**Figure 4.9**).

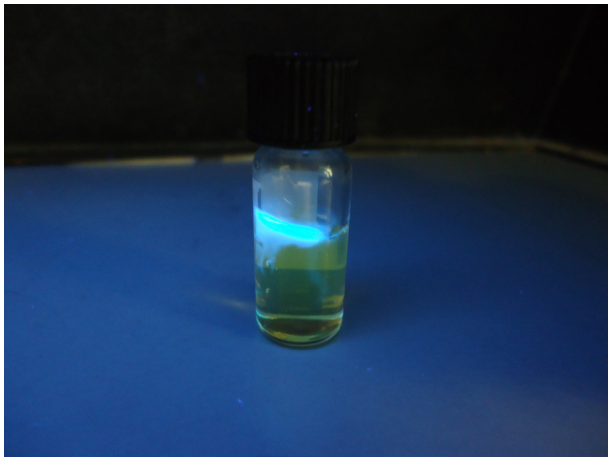

Figure 4.9. Azido-coumarin added on pre-formed gels with an imbalanced polymer ratio, showing fluorescence at the side of addition. Gels were prepared by adding $NaIO_4$ (1.0 eq per DHPA group) to a mixture of 8.89 mg star-PEG-DHPA (0.8 eq) and 11.11 mg star-PEG-BCN (1.0 eq). On top of the gel was added 0.5 eq N_3-coumarin (based on the excess of BCN-groups), after which the sample was illuminated with UV-light.

Next, we evaluated whether the SPOCQ and SPAAC reactions can also be performed in one-pot. For this experiment, hydrogels were prepared by adding a mixture of azido-coumarin and sodium periodate to a polymer mixture containing an imbalanced ratio of star-PEG-DHPA (0.8

eq) and star-PEG-BCN (1.0 eq). Immediate gelation was observed indicating that the presence of azido-coumarin did not interfere with the curing of the gel. Hydrogels containing a balanced ratio of star-PEG-DHPA (1.0 eq) and star-PEG-BCN (1.0 eq) were also prepared, which contained the same amount of azido-coumarin as for the imbalanced gel (0.8: 1.0). The gels were subsequently analyzed for coumarin fluorescence under UV-light and a marked difference in fluorescence was observed. As expected, the hydrogel with the imbalanced polymer ratio showed a much higher fluorescence than the hydrogel with the balanced polymer ratio (**Figure 4.10**). In order to quantify the observed differences in fluorescence, we prepared hydrogels in microwell plates and measured the fluorescence using a microplate reader. As seen in **Figure 4.10**, the fluorescence of the imbalanced gels (DHPA: BCN 0.8: 1.0) was significantly higher (40x) than the intensity of the balanced hydrogel (DHPA: BCN 1: 1).

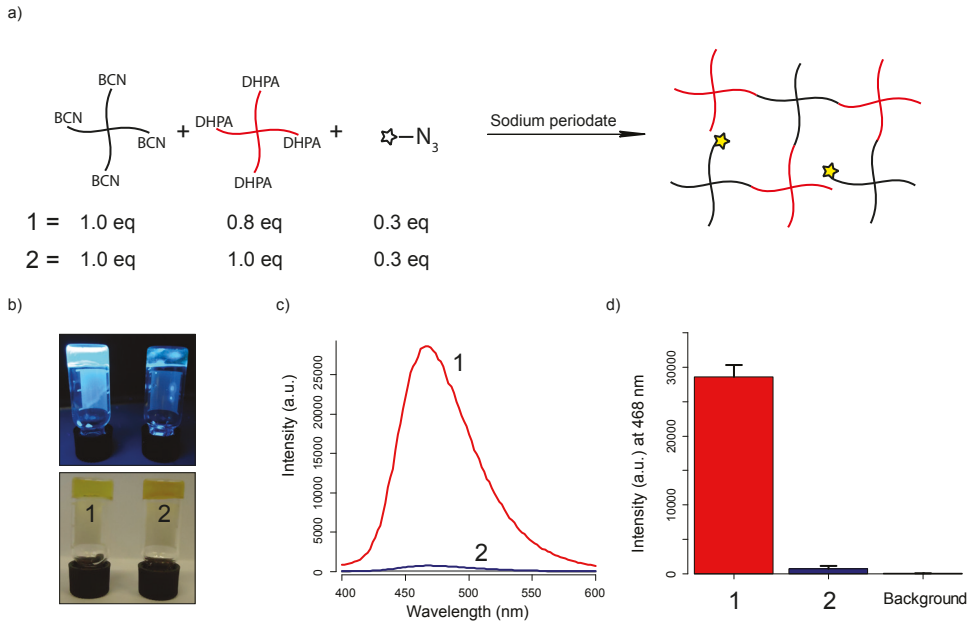

Figure 4.10. Incorporation of a functional group (azido-coumarin, fluorescence increases after reaction with alkynes) in SPOCQ-formed gels using SPAAC. A. Schematic overview B. Gels with an imbalanced polymer ratio (excess star-PEG-BCN, **1**) and a balanced ratio (**2**; top: picture under UV-light, bottom: regular picture). C. Fluorescence measurements showing that imbalanced hydrogels (**1**, red) display a 40x higher fluorescence intensity than balanced gels (**2**, blue). D. Emission at 468 nm of gels with an imbalanced ($2.9 \cdot 10^4 \pm 1.7 \cdot 10^3$)) and balanced ratio ($7.4 \cdot 10^2 \pm 3.4 \cdot 10^2$)) and a background measurement of only azido-coumarin (46 ± 3).

Moreover, the same trend was seen in MAS NMR, where a larger fraction of unreacted alkyne was present in imbalanced gels compared to the balanced hydrogel, further exemplifying the possibility to use the unreacted BCN groups for functionalization with azido compounds (**Figure 4.5**). These findings show that the SPOCQ and SPAAC reaction can be used in one

pot for the preparation of hydrogels (via SPOCQ) and the subsequent post-modification reaction (via SPAAC).

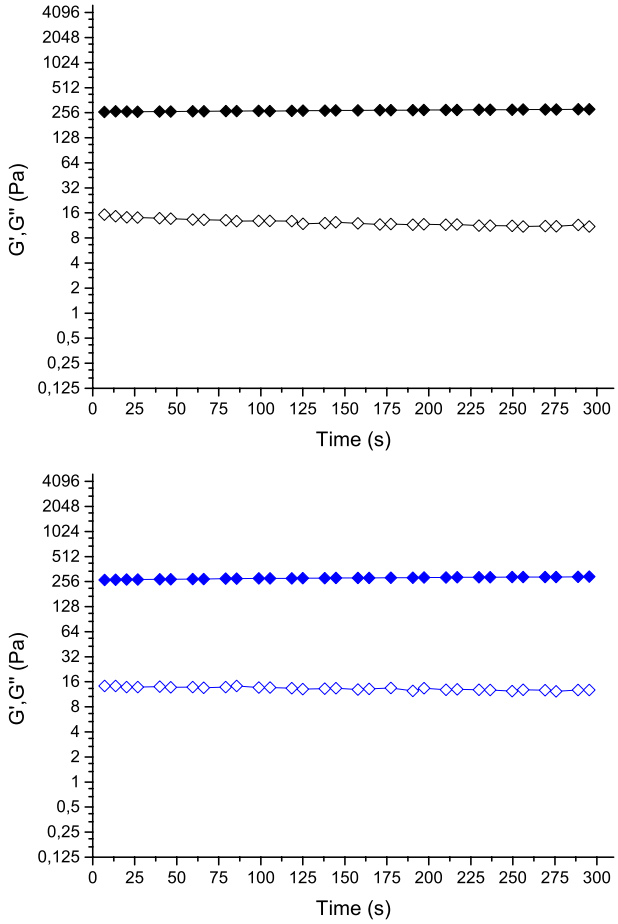

Figure 4.11. Rheology of imbalanced hydrogels (20 mg/mL) containing star-PEG-BCN and star-PEG-DHPA in a ratio of 1.0:0.8. G' is represented by closed symbols, G'' by open symbols. Top: time sweep measurement of non-functionalized imbalanced hydrogels (G' = 285 ± 23 Pa, n = 5) Bottom: time sweep measurement of azido coumarin-functionalized hydrogels (G' = 285 ± 48 Pa, n = 5). Incorporation of azido-coumarin does not change the mechanical properties of the hydrogel network.

In addition, incorporation of azido-coumarin did not change the mechanical properties of the network, since non-functionalized imbalanced hydrogels showed the same moduli (**Figure 4.11**). Using the same reactive group for cross-linking and functionalization can result in decreased hydrogel stiffness, as was shown for gels formed via the inverse electron demand Diels-Alder reaction.[23] The advantage of using SPOCQ for hydrogel formation and SPAAC for simultaneous hydrogel functionalization was further exemplified when we prepared hydrogels with a lower polymer concentration of 10 mg/mL (1 wt%). We again used an imbalanced

polymer ratio (0.8: 1.0) and added azido-coumarin (1.5 eq, based on excess BCN) to the samples. SPOCQ cross-linked samples composed of star-PEG-DHPA (0.8 eq), star-PEG-BCN (1.0 eq) and azido-coumarin still formed hydrogels almost instantaneously after addition of sodium periodate. Similarly, we also prepared hydrogels cross-linked with SPAAC, to compare those to the SPOCQ formed gels. When an imbalanced polymer ratio of star-PEG-N_3 (0.8 eq) and star-PEG-BCN (1.0 eq) were reacted in the presence of azido-coumarin, hydrogel formation did not occur. However, when azido-coumarin was not added to the polymer mixture, SPAAC cross-linked hydrogels were formed (**Figure 4.12, Table 4.3**). These findings show that azido-coumarin interferes with the gel formation when SPAAC is used as chemical crosslinking method. Due to the high reaction rate of SPOCQ, one-pot functionalization is possible, even at low polymer concentrations.

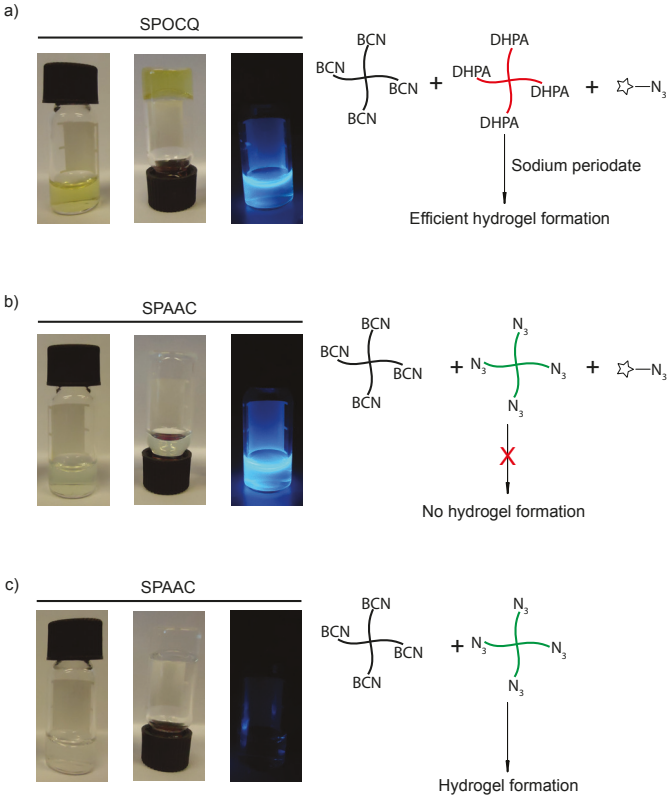

Figure 4.12. Competition experiment between SPOCQ and SPAAC, using a total polymer content of 10 mg/mL. A. Sample containing 0.8 eq star-PEG-DHPA, 1.0 eq star-PEG-BCN and azido-coumarin, cross-linked by SPOCQ. B. Sample containing 0.8 eq star-PEG-N_3, 1.0 eq star-PEG-BCN and azido-coumarin, cross-linked by SPAAC. Azido-coumarin hampered the formation of a hydrogel. C. Sample containing 0.8 eq star-PEG-N_3 and 1.0 eq star-PEG-BCN, resulting in SPAAC cross-linked hydrogels. Left: reacted samples; middle: inverted vial test (sample B did not form a hydrogel); right: under UV-light irradiation to detect coumarin fluorescence (sample C does not contain azido-coumarin).

4.4. Conclusion

In conclusion, we have shown that strain-promoted oxidation-controlled cyclooctyne-1,2-quinone cycloaddition (SPOCQ) is a fast and efficient cross-linking method for hydrogel formation. Cross-linking is activable and was achieved by addition of either a chemical oxidizing agent ($NaIO_4$) or an enzyme (mushroom tyrosinase) catalysing the oxidation of DHPA. We have also shown that the SPOCQ reaction can be regarded as an orthogonal reaction pair with SPAAC, which allows us to easily incorporate a second functionality during or after the curing process. We think that the combined usage of an imbalanced ratio of BCN and catechol groups for gel formation and the SPAAC reaction will provide a straightforward method to modify hydrogels with other functionalities or biomolecules, such as peptides for cell adhesion or biomineralization. Hydrogel modification can either be achieved directly in one-pot or sequentially on pre-formed gels. We expect these hydrogels to be ideal in those applications, where fast or spatiotemporally controlled gel formation is required.

4.5. Acknowledgements

Annika Borrmann is gratefully acknowledged for all her help with the design and performance of the experiments, for fruitful discussions and for co-authoring the manuscript. Ernst van Eck is thanked for help with the MAS NMR studies. Floris van Delft is thanked for useful discussions. Jan Dommerholt is kindly acknowledged for the synthesis of azido-coumarin. NWO, VICI grant 700.10.442 is thanked for financial support.

4.6. Materials and methods

Four-Armed poly(ethylene glycol)-NH_2 (10 kDa) salt was obtained from JenKem Technology (USA). (1*R*,8*S*,9*S*)-Bicyclo[6.1.0]non-4-yn-9-ylmethyl succinimidyl carbonate was purchased from SynAffix (Oss, The Netherlands). 3-Azido-7-hydroxycoumarin (N_3-coumarin) was kindly donated by Jan Dommerholt. All other chemicals were purchased from Sigma-Aldrich, Baker or Fluka and utilized as received.

^{1}H NMR spectra were recorded on a Varian Mercury (400 MHz). Chemical shifts are given using TMS as reference (δ = 0 ppm). Mass spectra were recorded on a Bruker Biflex MALDI-TOF (Bruker Daltronik, Bremen, Germany). As matrix, α-cyano-4-hydroxycinnamic acid was used. Column chromatography was performed with silica gel 60 (particle size 0.040 – 0.063 mm Merck) or aluminum oxide (basic activated, pore size 58 Å, Sigma-Aldrich). Thin-layer chromatography (TLC) was performed on silica gel coated plates (Merck 60, F-254). Visualization

was accomplished with UV-light and/or ninhydrin or permanganate staining. Lyophilization was achieved using an ilShin Freeze Dryer (ilShin, Ede, The Netherlands). Rheology measurements were performed on an AR2000ex rheometer (TA instruments, New Castle, USA). UV irradiation was performed with a CAMAG UV-lamp (366 nm). Fluorescence measurements were performed on a Tecan Infinite M200 Pro plate reader.

Star-PEG-BCN

To a dry reaction flask was added 4-armed poly(ethylene) glycol-NH_2 HCl salt (600 mg, 0.06 mmol), (1*R*,8*S*,9*S*)-bicyclo[6.1.0]non-4-yn-9-ylmethyl succinimidyl carbonate (BCN-OSu; 87.4 mg, 0.30 mmol) and 100 µL triethylamine (100 µL, 0.72 mmol) in dry DCM (25 mL). The reaction mixture was stirred at r.t. overnight under N_2 atmosphere and then washed with 2M NaOH (3 x 25 mL). The organic layer was dried over Na_2SO_4 and concentrated in vacuo. The residue was purified by column chromatography on silica gel (MeOH:DCM 2:98, followed by 10:90) to afford the product after freeze-drying from dioxane. The obtained white powder was stored at -20°C until further usage (406 mg, 63%).[44]
R_f = 0.36 (MeOH:DCM, 10:90)
^{1}H-NMR (400 MHz, $CDCl_3$, δ): 0.86 – 1.01 (m, 4H), 1.25 – 1.43 (m, 8H), 1.52 – 1.66 (m, 8H), 2.18 – 2.34 (m, 16H), 3.38 (m, 16H), 3.51 – 3.86 (m, $[CH_2CH_2O]_n$), 4.15 (d, J = 8.0 Hz, 8H)
MALDI-TOF (α-cyano-4-hydroxycinnamic acid): **Figure 4.13**.

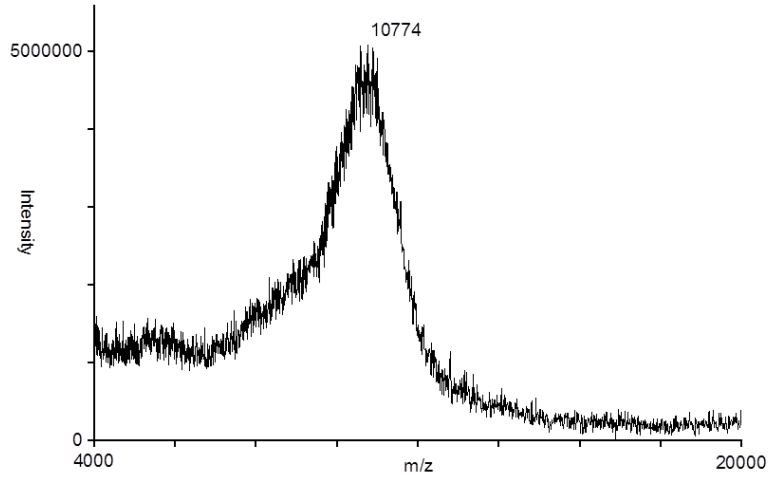

Figure 4.13. MALDI –TOF spectrum star-PEG-BCN; calculated m/z: 10791 for 222 ethylene glycol units

Star-PEG-DHPA

To star-poly(ethylene) glycol-NH_2 HCl salt (500 mg, 50 µmol) in DMF (13 mL) was added subsequently benzotriazol-1-yl-oxy-tris dimethylaminophosphonium hexafluorophosphate (BOP; 133 mg, 0.30 mmol), 3,4 dihydroxy phenylacetic acid (51 mg, 0.30 mmol), and D*i*PEA (210 µL, 1.2 mmol). The reaction mixture was stirred overnight at r.t., after which the DMF was evaporated in vacuo. The residue was dissolved in DCM and washed with 1 M $KHSO_4$ (3 x 40 mL) and brine (1 x 40 mL). The organic layer was dried over Na_2SO_4. The product was purified with column chromatography on basic aluminum oxide (MeOH: DCM; 10:90). Lyophilization from dioxane afforded the product as a white powder, which was stored at 4°C. (445 mg, 84%)

R_f = 0.25 (MeOH:DCM, 10:90)

^{1}H-NMR (400 MHz, $CDCl_3$, δ): 3.36 – 3.86 (m, $[CH_2CH_2O]_n$, $C\underline{H}_2$-Ar-CH), 6.61 – 7.03 (m, Ar-CH)

MALDI-TOF (α-cyano-4-hydroxycinnamic acid): **Figure 4.14**.

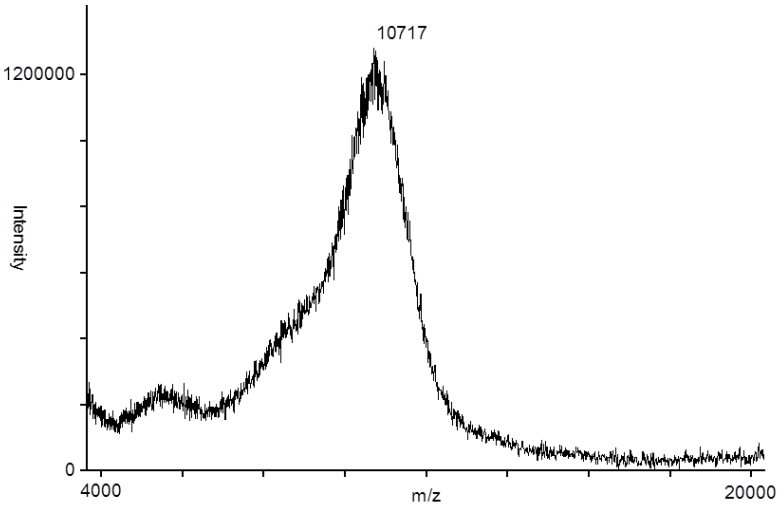

Figure 4.14. MALDI-TOF spectrum star-PEG-DHPA; calculated m/z: 10733 for 223 ethylene glycol units

Star-PEG-N_3

To star poly(ethylene) glycol-NH_2 HCl salt (800 mg, 80 µmol) in DCM (25 mL) was added subsequently BOP (283 mg, 0.64 mmol), azido acetic acid[45] (65 mg, 0.64 mmol) and D*i*PEA (328 µL 1.92 mmol). The reaction mixture was stirred overnight at r.t and extracted with 1 M $KHSO_4$ (5 x 50 mL) and brine (1 x 50 mL). The organic layer was dried over $MgSO_4$ and concentrated in vacuo. The compound was purified by column chromatography on basic aluminum oxide, using MeOH:DCM (10:90) as eluent. Freeze-drying from dioxane afforded the product as a white powder (760 mg, 92%)

R_f = 0.38 (MeOH:DCM, 10:90)
^{1}H-NMR (400 MHz, $CDCl_3$, δ): = 3.41 (s, 8H), 3.45 – 3.55 (m, 16H), 3.57 – 3.70 (m, $[CH_2CH_2O]_n$), 3.96 (s, 8H)
MALDI-TOF (α-cyano-4-hydroxycinnamic acid): **Figure 4.15**
IR = 2103.52 cm^{-1} (N_3).

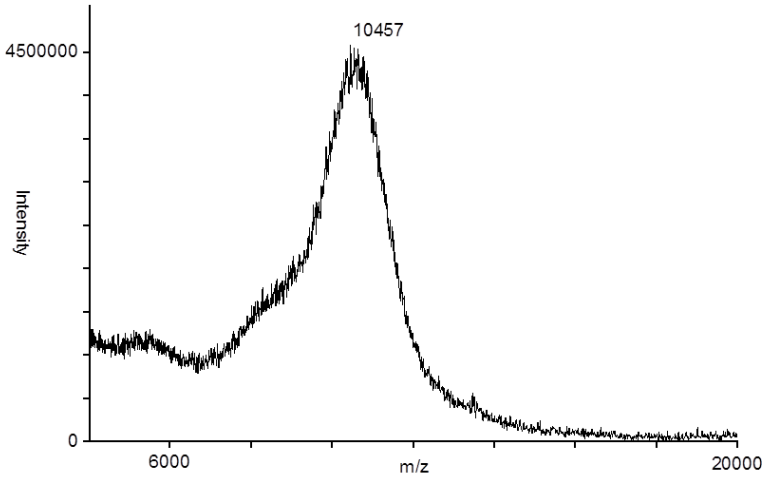

Figure 4.15. MALDI-TOF spectrum star-PEG-N_3; calculated m/z: 10463 for 223 ethylene glycol units

Hydrogel formation

Hydrogels were formed by addition of $NaIO_4$ or mushroom tyrosinase to an equimolar mixture of star-PEG-BCN and star-PEG-DHPA. Hydrogels were prepared in total polymer concentrations of 10, 20 and 30 mg/mL (1-3 wt%) in water ($NaIO_4$) or in PBS (tyrosinase). For a typical hydrogel, equal volumes of the polymer mixture and the oxidizing agent were mixed to the final concentration. For the polymer mixture, stock solutions of 20, 40 and 60 mg/mL of star-PEG-BCN and star-PEG-DHPA were first freshly prepared and then mixed in a 1:1 fashion. For hydrogels formed by sodium periodate, a stock solution containing 1 eq $NaIO_4$ (based on amount of DHPA groups, 4 eq $NaIO_4$ per star-PEG-DHPA) was prepared in MilliQ. Hydrogels formed by mushroom tyrosinase were formed in 1 x PBS (pH 7.5), which was purged with O_2 for 15 min prior to use. A tyrosinase stock solution was prepared in PBS containing twice as many units/mL as needed in the final gel sample.

Determination of gelation time

Gelation time was determined qualitatively using the inverted vial test. The test was not applied for hydrogels formed by sodium periodate, due to almost instant gel formation as soon as all components were mixed. For the enzymatically cross-linked hydrogels, the gelation times were

determined using a tyrosinase concentration series: 100 – 2000 units/mL. For this, a 4000 units/mL stock solution in PBS was first prepared, of which a dilution series was made. Hydrogels (20 mg/mL) were formed using the typical procedure. As soon as the enzyme solution was added to the polymer mixture, the time measurement was started. When the material stopped flowing, and the vial could thus be inverted, the measurement was ended. Gelation time measurements were performed in triplo (**Table 4.1**).

Rheology

The storage (G') and loss modulus (G'') of the hydrogels were measured using an AR2000ex rheometer (TA instruments). All measurements were performed using a flat steel plate geometry (20 mm, gap size 500 μM) and were performed at a temperature of 20°C. Hydrogels were prepared by loading 100 μL of a star-PEG-BCN/star-PEG-DHPA mixture directly on the testing platform. After addition of 100 μL $NaIO_4$ or mushroom tyrosinase stock solution, the upper plate was immediately lowered and the measurement was started. Initially, a strain sweep measurement was conducted to determine the linear viscoelastic range of the hydrogels, by measuring between 0.1 and 1000% strain at an angular frequency of 10 rad/s. Within this range, a strain percentage (1%) was chosen to perform further measurements. The values of G' and G'' for periodate-induced gels (10, 20 and 30 mg/mL) were determined using an oscillatory time sweep test for 5 min at a constant strain of 1% and an angular frequency of 10 rad/s. Time sweep measurements for enzyme-induced gels were performed for 2 h, using a final enzyme concentration of 500 units/mL. To minimize evaporation, a solvent trap was utilized which was filled with water. For frequency sweep measurements, the angular frequency was measured between 0.1 and 100 rad/s and a constant strain of 1%. All measurements were performed at least in triplicate. SPAAC cross-linked hydrogels were measured by loading an equimolar mixture of star-PEG-BCN and star-PEG-N_3 on the rheometer. Time sweep measurements were conducted for 16 h for 10 mg/mL hydrogels and for 2.5 h for 30 mg/mL gels, using the same settings as above.

Stability measurements

Star-PEG-DHPA and star-PEG-BCN solutions of 40 mg/mL were prepared in MilliQ and stored at 4°C and at room temperature for 1 week. In order to determine the stability of the polymers in solution, hydrogels of 20 mg/mL were prepared with the aged solutions using sodium periodate as oxidizing agent. Hydrogels prepared with polymers left at room temperature were less stiff, resulting in slightly lower G' values. For long term storage it is therefore advisable to store the polymers as solids at lower temperatures.

Magic-angle spinning (MAS) ^{1}H NMR

Hydrogels were prepared in final polymer concentrations of 30 mg/mL using the standard procedure with sodium periodate as oxidizing agent. Gels were prepared with three different ratios of star-PEG-BCN: star-PEG-DHPA of 1:1 (balanced), 1:0.8 and 1:0.5. The total sample volume used was 200 µL. NMR experiments were performed on a Varian 300 MHz solid state NMR spectrometer. Single pulse ^{1}H NMR experiments were performed using a 9.5 mm Chemagnetics probe, with magic-angle spinning at a frequency of 1605 Hz. The gels were prepared in a Teflon sample insert that fit snugly into the 9.5mm rotor. T_1 measurements were performed to ensure that the repetition delay of 10s was sufficiently long so that measurements were quantitative. For each preparation 256 scans were accumulated (**Figure 4.5**).

Fluorescence measurements

For post-functionalization: see **Figure 4.9**. Imbalanced hydrogels contained a polymer ratio of 0.8: 1.0 of star-PEG-DHPA and star-PEG-BCN. For example, a 200 µL hydrogel (20 mg/mL) contained 1.78 mg star-PEG-DHPA (0.8 eq) and 2.22 mg star-PEG-BCN (1.0 eq). Hydrogels were oxidized by sodium periodate, using 1 equivalent of $NaIO_4$ per DHPA group. Gels contained 1.5 equivalents 3-azido-7-hydroxycoumarin (N_3-coumarin) per BCN-group, based on the excess of star-PEG-BCN (in the example: 0.44 mg). Balanced hydrogels contained an equimolar polymer ratio (1:1, for example 2.0 mg star-PEG-DHPA and 2.0 mg star-PEG-BCN). The amount of N_3-coumarin remained equal for balanced hydrogels. For a typical hydrogel, a star-PEG-DHPA/star-PEG-BCN mixture (100 µL) was prepared, to which a N_3-coumarin/$NaIO_4$ mix (100 µL) was added. This N_3-coumarin/$NaIO_4$ mixture was prepared using a stock solution of N_3-coumarin in DMSO, in such a way that the maximum DMSO concentration in the mixture was 5%. Hydrogels were irradiated under UV-light (366 nm) using a UV-lamp (CAMAG). The fluorescence of N_3-coumarin containing hydrogels was measured using a Tecan Infinite M200 Pro plate reader. Hydrogels were prepared in a 96-wells plate, with a sample volume of 80 µL. Hydrogels were left for 15 min before the measurement was started. An emission scan was performed between 400 and 600 nm, using an excitation wavelength of 360 nm. To determine the background fluorescence, a mixture of star-PEG-DHPA, N_3-coumarin and $NaIO_4$ was measured. All fluorescence measurements were performed with n = 9.

Competition reaction SPOCQ and SPAAC.

Hydrogels with a total polymer content of 10 mg/mL were prepared with three different polymer compositions (**Table 4.3**). The first sample contained 0.8 eq star-PEG-DHPA, 1.0 eq star-PEG-BCN, 1.5 eq N_3-coumarin (based on the excess of BCN) and 1 eq $NaIO_4$ (per DHPA group), and was prepared in a similar manner as before. The second sample contained 0.8 eq star-PEG-N_3, 1.0 eq star-PEG-BCN and an equal amount of N_3-coumarin (1.5 eq), and was prepared by making a polymer mixture in MilliQ, to which a stock solution of N_3-coumarin in

DMSO (2.5%) was added. The third sample only contained the star-PEG-N_3 (0.8 eq) – star-PEG-BCN (1.0 eq) polymer mixture in MilliQ. Sample 2 and 3 were left overnight to allow gel formation to occur. The inverted vial test was utilized to check gel formation of the samples. The gels or solutions were examined under UV-light (366 nm) using a UV-lamp. Samples were prepared in triplicate.

Table 4.3. Overview sample composition for the SPOCQ/SPAAC competition experiment. Total sample volume: 400 µL. Total polymer concentration: 10 mg/mL. N_3-coumarin: from stock solution: 24.6 mM (in DMSO, 1.5 eq based on excess of BCN groups). $NaIO_4$: from stock solution: 3.54 mM (1 eq based on amount of DHPA groups). * = added together to a solution of star-PEG-DHPA and star-PEG-BCN.

	Sample 1	**Sample 2**	**Sample 3**
Star-PEG-BCN	2.22 mg	2.22 mg	2.22 mg
Star-PEG-DHPA	1.78 mg	-	-
Star-PEG-N_3	-	1.78 mg	1.78 mg
N_3-coumarin	10 µL*	10 µL	-
$NaIO_4$	190 µL*	-	-
MilliQ	200 µL	390 µL	400 µL

4.7. References

(1) Hoffman, A. S. *Adv. Drug Delivery Rev.* **2012**, *64*, 18-23.

(2) Lin, C.-C.; Anseth, K. S. *Pharm. Res.* **2008**, *26*, 631-643.

(3) Zhu, J. *Biomaterials* **2010**, *31*, 4639-4656.

(4) Peppas, N. A.; Hilt, J. Z.; Khademhosseini, A.; Langer, R. *Adv. Mater.* **2006**, *18*, 1345-1360.

(5) Hoare, T. R.; Kohane, D. S. *Polymer* **2008**, *49*, 1993-2007.

(6) Kharkar, P. M.; Kiick, K. L.; Kloxin, A. M. *Chem. Soc. Rev.* **2013**, *42*, 7335.

(7) Jonker, A. M.; Löwik, D. W. P. M.; van Hest, J. C. M. *Chem. Mater.* **2012**, *24*, 759-773.

(8) Nimmo, C. M.; Shoichet, M. S. *Bioconjugate Chem.* **2011**, *22*, 2199-2209.

(9) Jiang, Y.; Chen, J.; Deng, C.; Suuronen, E. J.; Zhong, Z. *Biomaterials* **2014**, *35*, 4969-4985.

(10) Tornoe, C. W.; Christensen, C.; Meldal, M. *J. Org. Chem.* **2002**, *67*, 3057-3064.

(11) Rostovtsev, V. V.; Green, L. G.; Fokin, V. V.; Sharpless, K. B. *Angew. Chem. Int. Edit.* **2002**, *41*, 2596-2599.

(12) Malkoch, M.; Vestberg, R.; Gupta, N.; Mespouille, L.; Dubois, P.; Mason, A. F.; Hedrick, J. L.; Liao, Q.; Frank, C. W.; Kingsbury, K.; Hawker, C. J. *Chem. Comm.* **2006**, 2774.

(13) Dijk, M. v.; Nostrum, C. F. v.; Hennink, W. E.; Rijkers, D. T. S.; Liskamp, R. M. J. *Biomacromolecules* **2010**, *11*, 1608-1614.

(14) Shih, H.; Lin, C.-C. *Biomacromolecules* **2012**, *13*, 2003-2012.

(15) Aimetti, A. A.; Machen, A. J.; Anseth, K. S. *Biomaterials* **2009**, *30*, 6048-6054.

(16) Gupta, N.; Lin, B. F.; Campos, L. M.; Dimitriou, M. D.; Hikita, S. T.; Treat, N. D.; Tirrell, M. V.; Clegg, D. O.; Kramer, E. J.; Hawker, C. J. *Nat. Chem.* **2010**, *2*, 138-145.

(17) Lutolf, M. P.; Raeber, G. P.; Zisch, A. H.; Tirelli, N.; Hubbell, J. A. *Adv. Mater.* **2003**, *15*, 888-892.

(18) Phelps, E. A.; Enemchukwu, N. O.; Fiore, V. F.; Sy, J. C.; Murthy, N.; Sulchek, T. A.; Barker, T. H.; García, A. J. *Adv. Mater.* **2012**, *24*, 64-70.

(19) Fairbanks, B. D.; Schwartz, M. P.; Halevi, A. E.; Nuttelman, C. R.; Bowman, C. N.; Anseth, K. S. *Adv. Mater.* **2009**, *21*, 5005-5010.

(20) Grover, G. N.; Lam, J.; Nguyen, T. H.; Segura, T.; Maynard, H. D. *Biomacromolecules* **2012**, *13*, 3013-3017.

(21) Wei, H.-L.; Yang, Z.; Zheng, L.-M.; Shen, Y.-M. *Polymer* **2009**, *50*, 2836-2840.

(22) Nimmo, C. M.; Owen, S. C.; Shoichet, M. S. *Biomacromolecules* **2011**, *12*, 824-830.

(23) Alge, D. L.; Azagarsamy, M. A.; Donohue, D. F.; Anseth, K. S. *Biomacromolecules* **2013**, *14*, 949-953.

(24) DeForest, C. A.; Polizzotti, B. D.; Anseth, K. S. *Nat. Mater.* **2009**, *8*, 659-664.

(25) Xu, J.; Filion, T. M.; Prifti, F.; Song, J. *Chem.-Asian J.* **2011**, *6*, 2730-2737.

(26) Zheng, J.; Smith Callahan, L. A.; Hao, J.; Guo, K.; Wesdemiotis, C.; Weiss, R. A.; Becker, M. L. *ACS Macro Letters* **2012**, *1*, 1071-1073.

(27) Borrmann, A.; van Hest, J. C. M. *Chem. Sci.* **2014**, *5*, 2123.

(28) Agard, N. J.; Prescher, J. A.; Bertozzi, C. R. *J. Am. Chem. Soc.* **2004**, *126*, 15046-15047.

(29) Codelli, J. A.; Baskin, J. M.; Agard, N. J.; Bertozzi, C. R. *J. Am. Chem. Soc.* **2008**, *130*, 11486-11493.

(30) Devaraj, N. K.; Weissleder, R.; Hilderbrand, S. A. *Bioconjugate Chem.* **2008**, *19*, 2297-2299.

(31) Lee, B. P.; Dalsin, J. L.; Messersmith, P. B. *Biomacromolecules* **2002**, *3*, 1038-1047.

(32) Ryu, J. H.; Lee, Y.; Kong, W. H.; Kim, T. G.; Park, T. G.; Lee, H. *Biomacromolecules* **2011**, *12*, 2653-2659.

(33) Brubaker, C. E.; Messersmith, P. B. *Biomacromolecules* **2011**, *12*, 4326-4334.

(34) Cencer, M.; Liu, Y.; Winter, A.; Murley, M.; Meng, H.; Lee, B. P. *Biomacromolecules* **2014**, *15*, 2861-2869.

(35) Holten-Andersen, N.; Harrington, M. J.; Birkedal, H.; Lee, B. P.; Messersmith, P. B.; Lee, K. Y. C.; Waite, J. H. *PNAS* **2011**, *108*, 2651-2655.

(36) Lee, B. P.; Konst, S. *Adv. Mater.* **2014**, *26*, 3415-3419.

(37) Borrmann, A.; Fatunsin, O.; Dommerholt, J.; Jonker, A. M.; Löwik, D. W. P. M.; van Hest, J. C. M.; van Delft, F. L. *Bioconjugate Chem.* **2015**, *26*, 257-261.

(38) Park, K. M.; Ko, K. S.; Joung, Y. K.; Shin, H.; Park, K. D. *J. Mater. Chem.* **2011**, *21*, 13180.

(39) Yang, Z.; Gu, H.; Fu, D.; Gao, P.; Lam, J. K.; Xu, B. *Adv. Mater.* **2004**, *16*, 1440-1444.

(40) Sperinde, J. J.; Griffith, L. G. *Macromolecules* **1997**, *30*, 5255-5264.

(41) Hu, B.-H.; Messersmith, P. B. *J. Am. Chem. Soc.* **2003**, *125*, 14298-14299.

(42) Ko, D. Y.; Shinde, U. P.; Yeon, B.; Jeong, B. *Prog. Polym. Sci.* **2013**, *38*, 672-701.

(43) Menyo, M. S.; Hawker, C. J.; Waite, J. H. *Soft Matter* **2013**, *9*, 10314.

(44) Dommerholt, J.; Schmidt, S.; Temming, R.; Hendriks, L. J. A.; Rutjes, F. P. J. T.; van Hest, J. C. M.; Lefeber, D. J.; Friedl, P.; van Delft, F. L. *Angew. Chem. Int. Edit.* **2010**, *49*, 9422-9425.

(45) Pfeiffer, H.; Rojas, A.; Niesel, J.; Schatzschneider, U. *Dalton T.* **2009**, 4292-4298.

Chapter 5

SPAAC and SPOCQ cross-linked hydrogels as matrices for encapsulation of aligned peptide amphiphile fibres

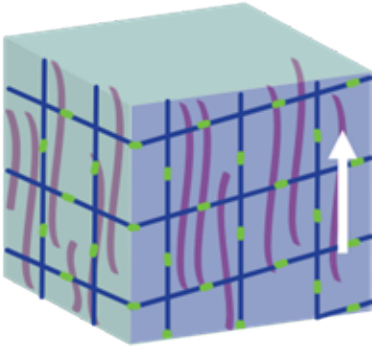

5.1. Introduction

5.1.1. Peptide amphiphile fibres

In nature, higher order structures, such as spheres, rods, disks, channels, sheets and fibres are commonly obtained via the self-assembly of amphiphilic molecules.[1,2] Amphiphiles have the ability to self-assemble in aqueous solution, in such a way that the hydrophilic domains are exposed to water, while the hydrophobic regions are hidden from the aqueous environment. A versatile class of amphiphiles is constituted by peptide amphiphiles, which are composed of a hydrophobic aliphatic tail and a hydrophilic peptide sequence, linked to each other via an amide bond. Potential applications of peptide amphiphiles lie in those areas where the formation of higher order structures is required, such as mimicking the extracellular matrix (ECM) (see also **Chapter 1.4.3**.). The ECM is the biological material that surrounds cells in tissue and is composed of proteoglycan filaments, collagen fibres and elastin. Peptide amphiphiles form β-sheet structures that resemble the architecture of natural fibres of the ECM. They can easily be synthesized using solid phase peptide synthesis (SPPS). Webber et al. for example used SPPS for peptide amphiphile synthesis by coupling of palmitic acid to the N-terminus of an RGDS-containing peptide. These constructs self-assembled in cylindrical micelles, forming nanometre wide fibres, micrometres in length. The potential of these amphiphiles in biological applications was proven by *in vitro* and *in vivo* studies with bone marrow derived cells.[3] The Tirrell group synthesized peptide amphiphiles via coupling of two palmitic acid tails to a peptide. The peptide component was derived from a T-cell epitope from the tumour antigen ovalbumin. The assembled cylindrical micelles were used for *in vivo* studies and showed protection from tumours by stimulation of ovalbumin-specific T-cells.[4]

5.1.2. Diacetylene-containing peptide amphiphile fibres

The mechanical integrity of nanofibres formed from peptide amphiphiles is, like many self-assembled structures held together by secondary interactions, usually limited, making the structures prone to disassemble.[5] A facile method to cross-link the individual components was presented by Hartgerink et al. The peptide amphiphiles contained four cysteine residues in the peptide sequence, which were used to form intermolecular disulfide bridges. This method to introduce stability is reversible; addition of mild reducing agents disconnects the disulfide bridges.[6] Another interesting method to prevent fibre disassembly is the incorporation of diacetylene moieties in the alkyl tails. Diacetylenes can be polymerised using UV irradiation, yielding highly conjugated backbones.[7] The topochemical polymerisation proceeds when the spacing between the monomers is 4.9 Å and when they are in an angle of 45°.[8,9] This conjugated π-system is highly ordered, accompanied by an intense blue colour of the polydiacetylenes. Upon environmental influences such as changes in temperature, pH and mechanical stress, the π-system becomes less ordered leading to a colour change from blue to pink (**Figure 5.1**).[10-13]

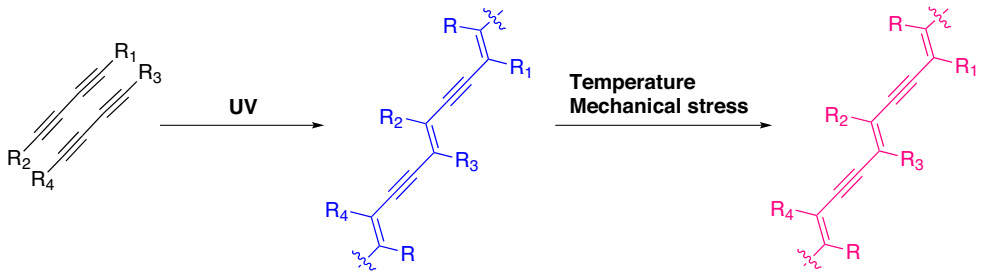

Figure 5.1. Diacetylenes can be polymerised using UV irradiation resulting in a characteristic blue colour. The colour change to pink occurs upon external environmental changes.

Diacetylene-containing peptide amphiphiles have been widely studied (**Figure 5.2**). The Stupp group for example showed that these compounds have a high degree of internal order and a characteristic ß-sheet structure. The replacement of linear by branched peptides led to a decrease in polymerisation efficiency.[14] Biesalski et al. showed the high degree of stability of peptide amphiphiles containing the cell binding motif RGDS as the peptide component. Polymerised fibres could be transferred to solid substrates and be removed without losing surface functionality. Fibroblasts were able to adhere to the fibres and showed a spread morphology.[15]

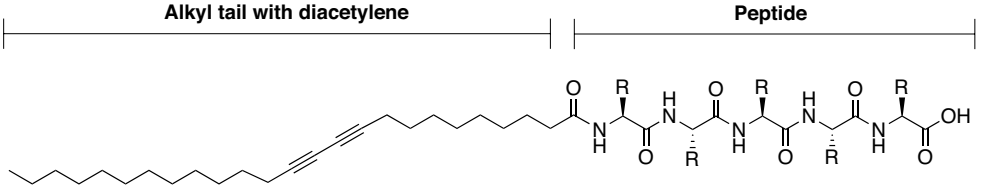

Figure 5.2. General structure of a diacetylene-containing peptide amphiphile.

Also in our group, a lot of research has been carried out on diacetylene-containing peptide amphiphiles. For example, a systematic study on the length of the alkyl tail was performed. Van den Heuvel clearly showed that a longer alkyl tail improves the stability of the formed nanofibres.[16] Furthermore, peptide amphiphiles were used as macro-initiator for atom transfer radical polymerisation (ATRP), by incorporation of α-bromo esters as initiator in the peptide component. Steric crowding introduced by performing the ATRP reaction led to the characteristic colour change from blue to pink.[13] Recently, our group showed that RGDS-containing fibres mixed with spacer fibres can be used to sense cell adhesion. Upon cellular adherence, the characteristic colour change from blue to pink was observed. In fact, this could be tuned by varying the C-terminal amino acid of the spacer amphiphile. The colour change was most prominent for lysine as the C-terminal residue.[17]

An interesting additional feature of certain peptide amphiphile fibres is the possibility to align them. Apart from the order obtained from spontaneous assembly, the fibres can thus be further organized at a macroscopic level. Our group showed the assembly of diacetylene-containing peptide amphiphiles with a peptide component derived from the CS protein of a malaria parasite (GANPNAAG). Upon applying a strong magnetic field (20 T), the fibres showed a high degree of alignment parallel to the magnetic field yielding materials with highly anisotropic optical properties.[18,19] The Stupp group reported the alignment of peptide amphiphile nanofibres containing cell-adhesion motif IKVAV using shear.[20] The IKVAV motif is present in the C-terminal coiled-coil domain of laminin-1 and is known to promote neurite outgrowth of several neuronal cell types.[21] The aim of the research was to control the directional growth of neuronal cells. For this purpose, neuronal cells were mixed with the peptide amphiphiles, resulting in nanofibre gels with encapsulated cells. Due to the presence of the IKVAV motif, neurite growth was promoted. These neurites grew along the direction of the aligned nanofibres, showing the ability to control the orientation of neuronal cells.[22,23]

In the abovementioned method, fibre alignment is achieved by pipetting of a peptide amphiphile solution into a $CaCl_2$ solution. The shear forces caused by pipetting led to alignment, whereas gel formation is triggered by the calcium ions that screen the charged amino acid residues. The drawback of this method is that the obtained gel is held together by physical interactions, which are often weak. When the gel disassembles, fibre alignment will also be disrupted. This could be circumvented if the peptide amphiphile fibres are captured in a covalently cross-linked matrix. We therefore set out to develop a novel system in which we can align and fixate peptide amphiphile fibres in a more permanent polymeric network structure based on our previously described hydrogels (**Figure 5.3, Chapters 3** and **4**). In order to obtain materials which are of potential interest to study directional neuronal cell growth IKVAV-containing fibres will be incorporated in a hydrogel. Contrary to the procedure described by Stupp, neuronal cells will be added after the preparation of the matrix material. As cellular ingrowth in the polymer network is thus required, a polymeric building block will be used containing a matrix metalloproteinase (MMP) sensitive peptide motif. MMPs are naturally occurring in the ECM where they are responsible for remodelling. This chapter first describes our investigations regarding the encapsulation of peptide amphiphile fibres in SPAAC cross-linked hydrogel matrices. It was tested whether fibres still displayed their characteristic topochemical polymerisation and whether network formation was still possible (**Paragraph 5.2.1; 5.2.2**). Our next step focussed on the alignment of the fibres in a strong magnetic field and the subsequent formation of a hydrogel network around these aligned fibres (**Paragraph 5.2.3**). Furthermore, we also investigated the possibilities of using the newly developed SPOCQ cross-linking method to create the matrix structure (**Paragraph 5.2.4**). Moreover, this chapter will provide an outlook what will be required to apply these gels for directing neuronal cell growth (**Paragraph 5.2.5**).

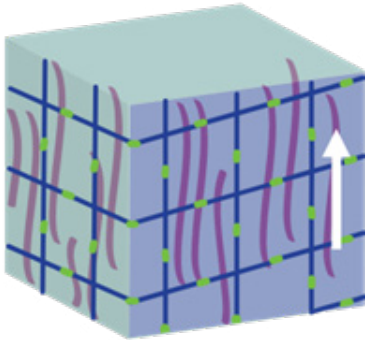

Figure 5.3. Schematic representation of the peptide amphiphile fibres aligned in a magnetic field and encapsulated in the hydrogel matrix. Aligned peptide amphiphile fibres are represented in purple, star-PEG polymers in blue and the cross-links between the polymeric constituents are represented in green. Both SPAAC and SPOCQ are examined as cross-linking method. The white arrow indicates the direction of the magnetic field.

5.2. Results and Discussion

5.2.1. Gel and fibre formation

We first investigated whether we could encapsulate fibres in a SPAAC cross-linked hydrogel network. Peptide amphiphiles were synthesized by solid phase peptide syntheses as described in earlier chapters. The peptide component was composed of a Gly-Ala-Gly-Ala-Glu pentapeptide. The GAGAE sequence was chosen since it is known to be most susceptible to environmental changes.[13] This peptide sequence was therefore used in the first gelation tests, and was later on lengthened to introduce the IKVAV motif (GAGAEIKVAV). Alkyl tail 10,12-pentacosadiynoic acid, containing the diacetylene moiety, was N-terminally coupled to the peptides to obtain the desired amphiphiles (**Figure 5.4**).[24]

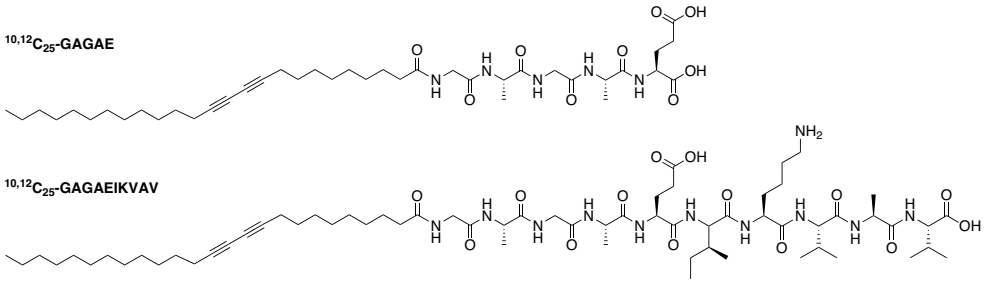

Figure 5.4. Structures of peptide amphiphiles with GAGAE and GAGAEIKVAV.

GAGAE fibres were prepared by heating a solution of the peptide amphiphiles in water to 90°C, which was allowed to cool slowly to room temperature. Polymerisation of the fibres was carried out next by illumination with UV-light for 15 minutes. Fibres prepared in this manner thus obtained their characteristic blue colour, indicative of the highly ordered packing of the alkyl tails within the fibres.[24] These polymerised fibres were mixed with polymers star-PEG-BCN and star-PEG-N_3, to test whether this could lead to fibre-containing hydrogels. Fibre solutions of 0.5 mg/mL and 1.0 mg/mL were added to a polymer mixture of 20 mg/mL and were left to allow gel formation. After approximately 75 minutes gelation occurred, which was similar to previous gelation times for SPAAC cross-linked hydrogels (see **Chapter 3**). The blue fibre-loaded gels were heated to test whether the fibres were still sensitive to environmental changes. Upon heating, the fibre-loaded gels showed indeed their characteristic colour change from blue to pink (**Figure 5.5**).

Figure 5.5. GAGAE fibre containing hydrogels. Left: unpolymerised peptide amphiphiles, resulting in a colourless hydrogel. Middle: polymerised GAGAE fibres, giving a blue gel. Right: upon heating a colour change to pink occurred.

We next tested whether polymerisation was also possible within the hydrogel network. A peptide amphiphile solution was mixed with the polymers to form a hydrogel. This colourless gel was polymerised under UV-light, which resulted in blue fibre-containing gels. Upon heating, pink gels were also obtained (**Figure 5.5**). These gelation tests show that the peptide amphiphile fibres still display their characteristic polymerisation behaviour when encapsulated in a hydrogel network.

5.2.2. Rheology

To test whether SPAAC cross-linking occurred efficiently, the mechanical properties of the fibre-loaded gels were measured by means of rheology. These tests were performed with samples containing 10, 20 and 30 mg/mL hydrogels and polymerised GAGAE fibres (0.5 and 1.0 mg/mL) (**Figure 5.6, Table 5.1**). Time sweep measurements resulted in comparable G' values as previously measured for non-fibre containing gels (see **Chapter 3**). The values for the loss modulus (G'' ± 13 Pa) were somewhat higher than before, indicating that the fibre-loaded hydrogel is more viscous (**Figure 5.6**).

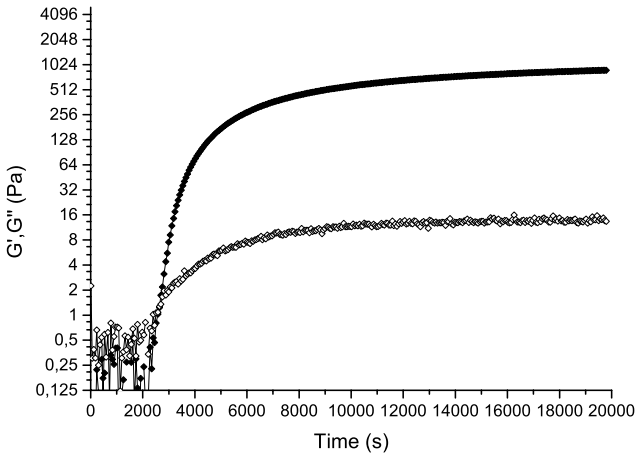

Figure 5.6. Time sweep measurement by rheology (5.5 h) on a 20 mg/mL hydrogel containing 1.0 mg/mL GAGAE fibres.

Moduli for the 20 mg/mL gels were somewhat lower than expected, but still in the same order of magnitude as before. There were no differences in the mechanical properties of gels containing 0.5 mg/mL or 1.0 mg/mL fibres. These data show that the mechanical properties of the SPAAC cross-linked gels are not affected when fibres are encapsulated in the polymer network (**Table 5.1**). An interesting observation was that due to a strain sweep measurement conducted on the blue fibre gels, the applied mechanical stress resulted in less ordered fibres as indicated by the occurrence of the typical pink colour. In summary, when combined, both the hydrogel and the peptide amphiphile fibres showed their characteristic behaviour. We can thus efficiently encapsulate fibres in our SPAAC cross-linked hydrogel network.

Table 5.1. Hydrogel strength G' (Pa) of fibre-containing SPAAC hydrogels measured by rheology. Values were recorded after set time points of 16h, 5.5h and 2.5h for 10 mg/mL, 20 mg/mL and 30 mg/mL, respectively, for gels containing 0.5 and 1.0 mg/mL GAGAE fibres. Rheology data for gels without fibres: see **Chapter 3**.

GAGAE Fibres	G' 10 mg/mL	G' 20 mg/mL	G' 30 mg/mL
0.5 mg/mL	16 Pa	876 Pa	2489 Pa
1.0 mg/mL	13 Pa	878 Pa	2379 Pa
No fibres	25 Pa	1192 Pa	2298 Pa

5.2.3. Magnetic alignment of GAGAE and GAGAEIKVAV fibres in SPAAC cross-linked hydrogels

After establishing the possibility to prepare hydrogels containing peptide amphiphile fibres, we proceeded with fibre alignment. Previous research by our group showed the possibility to align GANPNAAG-containing fibres using strong magnetic fields.[18] Since our peptide component (GAGAE / IKVAV) was different than the one reported in literature, we decided to first examine which magnetic field strength was required to obtain proper alignment of the fibres without the gel matrix. The level of alignment was determined by measuring the birefringence, which is the property that the refractive index of a material depends on the direction of light. In our experiments, we used a 32 T magnet equipped with a temperature controller and a set-up to measure birefringence *in situ*. The peptide amphiphile samples were loaded in a quartz optical cell, which was placed in the magnet. In order to get proper alignment, the fibres were first disassembled by heating the peptide amphiphiles to 80°C. After that, the magnetic field was switched on and the assembly was allowed to take place upon cooling to 20°C, while recording the birefringence to measure alignment. Birefringence was measured as retardation (in degrees); these terms are directly proportional when the path length is constant between measurements.

The experiments were first performed with GAGAE fibres at magnetic field strengths of 0, 5, 10, 15 and 20 T (**Figure 5.7**). As expected, we did not measure birefringence at 0 T, as the curve resembled the control sample with only water. With increasing field strength, increasing values of retardation were recorded, with the highest value being -8.9° (delta retardation) for the 20 T sample. Fibres are thus more aligned when a higher magnetic field is applied. The retardation is negative in value, meaning that the alkyl chains are orientated perpendicular to the magnetic field (**Figure 5.8**).[18,25]

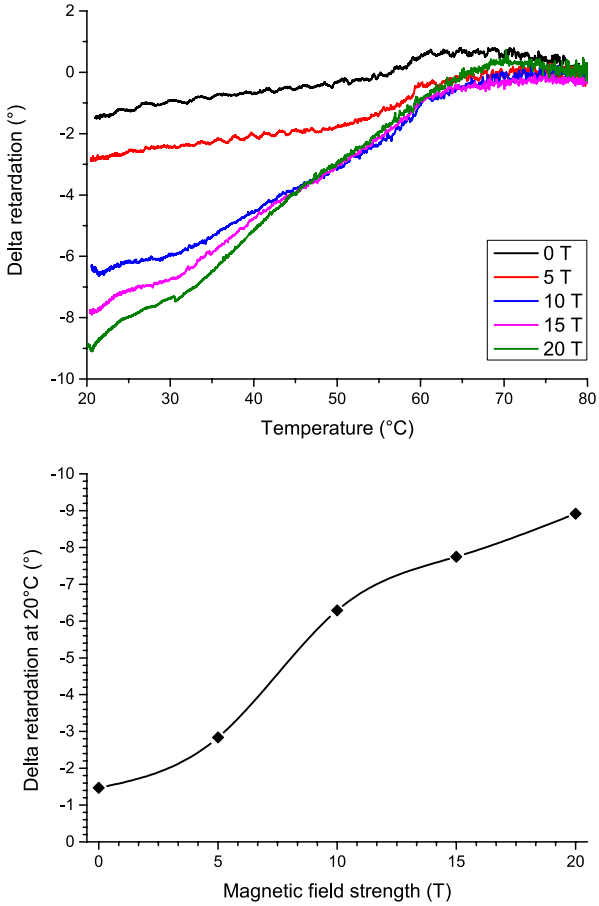

Figure 5.7. Birefringence values of GAGAE fibres when exposed to a magnetic field of 0, 5, 10, 15 and 20 T during cooling from 80°C to 20°C. Fibres were more aligned at higher magnetic fields, as larger negative retardation values were measured. Fibre alignment was not obtained at 0 T. Laser: λ = 632.8 nm; path length 0.001 m. Top: graphical representation. Bottom: graph with maximum delta retardation values (values at 20°C).

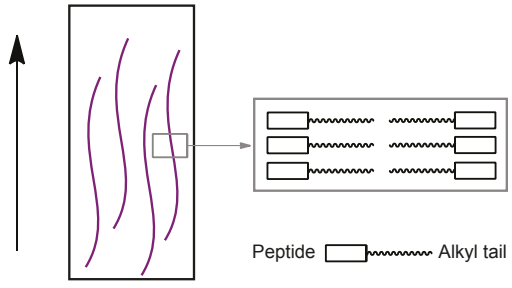

Figure 5.8. Schematic representation of aligned peptide amphiphile fibres (purple). The alkyl tails are orientated perpendicular to the applied magnetic field (black arrow).

After magnetic alignment, the fibres were polymerised by illumination with UV light for 15 minutes. Polymerised fibres showed their typical blue colour. The alignment of the fibres could easily be visualised by placing a polariser film on top of the sample. When the polariser was placed parallel to the direction of the applied magnetic field, the light was strongly absorbed in contrast to a perpendicular orientation of the polariser (**Figure 5.9**).

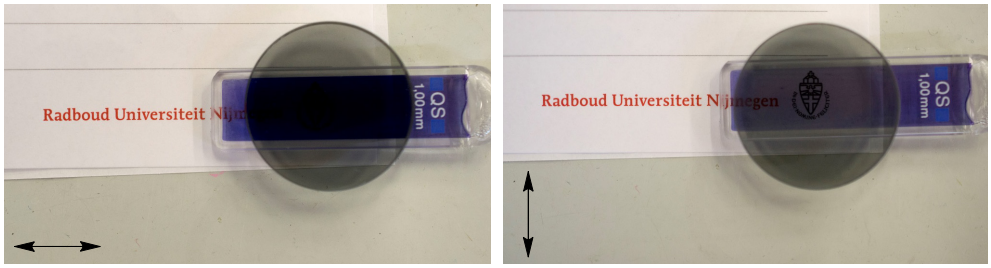

Figure 5.9. Polymerised peptide amphiphile fibre samples after magnetic alignment, analysed with a polariser film. Left: polariser film placed parallel to the direction of the magnetic field, leading to a strong absorbance of the light. Right: polariser film placed perpendicular to the applied field.

This effect could also be measured quantitatively when the polariser film was placed in a UV spectrometer. A large difference in absorbance was measured between the parallel and perpendicular orientation (**Figure 5.10 A**). Linear dichroism analysis of the UV-Vis spectra showed the same trend as the birefringence as alignment was largest for an applied magnetic field of 20 T. This was confirmed by the calculated dichroic ratio, obtained by dividing the absorbance in the parallel direction by the absorbance in the perpendicular direction for the absorbance maximum at 640 nm. (**Figure 5.10 B**).

The experiment was repeated with peptide amphiphile fibres which were composed of a mixture of GAGAEIKVAV and GAGAE peptide amphiphiles in a ratio of 1:6 (**Figure 5.4**).[17] The fibre mixture was placed in a magnetic field of 20 T, because this gave the best alignment for only GAGAE fibres. Comparable retardation values (delta retardation = -8.4°) were found, showing that GAGAEIKVAV containing fibres can also be aligned.

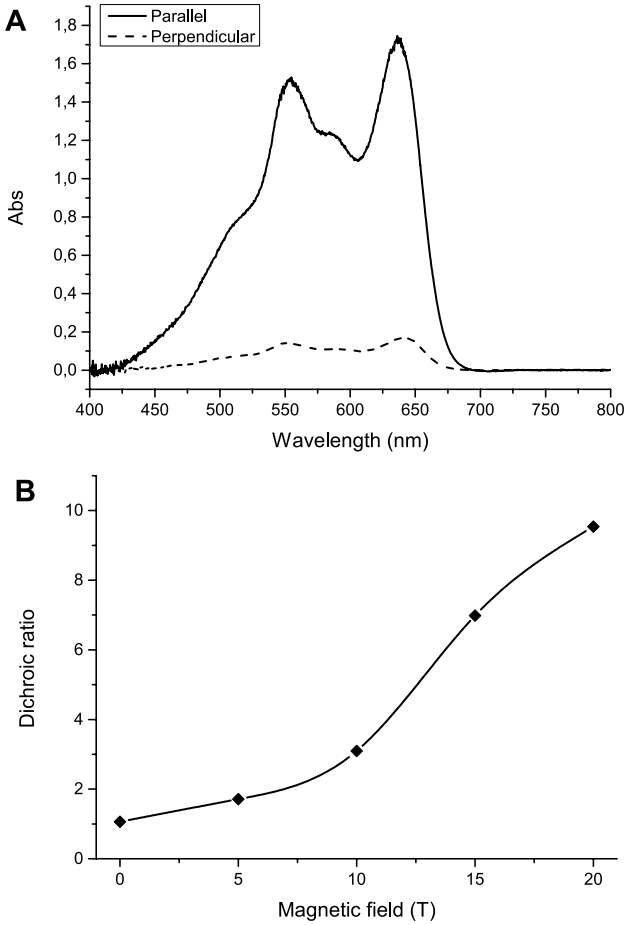

Figure 5.10. UV spectra of aligned GAGAE fibres. A) Differences in UV absorbance parallel and perpendicular to the applied magnetic field for the 20 T sample, showing fibre alignment. B) Dichroic ratios at the different magnetic field strengths, showing that differences in absorbance are largest at 20T, confirming that alignment is largest at 20 T.

After demonstrating the alignment of peptide amphiphile fibres, we proceeded with the encapsulation of the aligned fibres in our hydrogel network. For this purpose, we synthesized a new polymeric building block for hydrogel formation, containing an MMP-sensitive peptide motif. MMP stands for matrix metalloproteinases, which is a family of proteinases able to degrade a variety of extracellular matrix components. From literature it is known that generating space within the hydrogel network is important for cellular growth. By incorporating an MMP-sensitive peptide motif, a cellular cleavage site is present, leading to a more dynamic 3D cellular environment.[26-29] We chose to synthesize peptide N_3-GGPQGIAGQG, which contains the MMP-sensitive motif GPQG↓IAGQ. This 8-residue containing peptide is a known substrate

for several MMP family members.[30] Peptide N_3-GGPQGIAGQG (N_3-MMP) was coupled to star-PEG using the previously exploited coupling strategy with BOP and D*i*PEA (**Chapter 2**). Gelation of star-PEG-BCN and star-PEG-MMP-N_3 occurred as expected, which was simply examined using the inverted vial test (**Figure 5.12**). Next, we aimed for encapsulating aligned fibres in our SPAAC cross-linked hydrogels. For this purpose both star-PEG building blocks were mixed together in a 1:1 ratio with a total concentration of 20 mg/mL, with the GAGAE peptide amphiphiles (1.0 mg/mL). The sample was placed in the magnet, which was already heated to 80°C, after which the reaction mixture was cooled down to 20°C within approximately 45 minutes. We envisaged that fibre alignment could still occur before gel formation was complete, as it was previously shown that gelation of PEG gels occurred after 75 minutes at room temperature (see **Chapter 3**). During the cooling down process, retardation became initially indeed more negative in value, indicating the beginning of fibre alignment. Only a short time later however, the retardation values levelled off (**Figure 5.11**). Probably, cross-linking of the polymers proceeded too quickly and the alignment process was stopped as the solution became increasingly viscous. In order to slow down gelation, a lower hydrogel concentration, 15 mg/mL, was applied. Fibres indeed had more time to align, leading to higher retardation values than for the 20 mg/mL sample. However, also in this case alignment levelled off as soon as the hydrogel cross-linking occurred and remained low when compared to the alignment of fibres at 20 T without the presence of a hydrogel (**Figure 5.11**).

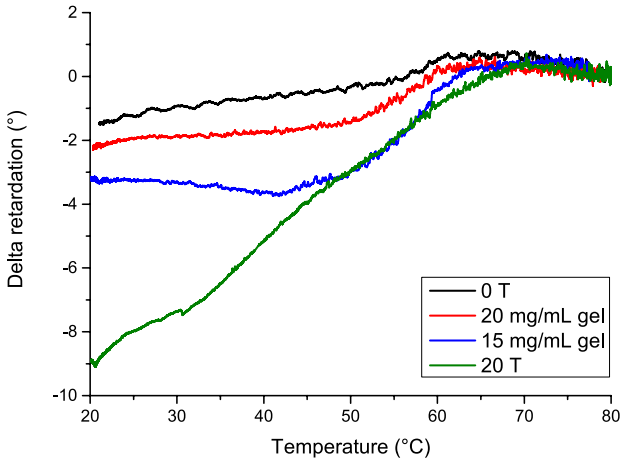

Figure 5.11. Birefringence values of GAGAE fibres entrapped in a hydrogel network, which was formed *in situ* during magnetic alignment. Hydrogel formation disrupts fibre alignment; especially in the 20 mg/mL sample hardly any birefringence was measured. For comparison, GAGAE fibres without any hydrogel components at 0 T and 20 T are displayed.

To prevent disturbance of the fibre alignment by concurrent hydrogel formation, we tested if it was possible to perform hydrogel cross-linking after fibre alignment. In this new approach, we mixed star-PEG-MMP-N_3 with GAGAE-fibres and performed alignment with a magnetic field strength of 20 T. After polymerisation of the fibres, a small volume of star-PEG-BCN was added on top of the sample in the optical cell. The sample was left overnight, to allow gelation to occur fully. The next day, a darker blue colour was observed in the upper part of the sample cell, which appeared to be the only part were gelation occurred. Star-PEG-BCN was thus not able to diffuse through the whole cell, resulting in local gelation at the site of addition. When the polariser film was placed on the dark blue upper part, the polariser effect was much smaller than in the non-gelled lower part of the sample cell. This again shows that gelation disrupted the alignment of the fibres. SPAAC-mediated hydrogel formation either in situ during the alignment process or after alignment leads thus in both cases to a disrupted alignment (process) of the peptide amphiphile fibres.

5.2.4. Magnetic alignment of GAGAE fibres and star-PEG-polymers in SPOCQ cross-linked hydrogels

As an alternative to the SPAAC chemistry, SPOCQ cross-linking was envisioned (see **Chapter 4**). A great advantage of this new cross-linking method is that it is activatable. Gelation only occurs after addition of an oxidizing agent, which can be either sodium periodate or the enzyme mushroom tyrosinase. Oxidizer $NaIO_4$ is a small molecule, which is therefore expected to diffuse easily through the sample. In this respect, we hypothesized that diffusion problems as previously seen for star-PEG-BCN were less likely to occur. It was tested whether SPOCQ can be used to cross-link fibre-containing hydrogels after magnetic alignment. A mixture of star-PEG-BCN, star-PEG-DHPA (**Figure 5.12**) and GAGAE fibres was loaded in the optical cell and placed in the magnet. After reaching a temperature of 80°C, the magnetic field strength was increased to 20 T. Fibres nicely aligned parallel to the applied field, as seen from the negative birefringence values.

Results were comparable to the values previously obtained for only GAGAE fibres (**Figure 5.7**), indicating that the presence of the two polymers did not hinder fibre alignment (**Figure 5.13 A**). After polymerisation with UV light, the polariser film indicated proper alignment of the peptide amphiphile fibres. The alignment was also measured with UV spectroscopy, showing a clear difference in absorbance between light in the parallel and the perpendicular direction (**Figure 5.13 B**).

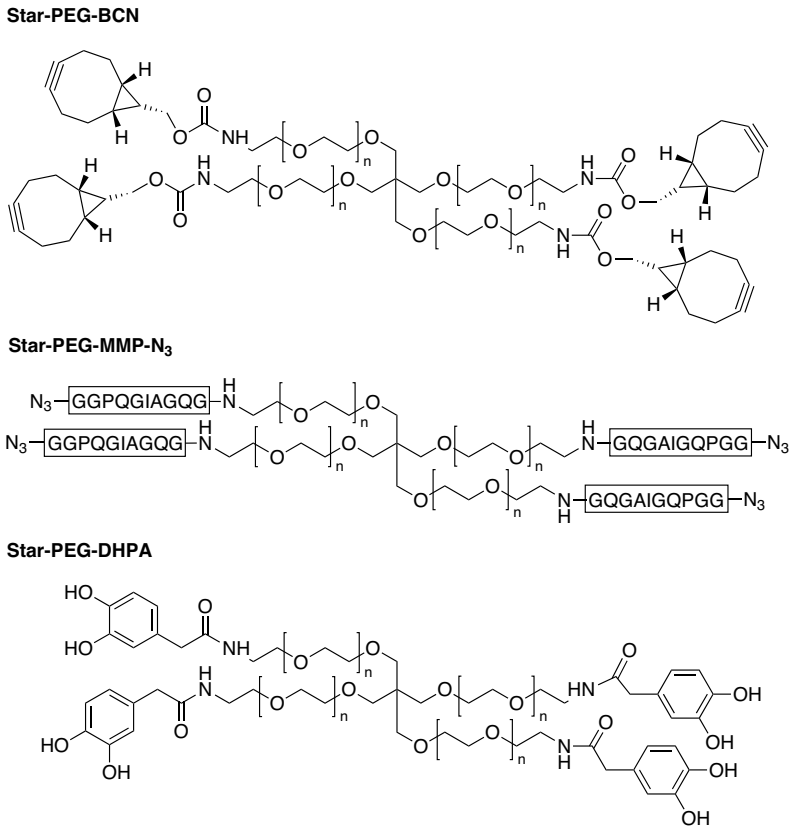

Figure 5.12. Structures of the polymers used for SPAAC cross-linking (star-PEG-BCN and star-PEG-MMP-N_3) and SPOCQ cross-linking (star-PEG-BCN and star-PEG-DHPA).

The magnetic alignment of the star-PEG-BCN, star-PEG-DHPA and GAGAE fibres mixture was performed twice, to obtain two identical samples. One of these samples was used to test gelation with sodium periodate as oxidizing agent, the other was used to test the enzyme mushroom tyrosinase. In both cases, a small volume of the oxidizing agent was added on top of the sample in the optical cell. Since oxidation of the DHPA groups results in a yellow colour, we expected to see the diffusion of the oxidizing agent throughout the optical cell. After addition of both $NaIO_4$ and the enzyme, the samples were left for 16 h. We observed a colour change in the upper part of both optical cells, especially for the enzyme sample, which turned orange. However, because of the blue colour of the aligned fibres, it was hard to visualize whether the oxidizing agent diffused throughout the whole cuvette. UV spectroscopy was used to measure the alignment. Absorbance values were slightly higher than before addition of the oxidizing agent (**Figures 5.13 B** and **5.14**), probably caused by the fact that oxidation results in a yellow colour. Importantly, a large difference in absorbance was still measured, indicating that alignment

was not affected. Samples were also examined after 2 and 14 days. The colour did not change significantly, making it hard to determine whether gelation occurred. UV measurements still showed a large difference between the two directions of light (**Figure 5.14**). However, this could also mean that gelation had not occurred, or as reported in previous research, the fibres remained aligned because they were closely packed between the two glass plates of the optical cell.[18,31]

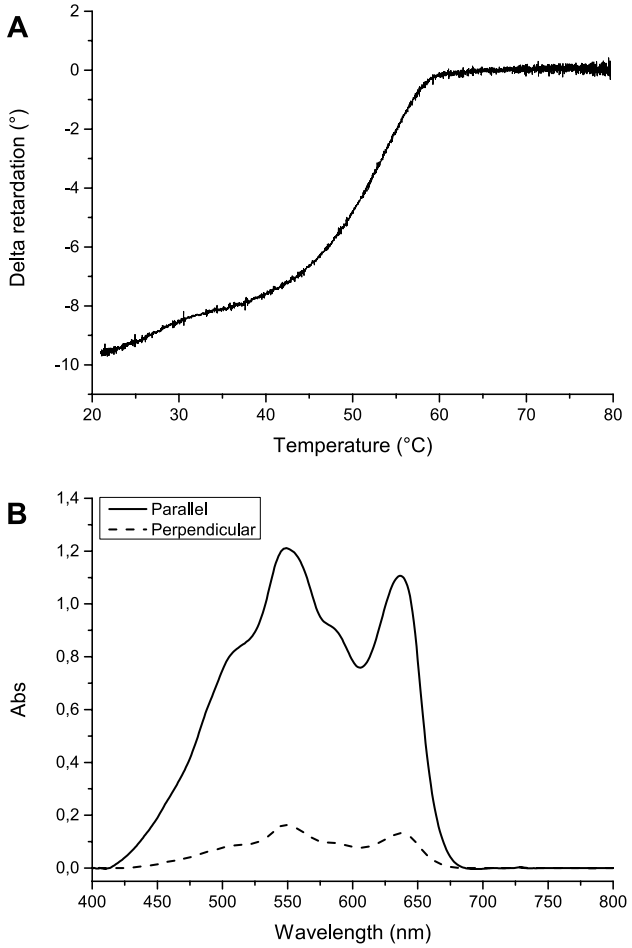

Figure 5.13. Magnetic alignment of a star-PEG-BCN / star-PEG-DHPA / GAGAE fibre mixture. A) Birefringence measurement, showing that the fibres are properly aligned. B) UV spectrum of aligned fibres, showing the expected large difference in absorbance between the parallel and perpendicular directions. The spectrum was recorded before addition of an oxidizing agent.

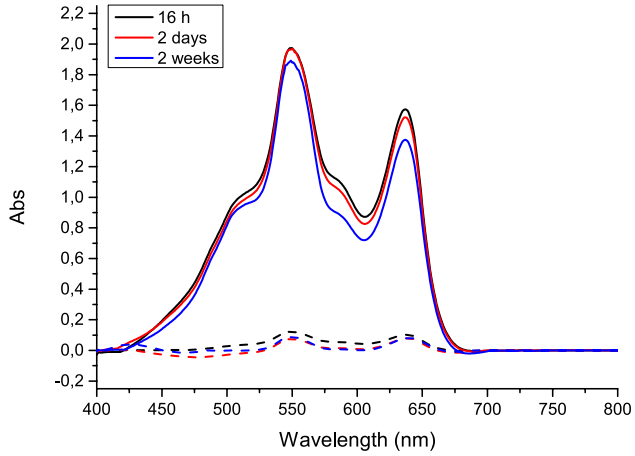

Figure 5.14. UV spectra for the $NaIO_4$ oxidized star-PEG-BCN / star-PEG-DHPA/ GAGAE fibre mixture, followed over time. The large differences in UV absorbance parallel (solid line) and perpendicular (dashed line) to the applied magnetic field remained, indicating that fibres are still aligned after 2 weeks.

In order to unambiguously determine whether gelation had taken place throughout the entire sample, we opened the optical cells containing the 2 week old samples. The enzyme-oxidized reaction mixture showed only gel formation in the upper part of the sample, revealing that once the enzyme starts with the formation of the polymeric network diffusion is strongly hampered. A large part of the sample was still a fibrous liquid (**Figure 5.15**). As expected, fibre alignment was completely lost, as was demonstrated with the polariser film experiment. Gratifyingly, opening of the periodate-oxidized reaction mixture showed a hydrogel throughout the whole sample. $NaIO_4$ is thus able to diffuse through the whole optical cell, leading to oxidation of the DHPA-groups and thus to gel formation (**Figure 5.15**). The polariser film showed that the fibres were still aligned. We thus managed to encapsulate magnetically aligned fibres in a SPOCQ cross-linked hydrogel network.

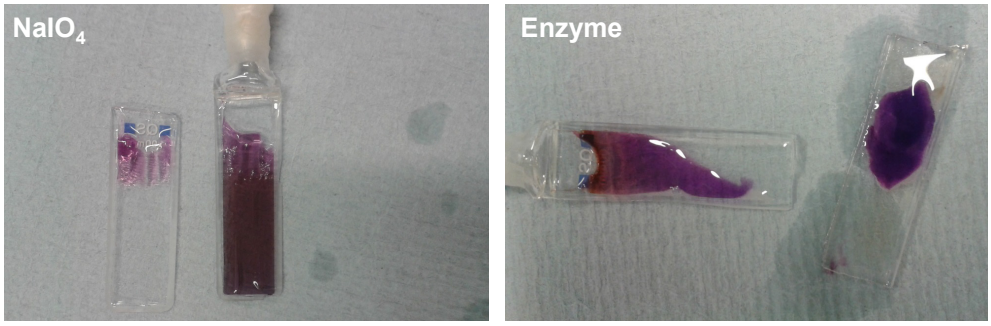

Figure 5.15. Magnet samples after opening of the optical cell. Left: $NaIO_4$ as oxidizing agent leads to hydrogel formation throughout the whole cell. Right: enzyme mushroom tyrosinase leads to a hydrogel network in the upper part (orange coloured), the remaining of the optical cell was a fibrous liquid.

As an extra proof to show alignment, transmission electron microscopy (TEM) was performed. As expected, TEM analysis of the enzyme-oxidized sample showed non-aligned fibres. For the periodate-oxidized sample, it was difficult to obtain good contrast, but aligned fibres were indeed observed (**Figure 5.16**). Scanning electron microscopy (SEM) on both samples was not successful, as this only showed porous structures, probably caused by the hydrogel surface. Thus, alignment of GAGAE fibres could easily be performed in presence of polymers star-PEG-BCN and star-PEG-DHPA using a magnetic field of 20 T. Oxidizing agent sodium periodate was added on top of the sample and was able to diffuse throughout the whole sample in a time period of 2 weeks. The fibres were encapsulated in the SPOCQ cross-linked hydrogel, and remained aligned as visualized with UV spectroscopy and TEM.

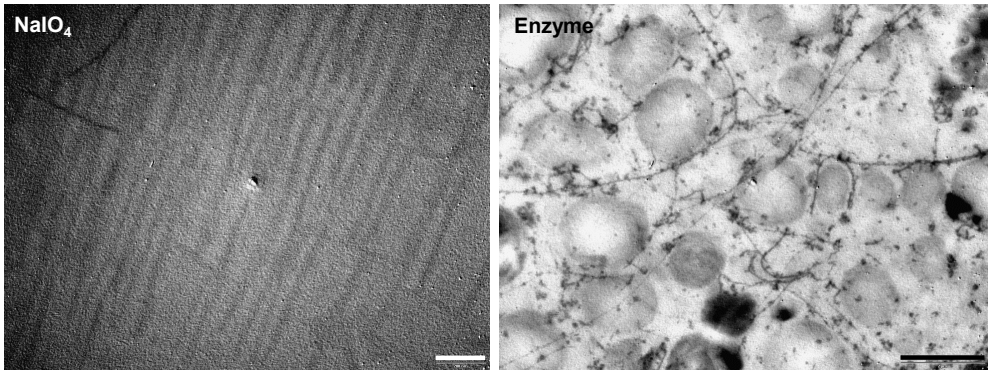

Figure 5.16. Transmission electron microscopy (TEM) pictures of magnetically aligned peptide amphiphiles. Left: with sodium periodate as oxidizing agent, a SPOCQ cross-linked hydrogel is formed with aligned fibres entrapped in the gel network (scale bar: 200 nm). Right: with enzyme mushroom tyrosinase, cross-linking does not lead to proper gel formation, peptide amphiphile fibres do not retain their alignment (scale bar: 2 μm).

5.2.5. Future research

After establishing a successful protocol to construct a hydrogel with aligned peptide amphiphile fibres, the main challenge that remains is to show biological activity of this material in cell culturing applications directed to neuronal outgrowth. Two biological motifs that were installed, the MMP cleavage domain and IKVAV should be tested whether they have retained their activity. Literature supports the hypothesis that incorporation of MMP cleavage domains in hydrogels has potential to enable successful cell culturing by allowing controlled degradation of the network.[27,32-37] An example is the research by Fonseca et al. who modified alginate with an MMP cleavable peptide. Human mesenchymal cells showed an elongated morphology with MMP peptide and RGD-containing alginate gels, but when this was repeated without the MMP motif only round cells were found.[27,32] Lutolf et al. reported Michael-type cross-linked PEG hydrogels with MMP-cleavable peptides. The MMP motif was required to make the hydrogel

network degradable, which was shown by the ability of fibroblasts to enter the network.[36] MMP motif containing PEG hydrogels were also used to study the proliferation and differentiation of human mesenchymal cells. The morphology of the cells depended on the degradability of the hydrogels, as cells able to remodel their environment express higher levels of specific differentiation markers.[37] All of these examples highlight the importance of MMP cleavable sequences in creating a dynamic cellular environment within the hydrogel network.[27,32-37]

A good starting point for future research would be to add HeLa cells or NIH3T3 fibroblasts to a SPAAC cross-linked MMP-hydrogel containing (unaligned) RGDS fibres. We hypothesize that this 3-D system results in proper cell adhesion to the RGDS fibres, as the MMP motifs create a cleavable hydrogel network and thus allow cells to find the adhesion motifs. This experiment should then be repeated with IKVAV-containing fibres and neuronal cells, to confirm that the IKVAV motif is a proper motif for cellular adhesion of this cell type. Due to our experience with SPAAC cross-linked hydrogels as suitable matrices in cell studies, this is suggested as a good starting point for cell culturing studies. However, we have also demonstrated that SPAAC cross-linking is not compatible with the magnetic alignment procedure. We therefore should gain more knowledge about using SPOCQ cross-linking in cell studies (see **Chapter 6**). Both suggested experiments with the RGDS and IKVAV containing fibres should thus also be performed with SPOCQ cross-linked MMP hydrogels. The final step would then be to magnetically align the IKVAV-containing fibres using a 20 T magnetic field. After hydrogel cross-linking, neuronal cells can be added, which are able to grow into the MMP-containing network. Finally, cell studies need to be performed with the neuronal cells, to investigate whether cells show directional growth along the IKVAV motifs of the aligned fibres.

5.3. Conclusion

Peptide amphiphiles fibres were successfully encapsulated in a SPAAC cross-linked hydrogel network, as both the fibres and the gel retained their characteristic behaviour. Fibres containing the GAGAE and GAGAEIKVAV peptide components were aligned in a magnetic field, up to a field strength of 20 T. UV analysis confirmed fibre alignment, as polarized light parallel to the direction of the applied field was strongly absorbed. Magnetic alignment was however disrupted both by *in situ* SPAAC cross-linking and by SPAAC based gel formation after alignment. The activatable SPOCQ cross-linking method provided a way to encapsulate aligned fibres in a hydrogel network. Fibre alignment was performed in presence of star-PEG-DHPA and star-PEG-BCN, after which oxidation with sodium periodate resulted in a hydrogel network. Future research should focus on 3-D cell culturing with degradable hydrogel networks, created by incorporation of a matrix metalloprotease (MMP) motif. By incorporation of adhesion motif

IKVAV on the aligned fibres, it should be possible to make a hydrogel network to direct neuronal cell growth.

5.4. Acknowledgements

Britta Ramakers is kindly acknowledged for her expertise on the peptide amphiphile fibres, for collaborating on all of the magnet experiments and for useful discussions. Roger Rikken is thanked for operating the magnet and for all helpful suggestions. Prof. Peter Christianen is acknowledged for fruitful discussions.

5.5. Materials and methods

General notes experimental section

Materials and methods and standard solid phase peptide synthesis (SPPS) can be found in **Chapter 2**. The preparation of polymers star-PEG-BCN and star-PEG-N_3 are described in **Chapter 3**. The synthesis of star-PEG-DHPA is outlined in **Chapter 4**.

Peptide N_3-GGPQGIAGQG (protected)

N_3-Gly-Gly-Pro-Gln(Trt)-Gly-Ile-Ala-Gly-Gln(Trt)-Gly-OH

MMP sensitive peptide N_3-GGPQGIAGQG was synthesized via standard SPPS using a 2-chlorotrityl resin. Azido-glycine was coupled as the N-terminal residue. A mild cleavage protocol was used by treatment of the resin with a mixture of dichloromethane (DCM), trifluoroethanol (TFE) and acetic acid (HOAc) (6:1:1) for 3 h. The solvents were evaporated under reduced pressure and co-evaporation was performed with chloroform (3 x 40 mL). The peptide was purified by preparative HPLC.

LCQ: m/z: 1351.1 $[M + H]^+$, 1373.5 $[M + Na]^+$ (calculated $[M + H]^+$ = 1351.62)

LC-MS: m/z: 1352.0 $[M + H]^+$, Rt = 10.76 min

HPLC: Rt = 28.02 min

Synthesis of star-PEG-MMP-N_3 (star-PEG-GQGAIGQPGG-N_3) (protected)

To star-poly(ethylene glycol)-NH_2 HCl salt (250 mg, 25 µmol) in DCM (20 mL) was added subsequently BOP (66 mg, 6 eq, 150 µmol), protected peptide N_3-GGPQGIAGQG (203 mg, 6 eq, 150 µmol), and D*i*PEA (102 µL, 24 eq, 0.60 mmol). The reaction mixture was stirred overnight at r.t. Extraction was performed with 1 M $KHSO_4$ (3 x 40 mL) and brine (1 x 40 mL), after which the organic layer was dried over Na_2SO_4. Column chromatography on basic aluminium oxide (MeOH: DCM; 10:90) afforded the protected peptide-polymer construct as a white powder after freeze-drying from dioxane (348 mg; 91%).

^{1}H-NMR (400 MHz, $CDCl_3$): δ = 0.70 – 0.98 (m), 1.22 – 1.58 (m), 1.82 – 2.61 (m), 3.45 – 3.75 (m, $[CH_2CH_2O]_n$,), 4.34 (m, Cα), 7.10 – 7.25 (m, Trt).
MALDI-TOF (DHB): m/z: 15477, calculated m/z: 15466 for 222 ethylene glycol units.

Deprotection of star-PEG-MMP-N_3 (star-PEG-GQGAIGQPGG-N_3)
Deprotection of the protected star-PEG-MMP-N_3 construct (320 mg) was performed by treatment with TFA: TIS: H_2O (95: 2.5: 2.5; 12 mL) for 4 h at r.t. The reaction mixture was partially concentrated and precipitated in Et_2O. Freeze drying from water afforded the product as a white solid (200 mg; 72%).
^{1}H-NMR (400 MHz, D_2O): δ = 0.66 – 0.79 (m), 0.95 – 1.09 (m), 1.21 – 1.35 (m), 1.69 (m), 1.75 – 1.92 (m), 2.00 (m), 2.09 – 2.28 (m) 3.38 – 3.71 (m, $[CH_2CH_2O]_n$,), 4.12 – 4.29 (m, Cα).
MALDI-TOF (alpha-cyano): m/z: 13404, calculated m/z: 13396 for 220 ethylene glycol units.

Synthesis peptide amphiphiles
Peptide amphiphiles containing GAGAE and GAGAEIKVAV as peptide component were prepared via standard solid phase peptide synthesis (SPPS) using a 2-chlorotrityl resin. In the final step, 10,12-pentacosadiyonic acid (3 eq) was coupled, using DIPCDI (3.3 eq) and HOBt (3.6 eq). Cleavage from the resin was performed by treatment of the resin with TFA: TIS: H_2O (95: 2.5: 2.5) for 3 h at r.t. The peptide amphiphile was afforded by precipitation in ether, followed by freeze-drying from acetic acid. Purification was performed using preparative HPLC.

$^{10,12}C_{25}$-Gly-Ala-Gly-Ala-Glu ($^{10,12}C_{25}$-GAGAE)
LC-MS: m/z: 760.12 $[M + H]^+$ (calculated $[M + H]^+$ = 760.48)
HPLC: Rt = 34.54 min

$^{10,12}C_{25}$-Gly-Ala-Gly-Ala-Glu-Ile-Lys-Val-Ala-Val ($^{10,12}C_{25}$-GAGAEIKVAV)
LC-MS: m/z: 1271.6 $[M + H]^+$ (calculated $[M + H]^+$ = 1270.83), Rt = 12.13 min.
HPLC: Rt = 30.45 min

Fibre formation
The peptide amphiphiles were dissolved in MilliQ, at a concentration of 1.0 mg/mL. Sonication of the samples was performed for 15 min at 25°C. Samples were heated to 90°C using a water bath and were allowed to cool to room temperature overnight in the water bath.

Fibre polymerisation
After fibre formation, samples were illuminated with UV-light for 15 minutes. Fibres were illuminated from above, with a distance of 3 cm between the lamp and the sample, using a Bluepoint 2 UV lamp. After UV treatment, fibres showed their characteristic blue colour.

Gelation and fibre formation studies

Star-PEG-BCN (4.0 mg) and star-PEG-N_3 (4.0 mg) were dissolved in 400 µL polymerised GAGAE fibre solution (1.0 mg/mL; blue). The mixture was left at room temperature to allow gelation (20 mg/mL). Similarly, gels with a polymer content of 10 and 30 mg/mL and a fibre content of 0.5 or 1.0 mg/mL were prepared. Hydrogels were heated to 90°C, showing their characteristic colour change from blue to pink. Rheology studies were conducted by measuring time sweeps of 16 h, 5.5 h and 2.5.h for gels with a polymer content of 10, 20 and 30 mg/mL, respectively and a fibre content of 0.5 or 1.0 mg/mL. Rheometer settings were equal as described before (see **Chapter 3** or **4**). Frequency and strain sweeps were also performed on the fibre-containing hydrogels.

Star-PEG-BCN (4.0 mg) and star-PEG-N_3 (4.0 mg) were dissolved in 400 µL GAGAE solution (1.0 mg/mL; not polymerised; colourless). The sample was kept in the dark. After gelation had occurred (20 mg/mL; 75 min), it was heated to 90°C and allowed to cool to room temperature to enable fibre formation. The sample was polymerised with UV light (15 min; resulting in the expected blue gel) and after that heated to 90°C (giving a pink gel).

Magnetic alignment of peptide amphiphile fibres

Prior to measuring the peptide amphiphile fibre samples, several temperature sweeps (20 → 80°C and 80 → 20 °C) were conducted on a water sample to check the temperature effect on the retardation values. Only small variations in retardation values were recorded, showing that temperature changes do not have an influence on the birefringence measurements. Peptide amphiphile fibres were formed as described above, in concentrations of 1.0 mg/mL. For the IKVAV-containing amphiphiles, a mixture of GAGAEIKVAV and GAGAE fibres in a ratio of 1:6 was prepared. Fibres (± 350 µL) were loaded in a quartz optical cell with a pathlength of 1 mm. Samples were measured on a 32 T Bitter magnet from the High Field Magnet Laboratory (HFML). This magnet has a power of 18 MW, a bore size of 50 mm and is equipped with a temperature controller and a birefringence set-up. In this set-up, the sample was placed between two crossed polarizers. Monochromatic light was produced by a HeNe laser (λ = 632.8 nm; pathlength 0.001 m). The birefringence set-up was furthermore equipped with a photo-elastic modulator (PEM) and a photodetector.[38] Samples were placed in the magnet, which was already heated to a temperature of 80°C. When the temperature was stable at 80°C, the magnet was switched on to the desired strength (5 T, 10 T, 15 T or 20 T) using a sweep rate of 80 mT/s. The temperature was lowered to 20°C in approximately 45 minutes, under constant measuring of the birefringence. The magnet was switched off when a temperature of 20°C was reached. As a control experiment, this procedure was repeated without magnetic field (0 T). For all experiments, the pathlength was kept constant (1 mm), meaning that birefringence and retardation are equal. The measured birefringence values were graphically represented

as delta retardation (°). The birefringence value recorded at 80°C was taken as the constant starting point; delta retardation was calculated by subtracting this constant value. After magnetic alignment, samples were polymerised with UV light for 15 minutes. All samples were examined using a polariser film.

Magnet samples for SPAAC cross-linking

Samples for in situ hydrogel formation were prepared by dissolving star-PEG-BCN in a GAGAE fibre solution (1.0 mg/mL) and by dissolving star-PEG-MMP-N_3 in a GAGAE fibre solution (1.0 mg/mL). Amounts of the polymers were chosen to yield a ratio of 1:1 between the BCN and N_3 groups and a final polymer concentration of 15 mg/mL or 20 mg/mL. Directly after mixing the two polymer-fibre solutions, the mixture (± 350 µL) was loaded in the optical cell and placed in the magnet (already at 80°C). Measurements were performed at 20 T as described above. The fibres in the resulting hydrogels were polymerised with UV light. The sample for hydrogel formation after magnetic alignment was prepared by dissolving star-PEG-MMP-N_3 in a GAGAE fibre solution (1.0 mg/mL). This solution (± 320 µL) was loaded in the optical cell and aligned using a magnetic field of 20 T. After polymerisation of the fibres, star-PEG-BCN (20 µL) was loaded on top of the sample. The total polymer concentration of the resulting hydrogel was 20 mg/mL (ratio BCN: N_3 1:1). As a control experiment, a birefringence measurement was performed on a mixture of polymers of star-PEG-BCN and star-PEG-MMP-N_3. The formed hydrogel was measured at 20 T. All samples were examined using a polariser film.

Magnet samples for SPOCQ cross-linking

Two equal samples were prepared by dissolving star-PEG-BCN in a GAGAE fibre solution (1.0 mg/mL) and by dissolving star-PEG-DHPA in a GAGAE fibre solution (1.0 mg/mL). A ratio of 1:1 between the BCN and catechol groups was taken with a final polymer concentration of 20 mg/mL. After mixing the two polymer-fibre solutions, the mixture (± 300 µL) was loaded in the optical cell and placed in the magnet (already at 80°C). Measurements were performed at 20 T as described above. The fibres in the resulting hydrogels were polymerised with UV light. Samples were examined with a polarizer film and measured in a UV spectrometer. To one of the samples, 50 µL sodium periodate (1 eq, based on amount of DHPA groups) was added on top of the material in the optical cell. To the other sample, 50 µL enzyme mushroom tyrosinase (500 units/mL) was added. Both samples were analysed using the polarizer film and UV spectroscopy 16 h, 2 days and 2 weeks after addition of the oxidizing agent. After 2 weeks, both optical cells were opened to check gel formation.

UV spectroscopy

UV spectra were recorded on a Jasco-v630 spectrometer at a wavelength range of 400 – 800 nm. Samples used for magnetic alignment (in a 1 mm quartz optical cell) were measured. A

polarizer film was placed in front of the light beam, to be able to measure parallel (0°) and perpendicular (90°) to the applied magnetic field. UV spectra were corrected by subtracting the background spectrum recorded for water. UV spectra were baseline corrected using the Origin software. To determine the dichroic ratio, maximum absorbance values for the peak around 640 nm were taken. The absorbance in the parallel direction divided through the absorbance in the perpendicular direction yields the ratio.

Transmission electron microscopy (TEM)

TEM samples were prepared for the two SPOCQ cross-linked samples (periodate and enzyme). A carbon-coated copper grid was placed on the samples for 1 min, followed by staining with a 1% uranyl acetate solution in MilliQ for 30 seconds. The grid was floated on MilliQ water for 1 min, after which the excess of water was removed by blotting with filter paper. A JEOL 1010 transmission electron microscope set was used for imaging, with an accelerating voltage of 60 kV.

5.6. References

(1) Löwik, D. W. P. M.; van Hest, J. C. M. *Chem. Soc. Rev.* **2004**, *33*, 234.

(2) Ramakers, B. E. I.; van Hest, J. C. M.; Löwik, D. W. P. M. *Chem. Soc. Rev.* **2014**, *43*, 2743.

(3) Webber, M. J.; Tongers, J.; Renault, M.-A.; Roncalli, J. G.; Losordo, D. W.; Stupp, S. I. *Acta Biomater.* **2010**, *6*, 3-11.

(4) Black, M.; Trent, A.; Kostenko, Y.; Lee, J. S.; Olive, C.; Tirrell, M. *Adv. Mater.* **2012**, *24*, 3845-3849.

(5) Nieuwland, M.; Ruizendaal, L.; Brinkmann, A.; Kroon-Batenburg, L.; van Hest, J. C. M.; Löwik, D. W. P. M. *Faraday Discuss.* **2013**, *166*, 361.

(6) Hartgerink, J. D. *Science* **2001**, *294*, 1684-1688.

(7) Wegner, G. *Makromol. Chem.* **1972**, *154*, 35-48.

(8) Baughman, R. H. *J. Polym. Sci. Polym. Phys. Ed.* **1974**, *12*, 1511-1535.

(9) Rhodes, D. G.; Frankel, D. A.; Kuo, T.; O'Brien, D. F. *Langmuir* **1994**, *10*, 267-275.

(10) Li, Z.; Fowler, F. W.; Lauher, J. W. *J. Am. Chem. Soc.* **2009**, *131*, 634-643.

(11) Charych, D. H.; Nagy, J.; Wayne Spevak; Bednarskit, M. D. *Science* **1993**, *261*, 585-588.

(12) Okada, S.; Peng, S.; Spevak, W.; Charych, D. *Acc. Chem. Res.* **1998**, *31*, 229-239.

(13) Ramakers, B. E. I.; van den Heuvel, M.; Tsichlis i Spithas, N.; Brinkhuis, R. P.; van Hest, J. C. M.; Löwik, D. W. P. M. *Langmuir* **2012**, *28*, 2049-2055.

(14) Hsu, L.; Cvetanovich, G. L.; Stupp, S. I. *J. Am. Chem. Soc.* **2008**, *130*, 3892-3899.

(15) Biesalski, M. A.; Knaebel, A.; Tu, R.; Tirrell, M. *Biomaterials* **2006**, *27*, 1259-1269.

(16) Van den Heuvel, M.; Löwik, D. W. P. M.; van Hest, J. C. M. *Biomacromolecules* **2008**, *9*, 2727-2734.

(17) Ramakers, B. E. I.; Bode, S. A.; Killaars, A. R.; van Hest, J. C. M.; Löwik, D. W. P. M. *J. Mater. Chem. B* **2015**, *3*, 2954-2961.

(18) Löwik, D. W. P. M.; Shklyarevskiy, I. O.; Ruizendaal, L.; Christianen, P. C. M.; Maan, J. C.; van Hest, J. C. M. *Adv. Mater.* **2007**, *19*, 1191-1195.

(19) Van den Heuvel, M.; Prenen, A. M.; Gielen, J. C.; Christianen, P. C. M.; Broer, D. J.; Löwik, D. W. P. M.; van Hest, J. C. M. *J. Am. Chem. Soc.* **2009**, *131*, 15014–15017.

(20) Silva, G. A.; Czeisler, C.; Niece, K. L.; Beniash, E.; Harrington, D. A.; Kessler, J. A.; Stupp, S. I. *Science* **2004**, *303*, 1352-1355.

(21) Powell, S. K.; Rao, J.; Roque, E.; Motoyoshi Nomizu; Kuratomi, Y.; Yamada, Y.; Kleinman, H. K. *J. Neurosci. Res.* **2000**, *61*, 302-312.

(22) Berns, E. J.; Sur, S.; Pan, L.; Goldberger, J. E.; Suresh, S.; Zhang, S.; Kessler, J. A.; Stupp, S. I. *Biomaterials* **2014**, *35*, 185-195.

(23) Zhang, S.; Greenfield, M. A.; Mata, A.; Palmer, L. C.; Bitton, R.; Mantei, J. R.; Aparicio, C.; Cruz, M. O. d. l.; Stupp, S. I. *Nat. Mater.* **2010**, *9*, 594-601.

(24) Ramakers, B. E. I. *PhD thesis - Synthesis and characterisation of peptide based materials* **2015**.

(25) Rosenblatt, C.; Yager, P.; Schoen, P. E. *Biophys. J.* **1987**, *52*, 295-301.

(26) West, J. L.; Hubbell, J. A. *Macromolecules* **1999**, *32*, 241-244.

(27) Fonseca, K. B.; Gomes, D. B.; Lee, K.; Santos, S. G.; Sousa, A.; Silva, E. A.; Mooney, D. J.; Granja, P. L.; Barrias, C. C. *Biomacromolecules* **2014**, *15*, 380-390.

(28) Lutolf, M. P.; Hubbell, J. A. *Nat. Biotechnol.* **2005**, *23*, 47-55.

(29) Wang, C.; Varshney, R. R.; Wang, D.-A. *Adv. Drug Delivery Rev.* **2010**, *62*, 699-710.

(30) Nagase, H.; Fields, G. B. *Biopolymers* **1976**, *40*, 399-416.

(31) Van den Heuvel, M. *PhD Thesis - Structure and properties of polydiacetlyene-containing peptide amphiphile fibres* **2011**.
(32) Fonseca, K. B.; Bidarra, S. J.; Oliveira, M. J.; Granja, P. L.; Barrias, C. C. *Acta Biomater.* **2011**, *7*, 1674-1682.
(33) Kang, M. K.; Colombo, J. S.; D'Souza, R. N.; Hartgerink, J. D. *Biomacromolecules* **2014**, *15*, 2004-2011.
(34) Sarig-Nadir, O.; Seliktar, D. *Biomaterials* **2010**, *31*, 6411-6416.
(35) Lau, H. K.; Kiick, K. L. *Biomacromolecules* **2015**, *16*, 28-42.
(36) Lutolf, M. P.; Raeber, G. P.; Zisch, A. H.; Tirelli, N.; Hubbell, J. A. *Adv. Mater.* **2003**, *15*, 888-892.
(37) Anderson, S. B.; Lin, C.-C.; Kuntzler, D.V.; Anseth, K. S. *Biomaterials* **2011**, *32*, 3564-3574.
(38) Gielen, J. *PhD Thesis - Supramolecular aggregates in high magnetic fields* **2010**.

Chapter 6

Dual cross-linked hydrogels by combining chemical and physical cross-linking

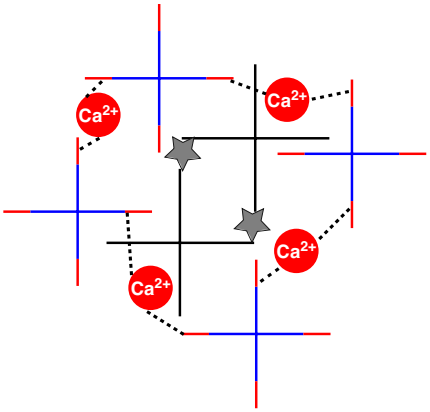

6.1. Introduction

As outlined in the introductory chapter, hydrogels can show distinctly different properties if they are cross-linked via either chemical or physical methods (**Chapter 1**). Chemical cross-linking often leads to stronger hydrogels of which the mechanical properties can easily be tuned by varying the cross-linking density. Physically cross-linked hydrogels, on the other hand, can be made stimuli responsive. These materials undergo a solution-to-gel state transition in response to external stimuli, such as temperature,[1,2] pH,[3] light and ionic strength.[4,5] A great advantage of physical cross-linking is that it does not depend on organic solvents or the addition of cross-linking reagents. Furthermore, the specific sub-set of *in situ* forming hydrogels holds great promise as drug delivery system, as these gels undergo the sol-to-gel transition upon administration in the body, which often is mediated by ionic crosslinking.[1,2,4,6,7] In particular carbohydrates have been used for this type of physically cross-linked hydrogels. Chitosan is a polysaccharide composed of the monomers β-2-acetamido-2-deoxy-D-glucopyranose and 2-amino-2-deoxy-D-glucopyranose. Chitosan is obtained by the deacetylation of chitin, which is the main component of the skeleton of crustaceans such as shrimps and crabs. Due to its biocompatibility and biodegradability, chitosan has already been used in several medical applications, for example as bioadhesive and mucoadhesive material.[8,9] In order to perform physical cross-linking, chitosan needs to be dissolved, which is enabled by protonation of the amine groups.[10] A straightforward way of gel formation was attained by the addition of various metal ions, such as Pt(II), which formed coordinate covalent bonds with these protonated amine groups by complexation.[11] Chitosan hydrogels were also obtained by addition of polyol phosphate salts (e.g. glycerol) to an aqueous chitosan solution. This transferred the gelation process from being purely pH-dependent to a combined pH and temperature-dependent system. The chitosan/polyol mixture remained a liquid at physiological pH and below room temperature, but formed a gel when the temperature was increased to 37°C.[10]

The most pronounced example of a physically cross-linked carbohydrate-based hydrogel is alginate. As also outlined in **Chapter 2**, alginate is a polysaccharide composed of the two monomers α-L-guluronic acid (G) and β-D-mannuronic acid (M). In the polymer, blocks of one of the monomers are present, as well as regions with alternating units. An important feature of alginate is its ability to form gels with divalent cations such as Ca^{2+}, Ba^{2+} and Sr^{2+}. Gelation is not induced by monovalent cations and by Mg^{2+}.[12-14] Alginate-based hydrogels have been used in several biomedical applications, including wound healing,[15,16] cell encapsulation,[17] drug delivery[18,19] and in tissue engineering.[20-22] An example is the work by Zhao et al. who developed an injectable calcium phosphate-alginate hydrogel. Human umbilical cord mesenchymal stem cells were encapsulated in the hydrogels and remained viable. Cells also showed osteodifferentiation and synthesized bone minerals, showing the potential of alginate-based hydrogels for bone tissue engineering.[20]

A class of synthetic polymers that can both be chemically and physically cross-linked are the polyphosphazenes. These organometallic polymers contain a backbone with alternating nitrogen and phosphorus atoms, whereby two side groups are attached to each phosphorus atom.[23] Polyphosphazenes with carboxylatophenoxy side groups were synthesized and their gelation behaviour was studied. These polymers were insoluble in neutral or acidic water, but dissolved in basic solutions. Upon addition of calcium ions rapid gelation occurred, via the formation of salt bridges between carboxylic acid groups of neighbouring polymers. These gels dissolved when calcium was replaced by monovalent ions.[24] Polyphosphazenes hydrogels are also temperature sensitive and therefore studied to be applied as responsive membranes.[23]

As already mentioned, purely physically cross-linked hydrogels have a few disadvantages, as they are usually weak and can lose their mechanical integrity over time.[25] Furthermore, studies on alginate showed that calcium cross-linking can give rise to non-uniform hydrogel structures.[26] Therefore, chemical cross-linking procedures have also been applied to the abovementioned carbohydrates. In case of chitosan, cross-linking agents such as glutaraldehyde and genipin were added to make bridges between the polymeric chains. Chemical cross-linking of chitosan using genipin occurred via a heterocyclic linkage and the formation of amide bonds.[8,27] In case of alginate, the polymers were modified to be able to use a chemical cross-linking procedure for hydrogel formation and to gain control over the mechanical properties. Alginate polymers were functionalized with tetrazine or norbornene groups, which can react together in a Diels-Alder cycloaddition reaction. The covalently cross-linked hydrogels were used for the encapsulation of NIH 3T3 cells, which could easily be performed with high cell viability. Furthermore, RGDS functionalized thiol-containing peptides were linked to the norbornene groups. This made the alginate gels cell-adhesive, as was shown by 2D and 3D cell culture studies.[28] For the polyphosphazenes, cross-linking was improved by making use of polymers with carboxylate functional substituents. These polymers were chemically cross-linked by ^{60}Co gamma radiation, to generate stable, pH sensitive hydrogels. In basic solutions, a higher swelling ratio was reported than in acidic solutions, which also led to faster release of an encapsulated fluorescent dye.[29] In a later study, it was found that the cross-linking between metal ions and the carboxylic acid side chains can be controlled by redox reactions.[30]

In most cases, only purely physical or purely chemical cross-linking methods have been applied to the carbohydrates. However, an interesting alternative is to combine the properties of both physically and chemically cross-linked hydrogels by making use of a dual cross-linking system. A recent study by the Alsberg group demonstrated this by using both ionic and photo cross-linking. Methacrylated alginate was first ionically cross-linked using calcium. The remaining carboxylic acid groups were then used for photo cross-linking using UV light. Hydrogels prepared via this dual cross-linking method showed increased stiffness and decreased swelling compared to single

cross-linking using one of the methods.[31] In another study, a two-step cross-linking protocol was performed with hyaluronic acid hydrogels. In the first step, a Michael-type reaction between a part of the acrylate groups and proteolytically degradable peptides was carried out. In the second step, the remaining acrylate groups were used for a free radical polymerisation using UV light. Rheology studies showed increased mechanical properties for hydrogels that were dually cross-linked. These gels were used for 3-D cell culturing, in which protease-mediated cellular remodelling was prevented when gels were also cross-linked by UV-light.[32]

In this chapter, we aim for developing a novel dual cross-linking procedure, by combining very efficient physical and chemical cross-linking methods. By making use of two complementary techniques for network formation, advanced hydrogels can be prepared, with improved mechanical properties. As chemical cross-linking method the SPOCQ conjugation reaction, as reported in **Chapter 4**, was employed.[33] This method was first optimized with respect to hydrogel formation capacity (**Paragraph 6.2.1** and **6.2.2**). Importantly, the biocompatibility of SPOCQ cross-linking was studied by employing cell adhesion studies, in order to test the potential of these gels for biomedical applications (**Paragraph 6.2.3**). As physical cross-linking method, we aimed for using ionic interactions with calcium ions. In **Chapter 2** of this thesis, these interactions were already studied by making use of polymers functionalized with Ca^{2+}-binding peptides, however, with limited success. Therefore, we first studied physical cross-linked hydrogels, by using the strong interaction between bisphosphonate alendronic acid and Ca^{2+} (**Paragraph 6.3**) After studying both cross-linking methods separately, we combined them and studied dual cross-linked hydrogels (**Paragraph 6.4**). Finally, we investigated the possibility to make stimuli responsive hydrogels, by addition of thermally triggerable calcium-containing liposomes to alendronic acid functionalized polymers (**Paragraph 6.5**).

6.2. Further research on SPOCQ cross-linked hydrogels

6.2.1. 8-armed SPOCQ cross-linked hydrogels

As described in **Chapter 4**, we developed the strain-promoted-oxidation-controlled cyclooctyne-1,2-quinone cycloaddition (SPOCQ) reaction as a fast and activatable cross-linking method for hydrogel formation. We showed that reaction of cycloctyne-functionalized PEG (star-PEG-BCN) and catechol-functionalized PEG (star-PEG-DHPA) yields hydrogels after oxidation by either sodium periodate or enzyme mushroom tyrosinase.[33] These studies were all carried out with 4-armed PEG (star-PEG), whereby each polymer thus contains 4 functional groups. We now extended this research by studying the gelation of 8-armed PEG constructs. In this way, we can obtain more insight in the mechanical properties of the hydrogels, by investigating the influence of the type of polymer on gel strength. This 8-armed poly(ethylene) glycol contains a tripentaerythritol core, as depicted in **Figure 6.1**.

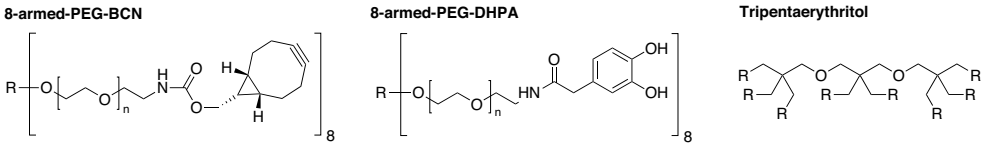

Figure 6.1. Structures of 8-armed-PEG-BCN and 8-armed-PEG-DHPA, with the tripentaerylthritol core (right).

Polymer 8-armed-PEG-NH_2 (M_n = 20000 Da) was first functionalized with cyclooctyne derivative bicyclo[6.1.0]non-4-yne (BCN) and with catechol 3,4-dihydroxyphenylacetic acid (DHPA) to obtain 8-armed-PEG-BCN and 8-armed-PEG-DHPA, respectively (**Figure 6.1**). We performed gelation studies at the same polymer concentrations (10, 20 and 30 mg/mL) as previously performed for the star-PEG (4-armed) constructs (**Chapter 4**). Oxidation of a mixture of 8-armed-PEG-BCN and 8-armed-PEG-DHPA with sodium periodate immediately resulted in hydrogel formation (**Figure 6.2**). Rheological analysis showed higher moduli than for the 4-armed-PEG-constructs, at the same polymer concentrations. In fact, the values for the elastic modulus G' were almost a factor 2 higher for 8-armed PEG, compared to 4-armed-PEG based hydrogels. By doubling the number of functional groups per polymer, the number of branching points is also twice as high. This gives rise to a denser polymeric network, which nicely corresponds with the rheological analysis (**Figure 6.2** and **Table 6.1**). This data shows that the strength of SPOCQ cross-linked gels can, apart from changing the polymer concentration, also be tuned using 8-armed PEG polymers. In view of time, we did not continue with these 8-armed gels, but use of these branched polymers can be valuable in further studies where control over the mechanical properties of hydrogels is demanded.

Table 6.1. Comparison of G' (Pa) values for 4-armed and 8-armed PEG hydrogels, oxidized by sodium periodate. Values were recorded on the rheometer during 5 min (4-armed: n = 5; 8-armed: n = 3)

	10 mg/mL	**20 mg/mL**	**30 mg/mL**
4-armed PEG	65 Pa ± 10	454 Pa ± 19	1375 Pa ± 21
8-armed PEG	104 Pa ± 3	834 Pa ± 30	2197 Pa ± 133

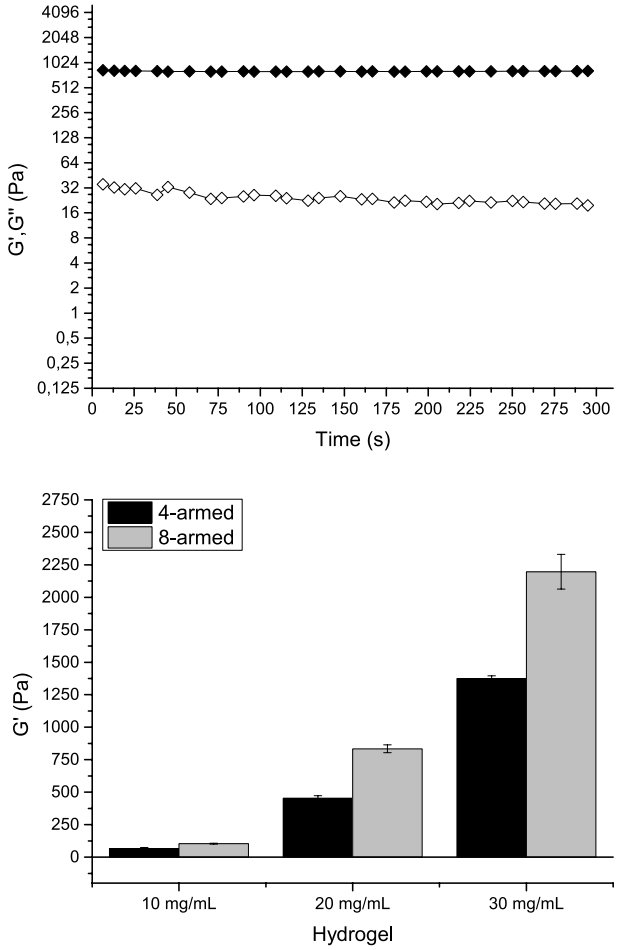

Figure 6.2. Rheological analysis of 8-armed SPOCQ cross-linked hydrogels oxidized by $NaIO_4$. Top: representative time sweep measurement of a 20 mg/mL hydrogel showing G' (closed symbols) and G'' values (open symbols). Bottom: G' values compared with 4-armed SPOCQ cross-linked hydrogels for 10, 20 and 30 mg/mL.

6.2.2. Vitamin B2 oxidation of the SPOCQ reaction

In order to be able to use SPOCQ cross-linked hydrogels in biomedical applications, it is important to investigate the biocompatibility of these gels. We therefore envision performing cell adhesion studies. As outlined before, the SPOCQ reaction was performed with oxidizing agents sodium periodate and mushroom tyrosinase. The toxicity of these reagents towards cells will be investigated, but before commencing these studies, we first focused on another possibility to perform oxidation. A biocompatible photo-oxidation of dopamine was reported using vitamin B2 (Riboflavin). Vitamin B2 photo-decomposes upon visible light or UV light,

leading to the formation of reactive oxygen species. The interaction of dopamine with vitamin B2 and the formed oxygen species cause oxidation of the catechol to the quinone.[34] The potential of vitamin B2 as biocompatible oxidizing agent for the SPOCQ reaction was studied. First, a solution of star-PEG-BCN, star-PEG-DHPA (4-armed) and vitamin B2 was illuminated with UV-light using a lamp with a wavelength range of 320 – 450 nm. The viscosity of the polymer solution increased after illumination for 45 minutes. Eventually, the formation of a soft hydrogel was observed. However, due to the long illumination time required and the heat generated by the lamp, a large part of the water was evaporated. In order to improve the photo-oxidation process, a high power UV-lamp was utilized. In this way, only a short exposure of the sample was required. Nevertheless, due to the small sample volume and the power of the lamp, still most of the water was evaporated, resulting in a polymer film. To use a more benign irradiation source, we used visible light by simply placing a vial containing star-PEG-BCN, star-PEG-DHPA and vitamin B2 in the windowsill. After 3 hours, the complete sample volume was converted to a hydrogel, with no evaporation taking place. In order to determine the mechanical properties of these photo-oxidized gels, gels were made in a mold and allowed to cross-link with visible light for one day. Rheological analysis confirmed the formation of a hydrogel as G' values exceeded G'' values. The photo-oxidized gels were very soft, as G' values of 96 Pa were obtained (**Figure 6.3**). These first gelation tests were performed with a polymer concentration of 50 mg/mL and with 0.5 eq vitamin B2 per DHPA group. Since the oxidation reaction depends on the interaction with vitamin B2, as well as on the generation of reactive oxygen species, the optimal amount of vitamin B2 was not exactly known. We therefore prepared samples with 0.25 eq, 0.5 eq and 1 eq vitamin B2 per DHPA group. We also changed the total polymer content to the previously used amount of 20 mg/mL in order to determine if the applied conditions still resulted in hydrogel formation. Rheology studies with these vitamin B2 ratios and polymers star-PEG-BCN and star-PEG-DHPA (20 mg/mL) showed only small differences in the moduli of the gels (**Figure 6.3**). As the ratio of vitamin B2 does not seem to influence the mechanical properties, we decided to continue with 0.5 eq vitamin B2, as this amount was also readily soluble. Since we aimed to investigate the biocompatibility of the SPOCQ reaction, we will use the established gelation procedure with vitamin B2 in cell adhesion studies (see **Paragraph 6.2.3**). In conclusion, vitamin B2 can be used as an oxidizing agent in the SPOCQ reaction by making use of illumination with visible light. The resulting hydrogels had poor mechanical properties. Based on this, and based on the lengthy illumination time, we conclude that the vitamin B2 oxidization process is not ideal. Optimization of this method can be achieved by using a UV-lamp with a more suitable wavelength, for example a blue LED lamp of 467 nm. Moreover, the addition of superoxide dismutase to the reaction mixture is recommended. This compound increases the production of reactive oxygen species and thereby enhances the reaction rate of the photo-oxidation. [34]

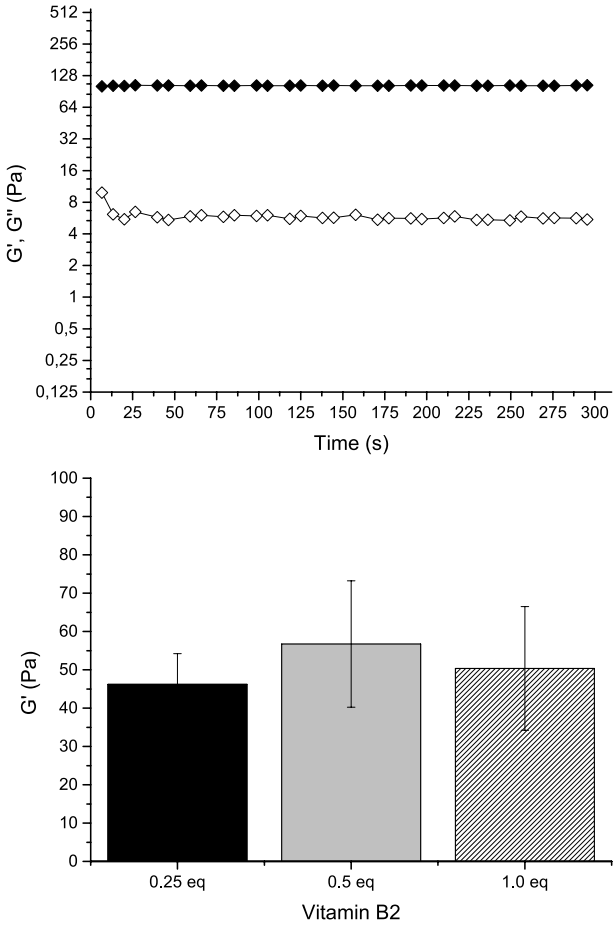

Figure 6.3. Rheological analysis of vitamin B2 oxidized hydrogels after exposure to visible light (24h). Top: representative time sweep measurement of a 50 mg/mL gel with 0.5 eq vitamin B2. Weak gels were obtained, as seen for the G' value of 96 Pa ± 22 (n = 3). Bottom: Comparison of 20 mg/mL hydrogels with 0.25, 0.5 and 1 eq vitamin B2 (per DHPA group) showing minimal differences in moduli.

6.2.3. Cell adhesion studies with SPOCQ cross-linked hydrogels

The biocompatibility of SPOCQ cross-linked hydrogels was investigated, by performing cell adhesion studies. Gels were prepared with all three oxidizers, in order to determine the toxicity of these reagents. In accordance with the cell adhesion studies performed for the SPAAC cross-linked gels (**Chapter 3**), cell adhesion motif RGDS was incorporated in the SPOCQ polymers. Peptide RGDS was synthesized using solid phase peptide synthesis and N-terminally functionalized with 3,4-dihydroxyphenylacetic acid (DHPA). The previously developed coupling strategy using BOP and D*i*PEA was applied, to afford polymer star-PEG-RGDS-DHPA. As expected, rapid gelation also occurred when this peptide-containing polymer was used in the

SPOCQ reaction with star-PEG-BCN. Three different oxidizing agents were now available to test in cell adhesion studies. A cell adhesion test was performed with RGDS-containing SPOCQ gels, oxidized via mushroom tyrosinase. This test showed that the use of the enzyme induced toxicity, as only cell parts or cells with a round morphology were found (data not shown). This behaviour was known from literature studies which indicated that mushroom tyrosinase triggers apoptosis.[35,36] We therefore decided to focus on sodium periodate and vitamin B2 as oxidizing agents for cell adhesion studies. Based on the research in **Chapter 3**, we started with an RGDS content of 50%. Hydrogels were prepared in a total polymer content of 20 mg/mL with 1 eq sodium periodate or 0.5 eq vitamin B2 (per DHPA group) for oxidation. All gels were left for one day to allow sufficient exposure of the vitamin cross-linked ones to visible light. After gel formation had been confirmed, the hydrogels were washed for 4 hours with PBS. Cell adhesion studies were carried out with NIH 3T3 fibroblasts, which were seeded onto the hydrogels and then incubated overnight. Cell viability was assessed by performing a live/dead assay. As expected, cells seeded on gels without adhesion motif RGDS gave red (or orange) fluorescent signals and showed a round morphology in their transmission images (**Figure 6.4**).

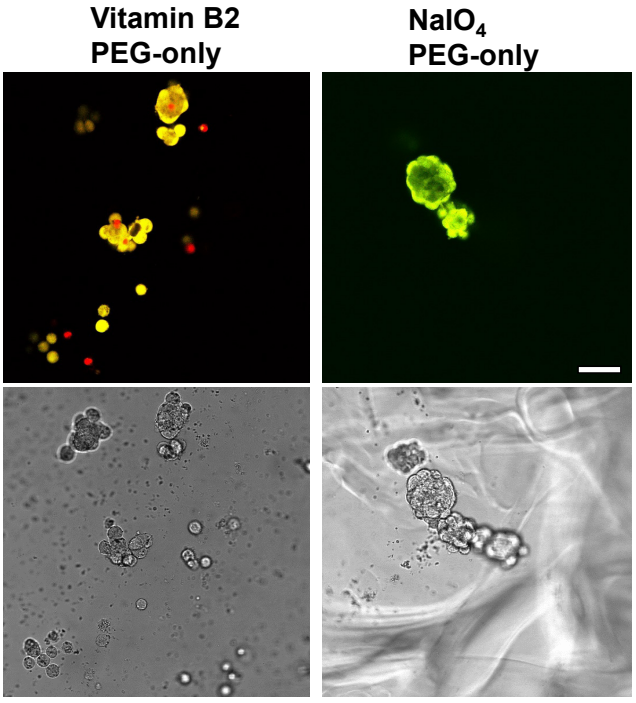

Figure 6.4. Cell viability images for the live/dead assay on 20 mg/mL SPOCQ cross-linked hydrogels. Images are composed from overlays of the calcein-AM (green, live cells) and ethidium homodimer-1 (EthD-1, red cells) channels. Gels without cell adhesion motif RGDS yielded red (or orange) fluorescent cells with a round morphology. Upper picture: confocal fluorescence, lower picture: transmission image. Scale bar represents 50 μm for all micrographs.

Incorporation of RGDS turned the SPOCQ cross-linked hydrogels into a good substrate for cellular adhesion. For both $NaIO_4$ and vitamin B2, a large number of green fluorescent cells were found which nicely showed their elongated morphology. For vitamin B2, the live/dead assay was also performed with gels containing 100% RGDS, also revealing nicely elongated fibroblasts (**Figure 6.5**). These cell studies confirmed that SPOCQ cross-linking can be used for the preparation of cell adherent hydrogels, and that both $NaIO_4$ and vitamin B2 are suitable oxidizing agents to provide biocompatible gels.

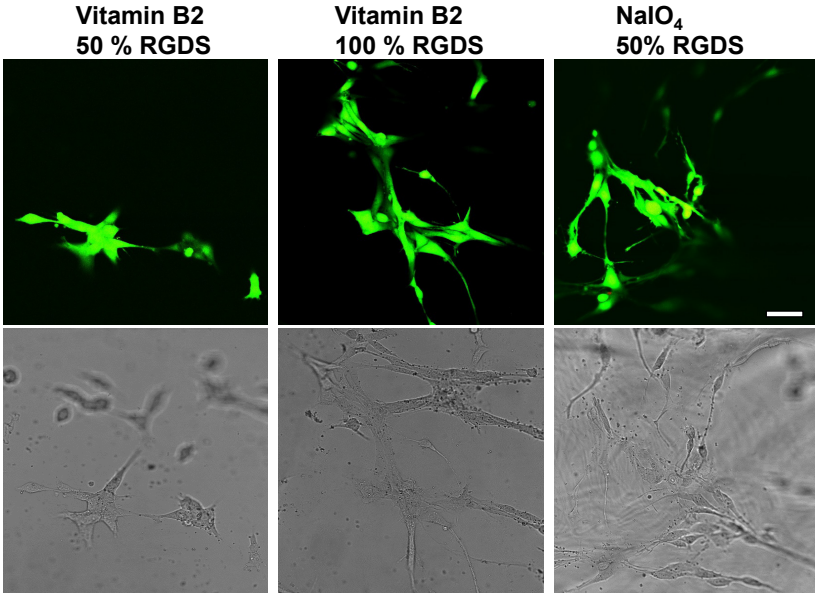

Figure 6.5. Cell viability images for the live/dead assay on 20 mg/mL SPOCQ cross-linked and RGDS-containing hydrogels, showing nicely elongated viable fibroblasts (green fluorescent). Images are composed from overlays of the calcein-AM and EthD-1 channels. Upper picture: confocal fluorescence, lower picture: transmission image. Left and middle: vitamin B2 as oxidizing agent, gels containing 50 and 100% RGDS, respectively. Right: sodium periodate as oxidizing agent, gel containing 50% RGDS. Scale bar represents 50 μm for all micrographs.

6.3. Physical cross-linking using Ca^{2+}

Now that we further studied the mechanical properties of SPOCQ cross-linked hydrogels and showed their biocompatibility, we investigated the second, physical, cross-linking technique that we want to apply in our dual cross-linked hydrogel, based on ionic interactions with calcium ions. In **Chapter 2**, the hydrogel formation of peptide-polymer constructs containing calcium-binding peptides was already studied. It was shown that addition of calcium did not result in gelation, probably because Ca^{2+}-binding to the peptides was too weak to make physical cross-links

between the polymers. In this chapter, we set out to further investigate physically cross-linked hydrogels with calcium. Bisphosphonates were identified as a particularly interesting class of Ca^{2+} binding small molecules. They contain two phosphate groups connected to the same carbon which induces the ability to coordinate divalent ions. Calcium binding occurs by coordination of the ion with one oxygen from each phosphate group. An important bisphosphonate is alendronic acid, in which the central carbon contains, apart from the two phosphates, also a hydroxyl group. This increases the calcium binding efficiency by formation of a tridentate conformation. Bisphosphonates are successfully used in the treatment of bone disorders such as osteoporosis, due to their high affinity towards bone mineral hydroxyapatite.[37-39]

It was shown that alendronic acid can be built in in a polymeric hydrogel network. Alendronic acid was functionalized with a vinyl group, which was used for reaction with 2-hydroxy methacrylate (HEMA). Upon gamma irradiation, a hydrogel was formed, containing alendronic acid as functional group.[40] Recently, a hydrogel system was prepared in which acrylated alendronic acid was reacted with poly(ethylene)glycol diacrylate. Upon addition of initiators, cross-linking was induced which resulted in hydrogel formation. In this research, swelling studies were conducted in which the monovalent NaCl was compared to the divalent $CaCl_2$. Upon soaking in the salt solutions, all gels shrank, but only the samples with NaCl were able to retain their initial size upon rinsing with MilliQ water. Furthermore, it was demonstrated that hydrogels containing calcium as reversible cross-linkers could be secured in a certain shape, which showed the relatively strong coordination between alendronic acid and calcium.[41]

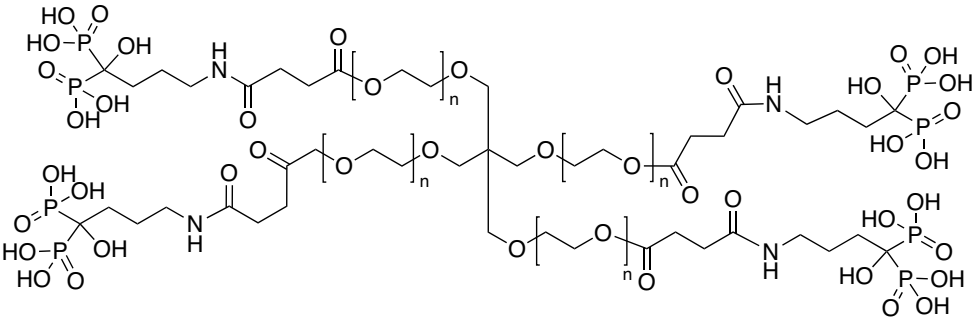

Figure 6.6. Structure of star-PEG-alendronic acid

The strong binding properties of alendronic acid towards calcium inspired us to use this bisphosphonate as a replacement for the calcium-binding peptides described in **Chapter 2**. We therefore synthesized polymer star-PEG-alendronic acid (**Figures 6.6** and **6.7**). For the preparation of this compound, a star-PEG construct was used in which each arm was functionalized with N-hydroxy succinimidyl ester (NHS). Coupling of alendronic acid to star-

PEG-NHS needed to be carried out under basic conditions, since this allows alendronic acid to dissolve. Attempts to perform the synthesis in basic water (by addition of NaOH, pH 10) or in normal PBS buffer (pH 7.4) were not successful. In both cases, the obtained products appeared to be insoluble in water, which is unlike what was expected for star-PEG-alendronic acid. Moreover, NMR and MALDI-TOF analysis did not confirm conversion to the product. As the reaction is likely to be pH sensitive due to the ionic character, we decided to use a stronger buffer and prepared PBS containing 100 mM phosphate. Alendronic acid was dissolved in this buffer, the pH was brought to 7.4 and star-PEG-NHS was added. After purification, the product could easily be dissolved in water. NMR and MALDI-TOF analysis confirmed the successful synthesis of star-PEG-alendronic acid.

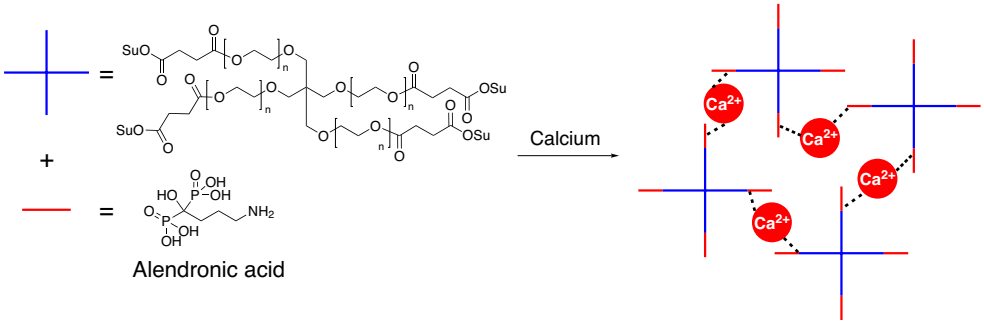

Figure 6.7. Physical cross-linking upon calcium addition using star-PEG polymers functionalized with bisphosphonate alendronic acid.

We next investigated the gelation of star-PEG-alendronic acid upon addition of calcium (**Figure 6.7**). A polymer concentration of 50 mg/mL (5 wt%) was first tested with 100 mM $CaCl_2$ which nicely and rapidly formed a hydrogel. A polymer content of 30 mg/mL (3 wt%) appeared to be the minimum concentration for gelation, as only viscous solutions were obtained at lower polymer concentrations. Rheology studies were carried out on a range of hydrogels formed from star-PEG-alendronic acid (30 – 100 mg/mL) and $CaCl_2$ (100 mM) (**Figure 6.8**). As expected, G' values increased with increasing polymer content. Moduli up to 8000 Pa were obtained for 100 mg/mL (10 wt%) star-PEG-alendronic acid gels.

A well-known advantage of physically cross-linked gels is their self-healing behaviour. We demonstrated this by cutting a hydrogel into two pieces. After only 5 min, these pieces fused together in such a way that the crack could not be detected anymore. This simple test showed the self-healing behaviour of the star-PEG-alendronic acid gels. Moreover, we could easily demonstrate the reversibility of the cross-linking method by addition of the strong calcium binder EDTA. This caused disassembly of the hydrogel network, as calcium binding to EDTA disrupts the ionic bridges between adjacent polymer chains.

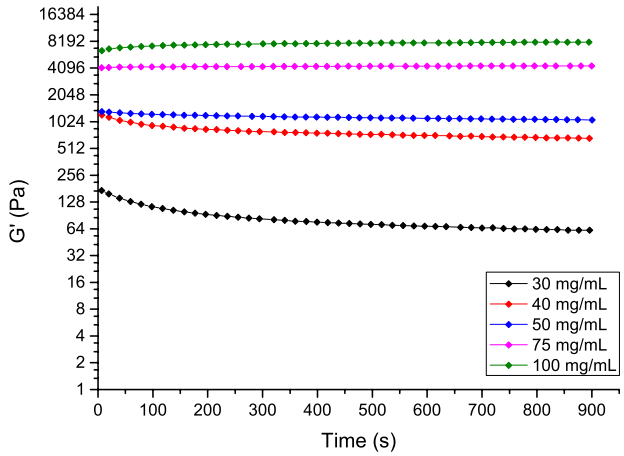

Figure 6.8. Rheology data of calcium cross-linked gels using star-PEG-alendronic acid in concentrations of 30,40, 50, 75 and 100 mg/mL. Moduli up to 8000 Pa were obtained for 100 mg/mL physically cross-linked gels.

6.4. Dual cross-linking: SPOCQ and Ca^{2+}

We next set out to combine both chemical and physical cross-linking techniques, in order to overcome the disadvantages of each of the separate methods. Especially the weak mechanical properties often encountered with purely physically cross-linked gels can be improved when a second (chemical) cross-linking procedure is incorporated.

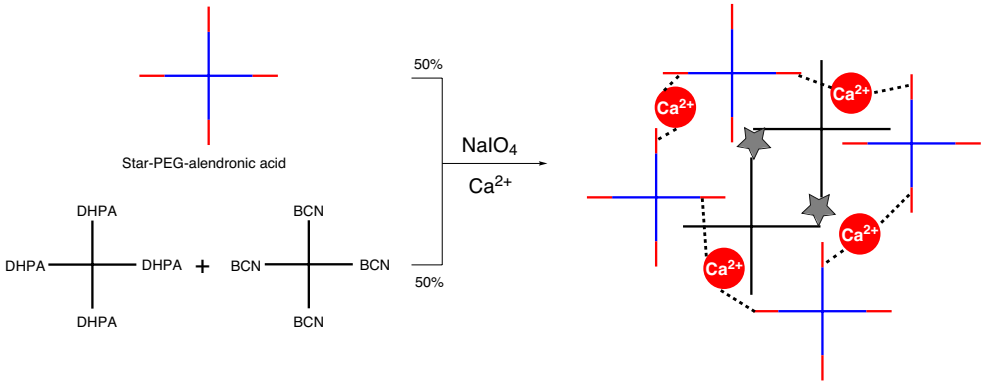

Figure 6.9. Schematic overview of dual cross-linked hydrogels. Star-PEG-BCN and star-PEG-DHPA are chemically cross-linked upon oxidation by $NaIO_4$ (represented by stars). Star-PEG-alendronic acid polymers are physically cross-linked by Ca^{2+}. Star-PEG-alendronic acid makes up 50% of the total polymer content, the other half is a mixture of star-PEG-BCN/star-PEG-DHPA (1:1).

In order to combine the chemical cross-linking method SPOCQ with the physical cross-linking procedure using calcium (**Figure 6.9**), we mixed polymers star-PEG-BCN and star-PEG-DHPA with star-PEG-alendronic acid. The first two can be chemically cross-linked using SPOCQ, while star-PEG-alendronic acid is able to make physical cross-links with calcium. Mixed gels were prepared with a total concentration of 60 mg/mL (6 wt%), in which half of the total polymer content was star-PEG-alendronic acid (30 mg/mL) and the other half was composed of a 1:1 mixture of star-PEG-BCN and star-PEG-DHPA (30 mg/mL). Oxidizing agent sodium periodate ($NaIO_4$) was added to the aqueous solution of these three polymers, to allow chemical cross-linking using SPOCQ. As expected, a hydrogel was rapidly formed. G' values of these single cross-linked hydrogels were lower than values reported before for 30 mg/mL SPOCQ cross-linked gels (**Chapter 4, Table 6.1**). This is probably caused by steric hindrance due to the presence of star-PEG alendronic acid polymers. This hypothesis was tested by addition of non-functionalized star-PEG to a mixture of star-PEG-BCN and star-PEG-DHPA. This gave comparable G' values as when star-PEG-alendronic acid was used, showing that steric hindrance indeed is a limiting factor. In order to allow dual cross-linking, a mixture of $NaIO_4$ and $CaCl_2$ was added to the solution of the three polymers. Also in this case, rapid gel formation occurred. Gels were prepared on the rheometer plate, to enable direct analysis of the mechanical properties. Gels directly obtained their final moduli. G' values of the dual cross-linked hydrogel were much higher than for gels only cross-linked by $NaIO_4$ (**Figure 6.10**). These results clearly showed that the chemically cross-linked network was strengthened by the calcium-induced ionic bridges. Single and dual cross-linking was also performed on hydrogels with a total polymer content of 80 and 100 mg/mL (8 and 10 wt%). Also in this case, dual cross-linked hydrogels were much stiffer than gels only cross-linked by sodium periodate (**Figure 6.10; Table 6.2**). As expected, moduli were higher than for the 60 mg/mL gels, due to the higher polymer concentration in these gels. These experiments show that a mixture of star-PEG-BCN, star-PEG-DHPA and star-PEG-alendronic acid can be chemically cross-linked using SPOCQ and at the same time physically using calcium binding. Hydrogels prepared via this dual cross-linking method showed improved mechanical properties, compared to gels that were only chemically cross-linked.

Table 6.2. G' values of single ($NaIO_4$) and dual cross-linked ($NaIO_4$ and Ca^{2+}) hydrogels. Values were recorded on the rheometer during 5 min (n = 3).

Hydrogel	60 mg/mL	80 mg/mL	100 mg/mL
$NaIO_4$	72 ± 13	126 ± 18	256 ± 17
$NaIO_4$ + Ca^{2+}	688 ± 58	1138 ± 107	1969 ± 302

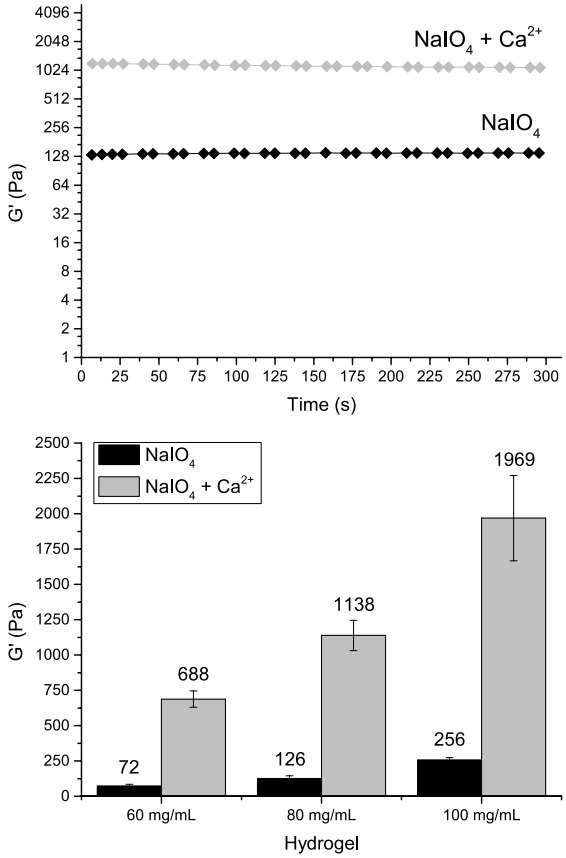

Figure 6.10. Rheology data of mixed hydrogels containing star-PEG-BCN, star-PEG-DHPA and star-PEG-alendronic acid. For single (chemical) cross-linking $NaIO_4$ was added, for dual (chemical and physical) cross-linking a mixture of $NaIO_4$ and Ca^{2+} was added. Top: representative time sweep of an 80 mg/mL hydrogel. Bottom: overview of G' values. Dual cross-linking gave much stiffer hydrogels than single cross-linking.

6.5. Stimuli responsive hydrogels using calcium-releasing liposomes

In order to control the physical gelation of star-PEG-alendronic acid, we investigated the possibilities to time the release of calcium. The Messersmith group studied calcium-containing thermally triggerable liposomes, which released the entrapped calcium upon an increase in temperature to 37°C.[42,43] We decided to adopt the procedure to prepare calcium-releasing liposomes and use them for gelation of star-PEG-alendronic acid. Liposomes were composed of phospholipids dipalmitoylphosphatidylcholine (DPPC) and dimyristoylphosphatidylcholine (DMPC) in a molar ratio of 90:10. A lipid cake of these phospholipids was first prepared, to which an aqueous solution of $CaCl_2$ was added. Encapsulation of the calcium was achieved by

sonication at 55°C. After removal of unencapsulated calcium via some centrifugation steps, calcium-containing liposomes were obtained.[42,43] The liposomes were added to a solution of star-PEG-alendronic acid (60 mg/mL). The sample was kept at room temperature (20°C) and remained liquid. Next, the liposome/star-PEG-alendronic acid mixture was heated to 37°C, which resulted in rapid gelation. The elevated temperature thus provided release of the entrapped calcium, leading to physical cross-linking of star-PEG-alendronic acid. The release profile of the calcium-loaded liposomes was determined with UV spectroscopy, using calcium-sensitive dye Arsenazo III. This clearly showed that the entrapped calcium is released around body temperature, as absorbance values rapidly increased upon reaching temperatures of 35°C and higher (**Figure 6.11**). The use of triggerable liposomes provided an on demand release of calcium and resulted in the preparation of stimuli-responsive hydrogels.

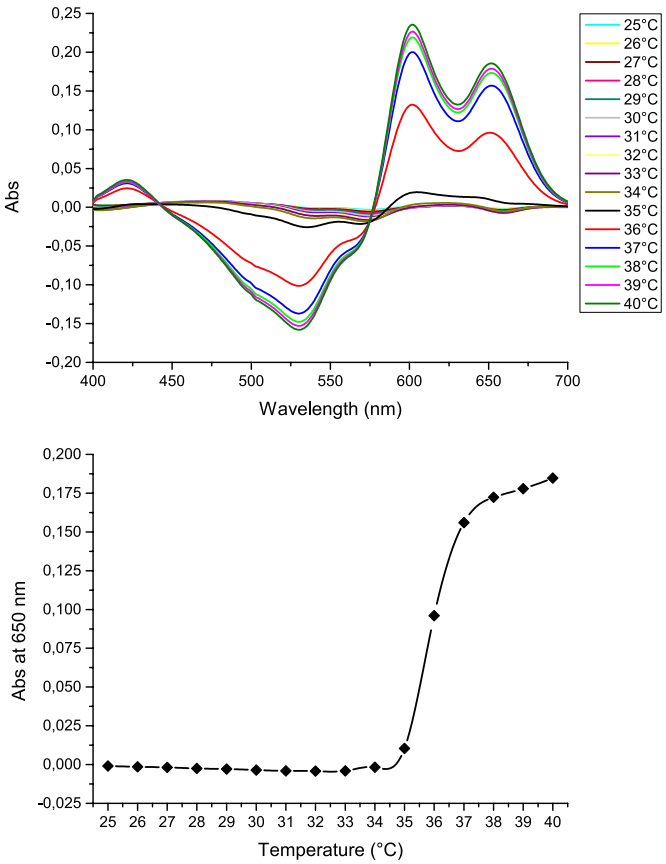

Figure 6.11. Release profile of calcium-loaded liposomes, determined via UV spectroscopy. Top: absorbance values of calcium-sensitive dye Arsenazo III. Bottom: absorbance values at 650 nm plotted against temperature, showing that release of calcium starts at 35°C and is close to its maximum value at 37°C.

6.6. Conclusion

In this chapter, dual cross-linked hydrogels were studied by combining chemical and physical cross-linking. First, the hydrogel forming capacity of chemical cross-linking method SPOCQ was further studied. We showed that 8-armed PEG constructs can also be cross-linked, leading to elastic moduli (G') which were almost a factor 2 higher than 4-armed hydrogels. Apart from sodium periodate and enzyme mushroom tyrosinase, we showed that vitamin B2 can be used as an oxidizing agent in the SPOCQ reaction. The biocompatibility of SPOCQ cross-linked hydrogels was shown by performing cell adhesion studies. RGDS-containing gels oxidized with $NaIO_4$ or with vitamin B2 were found to be good substrates for cell adhesion, giving viable and nicely elongated NIH 3T3 fibroblasts. Secondly, physical cross-linking was studied, by using the ionic interaction of calcium ions. Gelation of bisphosphonate containing polymer star-PEG-alendronic acid occurred rapidly upon addition of calcium, resulting in moduli up to 8000 Pa for 100 mg/mL (10 wt%) gels. Dual cross-linking was achieved by combining physical cross-linking (calcium) with chemical cross-linking (SPOCQ), leading to enhanced mechanical properties than for only chemically cross-linked gels. Finally, the physical cross-linked hydrogels were made stimuli responsive, by addition of thermally triggerable Ca^{2+}-containing liposomes. This is promising for biomedical applications such as bone tissue engineering where a controlled release of calcium is demanded.

As an outlook on further research concerning the research performed in this chapter, a good starting point will be to first optimize the SPOCQ oxidation protocol using vitamin B2. Next, the mechanical properties of the dual cross-linked gels can be further studied, for example by constructing a hybrid polymer, containing two different functional groups (DHPA/BCN and alendronic acid). In this way, one polymer can participate both in chemical cross-linking as well as in physical cross-linking. Thereby a more intricate network will be created, which likely will result in hydrogels with improved mechanical properties. Cell studies are interesting with the dual cross-linked gels, whereby the optimized vitamin B2 oxidization procedure can also be examined. These *in vitro* studies are also interesting for the physically cross-linked gels with star-PEG-alendronic acid, especially when using bone-marrow cells (see **Chapter 7**). Moreover, after studying the mechanical properties of the stimuli-responsive hydrogels, use of the triggerable liposomes will be a valuable addition for further *in vitro* studies with star-PEG alendronic acid hydrogels.

6.7. Acknowledgements

Imke Pijpers is gratefully acknowledged for performing many experiments described in this chapter, as well as for useful discussions. Sander Leeuwenburgh is thanked for introducing alendronic acid, and his expertise on this calcium-binding motif. Paula Lopez Perez is acknowledged for fruitful discussions on physically cross-linked hydrogels.

6.8. Materials and methods

General notes experimental section

Materials and methods and standard solid phase peptide synthesis (SPPS) can be found in **Chapter 2**. The preparation of polymers star-PEG-BCN and star-PEG-DHPA is described in **Chapter 4**. General information on rheology can be found in **Chapter 3**.

Materials and methods

8-Armed poly(ethylene glycol)-NH_2 (20 kDa) HCl salt, with a tripentaerythritol core, was obtained from JenKem Technology (USA). 4-armed PEG-NHS (N-hydroxy succinimidyl ester; 10 kDa) was purchased from NOF America Corporation (Sunbright; USA). Phospholipids 1,2-dipalmitoyl-sn-glycero-3-phosphocholine (DPPC) and 1,2-dimyristoyl-sn-glycero-3-phosphocholine (DMPC) were obtained from Avanti Polar Lipids, Inc. (USA). Arsenazo III was purchased from Sigma-Aldrich. For UV illumination, a Dr Hönle, Bluepoint 2 UV-lamp was used with a wavelength range of 320 – 450 nm (maximum 365 nm). Unless mentioned otherwise, a 1× PBS buffer (pH 7.4) was utilized containing 137 mM NaCl, 2.7 mM KCl, 10 mM Na_2HPO_4 and 1.8 mM KH_2PO_4.

8-armed-PEG-BCN

To a dry reaction flask was added 8-armed poly(ethylene glycol)-NH_2 HCl salt (M = 20000 Da, 400 mg, 20 µmol), (1*R*,8*S*,9*S*)-bicyclo[6.1.0]non-4-yn-9-ylmethyl succinimidyl carbonate (BCN-OSu; 58.3 mg, 0.2 mmol) and 67 µL triethylamine (0.48 mmol) in dry DCM (10 mL). The reaction mixture was stirred at r.t. overnight under N_2 atmosphere. Extraction was performed with 2M NaOH (3 × 15 mL). The organic layer was dried over Na_2SO_4 and concentrated in vacuo. The residue was purified by column chromatography on silica gel (MeOH:DCM 2:98, followed by 10:90). The product was afforded as a white powder after freeze-drying from dioxane (113 mg, 26%). ^{1}H-NMR (400 MHz, $CDCl_3$): δ = 0.86 – 1.01 (m, 8H), 1.29 – 1.45 (m, 16H), 1.52 – 1.65 (m, 16H), 2.15 – 2.34 (m, 32H), 3.37 (m, 32H), 3.45 – 3.91 (m, $[CH_2CH_2O]_n$), 4.14 (d, J = 8.0 Hz, 16H).

8-armed-PEG-DHPA

To 8-armed-poly(ethylene glycol)-NH_2 HCl salt (M = 20000 Da, 400 mg, 20 µmol) in DMF (10 mL) was added subsequently benzotriazol-1-yl-oxy-tris dimethylaminophosphonium hexafluorophosphate (BOP; 89 mg, 0.2 mmol); 3,4 dihydroxy phenylacetic acid (34 mg, 0.2 mmol), and D*i*PEA (279 µL, 1.6 mmol). The reaction mixture was stirred overnight at r.t., after which the DMF was evaporated in vacuo. The residue was dissolved in DCM and washed with 1 M $KHSO_4$ (3 x 15 mL) and brine (1 x 15 mL). The organic layer was dried over Na_2SO_4. The product was purified with column chromatography on basic aluminum oxide (MeOH: DCM; 10:90). Lyophilization from dioxane afforded the product as a white powder (292 mg, 69%).
^{1}H-NMR (400 MHz, $CDCl_3$, δ): 3.34 – 3.85 (m, $[CH_2CH_2O]_n$, $C\underline{H}_2$-Ar-CH), 6.62 – 6.87 (m, Ar-CH) MALDI-TOF (α-cyano-4-hydroxycinnamic acid): 21465, calculated m/z: 21465 for 446 ethylene glycol units.

DHPA-Gly-Arg(Pbf)-Gly-Asp(OtBu)-Ser(tBu)-Gly-OH

The peptide was synthesized using solid phase peptide synthesis, following the general protocol as described in **Chapter 2**. The synthesis was carried out with 1.0 g 2-chlorotrityl resin. In the final step, 3,4 dihydroxy phenylacetic acid (DHPA) was coupled, by addition of a solution of DHPA (2.0 eq), HOBt (3.5 eq) and triethylamine (3.5 eq) in DMF. After shaking for 3 minutes, a solution of HBTU (2.0 eq) in DMF was added and the coupling was left for 1 h. Cleavage from the resin was performed mildly, by treatment with a mixture of dichloromethane (DCM), trifluoroethanol (TFE) and acetic acid (HOAc) (6:1:1) for 3 h. The solvents were evaporated under reduced pressure and co-evaporation was performed with chloroform (3 x 40 mL). Freeze-drying from dioxane afforded the peptide as a white powder.
LCQ: m/z: 1062.3 $[M + H]^+$ (calculated $[M + H]^+$ = 1062.5)
HPLC: Rt = 22.24 min

DHPA-GRGDSG-Star-PEG (protected)

To star-poly(ethylene glycol)-NH_2 HCl salt (190 mg, 19 µmol) in DMF (10 mL) was added subsequently BOP (51 mg, 114 µmol), peptide DHPA-GRGDSG-OH (101 mg, 95 µmol), and D*i*PEA (79 µL, 0.46 mmol). The reaction mixture was stirred overnight at r.t. Evaporation of the DMF was performed and the residue was dissolved in DCM (30 mL). Extraction was performed with 1 M $KHSO_4$ (3 x 20 mL) and brine (1 x 20 mL), after which the organic layer was dried over Na_2SO_4. Column chromatography on basic aluminum oxide (MeOH: DCM; 10:90) afforded the product as a white powder after freeze-drying from dioxane (177 mg; 66%).
^{1}H-NMR (400 MHz, $CDCl_3$, δ): ^{1}H-NMR (400 MHz, $CDCl_3$): δ = 1.16 (s, 36H), 1.42 (s, 36H), 1.46 (s, 32H), 2.09 (s), 2.46 - 3.00 (m), 3.50 – 3.71 (m, $[CH_2CH_2O]_n$), 4.17 (m), 4.41 (m), 4.65 (m), 6.66 – 6.94 (m, Ar-CH).

DHPA-GRGDSG-Star-PEG

Deprotection of DHPA-GRGDSG-star-PEG (145 mg) was performed by treatment with TFA: TIS: H_2O (95:2.5:2.5; 8 mL) for 3 h at r.t. The reaction mixture was precipitated from diethyl ether. After overnight stirring in 1 M HCl, the product was dialysed against water using a membrane with a MW cut-off of 3500 Da. Freeze drying afforded the product as a white solid (93 mg; 71%)

^{1}H-NMR (400 MHz, D_2O): δ = 1.30 – 1.77 (m), 2.55 – 3.00 (m), 3.39 – 3.63 (m, $[CH_2CH_2O]_n$), 4.13 (m), 4.28 (m), 6.59; 6.69 (2m; Ar-CH).

MALDI-TOF (α-cyano-4-hydroxycinnamic acid): 12401 (calculated m/z: 12411 for 213 ethylene glycol units.

Star-PEG-alendronic acid

Prior to the synthesis a PBS solution containing 100 mM phosphate was freshly prepared by dissolving 9.95 mg KCl (2.67 mM), 403 mg NaCl (137.93 mM), 102 mg KH_2PO_4 (15 mM) and Na_2HPO_4 (85 mm) in 50 mL MilliQ water. The buffer was sonicated for 5 min. Alendronic acid (39.9 mg, 160 µmol) was dissolved in 10 mL PBS (100 mM phosphate) and the solution was brought to a pH of 7.4 with NaOH. Star-PEG-NHS (4-armed, M = 10000 Da; 200 mg, 20 µmol) was added and the reaction mixture was stirred overnight at r.t. The solution was transferred to a dialysis bag and dialyzed overnight against 600 mL water using membranes with a MW cut-off of 3500 Da. The product was afforded after freeze-drying as a white paper-like solid (188 mg; 86%).

^{1}H-NMR (400 MHz, $CDCl_3$, δ): 1.45 – 1.71 (m, NH-$CH_2C\underline{H}_2C\underline{H}_2$-C), 2.40; 2.53 (2t, C(O) $C\underline{H}_2C\underline{H}_2$C(O)), 2.96 – 3.06 (m, NH-$C\underline{H}_2CH_2CH_2$-C), 3.44 – 3.65 (m, $[CH_2CH_2O]_n$).

^{31}P-NMR δ: 35 ppm

MALDI-TOF (α-cyano-4-hydroxycinnamic acid): 11218, calculated m/z: 11210 for 221 ethylene glycol units.

Hydrogel formation – sodium periodate and vitamin B2

Hydrogels were formed by addition of $NaIO_4$ or vitamin B2 to an equimolar mixture of star-PEG-BCN and star-PEG-DHPA. Hydrogels were prepared in total polymer concentrations of 10, 20 and 30 mg/mL (1-3 wt%) in MilliQ. For a typical hydrogel, equal volumes of the polymer mixture and the oxidizing agent were mixed to the final concentration. For the polymer mixture, stock solutions of 20, 40 and 60 mg/mL of star-PEG-BCN and star-PEG-DHPA were first freshly prepared and then mixed in a 1:1 fashion. For $NaIO_4$, a stock solution of 1 eq sodium periodate in MilliQ (based on amount of DHPA groups, 4 eq $NaIO_4$ per star-PEG-DHPA) was prepared. For vitamin B2, a stock solution of 0.5 eq per DHPA group in MilliQ was prepared. Mixtures of the polymers with vitamin B2 were illuminated with visible light by placing them in front of the window for 24 h. The same procedures were used for hydrogel formation with 8-armed-PEG-BCN and 8-armed-PEG-DHPA.

Mixed gels: star-PEG-BCN, star-PEG-DHPA and star-PEG-alendronic acid

Hydrogels were prepared with a total polymer content of 60 mg/mL, 80 mg/mL and 100 mg/mL. For 60 mg/mL gels, a polymer mixture containing 6 mg star-PEG-BCN, 6 mg star-PEG-DHPA and 12 mg star-PEG-alendronic acid in 200 µL PBS was prepared. In the same way, polymer mixtures for 80 mg/mL and 100 mg/mL gels were prepared. A solution of the oxidizing agent was prepared in PBS, containing 1 eq $NaIO_4$ (based on amount of DHPA groups, 4 eq $NaIO_4$ per star-PEG-DHPA). For dual cross-linking, a mixture containing $NaIO_4$ (1 eq per DHPA group) and $CaCl_2$ (200 mM) in PBS was prepared. Hydrogels were prepared directly on the rheometer plate by mixing equal amounts of the polymer mixture (100 µL) and the oxidizing agent solution (100 µL; $NaIO_4$ or $NaIO_4$/$CaCl_2$) to obtain the final concentration (60, 80 or 100 mg/mL; $CaCl_2$: 100 mM). Oscillatory time sweep measurements were measured for 5 min at a constant strain of 1% and an angular frequency of 10 rad/s.

Hydrogel formation: star-PEG-alendronic acid with Ca^{2+}

Hydrogels were prepared with total star-PEG-alendronic acid concentrations of 30, 40, 50, 75 and 100 mg/mL (3, 4, 5, 7.5, 10 wt%). Twice as concentrated stock solutions were used, by dissolving star-PEG-alendronic acid in PBS (containing 100 mM phosphate), for example 6 mg in 100 µL for the 30 mg/mL gel. A 200 mM $CaCl_2$ stock solution was prepared in MilliQ. For each hydrogel, the star-PEG-alendronic acid and calcium stock solutions were mixed in a 1:1 fashion, to obtain the final concentrations (Ca^{2+} for every gel: 100 mM). Gels were prepared directly on the rheometer plate, to measure oscillatory time sweeps for 15 min at a constant strain of 1% and an angular frequency of 10 rad/s.

Live/dead assay

Hydrogel solutions were prepared in a total polymer content of 20 mg/mL, following the general protocol of hydrogel formation. Hydrogels containing 50% RGDS were prepared by mixing star-PEG-RGDS-DHPA and star-PEG-DHPA (1:1), for cross-linking to star-PEG-BCN. Gels were also prepared with 100% star-PEG-RGDS-DHPA. Hydrogels were oxidized by vitamin B2 or by $NaIO_4$ and were prepared in an 8-chambered coverslip (Nunc, Wiesbaden, Germany) in sample volumes of 150 µL for vitamin B2 and 50 µL for periodate. The coverslip containing the mixture with the vitamin B2 oxidizing agent was placed in the windowsill for exposure to visible light for one day. Hydrogels were washed with PBS for 4 hours. In each well, 40.000 cells in 250 µL medium were seeded. Wells coated with gelatin were used as positive control. NIH 3T3 fibroblasts were incubated overnight (37°C, 7.5% CO_2). After this incubation period, the cells were treated with the live/dead staining, which was prepared by diluting calcein-AM and ethidium homodimer-1 (EthD-1) in PBS to obtain a concentration of 1.33 mM calcein-AM and 2.67 mM EthD-1. The samples were allowed to rest for 10 minutes, after which they were immediately analyzed by confocal laser scanning microscopy. Calcein was excited with the 488

nm line of an argon ion laser, and emission was collected between 494 and 515 nm. EthD-1 was excited with the 561 nm line of a yellow diode laser and emission was collected between 600 and 625 nm. Using the ImageJ software, overlay images of the calcein and EthD-1 signals were produced.

Preparation of calcium-releasing liposomes

Liposomes were prepared from phospholipids 1,2-dipalmitoyl-sn-glycero-3-phosphocholine (DPPC) and 1,2-dimyristoyl-sn-glycero-3-phosphocholine (DMPC). A thin film of DPPC: DMPC (90:10 mol%) was prepared by drying a mixture of 9 mg DPPC and 0.92 mg DMPC in dichloromethane. To the lipid cake was added 2 mL $CaCl_2$ (0.2 M). The mixture was then stirred at 55°C for 30 min. Sonication was performed at 55°C, until an optically clear solution was obtained (2 hours). Ethanol was added to a final concentration of 4 M. The solution was left at r.t. for 15 min, after which it was heated to 50°C and bubbled with dry argon to remove the ethanol. To remove unencapsulated calcium, the liposomes were washed with 800 µL iso-osmotic buffered saline (0.2 M NaCl, 10 mM HEPES, 1 mM EDTA, pH 7.4) and centrifuged at 4°C (13000 rpm) for 10 minutes. This washing procedure was performed five times. For each washing step, 125 µL calcium sensitive dye Arsenazo III (500 µM) was added to 125 µL supernatant and the absorbance was determined at 650 nm using a plate reader. The low absorbance values for washing steps 4 and 5 confirmed removal of unencapsulated calcium.

Hydrogel formation star-PEG-alendronic acid and liposomes

To a solution of star-PEG-alendronic acid in PBS (60 mg/mL; PBS containing 100 mM phosphate) was added NaCl, to increase the osmolality to 525 mmol/kg. Three parts of the star-PEG-alendronic acid solution were mixed with one part of liposome material. The temperature was increased to 37°C, using a waterbath.

UV measurements on liposomes

UV spectra were recorded on a Jasco-v630 spectrometer at a wavelength range of 400 – 700 nm. A 0.04 mM Arsenazo III solution was prepared in 0.258 M NaCl. A mixture of 10 µL liposome material in 4 mL Arsenazo III solution was prepared, from which 2.5 mL was loaded in a cuvette. UV spectra were recorded at a temperature gradient of 1 °C/min, with a delay time of 20 seconds before measuring. A temperature range from 25°C to 40°C was utilized. Spectra were corrected by subtracting the background spectrum recorded for the liposome/Arsenazo III mixture at 25°C and were measured in triplo.

6.9. References

(1) Jeong, B.; Kim, S. W.; Bae, Y. H. *Adv. Drug Delivery Rev.* **2002**, *54*, 37-51.
(2) Ruel-Gariépy, E.; Leroux, J.-C. *Eur. J. Pharm. Biopharm.* **2004**, *58*, 409-426.
(3) Srividya, B.; Cardoza, R. M.; Amin, P. D. *J. Control. Release* **2001**, *73*, 205-211.
(4) He, C.; Kim, S. W.; Lee, D. S. *J. Control. Release* **2008**, *127*, 189-207.
(5) Hennink, W. E.; van Nostrum, C. F. *Adv. Drug Delivery Rev.* **2012**, *64*, 223-236.
(6) Hatefi, A.; Amsden, B. *J. Control. Release* **2002**, *80*, 9-28.
(7) Van Tomme, S. R.; Storm, G.; Hennink, W. E. *Int. J. Pharm.* **2008**, *355*, 1-18.
(8) Berger, J.; Reist, M.; Mayer, J. M.; Felt, O.; Peppas, N. A.; Gurny, R. *Eur. J. Pharm. Biopharm.* **2004**, *57*, 19-34.
(9) He, P.; Davis, S. S.; Illum, L. *Int. J. Pharm.* **1998**, *166*, 75-88.
(10) Chenite, A.; Chaput, C.; Wang, D.; Combes, C.; Buschmann, M. D.; Hoemann, C. D.; Leroux, J. C.; Atkinson, B. L.; Binette, F.; Selmani, A. *Biomaterials* **2000**, *21*, 2155-2161.
(11) Brack, H. P.; Tirmizi, S. A.; W. M. Risen, J. *Polymer* **1997**, *38*, 2351-2362.
(12) Pina, S.; Oliveira, J. M.; Reis, R. L. *Adv. Mater.* **2015**, *27*, 1143-1169.
(13) Tønnesen, H. H.; Karlsen, J. *Drug. Dev. Ind. Pharm.* **2002**, *28*, 621-630.
(14) George, M.; Abraham, T. E. *J. Control. Release* **2006**, *114*, 1-14.
(15) Murakami, K.; Aoki, H.; Nakamura, S.; Nakamura, S.-i.; Takikawa, M.; Hanzawa, M.; Kishimoto, S.; Hattori, H.; Tanaka, Y.; Kiyosawa, T.; Sato, Y.; Ishihara, M. *Biomaterials* **2010**, *31*, 83-90.
(16) Balakrishnan, B.; Mohanty, M.; Umashankar, P.; Jayakrishnan, A. *Biomaterials* **2005**, *26*, 6335-6342.
(17) Tan, W. H.; Takeuchi, S. *Adv. Mater.* **2007**, *19*, 2696-2701.
(18) Josef, E.; Zilberman, M.; Bianco-Peled, H. *Acta Biomater.* **2010**, *6*, 4642-4649.
(19) Dai, Y.-N.; Li, P.; Zhang, J.-P.; Wang, A.-Q.; Wei, Q. *Biopharm. Drug Dispos.* **2008**, *29*, 173-184.
(20) Zhao, L.; Weir, M. D.; Xu, H. H. K. *Biomaterials* **2010**, *31*, 6502-6510.
(21) Zhou, H.; Xu, H. H. K. *Biomaterials* **2011**, *32*, 7503-7513.
(22) Kim, W. S.; Mooney, D. J.; Arany, P. R.; Lee, K.; Huebsch, N.; Kim, J. *Tissue Eng. Pt A* **2012**, *18*, 737-743.
(23) Allcock, H. R. *Soft Matter* **2012**, *8*, 7521.
(24) Cohen, S.; Bañó, M. C.; Visscher, K. B.; Chow, M.; Allcock, H. R.; Langer, R. *J. Am. Chem. Soc.* **1990**, 7832-7833.
(25) Shoichet, M. S.; Li, R. H.; White, M. L.; Winn, S. R. *Biotechnol. Bioeng.* **1996**, *50*, 374-381.
(26) Kuo, C. K.; Ma, P. X. *Biomaterials* **2001**, *22*, 511-521.
(27) Mi, F.-L.; Sung, H.-W.; Shyu, S.-S. *J. Polym. Sci. Pol. Chem.* **2000**, *38*, 2804-2814.
(28) Desai, R. M.; Koshy, S. T.; Hilderbrand, S. A.; Mooney, D. J.; Joshi, N. S. *Biomaterials* **2015**, *50*, 30-37.
(29) Allcock, H. R.; Ambrosio, A. M. A. *Biomaterials* **1996**, *17*, 2295-2302.
(30) Fei, S.-T.; Phelps, M. V. B.; Wang, Y.; Barrett, E.; Gandhi, F.; Allcock, H. R. *Soft Matter* **2006**, *2*, 397.
(31) Samorezov, J. E.; Morlock, C. M.; Alsberg, E. *Bioconjugate Chem.* **2015**, *26*, 1339-1347.
(32) Khetan, S.; Burdick, J. A. *Biomaterials* **2010**, *31*, 8228-8234.
(33) Jonker, A. M.; Borrmann, A.; van Eck, E. R. H.; van Delft, F. L.; Löwik, D. W. P. M.; van Hest, J. C. M. *Adv. Mater.* **2015**, *27*, 1235-1240.
(34) Massad, W. A.; Barbieri, Y.; Romero, M.; García, N. A. *Photochem. Photobiol.* **2008**, *84*, 1201-1208.
(35) Frauenfeld, L.; Alzoubi, K.; Abed, M.; Lang, F. *Toxins* **2014**, *6*, 1096-1108.
(36) Russo, G. L.; De Nisco, E.; Fiore, G.; Di Donato, P.; d'Ischia, M.; Palumbo, A. *Biochem. Bioph. Res. Co.* **2003**, *308*, 293-299.

(37) Heymann, D.; Ory, B.; Gouin, F.; Green, J. R.; Rédini, F. *Trends Mol. Med.* **2004**, *10*, 337-343.
(38) Galezowska, J.; Gumienna-Kontecka, E. *Coordin. Chem. Rev.* **2012**, *256*, 105-124.
(39) Boanini, E.; Gazzano, M.; Rubini, K.; Bigi, A. *Adv. Mater.* **2007**, *19*, 2499-2502.
(40) Rayment, E. A.; Dargaville, T. R.; Shooter, G. K.; George, G. A.; Upton, Z. *Biomaterials* **2008**, *29*, 1785-1795.
(41) Nejadnik, M. R.; Yang, X.; Mimura, T.; Birgani, Z. T.; Habibovic, P.; Itatani, K.; Jansen, J. A.; Hilborn, J.; Ossipov, D.; Mikos, A. G.; Leeuwenburgh, S. C. G. *Macromol. Biosci.* **2013**, *13*, 1308-1313.
(42) Westhaus, E.; Messersmith, P. B. *Biomaterials* **2001**, *22*, 453-462.
(43) Messersmith, P. B.; Vallabhaneni, S.; Nguyen, V. *Chem. Mater.* **1998**, *10*, 109-116.

Chapter 7

Future perspectives

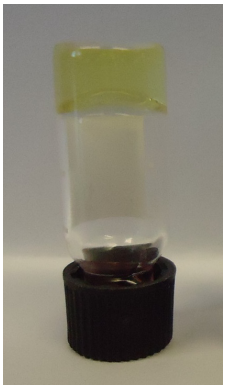

+

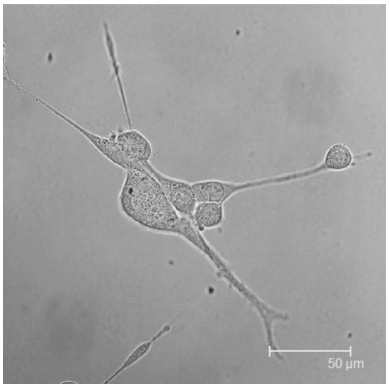

?

7.1. Brief summary

In this thesis, several bio-inspired cross-linking methods for hydrogel formation have been studied, aiming for biomedical applications. The first goal was to investigate hydrogels as bone tissue engineering scaffolds, by adopting the calcium-binding features found in bio-macromolecules such as bone sialoproteins and alginate. Physically cross-linked hydrogels were developed based on calcium-binding peptides (**Chapter 2**). These were linked to 4-armed polymer poly(ethylene)glycol (star-PEG), to obtain peptide-polymer constructs. The physical cross-linking of these constructs was studied by addition of calcium ions. The calcium binding ability of the peptides appeared to be insufficient to result in a cross-linked hydrogel network. We therefore switched our focus to chemically cross-linked hydrogels by making use of strain-promoted click (SPAAC) chemistry. In **Chapter 3**, the SPAAC reaction between ring-strained alkyne BCN and an azide was used to ensure cross-linking between star-PEG-BCN and star-PEG-N_3. This resulted in soft hydrogels with tunable mechanical properties. Incorporation of cell-binding peptide RGDS turned these hydrogels into good substrates for cell adhesion. Studies performed with NIH 3T3 fibroblasts and HeLa cells showed decreased cell adhesion to stiffer hydrogels. In contrast, the bone marrow derived HOS cells were able to adhere and spread independently of the mechanical properties of the hydrogels. In **Chapter 4**, we developed a novel chemical cross-linking method, called strain-promoted oxidation-controlled cyclooctyne–1,2-quinone cycloaddition (SPOCQ). Hydrogel formation between catechol functionalized star-PEG-DHPA and star-PEG-BCN occurred rapidly upon oxidation. This was achieved both chemically using sodium periodate and enzymatically with mushroom tyrosinase. We also showed that SPAAC and SPOCQ can function as an orthogonal reaction pair, by allowing gels to form rapidly using SPOCQ and to be functionalized subsequently using SPAAC. Both chemical cross-linking methods were used in **Chapter 5**, in which we constructed a hydrogel peptide amphiphile fibre composite material. These fibres, containing a diacetylene moiety in the alkyl tail, could easily be encapsulated in the hydrogel network, without losing their characteristic topochemical polymerisation. We furthermore showed that the fibres were aligned when assembled in a strong magnetic field. In order to stabilize the fibre alignment, SPAAC cross-linking was tested. However, formation of the polymeric network interfered with the fibre alignment process. Fortunately, the SPOCQ cross-linking method proved to be highly suited, as it could be activated after alignment was completed. In **Chapter 6**, we aimed for developing dual cross-linked hydrogels by combining physical and chemical cross-linking methods, in order to obtain advanced hydrogels with improved mechanical properties. Firstly, the hydrogel forming capacity of SPOCQ was further employed by using vitamin B2 as oxidizing agent and by cell adhesion studies demonstrating the biocompatibility of the chemically cross-linked gels. Secondly, we turned our attention to the ionic interactions of alendronic acid to develop physically cross-linked gels. The high affinity of this bisphosphonate towards calcium

resulted in the rapid physical gelation of star-PEG-alendronic acid. Finally, we combined SPOCQ cross-linking with Ca^{2+} binding, resulting in a dual cross-linked gel with enhanced mechanical properties compared to a single cross-linked system. Moreover, the physically cross-linked star-PEG-alendronic acid gels were made stimuli responsive, by incorporation of thermally triggerable calcium-releasing liposomes.

7.2. Future perspectives

7.2.1. Challenges for using hydrogels in biomedical applications

Hydrogels have great potential to be used in biomedical applications, such as tissue engineering and for the controlled delivery of drugs. However, in order to boost the clinical use of hydrogels, advanced gels should be developed which mimic the *in vivo* environment and which can easily be administered. Hence, the main challenges to focus on are injectability, degradability and mimicking the extracellular matrix. In this respect, the way in which cross-linking occurs is essential, as this determines the mechanical properties, the biocompatibility and influences hydrogel administration. This thesis focussed on several cross-linking methods, of which the potential for biomedical applications will now be discussed. This will be done based on the main challenges we need to overcome before hydrogels are routinely used in a clinical setting.

7.2.2. Chemical and/or physical cross-linking

An important factor that determines the biocompatibility of hydrogels is the way in which cross-linking occurs. Physical cross-linking methods are preferred, as chemical cross-linking often requires the use of organic solvents and/or reagents. The cytotoxicity caused by residual chemical reactants hampers the use of chemically cross-linked gels for biomedical applications. A valuable improvement for the chemical cross-linking procedures came from the rapid evolution of click chemistry in the past few years. These water-based chemistries are fast, modular, high-yielding and, importantly, bio-compatible. As described in literature and in this thesis, click chemistry has shown its value in the preparation of chemically cross-linked hydrogels. Click reactions such as SPAAC and SPOCQ allow precise control over the mechanical properties of the hydrogels (**Chapter 3** and **4**).[1] Physical cross-links, on the other hand, are advantageous due the fact that gelation can be designed to occur upon application of an external trigger (pH, temperature, stress, ionic). A drawback of this type of cross-linking is that these hydrogels often display weak mechanical properties. In this respect, a system in which chemical and physical cross-linking methods are combined is desired. We described such a system in **Chapter 6**, by making a network containing both physical and chemical cross-links, via Ca^{2+} binding to alendronic acid and the SPOCQ reaction, respectively. These mixed systems showed enhanced mechanical properties. This is an example of the emerging activities in the hydrogel field on

interpenetrating polymer networks. These hydrogels are formed when a second polymeric network is polymerised within a pre-polymerised gel. In most cases, natural polymers such as chitosan or alginate are combined with synthetic polymers. In this way, a dense network is easily generated, giving hydrogels with strong mechanical properties.[2,3] An example is the synthesis of hydrogel beads composed of alginate and pre-polymerised poly(N-isopropylacrylamide) (PNIPAAM). Drug indomethacin was directly mixed with the two polymers to ensure efficient loading. Cross-linking occurred upon injection into a Ca^{2+} solution. These hydrogel beads are temperature and pH-sensitive and give release rates up to 95% for indomethacin, which shows their potential for drug release.[4,5] The fact that interpenetrating polymer networks are based on natural polymers, also has some disadvantages for use as biomaterials. It is often difficult to obtain identical compositions when samples from natural sources are used, and their purification might be problematic. With this in mind, replacement of alginate with the synthetic star-PEG-alendronic acid can be beneficial. Apart from the combination with SPOCQ, star-PEG-alendronic acid can also be studied in combination with PNIPAAM. This will increase control over the physical properties of the gel, and by combination with polymer PNIPAAM, temperature and pH sensitivity can be introduced. In this way, a new class of stimuli-responsive interpenetrating hydrogels can be developed, with high potential as drug delivery vehicles.[2,3]

7.2.3. Injectability

As mentioned before, hydrogels are promising materials for the controlled delivery of drugs. Their high water content and porous morphology allows diffusion of molecules in and out of the polymeric network, making them suitable as drug delivery material. Ideal about hydrogels is the fact that they can be made injectable, by making use of their transition from solution to gel state. This in situ gelation allows the administration of hydrogels in a minimally invasive manner. Physically cross-linked hydrogels are often studied in this regard, as they show shear-thinning behaviour. This means that the material flows like a low viscosity solution when applying shear stress, but recovers into the gel state when the stress is removed. Additionally, the sol-to-gel transition can be achieved via the stimuli-responsiveness of physically cross-linked gels, as the encountered environmental changes upon administration to the body lead to gelation. For chemically cross-linked hydrogels, the covalent bonds are formed *in vivo*, meaning that biocompatibility is an essential criterion. Moreover, the reaction needs to be efficient and selective, as it must not interfere with the encapsulated pharmaceuticals. The emergence of the bio-orthogonal click reactions as well as the successful cell studies performed with these hydrogels, show that chemically cross-linked hydrogels are also promising as injectables. However, there are some points that need to be taken into account when studying the injectability of hydrogels. The first point is the gelation time, which is crucial for proper administration. If gelation occurs too slowly, the low viscous polymer solution can leak to surrounding tissues. On the other hand, with a too fast gelation rate, clogging in the syringe during injection is likely to occur. Apart

from the gelation time, the delivery time of the encapsulated drugs needs to be taken into account. A problem with the delivery of drugs is the initial burst release upon administration, as the drug can diffuse out of the system before gel formation. One way to improve this and to better control the delivery is by investigating the introduction of specific interactions between the polymer and the drug.[6-8] Further research on the hydrogel systems described in this thesis can focus on the injectability. For the SPAAC cross-linked gels, the slow reaction kinetics might be troublesome, as it might give rise to leakage before gelation. Increasing the polymer content could solve this issue, but this then also gives rise to stiffer gels. As outlined in **Chapter 3**, the stiffness range of most mammalian organs is between 100 and 10.000 Pa (G'). It is important to develop a hydrogel with a stiffness that matches the target tissue. A SPOCQ cross-linked gel could encounter clogging issues as gelation occurs rapidly. For this system, a double-barreled syringe can be studied, in which the oxidation agent and the polymeric building blocks are kept apart during injection. Upon reaching the target tissue, mixing of the two components leads to rapid *in situ* gelation, thereby minimizing leakage.

7.2.4. Degradability

Apart from the injectability studies, the degradability is another important aspect when investigating hydrogels for biomedical applications. When hydrogels are used in tissue engineering or for delivery of drugs or cells, long term stability is required. In this case, slow degrading polymers should be used. This also prevents the initial burst release issues, as discussed before. Furthermore, when studying the degradation profile of the hydrogels, one should also take into account what the degradation products are. It is for example known that the degradation products of polymers such as PLGA cause a decrease in pH, which might cause damage to proteins or lead to inflammation at the site of injection. However, in the design of our hydrogels, we chose to only use PEG, since the medical use of this polymer has already been approved by the FDA. In the design of hydrogels it is important to study the degradation rate, since this directly corresponds with the release rate of encapsulated drugs, proteins or cells. Ideally, the mechanical properties and the degradation profile should be balanced, to ensure proper functionality of the hydrogel.[8,9]

7.2.5. 3-D Cells studies & Mimicking the ECM

An important goal in the hydrogel field is mimicking of the extracellular matrix (ECM). The ECM is the biological material that surrounds cells in tissue. Important criteria to reach this goal are cell adhesion, cell migration and proteolytic degradation of hydrogels. This illustrates the importance of our cell adhesion studies. Both SPAAC and SPOCQ cross-linked hydrogels were found to be good substrates for cellular adhesion. In this thesis, only 2-D cell adhesion studies were performed. However, mimicking the ECM requires a 3-D cellular environment. An important way to achieve this is the incorporation of matrix metalloproteinase (MMP)

cleavable sequences, as this allows cells to actively remodel their surroundings. These MMPs are naturally occurring in the ECM, where they are responsible for remodelling. By incorporation of an MMP cleavable motif, a dynamic cellular environment is created within the hydrogel network. Further studies on our hydrogels should therefore concentrate on cellular adherence in three dimensions. As outlined in **Chapter 5**, an interesting system to start with is the MMP-motif containing hydrogels combined with IKVAV-containing peptide amphiphiles. The hydrogels contain both a cellular adhesion motif (IKVAV or RGDS) and an enzyme-cleavable MMP sequence, which allows cells to adhere in a 3-D fashion. Moreover, when magnetically aligned IKVAV-containing peptide amphiphile fibres are incorporated, these hydrogels can be studied as potential scaffolds for the directional growth of neuronal cells. Eventually, this could allow us to regenerate neural tissues in a controlled environment and manner. We consider the 3-D studies with the peptide amphiphiles containing hydrogels as a good starting point for achieving the goal to use our hydrogels for tissue engineering applications. Adjusting the peptide components in the hydrogel makes it easy to incorporate multiple functionalities in the network, which is an important step in mimicking the ECM.[7,10]

7.2.6. Bone tissue engineering

In **Chapter 6**, we introduced calcium-induced gelation of star-PEG-alendronic acid polymers. Further studies on this physically cross-linked hydrogel should aim for regeneration of bone tissue. Important in this aspect is that the material needs to have a high affinity for bone mineral hydroxy apatite. Our hydrogel contains bisphosphonate alendronic acid, which is known to be responsible for targeting and binding to bone via binding to calcium. Star-PEG-alendronic acid hydrogels are therefore promising as scaffold for bone tissue regeneration. In future research, cell studies with human bone marrow mesenchymal stem cells (hBMSC) are recommended. These cells can differentiate into the bone synthesizing osteoblasts. After harvesting from a patient, hBMSC can be cultured and combined with a scaffold to repair bone defects. hBMSC can be loaded in star-PEG-alendronic acid hydrogels, after which it is important to study their ability to differentiation into osteoblasts. The next step would then be to study them *in vivo* on their ability to repair cancellous bone defects. Moreover, we want to study the injectability of the star-PEG-alendronic acid hydrogels. Especially when aiming for bone tissue engineering, the injectability of the material is an important advantage. Without this, an open surgical procedure has to be carried out, which is highly invasive for the patient. Injectability of the physically cross-linked star-PEG-alendronic acid hydrogels is likely to be promising. Moreover, these gels have self-healing properties, which easily allows them to remodel and to fill any shape or defect. Additionally, our initial studies with calcium releasing liposomes showed that the hydrogels can be made stimuli responsive, which allows on demand release of calcium. This is a step forward in developing hydrogels in which the time, site and dose of release can be precisely controlled.[11-14]

7.3. References

(1) Nimmo, C. M.; Shoichet, M. S. *Bioconjugate Chem.* **2011**, *22*, 2199-2209.

(2) Dragan, E. S. *Chem. Eng. J.* **2014**, *243*, 572-590.

(3) Hoare, T. R.; Kohane, D. S. *Polymer* **2008**, *49*, 1993-2007.

(4) Shi, J.; Alves, N. M.; Mano, J. F. *Macromol. Biosci.* **2006**, *6*, 358-363.

(5) Zhang, G. Q.; Zha, L. S.; Zhou, M. H.; Ma, J. H.; Liang, B. R. *J. Appl. Polym. Sci.* **2005**, *97*, 1931-1940.

(6) Ko, D. Y.; Shinde, U. P.; Yeon, B.; Jeong, B. *Prog. Polym. Sci.* **2013**, *38*, 672-701.

(7) Altunbas, A.; Pochan, D. J. *Top Curr Chem* **2011**, *310*, 135-167.

(8) Annabi, N.; Tamayol, A.; Uquillas, J. A.; Akbari, M.; Bertassoni, L. E.; Cha, C.; Camci-Unal, G.; Dokmeci, M. R.; Peppas, N. A.; Khademhosseini, A. *Adv. Mater.* **2014**, *26*, 85-124.

(9) Nguyen, M. K.; Lee, D. S. *Macromol. Biosci.* **2010**, *10*, 563-579.

(10) Zhu, J. *Biomaterials* **2010**, *31*, 4639-4656.

(11) Zhao, L.; Weir, M. D.; Xu, H. H. K. *Biomaterials* **2010**, *31*, 6502-6510.

(12) Puppi, D.; Chiellini, F.; Piras, A. M.; Chiellini, E. *Prog. Polym. Sci.* **2010**, *35*, 403-440.

(13) Boanini, E.; Gazzano, M.; Rubini, K.; Bigi, A. *Adv. Mater.* **2007**, *19*, 2499-2502.

(14) Nejadnik, M. R.; Yang, X.; Mimura, T.; Birgani, Z. T.; Habibovic, P.; Itatani, K.; Jansen, J. A.; Hilborn, J.; Ossipov, D.; Mikos, A. G.; Leeuwenburgh, S. C. G. *Macromol. Biosci.* **2013**, *13*, 1308-1313.

Summary

Chapter 1 - Peptide- and protein based hydrogels

Hydrogels are three-dimensional, hydrophilic polymeric networks, capable of absorbing large amounts of water or biological fluids, up to thousand times their dry weight. They are insoluble due to the presence of cross-links between the constituents that form the polymeric network. An important hydrogel characteristic is the way in which cross-linking occurs, either chemically or physically. Chemically cross-linked hydrogels are formed via covalent bonds between the polymeric constituents. Advantageous about this cross-linking method is that it allows control over the mechanical properties of the formed hydrogels. A disadvantage is that chemical reactions often require the use of organic solvents and/or reagents, which hampers the use for biomedical applications. Physically cross-linked gels, on the other hand, are formed via self-assembly in response to external stimuli such as temperature, pH or ionic strength. These gels do not depend on the additions of chemical reagents and moreover, can be made stimuli-response. This makes them promising for use as injectable material. A disadvantage is that physical cross-linking methods often lead to gels with weak mechanical properties. The way in which cross-linking occurs is an important factor for hydrogel formation, as it determines the mechanical properties of the gel, the biocompatibility and also influences hydrogel administration. Control over the cross-linking method leads to control over the hydrogel properties, which facilitates their clinical use. This thesis therefore focusses on several bio-inspired cross-linking methods for hydrogel formation, aiming to develop adaptive scaffolds for bone tissue engineering.

Chapter 2 - Physical cross-linking of star-PEG polymers using calcium-binding peptides

Bone tissue is composed of cells embedded in an organic matrix, consisting of collagen and the calcium-containing hydroxyapatite. An important criterion in the search for scaffolds for bone tissue engineering is the ability to induce apatite formation. Materials that mineralize bone tissue are usually non-collagenous proteins, with strong calcium-binding features. These calcium-binding motifs are abundantly present in nature, such as bone sialoproteins, calmodulin and alginate. Our aim was the development of physically cross-linked hydrogels as bone tissue engineering scaffolds, by adopting the strong calcium-binding features found in nature. We first synthesized several peptides that were abundant in negatively charged carboxylate groups for binding to Ca^{2+}. Peptides such as Gly-Glu_7-Gly (GE_7G), $G[LEELLEE]_2G$ and the binding motifs from calmodulin were synthesized using solid phase peptide synthesis. The calcium-binding properties of these peptides were explored via analysis techniques such as circular dichroism spectroscopy (CD), dynamic light scattering (DLS) and isothermal calorimetry (ITC). The effect of calcium addition on the peptides secondary structure, the aggregation behaviour and the enthalpy of binding were determined. It was difficult to be conclusive about the ability of the peptides to bind calcium, as the analysis techniques mainly showed only weak effects upon

addition of calcium. Nevertheless, we decided to continue with our aim to develop calcium cross-linkable hydrogels by linkage of the peptides to star-shaped poly(ethylene)glycol (star-PEG). Coupling of peptide GE_7G to star-PEG was successful, affording the peptide-polymer construct star-PEG-GE_7G. Synthesis of the polymer constructs with peptide $G[LEELLEE]_2$ and with the calmodulin domains did not succeed, because the low solubility of these compounds hampered purification. Star-PEG-GE_7G was therefore used to test the possibility to make a physically cross-linked hydrogel using calcium as cross-linker. Unfortunately, addition of calcium to star-PEG-GE_7G did not result in gel formation. As the analysis techniques to determine the calcium-binding properties were also not convincing, we concluded that the interaction of calcium with the peptides is not strong enough to make physical connections between the polymers.

Chapter 3 - Soft PEG-hydrogels with independently tunable stiffness and RGDS-content for cell adhesion studies

We switched our attention to chemically cross-linked gels and especially focussed on the biocompatibility of the cross-linking procedure. Interesting in this respect are the so-called click reactions. These water-based chemistries are fast, modular, high-yielding and, importantly, biocompatible. We studied the copper-free click reaction named strain promoted azide-alkyne cycloaddition (SPAAC). Ring strained alkyne bicyclo[6.1.0]nonyne (BCN) and an azide were coupled to polymer star-PEG, to obtain star-PEG-BCN and star-PEG-N_3, respectively. Upon mixing of these two polymers in water, the SPAAC reaction commenced, leading to hydrogel formation. Cross-linking took place without the need of additional chemicals or further processing. We aimed for developing soft hydrogels, to mimic the stiffness range of most mammalian organs ($G' = 100 - 10.000$ Pa). Rheological analysis confirmed the soft nature of the SPAAC cross-linked gels, as elastic moduli of 25 Pa (10 mg/mL), 1192 (20 mg/mL) and 2298 Pa (30 mg/mL) were obtained. This also showed that the mechanical properties of the gels could easily be tuned by varying the total polymer content. In order to be able to ensure biocompatibility, cell adhesion peptide RGDS was incorporated in the polymeric network. Cell adhesion studies were performing using a live/dead assay, which contains a fluorescent dye to colour living cells (green) and a dye for dead cells (red). Three different cell types originating from different tissues were utilized to get insight in how cells interact with their surroundings. We found a large number of green fluorescent cells for the bone marrow derived HOS cells on all RGDS-containing hydrogels (10 – 30 mg/mL). This means that HOS cells remained viable on all hydrogel surfaces, independent of the stiffness. Both cell lines derived from softer tissues (HeLa and 3T3 NIH fibroblasts) also showed nicely spread and viable cells on the 10 and 20 mg/mL gels. Interestingly, cell adherence was clearly hampered on the stiffest hydrogel of 30 mg/mL, shown by the significantly lower amount of adherent cells. Since stiffness is the only difference between the 10, 20 and 30 mg/mL gels, we conclude that this seems to be a

determining factor in cellular adhesion of HeLa cells and NIH 3T3 fibroblasts. Importantly, our research showed that SPAAC cross-linked RGDS-containing hydrogels are a good substrate for cellular adhesion.

Chapter 4 - **A fast and activatable cross-linking strategy for hydrogel formation**
We demonstrated that the SPAAC reaction is a valuable method for the formation of chemically cross-linked hydrogels. However, as we also observed, the SPAAC reaction is often hampered by slow reaction kinetics. Moreover, the reaction is not activatable, which is a desired property for injectable hydrogels and for other biomedical applications where spatiotemporal control of hydrogel formation is demanded. We therefore developed a new cross-linking method called strain-promoted oxidation-controlled cyclooctyne–1,2-quinone cycloaddition (SPOCQ). This method is based on the reaction between alkyne BCN and catechol DHPA (3,4 dihydroxyphenylacetic acid), which proceeds after oxidation of the catechol to the quinone. We showed that hydrogel formation out of polymers star-PEG-BCN and star-PEG-DHPA proceeds extremely fast upon oxidation. Chemical oxidation using sodium periodate resulted in almost immediate gelation. Oxidation could also rapidly be performed using enzyme mushroom tyrosinase. By varying the enzyme concentration, the cross-linking rate could be controlled, as higher enzyme concentrations gave rise to lower gelation times. The SPOCQ reaction only commenced after addition of an oxidation agent, meaning that, for the first time, a fast and activatable cross-linking method for hydrogel formation is developed. Additionally, inspired by the large difference in reaction rate between SPOCQ and SPAAC, we hypothesized that we could use both reactions in one-pot. We indeed showed that both chemical cross-linking methods can be used in concert, SPOCQ for rapid hydrogel formation, and SPAAC for the simultaneous functionalization of the gel.

Chapter 5 - SPAAC and SPOCQ cross-linked hydrogels as matrices for encapsulation of aligned peptide amphiphile fibres
Both chemical cross-linking methods SPAAC and SPOCQ were used in **Chapter 5**, in which we combined the hydrogel network with peptide amphiphile fibres. These fibres are composed of a hydrophobic aliphatic tail and a hydrophilic peptide sequence. We used peptide amphiphiles with a diacetylene moiety in the alkyl tail, to introduce fibre stability. These fibres can be polymerised using UV irradiation, leading to highly ordered alkyl tails. Apart from this self-assembly, certain peptide amphiphiles fibres can be aligned using a strong magnetic field to further organize them at a macroscopic level. This is especially interesting when the peptide amphiphiles contain peptide motif IKVAV, which is known to promote neurite outgrowth of several neuronal cell types. Aligning IKVAV containing fibres opens up the possibility to develop a biomaterial to control the directional growth of neuronal cells. In order to avoid fibre disassembly after alignment, we aimed for capturing the aligned IKVAV containing peptide

amphiphile fibres in a hydrogel network. We confirmed that the peptide amphiphile fibres can be aligned using a strong magnetic field, and showed proper alignment with a field strength of 20 T. SPAAC cross-linking was first studied as polymeric matrix to fixate alignment. Unfortunately, the formation of the polymeric network occurred simultaneously with the alignment process, which thereby prevented proper alignment. We therefore continued with SPOCQ cross-linking, which has the great advantage of being activatable. In fact, this showed its value, because magnetic alignment of the fibres could be achieved in presence of polymers star-PEG-BCN and star-PEG-DHPA, as it was not hindered by gel formation. After alignment, oxidizing agent sodium periodate was added, which diffused through the sample cell, to provide formation of the polymeric network around the aligned fibres. We confirmed that the fibres remained aligned, and were thus entrapped in a polymeric matrix. This hydrogel is an interesting material for further research aiming for controlling the directional growth of neuronal cells.

Chapter 6 - Dual cross-linked hydrogels by combining chemical and physical cross-linking

Our hydrogels cross-linked with SPAAC and SPOCQ showed that chemically cross-linked gels allow precise control over the mechanical properties. Physical cross-linking, on the other hand, have the advantage that gelation occurs upon application of an external trigger (pH, temperature, stress, ionic strength). A disadvantage of physically cross-linked hydrogels is that they usually have weak mechanical properties. By combining chemical and physical cross-linking, advanced hydrogels can be developed with improved mechanical properties. Before studying these dual cross-linked hydrogels, we first further studied the gel forming capacity of SPOCQ cross-linking. We showed that vitamin B2 can also be used as oxidizing agent, by making use of illumination with visible light. With biomedical applications in mind, we continued by performing cell adhesion studies with SPOCQ cross-linked hydrogels. Gels were functionalized with adhesion motif RGDS and proved to be good substrates for cell adherence, when oxidized by sodium periodate or vitamin B2. We next studied physical cross-linking, based on the strong interaction of bisphosphonate alendronic acid with calcium. Polymer star-PEG-alendronic acid rapidly formed ionically cross-linked hydrogels upon addition of calcium. We also showed that these gels display self-healing behaviour. We now continued with dual cross-linked gels, by combining our chemical cross-linking method SPOCQ with the physical cross-linking procedure using calcium. Rheological analysis showed that these dual cross-linked gels showed improved mechanical properties, compared to gels that were only chemically cross-linked. Finally, we also made the physically cross-linked gels stimuli-responsive, by incorporation of thermally triggerable calcium-releasing liposomes. In this way, the release of calcium can be controlled, which is promising for biomedical applications such as bone tissue engineering.

Chapter 7 - Future perspectives

Hydrogels have great potential to be used in biomedical applications, such as tissue engineering and for the controlled delivery of drugs. In the final chapter, we focussed on the main challenges we need to overcome in order to boost the clinical use of hydrogels. We discussed the possibilities to make the hydrogels injectable. Both SPAAC and SPOCQ cross-linked gels are promising to study in this respect. Furthermore, the long term stability and degradability of the gels need to be investigated. An important guide when aiming for tissue engineering is mimicking of the extracellular matrix. Hydrogels are promising for creating this 3-D cellular environment, especially the gels containing the peptide amphiphile fibres as discussed in **Chapter 5**. The physical cross-linked gels from **Chapter 6** are interesting to study as bone tissue engineering scaffolds, as alendronic acid can bind to bones via binding to calcium. Future studies on the hydrogels described in this thesis, should directly aim for biomedical applications, which will give our gels the opportunity to find their way in clinical use.

Samenvatting

Hoofdstuk 1 - Peptide- en eiwit-gebaseerde hydrogels

Hydrogels zijn 3-dimensionale polymerische netwerken. Door hun hydrofiele karakter zijn ze in staat om grote hoeveelheden water of biologische vloeistoffen te absorberen, tot wel duizend keer hun eigen drooggewicht. De gels zijn onoplosbaar vanwege de aanwezigheid van cross-links (dwarsverbindingen) tussen de componenten die het polymerische netwerk vormen. Een belangrijk kenmerk van hydrogels is de manier waarop de cross-links ontstaan, wat zowel op een chemische als op een fysische manier kan plaatsvinden. Chemisch gecross-linkte hydrogels worden gevormd via covalente verbindingen tussen de polymerische componenten. Een belangrijk voordeel van deze cross-linkings methode is dat men controle heeft over de mechanische eigenschappen van de gevormde hydrogels. Een nadeel is dat de chemisch reacties vaak het gebruik van organische oplosmiddelen en/of reagentia vereisen, wat het inzetten van deze gels voor biomedische toepassingen verhindert. Fysische gecross-linkte hydrogels worden gevormd door zelf-assemblage van de polymerische componenten, in reactie op externe stimulansen, zoals temperatuur, pH of ionische sterkte. Deze gels zijn niet afhankelijk van de toevoeging van chemische reagentia. Ze kunnen zo worden ontwikkeld dat de vorming van de gel alleen plaats vindt als reactie op bepaalde stimulansen, wat deze hydrogels veelbelovend maakt als injecteerbaar materiaal. Een nadeel van fysische cross-linking is dat ze vaak gels geven met zwakke mechanische eigenschappen. De manier waarop cross-linking plaats vindt is een belangrijke factor in de vorming van hydrogels, aangezien het de mechanische eigenschappen bepaald, alsmede een invloed heeft op de biocompatibiliteit en op de mogelijkheden voor het toedienen van de gel. Controle over de cross-linkings methode leidt tot controle over de eigenschappen van de hydrogels, wat hun klinische gebruik vergemakkelijkt. Deze thesis richt zich op verschillende bio-geïnspireerde cross-linkings methoden voor het vormen van hydrogels, met als doel om deze in te zetten als adaptieve dragermaterialen voor het kweken van botweefsel.

Hoofdstuk 2 – Fysische cross-linking van ster-PEG polymeren met behulp van calcium-bindende peptides

Botweefsel bestaat uit cellen die door een organische matrix omringd worden. Deze matrix bestaat uit collageen en het calcium-bevattende hydroxyapatiet. Een belangrijk criterium in de zoektocht naar dragermaterialen voor het kweken van botweefsel, is dat het materiaal de mogelijkheid moet bieden om apatiet vorming te induceren. Materialen die botweefsel kunnen mineraliseren zijn vaak niet-collagene eiwitten, met sterke calcium-bindende eigenschappen. Deze calcium-bindende motieven zijn veel voorkomend in de natuur, zoals bijvoorbeeld bot sialo eiwitten, calmoduline en alginaat. Ons doel was de ontwikkeling van fysisch gecross-linkte hydrogels als dragermateriaal voor het kweken van botweefsel, met behulp van de

sterke calcium-bindende kenmerken uit de natuur. Eerst werden verschillende peptiden gesynthetiseerd, die rijk zijn in negatief geladen carboxylaat groepen, voor de binding aan Ca^{2+}. Peptiden zoals Gly-Glu_7-Gly (GE_7G), $G[LEELLEE]_2G$ en de bindingsmotieven van calmoduline werden gesynthetiseerd met behulp van vaste-fase peptide synthese. De calcium-bindende eigenschappen van deze peptiden werden onderzocht via analyse technieken zoals circulair dichroïsme spectroscopie (CD), dynamische licht verstrooiing (DLS) en isotherme calorimetrie (ITC). Zodoende werd het effect van het toevoegen van calcium op de secundaire structuur van het peptide, het aggregatie gedrag en de bindingsenthalpie bepaald. Het bleek lastig om een conclusie te trekken over het vermogen van de peptides om calcium te binden, omdat de analyse technieken voornamelijk zwakke bindingseffecten lieten zien na toevoeging van calcium. Desondanks besloten we om door te gaan met ons doel om hydrogels te ontwikkelen die cross-linken onder invloed van calcium. Dit werd gedaan middels het koppelen van de peptiden aan stervormig poly(ethylene)glycol (ster-PEG). Het koppelen van peptide GE_7G aan ster-PEG was succesvol en leidde tot het peptide-polymeer construct ster-PEG-GE_7G. De synthese van de polymeer constructen met peptide $G[LEELLEE]_2$ en met de calmoduline bindingsmotieven was niet geslaagd, omdat de lage oplosbaarheid van deze constructen de zuivering belemmerde. Daarom werd alleen ster-PEG-GE_7G gebruikt om te testen of hiermee een fysisch gecross-linkte hydrogel kon worden gemaakt, waarbij calcium de cross-linker is. Helaas resulteerde de toevoeging van calcium aan ster-PEG-GE_7G niet tot de vorming van een gel. Omdat de gebruikte analyse technieken om de calcium-bindende eigenschappen te bepalen ook niet overtuigend waren, concluderen we dat de interactie van calcium met de peptides niet sterk genoeg is om fysische connecties tussen de polymeren te maken.

Hoofdstuk 3 – Zachte PEG-hydrogels met onafhankelijk aanpasbare stijfheid en RGDS-hoeveelheid voor cel adhesie studies

We hebben onze aandacht verlegd naar chemische gecross-linkte gels en ons daarbij speciaal gericht op de biocompatibiliteit van de cross-linkings methode. Interessant hierbij zijn de zogenoemde click reacties. Deze op water gebaseerde chemische reacties zijn snel, aanpasbaar, geven een hoge opbrengst, en hebben als belangrijkste voordeel dat ze biocompatibel zijn. We hebben de kopervrije click reactie genaamd 'spannings-gestimuleerde cycloadditie tussen een azide en een alkyn' (SPAAC) bestudeerd. Ring gespannen alkyn bicyclo[6.1.0]nonyne (BCN) en een azide werden gekoppeld aan polymeer ster-PEG, om zo respectievelijk ster-PEG-BCN en ster-PEG-N_3 te verkrijgen. Nadat deze twee polymeren in water werden opgelost en gemengd, startte de SPAAC reactie, welke resulteerde in de vorming van een hydrogel. Dit cross-linkings proces vond plaats zonder verdere handelingen en zonder dat er extra chemicaliën dienden te worden toegevoegd. We hebben ons als doel gesteld om zachte hydrogels te maken, die de stijfheid van de meeste organen van zoogdieren ($G' = 100 – 10.000$ Pa) nabootsen. Analyse van de hydrogels met behulp van rheologie bevestigde het zachte karakter van de SPAAC

gecross-linkte hydrogels, aangezien elastische moduli van 25 Pa (10 mg/mL), 1192 (20 mg/mL) en 2298 Pa (30 mg/mL) werden verkregen. Dit liet ook zien dat de mechanische eigenschappen van de gels gemakkelijk kunnen worden aangepast, middels het variëren van de totale polymeer hoeveelheid. Om verzekerd te zijn van biocompatibele gels, werd cel adhesie peptide RGDS in het polymerisch netwerk ingebouwd. Cel adhesie studies werden uitgevoerd met een 'live/dead' assay, welke twee fluorescente stoffen bevat, om levende cellen te kleuren (groen) en om dode cellen te kleuren (rood). Er werden drie verschillende celtypes gebruikt, afkomst van verschillende weefsels, om zo een beeld te krijgen van hoe cellen interactie hebben met hun omgeving. Op alle RGDS-bevattende hydrogels (10 – 30 mg/mL) werd een groot aantal groen fluorescerende cellen gevonden voor de van botweefsel afkomstige HOS cellen. Dit betekent dat de HOS cellen in leven blijven op alle hydrogel oppervlaktes, onafhankelijk van de stijfheid van de gel. Voor beide cel types die afkomstig zijn van zachtere weefsels (HeLa en 3T3 NIH fibroblasten) werden mooi gespreide en levende cellen gevonden op de gels van 10 en 20 mg/mL. Interessant bij deze studies was dat de cel adhesie duidelijk gehinderd werd op de stijfste hydrogel (30 mg/mL), welke een significant lager aantal aangehechte cellen liet zien. Aangezien stijfheid de enige factor is waarin de 10, 20 en 30 mg/mL hydrogels van elkaar verschillen, concluderen we dat dit de bepaalde factor lijkt in de cel adhesie van HeLa cellen en 3T3 NIH fibroblasten. Belangrijk is dat dit onderzoek laat zien dat SPAAC gecross-linkte RGDS-bevattende hydrogels een goed substraat zijn voor cellulaire adhesie.

Hoofdstuk 4 – Een snelle en activeerbare cross-linkings methode voor het vormen van hydrogels

We hebben laten zien dat de SPAAC reactie een waardevolle methode is voor de vorming van chemisch gecross-linkte hydrogels. Echter, wat we ook geobserveerd hebben, is dat de SPAAC reactie vaak gehinderd wordt door de langzame reactie kinetiek. Bovendien is de reactie niet activeerbaar, wat vaak een gewenste eigenschap is voor injecteerbare hydrogels en voor andere biomedische toepassingen waar controle op het moment van gelvorming noodzakelijk is. We hebben daarom een nieuwe cross-linkings methode ontwikkeld, genaamd 'spanningsgestimuleerde oxidatie gecontroleerde cycloadditie met behulp van een 1,2-quinone' (SPOCQ). Deze methode is gebaseerd op de reactie tussen alkyn BCN en catechol DHPA (3,4 dihydroxy fenyl azijnzuur), welke plaatsvindt na de oxidatie van het catechol naar het quinone. We hebben laten zien dat de vorming van hydrogels uit polymeren ster-PEG-BCN en ster-PEG-DHPA extreem snel plaatsvindt na oxidatie. Chemische oxidatie met behulp van natrium periodaat resulteerde in bijna onmiddellijke gelvorming. Oxidatie kon ook snel worden uitgevoerd met behulp van enzym 'mushroom tyrosinase'. Door het variëren van de enzym concentratie kon de cross-linkings snelheid worden gecontroleerd, omdat hogere enzym concentraties resulteerde in kortere tijden tot het vormen van de gel. De SPOCQ reactie vindt alleen plaats nadat het oxidatie middel is toegevoegd, wat betekent dat we, voor de eerste keer, een snelle en

activeerbare cross-linkings methode voor het vormen van hydrogels hebben ontwikkeld. Door het grote verschil in reactiesnelheid tussen SPAAC en SPOCQ werden we ook geïnspireerd om beide reacties in één pot uit te voeren. We hebben hierbij laten zien dat beide cross-linkings methoden samen kunnen worden gebruikt, SPOCQ voor het snelle vormen van hydrogels en SPAAC voor het simultaan functionaliseren van de gel.

Hoofdstuk 5 - SPAAC en SPOCQ gecross-linkte hydrogels als matrices voor het vastzetten van uitgelijnde peptide amfifiele vezels

Beide chemische cross-linkings methoden SPAAC en SPOCQ werden gebruikt in **Hoofdstuk 5**, waarin we het hydrogel netwerk hebben gecombineerd met peptide amfifiele vezels. Deze vezels zijn opgebouwd uit een hydrofobe alifatische staart en een hydrofiele peptide sequentie. We hebben peptide amfifielen gebruikt met een diacetyleen functionaliteit in de alkyl staart, om vezel stabiliteit te introduceren. Deze vezels kunnen worden gepolymeriseerd door middel van bestraling met UV licht, wat leidt tot een hoge mate van ordening van de alkyl staarten. Behalve deze zelf-assemblage, kunnen bepaalde peptide amfifiele vezels ook worden uitgelijnd in een sterk magneetveld, wat leidt tot een verdere ordening op macroscopisch niveau. Dit is vooral interessant wanneer de amfifiele vezels peptide domein IKVAV bevatten, omdat dit in staat is om de uitgroei van neurieten van bepaalde zenuwcellen te stimuleren. Het uitlijnen van IKVAV-bevattende vezels opent mogelijkheden om een biomateriaal te ontwikkelen die de groeirichting van zenuwcellen controleert. Om te voorkomen dat de vezels deassembleren nadat ze uitgelijnd zijn, was ons doel om de IKVAV bevattende vezels vast te zetten in een hydrogel netwerk. We hebben bevestigd dat de peptide amfifiele vezels kunnen worden uitgelijnd met behulp van een sterk magneetveld, aangezien er een nette uitlijning werd gevonden bij een veldsterkte van 20 T. SPAAC cross-linking werd als eerste bestudeerd als polymerische matrix om de uitgelijnde vezels in vast te zetten. Helaas vond de vorming van het polymerisch netwerk gelijktijdig plaats met het uitlijningsproces, waardoor de vezels niet naar behoren werden uitgelijnd. We gingen daardoor verder met SPOCQ cross-linking, welke als groot voordeel heeft dat het activeerbaar is. Dit liet zijn meerwaarde zien, omdat de magnetische uitlijning kon plaatsvinden in aanwezigheid van polymeren ster-PEG-BCN en ster-PEG-DHPA, maar niet gehinderd werd door de vorming van de gel. Na de uitlijning kon het oxiderende middel natrium periodaat worden toegevoegd, welke diffundeerde door het monster, en zorgde voor de vorming van een polymerisch netwerk rondom de uitgelijnde vezels. We hebben bevestigd dat de vezels uitgelijnd bleven, en zijn dus in staat om de uitlijning vast te zetten in een polymerische matrix. Dit levert een hydrogel op welke interessant is voor verder onderzoek naar het controleren van de groeirichting van zenuwcellen.

Hoofdstuk 6 – Dubbel gecross-linkte hydrogels door het combineren van chemische en fysische cross-linking

Onze hydrogels gecross-linkt met SPAAC en SPOCQ hebben laten zien dat chemische cross-linkings methoden de mogelijkheid bieden om de mechanische eigenschappen van de gels te controleren. Aan de andere kant hebben fysische cross-linkings methoden het voordeel dat de gelvorming plaats vindt als reactie op een externe trigger (pH, temperatuur, stress en ionische sterkte). Een nadeel van de fysisch gecross-linkte hydrogels is dat ze vaak zwakke mechanische eigenschappen hebben. Door het combineren van zowel chemische als fysische cross-linking, kunnen geavanceerde hydrogels worden ontwikkeld met verbeterde mechanische eigenschappen. Voordat we deze dubbel gecross-linkte gels bestuderen, kijken we eerst verder naar de gel vormingscapaciteiten van de SPOCQ reactie. We hebben laten zien dat vitamine B2 ook gebruikt kan worden als oxiderend middel, met behulp van bestraling met zichtbaar licht. Met biomedische toepassingen in gedachten, zijn we ook doorgegaan met de cel adhesie studies, nu met de SPOCQ gecross-linkte hydrogels. De gels werden gefunctionaliseerd met adhesie motief RGDS en hebben bewezen goede substraten voor celadhesie te zijn, wanneer ze geoxideerd zijn met natrium periodaat of vitamine B2. Hierna hebben we fysische cross-linking bestudeerd, gebaseerd op de sterkte interactie van bisfosfonaat alendronine zuur met calcium. Polymeer ster-PEG-alendronine zuur vormde snel ionisch gecross-linkte hydrogels na de toevoeging van calcium. We hebben ook laten zien dat deze gels zelfhelend gedrag vertonen. We zijn daarna verder gegaan met de dubbel gecross-linkte gels, door chemische cross-linkings methode SPOCQ te combineren met de fysische procedure met calcium. Analyse met behulp van rheologie liet zien dat deze dubbel gecross-linkte gels verbeterde mechanische eigenschappen hebben in vergelijking tot gels met alleen chemische cross-linking. Tot slot hebben we de fysisch gecross-linkte gels ook zo ontwikkeld dat ze reageren op een externe stimulans. Dit hebben we gedaan door het toevoegen van temperatuur gevoelige, calcium vrijlatende liposomen. Op deze manier kan de afgifte van calcium worden gecontroleerd, wat veelbelovend is voor biomedische toepassingen zoals het kweken van botweefsel.

Hoofdstuk 7 – Toekomst perspectieven

Hydrogels hebben veel potentie om te worden gebruikt in biomedisch toepassingen, zoals voor het kweken van weefsels en in de gecontroleerde afgifte van medicijnen. In het laatste hoofdstuk hebben we ons gericht op de belangrijkste uitdagingen die we moeten overwinnen om het klinisch gebruik van hydrogels te stimuleren. We hebben de mogelijkheden besproken om hydrogels injecteerbaar te maken. Zowel SPAAC als SPOCQ gecross-linkte gels zijn veelbelovend om gebruikt te worden als injecteerbaar materiaal. Verder moet de stabiliteit over lange termijn en de degradeerbaarheid van de gels worden onderzocht. Een belangrijke richtlijn voor het kweken van weefsels is om de extracellulaire matrix na te bootsen. Hydrogels hebben potentie om deze 3-D cellulaire omgeving te creëren, zeker als ze peptide amfifiele

vezels bevatten, zoals besproken in **Hoofdstuk 5**. De fysisch gecross-linkte gels van **Hoofdstuk 6** zijn interessant om te bestuderen als dragermateriaal voor het kweken van botweefsels, omdat alendronine zuur kan binden aan botten, via de binding aan calcium. Toekomstige studies aan de hydrogels beschreven in deze thesis, zullen zich direct moeten richten om biomedische toepassingen, waardoor onze gels de kans krijgen om zich te bewijzen in klinisch gebruik.

Dankwoord

Na vier jaar (of eigenlijk al bijna 5) is dit dan het moment om een van de leukste dingen van je boekje te schrijven, het dankwoord! En een belangrijk onderdeel ook, want er zijn veel mensen die ik wil bedanken voor de mooie bijdrage die ze hebben geleverd aan dit proefschrift.

Als eerste is dat uiteraard **Dennis**. Bedankt voor je enthousiaste begeleiding! Ik waardeer het erg dat ik altijd binnen kon lopen, en ook dat je regelmatig langs kwam op het lab om gewoon even te vragen hoe het gaat. Dat leverde dan vaak weer van die praktische tips op, waardoor ik weer nieuwe ideetjes had om vooruit te komen. Bedankt ook voor de hulp met 'onze grote vriend', de HPLC, die toch geregeld jouw technische kennis nodig had, en waardoor ik inmiddels ook weet wat een ferrule is.
Natuurlijk is **Jan** de volgende die ik graag wil bedanken. Het was vooral heel fijn dat je altijd de grotere lijn zag van het onderzoek. Je dacht eigenlijk al een paar stappen verder en zag al meteen veel mooie (publiceerbare) resultaten, wat mij enorm motiveerde. Ondanks dat het soms toekomstmuziek leek voor mij, was je vastberaden, en ben ik erg blij dat ik (zeker ook doordat ik wat langer mocht blijven) nu een mooi boekje heb kunnen schrijven!

Wat betreft begeleiding wil ik ook **Sander Leeuwenburgh** bedanken. Je maakte altijd even tijd als ik ergens mee in de knoop zat, en ik heb veel aan je expertise over hydrogels en rheologie gehad. Jouw inbreng van alendronic acid als nieuw calciumbindend motief, heeft gelukkig ook geresulteerd in de fysische hydrogels van hoofdstuk 6. Ook heb ik prettig kunnen samenwerken met verschillende mensen op de afdeling **Biomaterialen**, waaronder **Reza Nejadnik**, **Timothy Douglas** en **Paula Lopez Perez**. Paula, you always shared your expertise on hydrogels and alendronic acid and I enjoyed our conversations about research at the rheometer.

Graag wil ook de manuscript commissie, **Alan Rowan**, **Rint Sijbesma** en **Kim Bonger**, bedanken voor het kritisch lezen van mijn proefschrift. Voor hoofdstuk 5 had ik de eer om met een grote magneet te mogen werken, bedankt voor jullie expertise en hulp hierbij, **Roger Rikken** en **Peter Christianen**. Graag wil ik **Floris van Delft** bedanken voor de waardevolle discussies voor hoofdstuk 4 en voor je expertise over click chemie. Dit hoofdstuk kreeg door **Ernst van Eck** een mooie toevoeging, dank voor de hulp met magic-angle spinning NMR.

Zonder de vaste medewerkers van de afdeling, zou alles een stuk moeizamer gaan! **Hans**, geen enkel peptide is hetzelfde, en daarom kwam jouw uitgebreide kennis regelmatig van pas. Bedankt ook voor de organisatie op het lab, de peptide benodigdheden waren altijd prima op orde. **Marieke**, dank dat alles altijd zo prima geregeld was, maar vooral ook bedankt voor de gezelligheid! Ik kon altijd van alles bij je kwijt, wat toch wel opluchtte. Ook **Desiree** wil ik hier

zeker noemen, bedankt dat je zo begripvol bent en, ondanks alles, altijd interesse in mij toonde. **Peter**, even een bestelling plaatsen of iets bij je ophalen, duurde altijd langer dan gedacht, omdat het zo gezellig was om een praatje met je te maken! **Jan Dommerholt**, bedankt voor het bestellen van BCN, en uiteraard voor je bijdrage aan hoofdstuk 4. **Peter van Galen** en **Helene**, bedankt voor het onderhoud aan de LC-MS en HPLC. Ook wil ik **Jacky** en **Paula** bedanken voor de administratieve hulp.

Zonder financiële ondersteuning was dit onderzoek niet mogelijk geweest, daarom mag **Agentschap NL** niet ontbreken. **Sybrand van der Zwaag** en **Annette Steggerda**, dank voor jullie enthousiasme en interesse in mijn project, en voor de leuke activiteiten en symposia die jullie organiseerden!

Tijdens mijn promotie heb ik het voorrecht gehad om drie studenten te begeleiden. **Addie Kusters**, je begon met het moeizame werk aan hoofdstuk 2, maar legde uiteindelijk de basis voor hoofdstuk 3. Het was leuk om te zien hoeveel plezier je daarin had, en hoe netjes je de verschillende combinaties van polymeren voor SPAAC hebt uitgetest. Ook ben je gestart met de eerste celtesten, en hebben we dit kunnen uitbouwen tot een mooi artikel. **Lindsey Lelieveld**, je was er alleen voor de bachelorstage, maar was erg gemotiveerd, zelfs om 's ochtends vroeg bij de handmatige ITC te proberen om luchtbellen te voorkomen. Een paar van jouw analyses heb ik kunnen gebruiken in hoofdstuk 2. **Imke Pijpers**, achter ideale student in het woordenboek vind je jouw naam zeker terug. Je kwam op het laatste stukje van mijn promotie, en terwijl ik door het hele land reisde, werkte jij zelfstandig aan je eigen hydrogels. Je was creatief in oplossingen vinden, onder andere om hydrogels onder UV licht te laten cross-linken, en hebt daardoor een groot deel van het werk in hoofdstuk 6 uitgevoerd. Jammer dat de tijd op was! Je hebt hard gewerkt en ik vond het erg gezellig!

Ik heb een hele gezellige tijd gehad in Nijmegen, wat natuurlijk komt door de collega's! Vooral de peptide angels, **Britta** en **Saskia**, waren mijn 'partners in crime'! **Britta**, je was de eerste die ik sprak, zelfs nog voordat ik begonnen was, en het was eigenlijk meteen goed! Ik kon altijd bij je terecht voor hulp met het onderzoek, maar ook zeker op persoonlijk vlak. Mooi om te zien dat je soms zo lekker nuchter bent, maar er wel altijd volledig voor gaat. Dank voor de gezellige etentjes, het samen organiseren van de Streepjesborrels, het shoppen, onze zangkunsten (Enrique!), mijn vraagbaak zijn voor allerlei Engelse vragen en, ondanks dat we nog net geen nieuwe ruggengraat gemaakt hebben, de prima samenwerking aan hoofdstuk 5!

Saskia, zonder jou had ik nooit kennis gemaakt met de wondere wereld van cell-babies! Ik ben heel blij dat je mijn paranimf bent! Samen hebben we hard gewerkt aan hoofdstuk 3, wat echt met vallen en opstaan ging. Ik heb veel van je geleerd over *in vitro* studies, en denk graag terug aan

de gezellige momenten achter de confocal! Ik waardeer je positiviteit en doorzettingsvermogen, en mede daarom hebben we uiteindelijk toch de mooie beloning van een artikel voor elkaar gekregen. Heel fijn dat je er altijd voor me bent en we samen zoveel leuke dingen hebben kunnen doen! Dank je wel voor de leuke en lekkere etentjes, het knuffelen met nijntjes, de shoptripjes en altijd gezellige gesprekken!

Annika, zonder jou was hoofdstuk 4 er niet geweest! Heel gaaf dat je mijn paranimf bent! Onze samenwerking was top, we hebben in korte tijd onze SPOCQ gels in Advanced Materials gekregen, waarbij ik onze reactie na de submissie 'Hij is niet afgewezen!' nooit zal vergeten. Mooi om jouw talent om dingen te regelen en je fanatieke werkhouding te zien. Ik denk ook met plezier terug aan de hydrogel fotosessies, waarbij niet alle gels zo fotogeniek bleken. Danke schön voor de gezellige treinreizen naar Arnhem, etentjes, leuke 'Wie is de Mol'-discussies en natuurlijk de Streuseltalers!

Wil ik hier natuurlijk ook even de 'partners van' noemen, **René**, **Stijn** en **Arne,** dank voor de gezellige avonden! **Ruud**, ondanks dat je nooit helemaal begrepen hebt dat Almere toch echt een stad is, vond ik het super gezellig om jou als bureau buurman te hebben! Ook had je altijd tijd om je even in de wereld van hydrogels te verdiepen en heb je zelf een prachtig boekje gemaakt! Dan zijn er nog veel andere mensen die ik wil bedanken voor hun hulp, tijd om even te overleggen en hun gezelligheid op het lab, tijdens de lunch (om 12:30 uur precies uiteraard) en tijdens borrels: **Matthijs** (mooi roze is niet lelijk), **Marcel** (lunch!), **Joep**, **Nanda**, **Morten** (Hot & Spicy zonder kaas), **Mark**, **Mariëlle**, **Zhipeng**, **Petra**, **René B.**, **Marjoke**, **Angelique**, **Lise**, **Lianne, Selma, Silvie, Jorgen, Stefan, Bram** en de rest van vleugel 1! **Rosa**, thanks for the nice collaboration on the review. Ook waren er een aantal studenten die zeker hebben bijgedragen aan de gezellige sfeer op het peptide lab: **Carim**, **Dennis** en **Pascal**. Gelukkig heb ik ook veel cel studies mogen uitvoeren, waarbij ik fijne hulp heb gehad van **Stéphanie** en **Liesbeth**.

Naast alle mensen die ik in Nijmegen heb leren kennen, wil ik ook graag het thuisfront bedanken. Het was elk weekend heerlijk om in Almere te zijn, en de promotie-perikelen lekker in het zuiden achter te laten.

Lieve **papa** en **mama**, heel erg bedankt voor jullie steun! Ik keek er altijd erg naar uit om op vrijdag in de auto te stappen en naar jullie (en Boemel :P) te rijden! Ik vind het super dat jullie mij altijd weer hebben gemotiveerd. De ritjes terug naar Arnhem, met mijn hele auto vol bakjes, shopdagen met mama, en klusjes met papa in mijn huisje, ik zal er altijd met veel plezier aan terugdenken! Lieve **Nils**, scheikunde is voor jouw een compleet andere wereld, verder dan H_2NX_4 kom je niet (ik vraag me nog steeds af wat voor bijzonder element X is :P), maar je

was altijd geïnteresseerd in mijn wetenschappelijke avonturen. Ik vind het erg gezellig dat we nu 'buren' zijn in Amsterdam! **Angela**, heel leuk om er zo'n gezellig schoonzus bij te krijgen. Super bedankt voor het prachtige ontwerp van de voorkant!

Lieve **Mavis**, **Gerrit**, **Kimberly** en **Lindsey**: naar Almere gaan betekende uiteraard ook een bezoekje aan jullie! Dank jullie wel voor de leuke weekenden, waar we het over van alles en nog wat hebben (en niet te vergeten vaak over lekker eten), en juist niet over wetenschap, wat mijn weekenden heerlijk ontspannen maakte! Ik ben blij met jullie, en de rest van de gezellige en gastvrije familie!

Een speciaal woordje ook voor mijn tante **Pauline**, je lieve appjes maken mij altijd blij! Ook stond ik vol trots op de Via Gladiola, om je te zien finishen na weer een succesvolle 4-daagse!

Dan tot slot, ondanks dat ik weet dat je dit cliché gaat vinden, zijn de laatste woorden toch echt voor jou! Lieve **Marc**, van mijn high-school lover, tot inmiddels ruim 10 jaar verder, maar het verveelt echt nooit! Dank je wel voor al je steun, ook al was het helaas vaak op afstand. Gelukkig heb je op mij gewacht in Amsterdam! Ik ben gek op je, en hoop nog lang met je samen te zijn!

★ ★ ★

Publications

- Jonker, A.M.; Bode, S.A.; Kusters, A.H.; van Hest, J.C.M.; Löwik, D.W.P.M.; *Soft PEG-hydrogels with independently tunable stiffness and RGDS-content for cell adhesion studies*; **Macromol. Biosci. 2015**, *15*, 1338-1347

- Jonker, A. M.; Borrmann, A.; van Eck, E. R. H.; van Delft, F. L.; Löwik, D. W. P. M.; van Hest, J. C. M.; *A fast and activatable cross-linking strategy for hydrogel formation*; **Adv. Mater. 2015**, *27*, 1235-1240.

- Borrmann, A.; Fatunsin, O.; Dommerholt, J.; Jonker, A. M.; Löwik, D. W. P. M.; van Hest, J. C. M.; van Delft, F. L.; *Strain-Promoted Oxidation-Controlled Cyclooctyne-1,2-Quinone Cycloaddition (SPOCQ) for fast and activatable protein conjugation*; **Bioconjugate Chem. 2015**, *26*, 257-261.

- Félix Lanao, R.P.; Jonker, A.M.; Wolke, J.G.C.; Jansen, J.A.; van Hest, J.C.M.; Leeuwenburgh, S.C.G.; *Physicochemical properties and applications of poly(lactic-co-glycolic acid) for use in bone regeneration*; **Tissue Eng. Pt. B 2013**, *19*, 380-390.

- Jonker, A. M.; Löwik, D. W. P. M.; van Hest, J. C. M.; *Peptide- and protein-based hydrogels;* **Chem. Mater. 2012**, *24*, 759-773.

- Tschan, S.; Brouwer, A.J.; Werkhoven, P.R.; Jonker, A.M.; Wagner, L.; Knittel, S.; Nigel Aminake, M.; Pradel, G.; Joanny, F.; Liskamp, R.M.J.; Mordmüller, B.; *Broad-spectrum antimalarial activity of peptido sulfonyl fluorides, a new class of proteasome inhibitors*; **Antimicrob. Agents Ch. 2013**, *57*, 3576-3584

- Geurink, P.P.; El Oualid, F.; Jonker, A.; Hameed, D.S.; Ovaa, H.; A general chemical ligation approach towards isopeptide-linked ubiquitin and ubiquitin-like assay reagents; **ChemBioChem 2012**, *13*, 293-297

- Brouwer, A.J.; Jonker, A.; Werkhoven, P.; Kuo, E.; Li, N.; Gallestegui, N.; Kemmink, J.; Florea, B.I.; Groll, M., Overkleeft, H.S.; Liskamp, R.M.J.; *Peptido sulfonyl fluorides as new powerful proteasome inhibitors*; **J. Med. Chem. 2012**, *55*, 10995-11003

- Brouwer, A.J.; Ceylan, T.; Jonker, A.M.; van der Linden, T.; Liskamp, R.M.J.; *Synthesis and biological evaluation of novel irreversible serine protease inhibitors using amino acid based sulfonyl fluorides as an electrophilic trap*; **Bioorgan. Med. Chem. 2011**, *19*, 2397-2406

About the author

Anika Maartje Jonker was born on 30 March 1987 in Almere, the Netherlands. She received her VWO-diploma in 2005 at Het Baken in Almere. After this, she studied Chemistry at the Utrecht University, where she obtained her Bachelor degree in 2008. She continued with the Master Drug Innovation, with her first internship in the Medicinal Chemistry and Chemical Biology group of Prof. Dr. R.M.J. Liskamp. Under the supervision of Arwin Brouwer she worked on the synthesis and evaluation of β-aminoethane sulfonyl fluorides as potent proteasome inhibitors. She performed her second internship at the Netherlands Cancer Institute (NKI) in Amsterdam. In the group of Huib Ovaa and Farid El Oualid, she studied the development and use of novel assay reagents for the high-throughput screening of deubiquitinating enzyme (DUB) inhibitors. After graduating in summer 2010, she started her PhD research at the Radboud University Nijmegen under the supervision of Prof. Dr. J.C.M. van Hest and Dr. D.W.P.M. Löwik. The results of this research project are described in this thesis. Since September 2015, Anika is working as a Chemistry teacher at Hogeschool Utrecht.

ISBN: 978-94-6233-183-9